



HAL
open science

Towards an integrated combination of membrane processes and ozonation for the removal of micropollutants in wastewater and urine

Hui Deng

► **To cite this version:**

Hui Deng. Towards an integrated combination of membrane processes and ozonation for the removal of micropollutants in wastewater and urine. Chemical and Process Engineering. INSA de Toulouse, 2019. English. NNT : 2019ISAT0046 . tel-03633025

HAL Id: tel-03633025

<https://theses.hal.science/tel-03633025>

Submitted on 6 Apr 2022

HAL is a multi-disciplinary open access archive for the deposit and dissemination of scientific research documents, whether they are published or not. The documents may come from teaching and research institutions in France or abroad, or from public or private research centers.

L'archive ouverte pluridisciplinaire **HAL**, est destinée au dépôt et à la diffusion de documents scientifiques de niveau recherche, publiés ou non, émanant des établissements d'enseignement et de recherche français ou étrangers, des laboratoires publics ou privés.



THÈSE

En vue de l'obtention du **DOCTORAT DE L'UNIVERSITÉ DE TOULOUSE**

Délivré par l'Institut National des Sciences Appliquées de
Toulouse

Présentée et soutenue par

Hui DENG

Le 15 juillet 2019

**Intérêt du couplage de procédés membranaires et d'ozonation
pour le traitement des micropolluants dans les filières de
traitement des eaux usées et des urines**

Ecole doctorale : **MEGEP - Mécanique, Energétique, Génie civil, Procédés**

Spécialité : **Génie des Procédés et de l'Environnement**

Unité de recherche :

LISBP - Laboratoire d'Ingénierie des Systèmes Biologiques et des Procédés

Thèse dirigée par

Christelle GUIGUI et Jean-Stephane PIC

Jury

Mme Annabelle COUVERT, Rapporteur

Mme Julie MENDRET, Rapporteur

M. Wolfgang GERNJAK, Examinateur

Mme Isabelle POLAERT, Examinatrice

Mme Christelle GUIGUI, Co-directrice de thèse

M. Jean-Stephane PIC, Co-directeur de thèse

**Towards an integrated combination of membrane
processes and ozonation for the removal of micropollutants
in wastewater and urine**

Abstract

In a context of growing water scarcity, wastewater reclamation or reuse has been increasingly recognized as an alternative source of water supply. However, trace micropollutants are not removed effectively by conventional treatment technologies in the wastewater treatment plants (WWTPs). To ensure safe reuse of municipal wastewater, it is necessary and important to establish advanced technologies, such as reverse osmosis (RO) process and ozonation, to reduce these non-desirable compounds to an acceptable level. In addition, a large fraction of trace micropollutants in the municipal wastewater, which are mainly referred to pharmaceutically active compounds (PhACs), mainly originate from urine wastewater. Thus, separation and treatment of urine at source not only provides an opportunity for urine valorisation by recovering N/P nutrients but also reduces the quantity of micropollutants in the municipal wastewater.

The objective of the present thesis is to assess the potential of the RO process and of ozonation for the emerging PhACs removal from two different types of wastewaters (municipal membrane bioreactor (MBR) permeate and urine). The performance of the RO process for MBR permeate was first examined in terms of RO membrane fouling and retention capacity for the target PhACs and for common water quality parameters. A combination of RO and ozonation was then investigated to remove PhACs from real urine. Before the treatment of real urine, impacts of water matrix, including ions, ammonia and organic matters, on removal efficiencies of trace PhACs removal by ozonation and ozone consumption was studied.

Results exhibited an excellent retention capacity of the RO membrane for the constituents present in MBR permeate, >80% for dissolved organic carbon (NPOC) and conductivity, and >90% for target PhACs. However, high rejection of the RO membrane meant that almost all the organic and inorganic substances were accumulated in RO concentrate, which was possibly related to the toxicity potential on the environment and human health. In order to reduce the quantity of RO concentrate releasing to the environment, RO concentrate, used as a part of MBR influents, was continuously recirculated to the MBR in an integrated MBR-RO system. On the other hand, ozonation was applied to degrade the trace PhACs from RO concentrate, aiming to minimize the environmental effect of RO concentrate.

The RO membrane in the MBR-RO system with RO concentrate recycling still maintained a relatively stable and effective retention capacity for the global water quality parameters and for the target PhACs (carbamazepine, diclofenac and ketoprofen). However, during RO concentrate recycling, the concentration of organic matters and inorganic ions in both MBR permeate and RO concentrate increased significantly. As a result, the fouling propensity of the RO membrane was enhanced in terms of RO permeate flux decline, which was mainly due to an increase of the osmotic pressure of retained ions at the RO membrane surface. In addition, ozonation was a feasible solution to manage RO concentrate with respect to micropollutant removal. 0.79 mg consumed O₃ per mg initial NPOC could achieve a >90% removal for the tested PhACs (carbamazepine, diclofenac, ibuprofen and propranolol)

from RO concentrate.

With respect to the treatment of urine wastewater, struvite precipitation was successful in recovering P nutrients from the urine solutions. However, most of the target PhACs (carbamazepine, diclofenac, ibuprofen, etc.) still remained in the urine solutions after the struvite precipitation tests, and thus ozonation was applied for their removal. As compared to the ozonation of saline solution with ions and synthetic urine (containing ions and ammonia), a higher ozone dose was required to remove the same quantity of the target PhACs from real urine solutions (containing ions, ammonia and organic matters), mainly due to the competitive reactions of constituents with molecular ozone. Indeed, ammonia and organic matters have been proved to be two main constituents to strongly inhibited the ozonation efficiencies of PhACs.

Keywords

Reverse osmosis; Ozonation; Micropollutants; Wastewater reclamation; Source-separated urine; RO membrane fouling

Résumé

La réutilisation des eaux usées est devenue une priorité dans le contexte du réchauffement climatique et de la rareté de la ressource. Cependant, les micropolluants n'étant pas éliminés par les technologies de traitement classiques des stations d'épuration, il est nécessaire de mettre en place des technologies avancées telles que le processus d'osmose inverse (OI) et l'ozonation afin de ramener ces composés indésirables à un niveau acceptable dans le contexte de la réutilisation. De plus, une majorité des micropolluants des eaux usées sont des composés pharmaceutiques (PhACs), et proviennent principalement des urines. La séparation et le traitement de l'urine à la source qui permettent non seulement de valoriser l'urine en récupérant les éléments nutritifs N/P, mais aussi de réduire la charge de micropolluants dans les eaux usées municipales, est une alternative de choix dans le contexte de la réutilisation et de la qualité sanitaire des eaux. L'objectif de ce travail était d'évaluer le potentiel de la combinaison de l'osmose inverse et de l'ozonation pour l'élimination des PhACs dans deux types d'eaux usées différentes (perméat de bioréacteur à membrane et urine). Les performances du procédé d'OI en traitement tertiaire après bioréacteur à membrane (BAM) ont tout d'abord été examinées en termes de colmatage et de rétention des PhACs et des paramètres de qualité d'eau classique. L'ozonation des concentrats a ensuite été réalisée. Dans un second temps, une combinaison précipitation/OI/ozonation a été étudiée pour la valorisation de l'urine en ce qui concerne la récupération du phosphore et l'élimination des PhACs.

L'OI a montré une excellente capacité de rétention pour les constituants présents dans le perméat BAM, > 80% pour le carbone organique dissous (NPOC) et la conductivité, et > 90% pour les PhACs. Afin de minimiser l'impact du concentrat d'OI sur l'environnement en cas de rejet, les concentrats ont été recirculés vers le BAM et l'intérêt d'une ozonation a été étudié. Les résultats ont montré que la membrane d'OI dans le système BAM-OI présente toujours une capacité de rétention relativement stable et efficace pour les paramètres globaux de qualité de l'eau. Cependant, après le recyclage du concentrat d'OI, le flux de perméat de la membrane d'OI diminue principalement en raison d'une augmentation de la pression osmotique des ions retenus à la surface de la membrane d'OI. Les PhACs retenus dans le concentré OI peuvent être éliminés efficacement par ozonation.

En ce qui concerne le traitement de l'urine, la précipitation de struvite a permis de valoriser le phosphore de l'urine. Cependant, les PhACs sont demeurés dans la solution et ont dû être traités par ozonation. L'approche a été d'étudier l'effet de la matrice dans laquelle se trouvent les PhACs sur les performances et les mécanismes d'ozonation. Ainsi une dose d'ozone supplémentaire est nécessaire pour réduire la même quantité de PhACs des solutions d'urine réelles (contenant des ions, de l'ammoniac et

des matières organiques) en comparaison aux solutions salines et sans matières organiques. Ceci est la conséquence de réactions compétitives des sels, de l'ammoniac et des matières organiques avec l'ozone moléculaire.

Mots clés

Osmose inverse; Ozonation; Micropolluants; Réutilisation; Urine; Colmatage

Acknowledgments

First of all, I would like to thank my jury members, Pro. Annabelle COUVERT and Dr. Julie MENDRET as reviewers for my thesis, and Pro. Wolfgang GERNJAK and Dr. Isabelle POLAERT as examiners for my Ph.D. study. During my thesis defence, they provide very important and valuable comments to improve the quality of my thesis.

I would like to express my most heartfelt appreciations and thanks to my co-supervisor Pro. Christelle GUIGUI for her step-by-step guidance. She leads me into the area of membrane technology for wastewater treatment. She introduces and assists me in how to propose scientific questions and practice an idea with theoretical and experimental method. In addition, she gives me many valuable suggestions to improve the quality of scientific publications.

I would also like to express my special gratitude to my co-supervisor Dr. Jean-Stephane PIC for his endless guidance in developing semi-batch ozonation experiments used during this work and answering to my question about experimental theory and corresponding parameters calculation. Without his support and help, this work would not have been so successful.

A very big thank to Technician Manon MONTANER, Bernard REBOUL and Colette KRASICKI for considerable assistance with training, preparation and maintenance of reverse osmosis pilot and of ozonation reactor. I am particularly grateful to Technician Aurore DIDI, who made great contributions to the analysis of water quality parameters and the quantification of micropollutants present in municipal wastewater. I would also like to thank Technician Laetitia CAVAILLE for the analysis of micropollutants concentration in real urine, and Technician Mansour BOUNOUBA for the training of ionic concentration measurement.

I also want to give a huge thank to my Chinese friends in France, Dan FENG, Bomin FU, Xi LIN, Shengyue DENG and Qi GAO, who always give me their endless encouragement during my Ph.D. journey. Many thanks belong to my colleagues: Qiuming MA, Feishi XU, Noemie GAMBIER, Paul JACOB, Naila BOUAYED, Tianyi Zhang, Zou SHEN, Dylan LORFING, Marine TOURNOIS and Hà HOANG for sharing a pleasing working environment.

China Scholarship Council (CSC) is also acknowledged for financial support during my Ph.D. studies.

My special appreciation and great thankfulness belong to my parents, my brother, and my sister for their love, encouragement and unconditional support. And last but not least, I am deeply grateful to my husband and constant companion Jianxiong HE for never-ending support in many aspects and sharing cheerfulness with me.

List of scientific publication

Journal papers

Hui DENG, Matthieu JACOB, Manon MONTANER, Jean-Stéphane PIC, Christelle GUIGUI.

Effect of Reverse Osmosis Concentrate Recirculation to Membrane Bioreactor on Performance of Reverse Osmosis in An Integrated MBR-RO Process for Municipal Wastewater Treatment.

(submitted)

Hui DENG, Christelle GUIGUI, Jean-Stéphane PIC.

Effect of Water Matrix on The Mechanisms and Performance of Ozonation for Micropollutant Removal.

(submitted)

Oral presentation

Hui DENG, Christelle GUIGUI, Jean-Stéphane PIC

Ozonation Performance for Micropollutants Removal from Source-Separated Urine.

International Conference of Ozone and Advanced Oxidation: Solutions for Emerging Pollutants of Concern to The Water and The Environment. 5-7 September, 2018, Lausanne, Switzerland.

Hui DENG, Hà HOANG, Jean-Stéphane PIC, Christelle GUIGUI

Combination of Membrane Processes and Ozonation for Source-Separated Urine Valorisation

9th International Water Association (IWA) Membrane Technology Conference & Exhibition for Water and Wastewater Treatment and Reuse (IWA-MTC 2019). 23-27 June, 2019, Toulouse, France.

Table of Contents

Abstract	i
Résumé	iii
Acknowledgments	v
List of scientific publication	vi
Table of Contents	vii
List of Tables	xi
List of Figures	xiv
Nomenclature	xvii
List of Abbreviations	xix
Introduction	1
Chapter I Background and Literature Review	7
I.1 Pharmaceutically active compounds	9
I.1.1 General information on pharmaceutically active compounds	9
I.1.2 Occurrence of PhACs in surface water	10
I.1.3 Occurrence of PhACs in sewage treatment plant effluents	10
I.2 Reverse osmosis process for wastewater reclamation	14
I.2.1 General information on reverse osmosis process	14
I.2.2 Rejection capacity of reverse osmosis membrane for micropollutants	14
I.2.3 RO membrane fouling.....	15
I.2.3.1 Membrane foulants and fouling type.....	16
I.2.3.2 RO membrane fouling mechanisms	17
I.2.3.3 Fouling behaviour of RO membrane for municipal wastewater reuse	19
I.2.4 Characteristics and disposal of RO concentrate	22
I.2.4.1 Characteristics of RO concentrate	22
I.2.4.2 Occurrence of PhACs in RO concentrate	23
I.2.4.3 Recirculation of RO concentrate into the biological unit	24
I.2.4.4 Treatment of RO concentrate by advanced oxidation processes	27
I.3 Ozonation application for decontamination of PhACs	29
I.3.1 Ozone decomposition and the formation of hydroxyl radicals	30
I.3.2 Expected attack site of micropollutants towards ozone	31
I.3.3 Micropollutants decontamination in wastewater by ozonation	32
I.3.4 Impact of water matrix on the degradation of PhACs by ozonation	35
I.3.4.1 Effect of scavengers.....	35
I.3.4.2 Impact of organic matters and alkalinity on ozone lifetime	35
I.3.5 Formation and toxicity of transformation products.....	36
I.4 Urine wastewater	37

I.4.1 Characteristics of source-separated urine.....	37
I.4.2 Occurrence of PhACs in source-separated urine.....	38
I.4.3 Urine valorisation and treatment of source-separated urine.....	39
I.4.3.1 Struvite precipitation	39
I.4.3.2 Reverse osmosis process	39
I.4.3.3 Ozonation process	40
I.5 Summary of literature review.....	40
Chapter II Materials and Methods.....	43
II.1 Target micropollutants.....	45
II.1.1 Properties of the target micropollutants	45
II.1.2 Preparation of stock solution of the target micropollutants	47
II.2 Description of RO process	47
II.2.1 RO membrane used.....	47
II.2.2 Dead-end RO cell configuration	48
II.2.3 Cross-flow RO pilot.....	48
II.2.4 RO process parameters	49
II.2.5 Saturation index calculation.....	50
II.3 Semi-batch ozonation.....	50
II.3.1 Description of ozonation pilot	50
II.3.2 Concentration profile of ozone in ultra-pure water and mass balance of ozone	51
II.3.2.1 Mass balance of ozone in the gaseous and liquid phase.....	52
II.3.2.2 Rate constant of ozone self-decomposition.....	53
II.3.2.3 Volumetric mass-transfer coefficient.....	53
II.3.3 Ozone dose.....	53
II.3.4 Ozone solubility in the ionic solution	54
II.4 Analysis of chemicals.....	54
II.4.1 pH and conductivity.....	54
II.4.2 Dissolved organic carbon and dissolved inorganic carbon	54
II.4.3 Chemical oxygen demand.....	55
II.4.4 Ions analysis.....	55
II.4.5 Ultraviolet absorbance	55
II.4.6 Size-exclusion high performance liquid chromatography	55
II.4.7 Polysaccharides and proteins	56
II.4.8 Micropollutants	56
Chapter III Combining RO and ozonation process for municipal wastewater reuse: RO membrane fouling and emerging micropollutants removal	57
Introduction	59
III.1 Experimental protocols	59
III.2 Characteristics of MBR permeate.....	60
III.3 RO performance with RO concentrate recirculation to MBR (Set 1).....	62
III.3.1 MBR-RO process with RO concentrate recycling.....	62

III.3.2 Characteristics of MBR permeate produced before and during RO concentrate recycling....	64
III.3.3 Influence of RO concentrate recycling on RO retention capacity for NPOC, COD and ions	66
III.3.4 Influence of RO concentrate recycling on RO membrane fouling propensity	69
III.3.4.1 RO membrane fouling in terms of RO permeate flux decline	70
III.3.4.2 Impact of osmotic pressure gradient of salts on RO permeate flux decline.....	71
III.3.4.3 Scaling potential analysis based on saturation index model	73
III.3.4.4 Organic fouling potential analysis	74
III.3.5 Influence of RO concentrate recycling on the retention capacity for PhACs.....	76
III.3.6 Conclusions on the impacts of RO concentrate recycling to MBR on RO performance	77
III.4 Removal of micropollutants by RO process combining ozonation (Set 2).....	78
III.4.1 RO retention capacity for micropollutants	78
III.4.2 Removal efficiency of PhACs from RO concentrate by ozonation.....	80
III.4.3 Removal efficiency of organic matters from RO concentrate by ozonation.....	83
III.4.4 Conclusions on performance of RO process + ozonation for PhACs removal.....	83
III.5 Conclusions of this chapter	84
Chapter IV Effect of water matrix on the mechanisms and performance of ozonation for micropollutants removal.....	87
Introduction	89
IV.1 Experimental protocols	89
IV.1.1 Preparation of organic matter-free solutions spiked with CBZ and KET	90
IV.1.2 Real urine collection and pre-treatment	90
IV.1.3 Ozonation operating conditions	91
IV.2 Ozonation kinetic regime and ozone mass transfer.....	92
IV.2.1 Mass transfer with chemical reactions	92
IV.2.2 Mass balance of ozone with chemical reactions	93
IV.3 Investigation of the oxidation mechanism of CBZ and KET	94
IV.4 Impacts of solution matrix on the efficiency of PhACs removal by ozonation.....	97
IV.4.1 Ozonation of CBZ and KET in saline solution and synthetic urine.....	97
IV.4.2 Ozonation of CBZ in real urine	100
IV.4.3 Variation of the concentration of ionic salts and N-NH_4^+	102
IV.4.4 Comparison of removal efficiencies of CBZ and KET in the different matrix.....	103
IV.5 Effect of water matrix on ozonation consumption and kinetic regimes.....	105
IV.5.1 Hatta number and enhancement factor	105
IV.5.2 Ozone effectiveness yield	106
IV.6 Conclusions of this chapter	108
Chapter V A combination process of struvite precipitation, reverse osmosis and ozonation for the reclamation of source-separated urine: nutrient valorisation and micropollutants removal.....	111
Introduction	113
V.1 Description of the treatment line.....	113

V.1.1 Characteristics of urine-based solutions and the target PhACs spike	116
V.1.2 Struvite precipitation	119
V.1.3 Dead-end RO filtration.....	119
V.1.4 Ozonation experiment	120
V.2 Recovery of P nutrient from urine-based solutions as struvite crystals	121
V.2.1 Identification of crystals.....	121
V.2.2 Removal of P by struvite precipitation.....	122
V.2.3 Removal of organic compounds during struvite precipitation	124
V.3 RO performance for urine treatment	126
V.3.1 Retention capacity of RO membrane for target micropollutants.....	126
V.3.2 Retention efficiencies for ionic species	130
V.3.3 Variation of RO permeate flux versus RO permeate volume	132
V.4 Ozonation of the urine-based solutions	133
V.4.1 Ozonation efficiencies of real urine	133
V.4.1.1 Ozonation of HUM-1.....	133
V.4.1.2 Ozonation of HUM-2.....	136
V.4.1.3 Ozonation of HUM-3 RO concentrate and HUM-3 RO permeate.....	137
V.4.1.4 Ozonation of SUM-RO concentrate and -RO permeate	140
V.4.2 Ozone kinetic regimes and ozone consumption during the ozonation of real urine.....	141
V.5 Comparison of P recovery and PhACs removal from source-separated urine by the combination process	144
V.6 Conclusions of this chapter.....	147
Conclusions and Future research.....	149
REFERENCES	154
Appendix	173

List of Tables

Chapter I

Table 1.1 Commonly prescribed drugs in the U.S. in 2016

Table 1.2 Residual concentration of common PhACs in surface water

Table 1.3 Concentration of trace micropollutants in the WWTPs influents and effluents, and their removal efficiencies

Table 1.4 Removal (%) of micropollutants from water by RO process

Table 1.5 Fouling types of RO membrane

Table 1.6 Summary of the fouling studies of RO membrane for municipal wastewater reuse

Table 1.7 Main characteristics of RO concentrate from municipal wastewater treatment

Table 1.8 Concentrations of micropollutants in RO concentrate

Table 1.9 Impacts of NF or RO concentrate recycling to a biological unit on NF or RO performance

Table 1.10 Removal efficiency of organics by AOPs from municipal RO concentrate

Table 1.11 Complication of ozonation removal of micropollutants in wastewater effluents

Table 1.12 Compositions of fresh and hydrolysed urine

Table 1.13 Concentration of PhACs found in urine from a public toilet

Table 1.14 Treatment processes of source-separated urine

Chapter II

Table 2.1 Relevant properties of the target PhACs

Table 2.2 Concentration of target micropollutants in the stock solution

Table 2.3 Characteristics of ESPA2 RO membrane

Chapter III

Table 3.1 Characteristics of two tested MBR permeate (as RO feed)

Table 3.2 Operating conditions of MBR pilot and RO process

Table 3.3 Compositions of wastewater and MBR permeate (RO feed) without and with RO concentrate recycling to MBR

Table 3.4 RO membrane retention capacities for anions and cations

Table 3.5 Diffusion coefficient, Reynolds Number, Schmidt Number, Sherwood Number, and transfer coefficient of different ions

Table 3.6 Ionic concentration at the RO membrane surface before and during RO concentrate

recirculation

Table 3.7 Saturation index of three common scalants before and after RO concentrate recirculation

Table 3.8 The retention rate of the tested PhACs before and during RO concentrate recycling

Table 3.9 Concentration of the selected indicators and their observed retention by the RO membrane

Table 3.10 Operating conditions of ozonation process for RO concentrate

Table 3.11 Removal of four PhACs by ozonation from RO concentrate

Chapter IV

Table 4.1 Characteristics of the tested solutions before ozonation

Table 4.2 Operating conditions of ozonation for different solution matrix

Table 4.3 Hatta number and the kinetic regime

Table 4.4 $k_{O_3-i} \times [i]$ values of the different compounds before ozonation

Table 4.5 Variation of PhACs, organic carbon and ionic salts after ozonation

Table 4.6 Hatta number, instantaneous enhancement factor (E_i) and enhancement factor from the experimental result (E_{exp}) in PWM-2, SAM, SUM and HUM

Table 4.7 Transferred ozone yield and ratio of consumed ozone dose to transferred ozone dose at the end of reaction time

Chapter V

Table 5.1 Characteristics of synthetic urine and of hydrolysed urine after UF pre-treatment

Table 5.2 Concentration of target PhACs in the tested solutions before precipitation or RO process

Table 5.3 Relevant properties of the target PhACs

Table 5.4 Operating conditions of the dead-end RO process for different solutions

Table 5.5 Operating conditions of semi-batch ozonation for different solutions

Table 5.6 Compositions of crystals from this study and the elements of struvite reported by the previous literature

Table 5.7 Removal efficiencies of global parameters from urine-based solutions during the struvite precipitation

Table 5.8 Mass of crystals from a test and a theoretical calculation

Table 5.9 Residual concentration of organic compounds before and after the precipitation experiments

Table 5.10 Concentration of organic compounds in RO solutions and their observed retention

Table 5.11 Concentration of global parameters in RO solutions and their observed retention

Table 5.12 Concentration of PhACs, carbon compounds and N compounds and cumulated consumed ozone dose during the ozonation of HUM-1 (20 times dilution)

Table 5.13 Concentration of PhACs, carbon compounds and N compounds and cumulated consumed ozone dose during the ozonation of HUM-2 (10 times dilution)

Table 5.14 Concentration of PhACs, carbon compounds and N compounds and cumulated consumed ozone dose during the ozonation of HUM-3-ROC (10 times dilution)

Table 5.15 Concentration of PhACs, carbon compounds and N compounds and cumulated consumed ozone dose during the ozonation of HUM-3-ROP (10 times dilution)

Table 5.16 Concentration of PhACs, carbon compounds and N compounds and cumulated consumed ozone dose during the ozonation of SUM-ROC

Table 5.17 Concentration of PhACs, carbon compounds and N compounds and cumulated consumed ozone dose during the ozonation of SUM-ROP

Table 5.18 Initial E_{exp} values and initial ozone demand (IOD) during the ozonation of HUM-based solutions

Table 5.19 Removal efficiencies of organic C from PhACs by ozonation

Table 5.20 Ozone consumption and the elimination of carbon and N-NH₄⁺ during the ozonation of the real urine solutions

List of Figures

Figure 1 Structure of the present thesis

Chapter I

Figure 1.1 Number of diclofenac and propranolol prescriptions over time in the U.S. (2006 - 2016)

Figure 1.2 Schema of RO process and the rejection mechanism for solutes

Figure 1.3 Four different fouling in terms of foulants

Figure 1.4 Schema of concentration polarization and membrane fouling

Figure 1.5 Schema of RO membrane fouling mechanism

Figure 1.6 Schematic of RO concentrate treatment by AOPs

Figure 1.7 Oxidation pathways of micropollutants in water

Figure 1.8 Expected attack site of micropollutants towards molecular ozone

Figure 1.9 Ozonation of specific moiety (aromatic ring and amine)

Figure 1.10 Different types of micropollutants and their elimination by ozone

Figure 1.11 Effect of water matrix on the removal efficiency of organic micropollutants

Chapter II

Figure 2.1 Expected attack site of PhACs towards molecular ozone and their ozone kinetic rate constant.

Figure 2.2 Device for RO filtration with dead-end mode

Figure 2.3 Schematic of cross-flow RO pilot

Figure 2.4 Ozonation pilot with a semi-batch reactor

Figure 2.5 Typical ozone concentration profiles

Chapter III

Figure 3.1 Treatment schema of MBR permeate

Figure 3.2 Schematic of cross-flow RO pilot with recirculation of RO concentrate to the MBR unit

Figure 3.3 Variation of NPOC (a) and COD (b) in RO flows with the recirculation of RO concentrate

Figure 3.4 Variation of conductivity in RO flows as a function of operation time

Figure 3.5 Effect of RO concentrate recycling on the concentration of ionic salts in the RO flows

Figure 3.6 RO permeate flux behaviour throughout the operating time

Figure 3.7 Variation of the osmotic pressure gradient of retained ions and RO permeate flux as a function of operation time

Figure 3.8 HPLC-SEC analysis of RO flows before and after RO concentrate recirculation to MBR unit

Figure 3.9 Concentration of proteins and polysaccharides in RO flows before and after RO concentrate

recirculation

Figure 3.10 Concentration of the target PhACs in RO flows before and during RO concentrate recirculation

Figure 3.11 Observed retention of PhACs during the RO process of MBRP-2

Figure 3.12 Residual concentration of PhACs selected during the ozonation of RO concentrate from the RO process of MBRP-2

Figure 3.13 Residual concentration of NPOC during the ozonation of RO concentrate from the RO process of MBRP-2

Chapter IV

Figure 4.1 Experimental protocols applied to study the impact of water matrix on the ozonation of PhACs

Figure 4.2 Mass transfer with chemical reactions in the case of ozone of low solubility

Figure 4.3 PhACs residual, pH and concentration of ozone gas-out and of dissolved ozone as a function of cumulated consumed ozone dose during the ozonation of PWM-1 and PWM-2

Figure 4.4 Proposed primary reaction products of molecular ozone towards CBZ and KET

Figure 4.5 PhACs residual, concentration of ozone gas-out and of dissolved ozone as a function of cumulated consumed ozone dose during the ozonation of SAM, SUM and HUM

Figure 4.6 Residuals of organic carbon and COD as a function of cumulated consumed ozone dose

Figure 4.7 pH variation as a function of cumulated consumed ozone dose

Figure 4.8 Variation of ionic concentration during the ozonation of SAM, SUM and HUM-2

Figure 4.9 Cumulated consumed ozone dose as a function of applied ozone dose during the ozonation of 5 solution matrices

Chapter V

Figure 5.1 Experimental treatment line of urine valorisation

Figure 5.2 Treatment of urine-based solutions by precipitation, RO and ozonation

Figure 5.3 Device for precipitation reactor

Figure 5.4 SEM image and EDX spectrum of the crystals from the precipitation of SUM and HUM-3 with $MgCl_2$ as Mg^{2+} source

Figure 5.5 Observed retention of the target PhACs by the RO membrane in different solutions

Figure 5.6 Variation of permeate flux over RO permeate volume during the filtration of PWM, SUM and HUM- 3

Figure 5.7 Variation of organic C residual and COD as a function of cumulated consumed ozone dose

Figure 5.8 Conversion of N-NH_4^+ to N-NO_3^- during the ozonation of HUM-based solutions with 10 times dilution

Figure 5.9 Concentration profile of ozone in either gaseous phase or liquid solution as a function of reaction time during the ozonation of the real urine solutions

Figure 5.10 Cumulated consumed ozone dose versus applied ozone dose

Nomenclature

ρ	Volumetric mass density (kg m^{-3})
μ	Viscosity of solution (mPa s)
ε_{sp}	Spacer porosity (0.8)
$\Delta\pi$	Osmosis pressure gradient (bar)
ΔP	Transmembrane pressure (bar)
π_{m}	Osmotic pressure at the membrane surface (Pa or bar)
π_{p}	Osmotic pressure in RO permeate side (Pa or bar)
A_{m}	Surface area of membrane (m^2)
C_{c}	Concentration of an indicator in RO concentrate (mg L^{-1} or mol L^{-1})
C_{f}	Concentration of an indicator in RO inflow (mg L^{-1} or mol L^{-1})
C_{m}	Concentration of an indicator at the membrane surface (mg L^{-1} or mol L^{-1})
C_{p}	Concentration of an indicator in RO permeate (mg L^{-1} or mol L^{-1})
D_{i}	Diffusivity of compound i in water ($\text{m}^2 \text{s}^{-1}$)
D_{O_3}	Diffusivity of ozone in water ($\text{m}^2 \text{s}^{-1}$)
d_{H}	Hydraulic diameter for a rectangular channel
E_{i}	Instantaneous enhancement factor
E_{exp}	Enhancement factor from experimental data
H	Spacer thickness (0.00063 m)
J	Membrane permeate flux ($\text{L h}^{-1} \text{m}^{-2}$)
k_{i}	Mass transfer coefficient of ion i (m s^{-1})
k_{La}	Ozone volumetric mass transfer coefficient (s^{-1})
k_{L}	Mass transfer coefficient (m s^{-1})
K_{sp}	Solubility product constant
$k_{\text{O}_3\text{-i}}$	Apparent rate constant of compound i with ozone ($\text{L mol}^{-1} \text{s}^{-1}$)
$k_{\text{OH}\cdot\text{i}}$	Apparent rate constant of compound i with $\cdot\text{OH}$ radicals ($\text{L mol}^{-1} \text{s}^{-1}$)
L_{p}	Permeability of RO membrane ($\text{L h}^{-1} \text{m}^{-2} \text{bar}^{-1}$)
$\text{Log}K_{\text{ow}}$	Ratio of concentration of a solute between water and octanol in logarithmic terms
m	Ozone solubility parameter
m_{ini}	Mass of a selected parameter in the initial urine solution (mg or μg)
m_{fil}	Mass of selected parameter in the urine solution after Buchner filtration (mg or μg)
$\text{O}_3_{\text{applied}}$	Applied ozone dose (mg)
$\text{O}_3_{\text{transferred}}$	Transferred ozone dose (mg)
$\text{O}_3_{\text{consumed}}$	Consumed ozone dose (mg)
$\text{p}K_{\text{a}}$	Acid dissociation constant at a logarithmic scale

P_c	Pressure in RO concentrate side (bar)
P_f	Pressure in RO feed side (bar)
P_p	Pressure in RO permeate side (bar)
Q_c	RO concentrate flow rate ($L h^{-1}$)
Q_f	RO inflow flow rate ($L h^{-1}$)
Q_g	Ozone gas flow rate ($L h^{-1}$)
Q_p	RO permeate flow rate ($L h^{-1}$)
R_{obs}	Observed retention capacity of an indicator (%)
R	The universal gas constant ($8.3145 J mol^{-1} K^{-1}$)
r_{appO_3}	Apparent ozone decomposition rate ($mol L^{-1} s^{-1}$)
T_{O_3}	Amount of ozone transferred from the gaseous to the liquid phase ($mg L^{-1}$ or $mol L^{-1}$)
t	Reaction time (s, min or h)
U	Tangential velocity of RO concentrate ($m s^{-1}$)
V_1	Valve of RO concentrate side
V_{liq}	Liquid solution volume (L)
V_g	Ozone gas volume (L)
V_c	RO concentrate volume (L)
V_f	RO feed volume (L)
V_p	RO permeate volume (L)
z_i	Valency of ion i
γ_i	Stoichiometric ratio of compound i with molecular ozone
$\cdot OH$	Hydroxyl radicals
$[B]_L$	Concentration of compound B in the liquid phase ($mg L^{-1}$ or $mol L^{-1}$)
$[B]_L^i$	Concentration of compound B at the liquid interface ($mg L^{-1}$ or $mol L^{-1}$)
$[i]$	Concentration of compound i ($mg L^{-1}$ or $mol L^{-1}$)
$[O_3]_{gas in}$	Concentration of ozone in the inlet stream ($mg L^{-1}$ or $mol L^{-1}$)
$[O_3]_{gas out}$	Concentration of ozone in the outlet stream ($mg L^{-1}$ or $mol L^{-1}$)
$[O_3]_G$	Concentration of ozone in the gas phase ($mg L^{-1}$ or $mol L^{-1}$)
$[O_3]_G^i$	Concentration of ozone at the gas interface ($mg L^{-1}$ or $mol L^{-1}$)
$[O_3]_L$	Concentration of ozone in the liquid phase ($mg L^{-1}$ or $mol L^{-1}$)
$[O_3]_L^i$	Concentration of ozone at the liquid interface ($mg L^{-1}$ or $mol L^{-1}$)
$[O_3]_L^*$	Concentration of dissolved at equilibrium ($mg L^{-1}$ or $mol L^{-1}$)

List of Abbreviations

AOPs	Advanced oxidation processes
B	Compound B
CAF	Caffeine
CBZ	Carbamazepine
CF	Concentration factor
COD	Chemical oxygen demand
DIC	Dissolved inorganic carbon
DIF	Diclofenac
DOC	Dissolved organic carbon
DOM	Dissolved organic matters
E	Enhancement factor
EPS	Extracellular polymeric substances
HRT	Hydraulic retention time
HU	Hydrolysed urine
HUM	Hydrolysed urine with micropollutants spike
i	Compound i
IAP	Ionic activity product
IBP	Ibuprofen
IC	Ionic chromatography
IOD	Initial ozone demand
KET	Ketoprofen
MBR	Membrane bioreactor
MBRP	Membrane bioreactor permeate
MF	Microfiltration
MW	Molecular weight
MWCO	Molecular weight cut off
MWWTPs	Municipal wastewater treatment plants
NF	Nanofiltration
NOM	Natural organic matters
NPOC	Non-purgeable organic carbon
Organic C	Organic carbon
OFL	Ofloxacin
OXA	Oxazepam
PhACs	Pharmaceutically active compounds

PRO	Propranolol
PWM	Ultra-pure water with micropollutants
QuEChERS	Quick, Easy, Cheap, Effective, Rugged, Safe
Re	Reynolds number
RO	Reverse osmosis
ROC	RO concentrate
ROP	RO permeate
Sc	Schmidt number
Sh	Sherwood number
SA	Saline solution
SAM	Saline solution with micropollutants
SMPs	Soluble microbial products
SMX	Sulfamethoxazole
SU	Synthetic urine
SUM	Synthetic urine with micropollutants
TOC	Total organic carbon
TOD	Transferred ozone dose
UF	Ultrafiltration
UVA	Ultraviolet absorbance
VRF	Volumetric reduction factor
WWTPs	Wastewater treatment plants
2OH-IBP	2-hydroxyibuprofen

Introduction

Over the past decades, population growth, water quality deterioration and climate change lead to greater pressures on the availability of water resources throughout the world. It is reported that one-third of the Europe territory is experiencing water stress (EUROPEAN COMMISSION, 2018). Moreover, in the coming years and decades, water shortage/scarcity will become more serious in many countries and regions of the world. In 2040, 33 countries will suffer from extremely high water stress, and more than half of the world population will face medium to extremely high water stress. To face this problem, therefore, it is of great importance to look for tools for the better management of the water resources.

In a context of growing water scarcity, water reuse - the use of treated wastewater, also referring to as water reclamation or water recycling, has been recognized increasingly as an alternative source of water supply. Even if wastewater represents a source of contamination, wastewater treated by technologies has been reused in many applications, both potable and nonpotable use. Many countries around the world, such as U.S., Saudi Arabia, etc., have taken great efforts in reusing wastewater to meet the growing water demand (Jiménez Cisneros and Asano, 2008). In Europe, at present, about 1 billion cubic metres of treated urban wastewater is reused annually, which accounts for approximately 2.4% of the treated urban wastewater effluents and less than 0.5% of annual Europe freshwater withdrawals (EUROPEAN COMMISSION, 2018). However, it ensures that the reuse of treated wastewater for agricultural irrigation, industrial use, or urban development, must be safe.

Effluents of municipal wastewater treatment plants (MWWTPs) are thought as an available source of reusable water. In fact, conventional water treatment technologies are not sufficient to remove a wide range of contaminants from suspended solids to smaller inorganic ions (Wintgens et al., 2005). Therefore, some trace micropollutants, especially for whom with poor biodegradation and low adsorption on the sludge, are detected frequently in MWWTPs effluents, at a concentration ranging from a few ng L^{-1} to several $\mu\text{g L}^{-1}$, even up to mg L^{-1} (Ashfaq et al., 2017; Blair et al., 2015; Guillosoy et al., 2019; Yu et al., 2013). Occurrence of trace micropollutants and their metabolites have been recognized as one of the most important concerns for wastewater reuse, due to their potential environmental risk even at a low concentration (Kołodziejaska et al., 2013). In order to safely reuse water, therefore, advanced wastewater technologies, such as reverse osmosis process (RO) and ozonation, need to be well established to eliminate trace micropollutants from MWWTPs effluents and to produce high-quality water before water reuse.

Even though human urine stream only makes up one percent of the total flow of municipal wastewater, the presence of a broad spectrum of pharmaceutically active compounds (PhACs) in the municipal wastewater is mainly due to the direct discharge of urine wastewater (Dodd et al., 2008; Landry and Boyer, 2016). On the other hand, the discharge of nutrients-enrich urine (N, P, K) to urban sewer system also increases nutrient load in wastewater, so that more energy costs are required by WWTPs for these nutrients removal (Maurer et al., 2006). To reduce the related ecotoxicity concern and to improve urine valorisation, thus, it is essential to recover these nutrients for an agricultural purpose and to remove unwanted micropollutants from urine at the source.

Reverse osmosis (RO), a common membrane technology, has gained worldwide acceptance for the reclamation of municipal wastewater, which is due to its high efficiencies in rejecting a wide range of organic pollutants, bacteria, dissolved organic matters and inorganic salts (Bellona et al., 2004; Dolar et al., 2012; Ganiyu et al., 2015; Jacob et al., 2012; Malaeb and Ayoub, 2011). When RO process is applied for the reclamation of municipal wastewater, it is extremely important to investigate RO membrane fouling, because which relates to the quality and the production of RO permeate. On the other hand, the application of RO process for wastewater reuse generates an inevitable concentrated stream, termed as RO concentrate or RO retentate. In the case of wastewater treatment by RO process, the volume recovery is only 40 - 90% (Van der Bruggen et al., 2003). RO concentrate is characterized by high levels of inorganic salts, organic substances and trace micropollutants, which may associate to the potential toxicity to receiving bodies (Bagastyo et al., 2011a; Comstock et al., 2011; Pérez et al., 2010). However, to date, there is a few information on the management of RO concentrate. The disposal of RO concentrate is still a big constraint for the sustainable application of RO process for wastewater reuse. Therefore, it is of great importance to treat RO concentrate by advanced treatment technologies to reduce the harmful effects on the environment.

Ozonation, one of the most used advanced oxidation processes (AOPs), has been confirmed having a great performance for the elimination of a large spectrum of organic chemicals (e.g., pharmaceuticals, pesticides, synthetic compounds) in WWTPs (Benner et al., 2008; Huber et al., 2005). As a further complement technology or a promising tertiary treatment alternative, therefore, it is widely and increasingly applied for the purification of water or the reclamation of wastewater (Domenjoud et al., 2015; Nebout et al., 2015). The potential efficacy of ozonation for organic micropollutants' removal is mainly ascribed to the combination of molecular ozone with selectivity and radical reactions generally involving hydroxyl radicals ($\cdot\text{OH}$) with non-selectivity (Beltrán, 2004; F et al., 1991; Prasse et al., 2012; Tizaoui and Grima, 2011). To the best of our knowledge, up to now, there are a few information on the ozonation efficiency of PhACs present in such as complicated matrix, such as municipal RO concentrate and source-separated urine.

In the last 10 years, many works regarding the wastewater treatment by membrane bioreactor (MBR), RO process, and ozonation have been done at INSA-LISBP, France. Jacob (2011) applied MBR, RO and nanofiltration (NF) process to treat municipal wastewater, where membrane fouling behavior and the fate of micropollutants and of microorganisms along the treatment line were studied. Li (2014) investigated the effects of carbamazepine micropollutant on MBR fouling, and the results demonstrated that the addition of carbamazepine in MBR increased MBR fouling. More recently, Vu (2017) reported the impacts of RO concentrate recirculation on the MBR performances in an MBR-RO system. In this thesis, the recirculation of RO concentrate to MBR in the MBR-RO system was proven to be a good alternative for the reduction of RO concentrate quantities. Merle (2009) and Crousier et al. (2016) applied ozonation process to eliminate recalcitrant organics from wastewater. Triger (2012) focused on a treatment line including struvite precipitation and ultrafiltration (UF) separation for the treatment and

valorization of urine. Based on these works, the present thesis investigates and evaluates the performance of the RO process, ozonation, or their combination for wastewater reuse including municipal MBR permeate and source-separated urine. The main objectives are:

- to examine the impacts of the continuous recirculation of RO concentrate to MBR on RO performance in an integrated MBR-RO system;
- to investigate the removal efficiencies of micropollutants by the RO process combining ozonation for municipal wastewater reuse.
- to test whether a process consisted of struvite precipitation, RO process and ozonation is available for urine treatment in terms of nutrients recovery and PhACs removal.

This thesis is conducted to address the following research questions:

- how does RO concentrate recirculation back to MBR affect the retention capacity of the RO membrane for common water quality parameters (organic matters, ions, etc.)?
- what are constituents responsible for the RO membrane flux decline during the RO concentrate recirculation to MBR?
- is RO process combining ozonation effective for the removal of trace PhACs from municipal MBR permeate?
- which constituent (ionic salts, ammonia and organic matters) is more pronounced in affecting the degradation level of PhACs and ozone consumption during the ozonation of complex matrices (real urine and RO concentrate)?

Figure 1 displays the structure of this thesis.

Chapter I provides an extensive and critical review of the literature on: (1) the occurrence of micropollutants in the municipal wastewater (2) the application of RO process for wastewater reuse including membrane fouling and the disposal of RO concentrate; (3) the ozonation of wastewater and the removal efficiency of micropollutants; and (4) the characteristics and treatment of source-separated urine;

Chapter II presents the Materials and Methods used to conduct this research.

Chapter III focuses on a combination of the RO and the ozonation process for municipal wastewater reuse. RO performance in an MBR-RO process with RO concentrate recirculation to MBR for municipal wastewater reclamation are first investigated in terms of RO membrane fouling and the rejection efficiency of common parameters for water quality. Moreover, the retention capacities of the RO membrane for trace PhACs are also examined. At last, ozonation process is followed to remove PhACs from RO concentrate produced during the RO treatment of MBR permeate, aiming to reduce the environmental impacts of RO concentrate.

Chapter IV evaluates the effect of water matrix (ionic salts, ammonia and organic matters) on the mechanisms and performance of ozonation for PhACs removal. The purpose is to better understand the ozonation behaviour of real urine.

Chapter V is a process study on the reclamation of source-separated urine with a combination process of struvite precipitation, RO and ozonation. In this combination process, struvite precipitation is used to recover P nutrients from urine; RO process allows to retain PhACs to a higher concentration; and the application of ozonation is to degrade PhACs present in the real urine solutions. In addition to the real urine, synthetic urine without organic matters is also investigated, aiming to provide more information on the treatment of wastewater with highly concentrated ions.

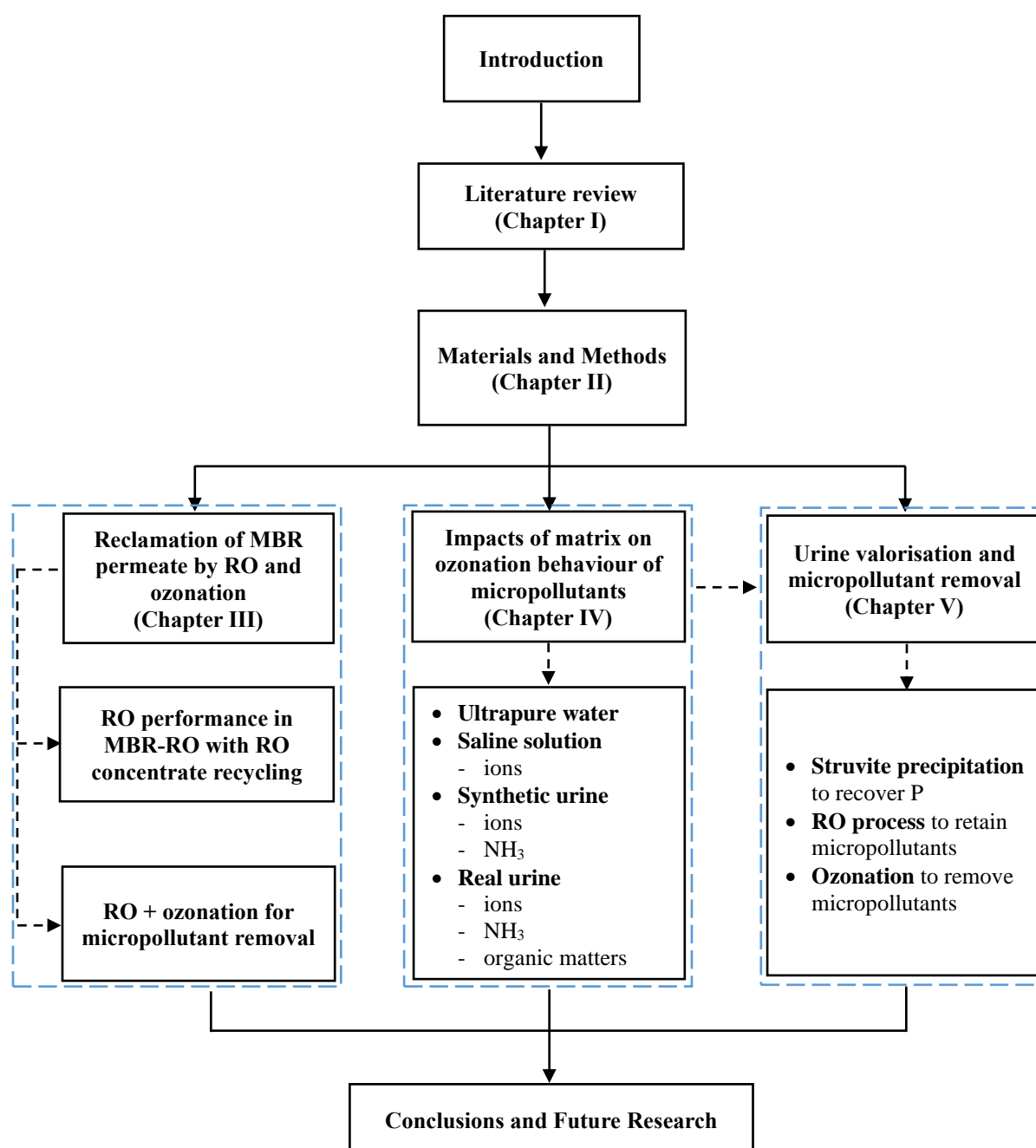


Figure 1 Structure of the present thesis

Chapter I Background and Literature Review

I.1 Pharmaceutically active compounds

I.1.1 General information on pharmaceutically active compounds

Pharmaceutically active compounds (PhACs), a group of chemicals including analgesics, anti-convulsants, anti-depressants, anti-inflammatories, hormones, antibiotics, etc., are used to maintain the healthy conditions of human and animals. Table 1.1 shows the most commonly prescribed drugs in the U.S. in 2016 (Provided by the ClinCalc DrugStats Database, available online: <https://clincalc.com/DrugStats/Top200Drugs.aspx>). A large number of PhACs from the different family group are consumed annually throughout the world. Figure 1.1 presents the number of prescription for two commonly used PhACs (diclofenac and propranolol) over time (2006 - 2016) in the U.S.. At present, pollution caused by human and veterinary pharmaceutical substances has become an emerging environmental problem, due to a health risk for humans and ecological system (Bendz et al., 2005; Nikolaou et al., 2007).

Table 1.1 Commonly prescribed drugs in the U.S. in 2016

Drug groups	Specific drug
Analgesic/ anti-inflammatory	Acetaminophen, Tramadol, Ibuprofen, Meloxicam, Cyclobenzaprine, Diclofenac, Prednisone
Anti-anxiety	Alprazolam, Buspirone, Temazepam, Oxazepam
Anti-anginal	Propranolol, Diltiazem, Isosorbide Mononitrate
Antibiotic	Amoxicillin, Azithromycin, Sulfamethoxazole, Trimethoprim, Ciprofloxacin
Anti-convulsant	Gabapentin, Clonazepam, Lorazepam, Pregabalin, Diazepam
Anti-depressant	Sertraline, Fluoxetine, Citalopram, Trazodone, Bupropion, Duloxetine
Anti-hypertensive	Lisinopril, Metoprolol, Atenolol, Furosemide, Carvedilol
Hormone	Estrogen Hormones

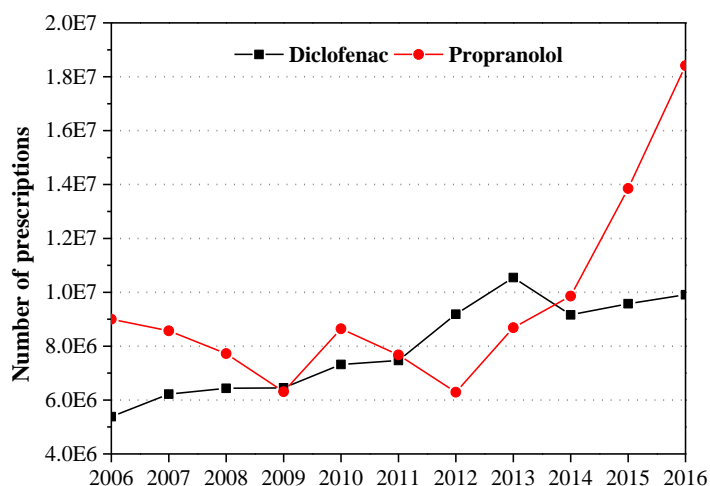


Figure 1.1 Number of diclofenac and propranolol prescriptions over time in the U.S. (2006 - 2016)

I.1.2 Occurrence of PhACs in surface water

A wide spectrum of PhACs and their metabolites have been detected frequently at a low concentration in soils, sediments, surface and groundwater, even in drinking water (Nikolaou et al., 2007; Silva et al., 2011). Table 1.2 shows the residual concentration of common PhACs in surface water based on the reported literature (Dai et al., 2015; Kasprzyk-Hordern et al., 2008; Kim et al., 2007; Silva et al., 2011). The concentration of these PhACs is mainly at the trace level in the ng L⁻¹ and µg L⁻¹ range.

Table 1.2 Residual concentration of common PhACs in surface water

ng L ⁻¹	Taff and Ely River, UK ^a	Ebro River basin, Spain ^b	Baiyun River, China ^c	South Korea ^d
Amoxicillin	<10 - 622	-	-	-
Atenolol	<1 - 560	<LOQ ² - 1237	-	-
Caffeine	- ¹	-	33.3 - 9785	2.9 - 194
Carbamazepine	<0.5 - 684	<LOQ - 53.8	n.d. ³ - 189	4.5 - 61
Diclofenac	<0.5 - 261	<LOQ - 148	7.8 - 170	1.1 - 6.8
Gabapentin	<0.6 - 1887	-	-	-
Ibuprofen	<0.3 - 100	<LOQ - 541	-	11 - 38
Ketoprofen	<0.5 - 14	<LOQ - 1060	n.d. - 509	-
Metoprolol	<0.5 - 12	<LOQ - 11.1	11.3 - 448	-
Naproxen	<0.3 - 146	<LOQ - 109	-	1.8 - 18
Paracetamol	<1.5 - 2382	-	-	-
Propranolol	<0.5 - 91	-	n.d. - 37.0	-
Sulfamethoxazole	<0.5 - 4	-	-	1.7 - 36
Trimethoprim	<0.5 - 183	<LOQ - 29.9	n.d. - 538	4.1 - 73

(a) The concentration from the lowest to the highest, from Kasprzyk-Hordern et al. (2008). (b) from Silva et al. (2011).

(c) from Dai et al. (2015). (d) from Kim et al. (2007).

(1) -: not analysed. (2) LOQ: limit of quantification. (3) n.d.: not detected

PhACs mainly enter the aquatic environment through: (1) the discharge of sewage treatment plant effluents; (2) the spreading of animal manure; and (3) aquaculture where PhACs are often dispensed with animal feed (EUROPEAN COMMISSION, 2019). Some studies have pointed out that a main source of PhACs in the environment is the discharge of WWTPs effluents. Because wastewater containing many emerging contaminants from houses, hospitals, manufacturing plants, farming and livestock impoundments, are received and assembled in the WWTPs (Bendz et al., 2005; Ganiyu et al., 2015; Kimura et al., 2005).

I.1.3 Occurrence of PhACs in sewage treatment plant effluents

Based on the recent studies, data on the occurrence of the most frequently detected emerging PhACs in the WWTPs influents and effluents are summarized in Table 1.3 (Ashfaq et al., 2017; Blair et al.,

2015; Guillosoou et al., 2019; Yu et al., 2013). From this table, it is possible to conclude that: (1) the concentration of trace PhACs in the WWTPs influents and effluents is highly variable, ranging from a few ng L^{-1} to $\mu\text{g L}^{-1}$. It is linked to some factors, such as metabolism (human and animal excretion), the size of WWTPs, elimination efficacy of WWTPs, etc. (Luo et al., 2014); and (2) treatment technologies in the WWTPs is not sufficient to remove or to degrade most of PhACs from wastewater.

Even though municipal sewer is one of the most important sources of the reclaimed water, the presence of these PhACs and their metabolites in the WWTPs effluents might limit the reclamation of wastewater, due to their potential hazards to the environment and human health even at low concentrations. Kołodziejska et al. (2013) have found that micropollutants can affect reproductive and endocrine system, and have a strongly adverse impact on algae and duckweed as well. Therefore, advanced treatment processes, such as reverse osmosis process (RO) and ozonation, should be established for a higher elimination of trace PhACs, the final aim being to improve water quality for safe reuse.

Table 1.3 Concentration of trace micropollutants in the WWTPs influents and effluents, and their removal efficiencies

Micropollutants	WWTP process	Influents (ng L ⁻¹)	Effluents (ng L ⁻¹)	Removal ¹ (%)	Reference
Atenolol	Physico-chemical lamellar settling + biofiltration	873 ± 142	288 ± 61	67 ± 6	Guillossou et al. (2019)
Caffeine	Screen + grit chamber + anaerobic-anoxic/oxic + settling tank + UV	2440 - 3160	9.82 - 55.6	-	Ashfaq et al. (2017)
	Grit channels + primary clarify + conventional activated sludge	11000	- ²	99	Blair et al. (2015)
Carbamazepine	Physico-chemical lamellar settling + biofiltration	410 ± 72	337 ± 76	19 ± 8	Guillossou et al. (2019)
	Screen + grit chamber + anaerobic-anoxic/oxic + settling tank + UV	1.62 - 3.08	4.58 - 6.34	-	Ashfaq et al. (2017)
	Grit channels + primary clarify + conventional activated sludge	220	-	92	Blair et al. (2015)
	Screen + settling tank + biological treatment	34 - 350	n.d. ³ - 81	-	Yu et al. (2013)
Diclofenac	Physico-chemical lamellar settling + biofiltration	687 ± 209	510 ± 128	24 ± 7	Guillossou et al. (2019)
	Screen + grit chamber + anaerobic-anoxic/oxic + settling tank + UV	4.04 - 26.0	5.68 - 31.6	-	Ashfaq et al. (2017)
	Screen + settling tank + biological treatment	86 - 580	n.d. - 120	-	Yu et al. (2013)
Ibuprofen	Physico-chemical lamellar settling + biofiltration	5597 ± 851	320 ± 213	95 ± 6	Guillossou et al. (2019)
	Screen + grit chamber + anaerobic-anoxic/oxic + settling tank + UV	75.6 - 262	7.66 - 35.8	-	Ashfaq et al. (2017)
	Grit channels + primary clarify + conventional activated sludge	4500	-	>99	Blair et al. (2015)
	Screen + settling tank + biological treatment	8600 - 56500	13 - 92	-	Yu et al. (2013)
Ketoprofen	Physico-chemical lamellar settling + biofiltration	1169 ± 121	240 ± 47	79 ± 4	Guillossou et al. (2019)
	Screen + grit chamber + anaerobic-anoxic/oxic + settling tank + UV	16.3 - 120	4.32 - 16.1	-	Ashfaq et al. (2017)
	Screen + settling tank + biological treatment	150 - 1300	n.d. - 65	-	Yu et al. (2013)
Naproxen	Physico-chemical lamellar settling + biofiltration	2302 ± 450	205 ± 111	91 ± 6	Guillossou et al. (2019)
	Screen + grit chamber + anaerobic-anoxic/oxic + settling tank + UV	1.58 - 10.2	0.64 - 1.95	-	Ashfaq et al. (2017)
	Grit channels + primary clarify + conventional activated sludge	3000	-	96	Blair et al. (2015)
	Screen + settling tank + biological treatment	9300 - 210000	n.d. - 150	-	Yu et al. (2013)

Micropollutants	WWTP process	Influents (ng L ⁻¹)	Effluents (ng L ⁻¹)	Removal ¹ (%)	Reference
Ofloxacin	Physico-chemical lamellar settling +biofiltration	429 ± 28	333 ± 101	21 ± 28	Guillossou et al. (2019)
	Screen + grit chamber + anaerobic-anoxic/oxic + settling tank + UV	320 - 616	103-162	-	Ashfaq et al. (2017)
	Grit channels + primary clarify+ conventional activated sludge	2100	-	-124	Blair et al. (2015)
Oxazepam	Physico-chemical lamellar settling +biofiltration	1089 ± 226	844 ± 215	23 ± 10	Guillossou et al. (2019)
Propranolol	Physico-chemical lamellar settling +biofiltration	-	181 ± 45	-	Guillossou et al. (2019)
	Screen + grit chamber + anaerobic-anoxic/oxic + settling tank + UV	n.d. - 56.6	n.d.	-	Ashfaq et al. (2017)
Sulfamethoxazole	Physico-chemical lamellar settling +biofiltration	1057 ± 432	1312 ± 629	-29 ± 53	Guillossou et al. (2019)
	Screen + grit chamber + anaerobic-anoxic/oxic + settling tank + UV	30 - 62.2	7.50-37.5	-	Ashfaq et al. (2017)
	Grit channels + primary clarifies+ conventional activated sludge	7400	-	-36	Blair et al. (2015)

(1) Removal (%) is calculated based on the concentration of micropollutants in the WWTPs influents and effluents. (2) -: not analysed. (3) n.d.: not detected.

I.2 Reverse osmosis process for wastewater reclamation

I.2.1 General information on reverse osmosis process

RO, a membrane technology, is widely applied in seawater desalination, drinking water production, brackish water treatment and wastewater reclamation, due to high water permeability and salt rejection (Greenlee et al., 2009; Malaeb and Ayoub, 2011). Over the past decades, RO process has gained worldwide acceptance for the reclamation of municipal wastewater due to its high efficiency in rejecting a wide range of organic pollutants, bacteria, dissolved organic matters and inorganic salts (Jacob et al., 2012; Malaeb and Ayoub, 2011; Xu et al., 2005). Figure 1.2 displays three main rejection mechanisms of RO for solutes in wastewater, including size exclusion (steric hindrance effect), charge exclusion, hydrophobic interactions between solutes, solvent and membrane (Bellona et al., 2004; Dolar et al., 2012; Ganiyu et al., 2015; Jacob et al., 2012; Malaeb and Ayoub, 2011).

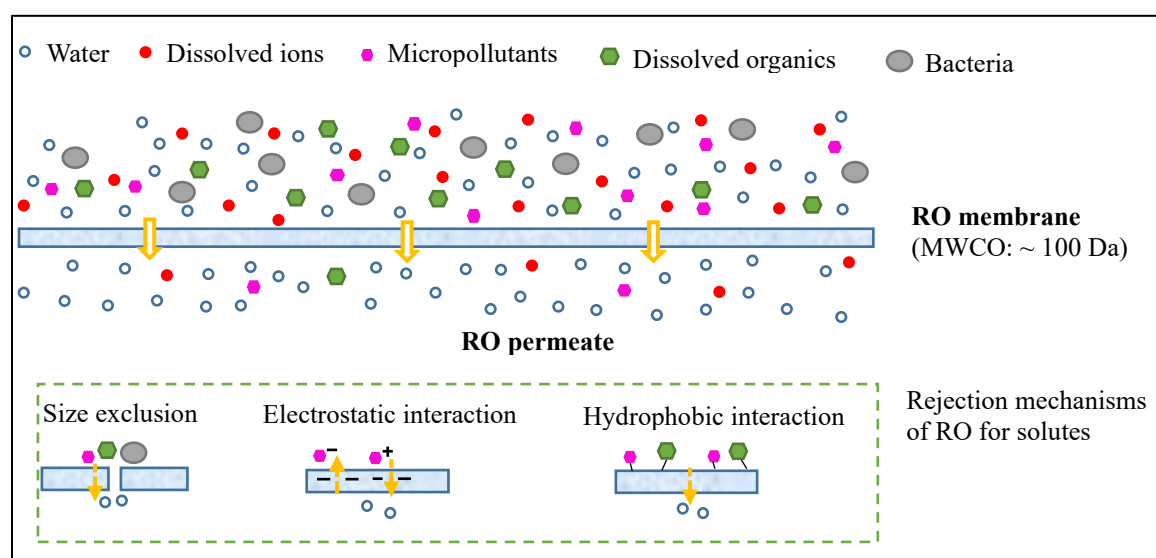


Figure 1.2 Schema of RO process and the rejection mechanism for solutes

I.2.2 Rejection capacity of reverse osmosis membrane for micropollutants

Studies with respect to the application of RO process to remove micropollutants from municipal wastewater have been published frequently in recent years (Alturki et al., 2010; Dolar et al., 2012; Jacob et al., 2012; Mamo et al., 2018). Based on the literature published, Table 1.4 summarizes the removal efficiencies of RO membrane for micropollutants in wastewater, surface water and groundwater.

It is observed that RO process exhibits a relatively high removal rate for micropollutants present in wastewater, with a removal higher than 90% for most of micropollutants. The higher rejection of micropollutants by RO membrane could be achieved by one or a combination of three basic mechanisms as mentioned above (Ganiyu et al., 2015; Radjenović et al., 2008). The rejection of uncharged micropollutants (such as carbamazepine) by RO membrane is predominantly affected by size exclusion, whereas electrostatic attraction or repulsion force could influence the removal of micropollutants with charge (like diclofenac) by RO membrane (Dolar et al., 2012; Kimura et al., 2005; Radjenović et al.,

2008). In addition, hydrophobic adsorption at the membrane-solute interface is a non-neglected role (Mamo et al., 2018). In contrast, the adsorption of hydrophilic micropollutants (such as sulfamethoxazole) to RO membrane is not significant (Alturki et al., 2010).

Table 1.4 Removal (%) of micropollutants from water by RO process

Reference	Mamo et al. (2018) ¹	Dolar et al. (2012) ²	Alturki et al. (2010) ²	Comerton et al. (2008) ²		Radjenović et al. (2008) ²
	MBR permeate	MBR permeate	MBR permeate	MBR permeate	Surface water	Groundwater
RO membrane	ESPA2	TR70-4021-HF	BW30, ESPA2	X20	X20	BW30LE-440
Atenolol	- ³	>99	>95	-	-	-
Acetaminophen	>99	-	-	99.7	82.1	85.6
Caffeine	-	-	>95	97.0	86.5	-
Carbamazepine	>99	>99	>95	97.0	91.0	98.5
Diazepam	>99	>99	-	-	-	-
Diclofenac	>99	-	>90	-	-	99.9
Gemfibrozil	-	-	>95	98.5	97.7	49.9
Ibuprofen	-	-	>95	-	-	-
Ketoprofen	-	-	>95	-	-	98.1
Metoprolol	>99	>99	-	-	-	-
Ofloxacin	-	>99	-	-	-	-
Propranolol	-	>99	-	-	-	-
Sulfamethoxazole	>99	>99	>95	98.8	94.1	99.9

(1) removal (%) is calculated based on the concentration of micropollutants in RO permeate and at the membrane surface.

(2) removal (%) is calculated based on the concentration of micropollutants in RO permeate and RO feed. (3) -: not analysed.

During the RO filtration process, the rejection rate for micropollutants is affected by membrane properties (pores size, charge), the chemistry of feed stream (pH, ionic strength, organic matters), physicochemical properties of constituents (molecular weight, pK_a , charge, and hydrophobic nature), and RO operating conditions (Joo and Tansel, 2015; Mamo et al., 2018; Taheran et al., 2016).

1.2.3 RO membrane fouling

RO membrane fouling is still an inevitable issue as it limits the competitiveness of RO process (Jiang et al., 2017). Membrane fouling is a process resulting in loss of performance of a membrane due to the deposition of suspended or dissolved substances on its external surfaces, at its pore openings, or within its pores (Koros et al., 1996). Membrane fouling is also described as a reduction of permeate flux and of salt rejection because of the accumulation of undesired substances on the membrane surface or inside the membrane pores (Jiang et al., 2017; Malaeb and Ayoub, 2011). RO membrane fouling could

reduce water production and the quality of permeate. Moreover, the operating cost increases, which is due to increased energy demand, application of pre-treatment unit, frequent chemical cleaning, shorter membrane lifetime, as well as additional labour for maintenance (Guo et al., 2012; Jiang et al., 2017). Several authors have provided a comprehensive review regarding the major foulants, principal RO membrane fouling mechanisms, and strategies for control RO membrane fouling (Guo et al., 2012; Jiang et al., 2017; Malaeb and Ayoub, 2011; She et al., 2016).

I.2.3.1 Membrane foulants and fouling type

Table 1.5 lists the fouling types of RO membrane.

Table 1.5 Fouling types of RO membrane

Fouling places	Foulant type	Attachment strength of solutes
External (surface) fouling	Colloidal fouling	Reversible fouling
Internal fouling	Inorganic fouling	Irreversible fouling
-	Organic fouling	-
-	Biofouling	-

In terms of fouling places, fouling can be classified into external (surface) fouling and internal fouling (Jiang et al., 2017; She et al., 2016). For RO membrane with nonporous nature, external fouling is more frequent compared to internal fouling (Greenlee et al., 2009). Increasing feed water hydrodynamic conditions or chemical cleaning could control external fouling (She et al., 2016). However, in some cases, both external fouling and internal fouling are irreversible, which depends on the compositions of feed water and the interactions between solutes and membrane (Jiang et al., 2017).

In terms of foulants, RO membrane fouling can be categorized into colloidal fouling, inorganic scaling, organic fouling and biofouling (Jiang et al., 2017), as depicted in Figure 1.3. Colloidal/particulate fouling refers to fouling caused by colloids (fine suspended particles) that have a size range from a few nm to a few μm (Schäfer, 2006). Colloids are ubiquitous in the natural water and wastewater, including inorganic compounds (silica, clays, metal oxides and salt precipitates), and organic macromolecules such as polysaccharides, proteins and some natural organic matters (Jiang et al., 2017; Schäfer, 2006). Inorganic scaling, also scale formation or precipitation scaling, is the depositions of inorganic precipitates on the membrane surface or inside the membrane pores (Jiang et al., 2017). As the solubility of some inorganic salts is relatively low or the concentration of some ionic species in the water or wastewater is relatively high, when an ionic product of a sparingly soluble salt exceeds its equilibrium solubility product, the relevant precipitate is formed and then deposits on the membrane surface, resulting in an increase in transmembrane pressure or a decline in permeate flux (Guo et al., 2012; Jiang et al., 2017; Schäfer, 2006). Studies published in the past 10 years shows that calcium sulphate (42%) and calcium carbonate (38%) are two common studied inorganic scalants, and other common scalants include calcium phosphate, barium sulphate, calcium fluoride, etc. (Jiang et al.,

2017). Organic fouling is caused by organic matters (humic substances, polysaccharides, proteins, lipids, nucleic acids and amino acids, etc.) (Jiang et al., 2017). In the case of wastewater treatment, effluents organic matters (EfOM, such as humic substances and polysaccharides) could result in membrane fouling by adsorption, surface accumulation or pore blocking (Malaeb and Ayoub, 2011). Biofouling is a process of the accumulation of microorganism on the membrane surface, including deposition, growth and metabolism of bacteria (Guo et al., 2012).

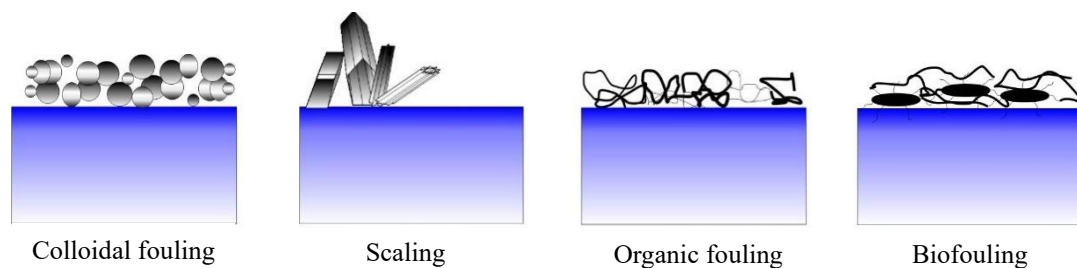


Figure 1.3 Four different fouling in terms of foulants. From Tiraferri (2014) <http://www.colloid.ch/membranes>

Membrane fouling is also classified into reversible fouling and irreversible fouling based on the attachment strength of solutes to the membrane surface. Some studies state that reversible fouling results from concentration polarization and particle deposit, which is removed by physical means, including relaxation and periodic backwashing (Choi et al., 2005; Huyskens et al., 2008). Irreversible fouling is mainly referred to a strong adherence to the membrane such as adsorption, pore plugging and solute gelation on the membrane (Schäfer, 2006), which is not removed with mechanical means but can be by chemical cleaning, or not at all.

1.2.3.2 RO membrane fouling mechanisms

As well known, permeate flux membrane lifetime are primarily influenced by concentration polarization and membrane fouling (Sablani et al., 2001). Surface adsorption, pore blocking, inorganic precipitation, gel or cake formation, biological fouling are the main mechanism for membrane fouling (H. Li et al., 2016; Schäfer, 2006). Actually, RO membrane fouling is complicated and caused by complex interactions between fouling constituents and the membrane, and which constituents govern for RO membrane fouling depends on the properties of RO membrane (surface morphology, hydrophobicity, charge and MWCO), the matrix of RO feed (pH, ionic strength, etc.), and RO operating conditions (water recovery, cross-flow velocity, temperature, etc.) (Guo et al., 2012; Jiang et al., 2017).

1.3.3.2.1 Concentration polarization / osmotic pressure

Concentration polarization (CP) is a phenomenon that the concentration of solutes or particles (salts and organic matters) near the membrane surface is higher compared to the bulk solution (Figure 1.4), due to the accumulation of solutes/particles at the membrane surface (Guo et al., 2012; She et al., 2016). Retained solutes/particles are brought into the bulk solution by back diffusion. The elevated concentration of inorganic and organic substances at the membrane surface leads to an increase in osmotic pressure, decreasing the effective transmembrane pressure and further reducing the permeate

flux. The osmotic pressure of solutes on the side of RO concentrate and RO permeate can be determined by using Van't Hoff equation and the measured solute concentration on each side (Schäfer, 2006).

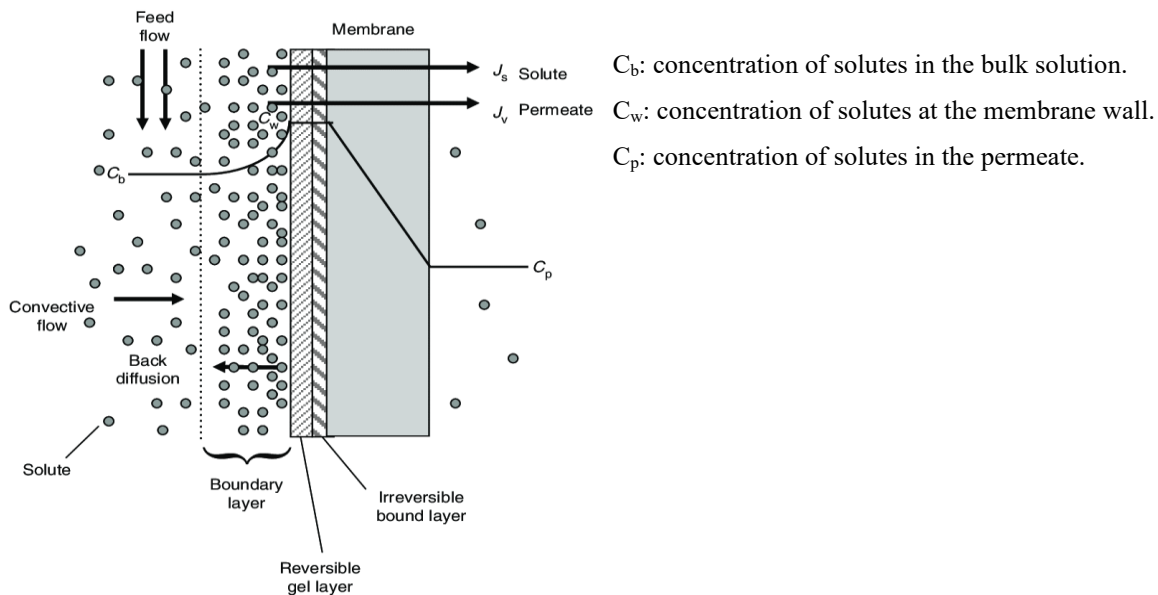


Figure 1.4 Schema of concentration polarization and membrane fouling. From Pabby (2015)

During the initial period of RO process, CP is a primary reason for a decline in permeate flux due to an increased osmotic pressure at the membrane surface (Sablani et al., 2001). In addition, higher solute concentration at the membrane surface might increase the tendency of RO membrane fouling due to inorganic scaling, adsorption of solute, and a gel or cake layer formation (Guo et al., 2012; Schäfer, 2006; She et al., 2016), possibly causing an additional loss in permeate flux. Therefore, CP is thought as a fouling precursor. CP is often considered to be reversible and can be minimized with turbulence promoters on the side of the membrane (spacer or velocity adjustment) (Sablani et al., 2001; Schäfer, 2006).

I.3.3.2.2 Adsorption of organic matters

Adsorption, a specific interaction between organics and membrane, may take place on the membrane surface or inside pores. Organic fouling is quite often irreversible with respect to adsorption (H. Li et al., 2016; Sablani et al., 2001). A previous study reports that the solute adsorption is reversible, but which could transit to irreversible fouling (Nikolova and Islam, 1998). Quartz crystal microbalance, thermogravimetric method, and Fourier transform infrared spectrometry are used to determine adsorption of organics on the membrane surface (H. Li et al., 2016).

I.3.3.2.3 Gel/cake layer

The formation of a gel/cake layer is due to the deposition of organic matters or colloids on the membrane surface (Jiang et al., 2017; Schäfer, 2006). Once the concentration of solutes reaches a limit value, a gel layer starts to form, and then develops until a critical flux reaches (H. Li et al., 2016). Figure 1.5 describes the transition of CP to gel/cake layer formation. The presence of gel/cake layer

increases the effective membrane thickness, resulting in an additional hydraulic resistance so that membrane permeation reduces (Jiang et al., 2017; Sablani et al., 2001).

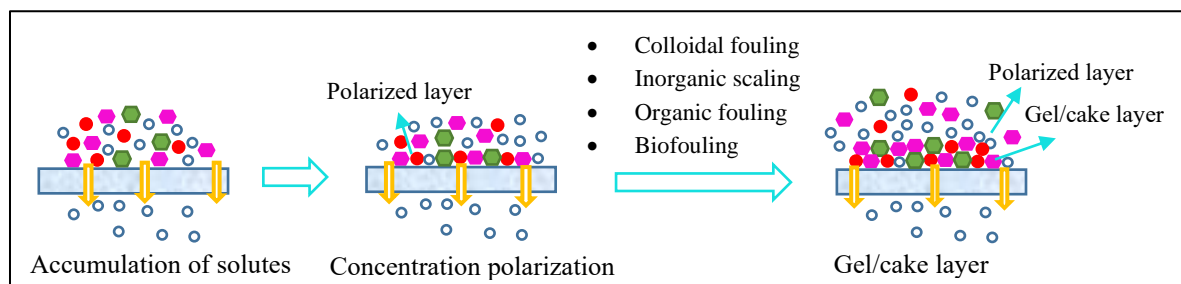


Figure 1.5 Schema of RO membrane fouling mechanism

I.2.3.3 Fouling behaviour of RO membrane for municipal wastewater reuse

Table 1.6 summarizes the major findings of studies regarding the fouling behaviour of RO membrane during municipal wastewater reuse. It is clearly seen that, RO membrane fouling mechanism is complicated due to the complex nature of municipal wastewater and the complex interactions of foulants and RO membrane. Organic matters, including microbial-derived organic matters, humic-like organics, polysaccharide, etc., are major constituents to lead to RO membrane fouling. Soluble microbial products (SMPs) present in MBR permeate is found to play an important role in the fouling behaviour of the RO membrane, and the presence of silica and calcium in combination of organic matter could accelerate RO permeate flux decline due to their interaction at the RO membrane surface (Kimura et al., 2016; Lee et al., 2006). A recent study observes that RO permeate flux reduction is synergistically enhanced in the coexistence of organics and silica in the RO feed (Quay et al., 2018). In addition, inorganic salts in the MBR effluents also cause the severe RO membrane fouling in an MBR-RO system for real domestic wastewater reuse (W. Luo et al., 2017; Moreno et al., 2013). RO membranes fouling is prone to occur in different forms (inorganic scaling, organic fouling, biofilm and colloidal fouling), and which constituents (inorganic ions, organic matters, or both) govern for RO membrane fouling depends on the properties of RO membrane, MBR operating conditions, the matrix of MBR permeate, and RO operating conditions (Jiang et al., 2017).

The studies obtained from Farias et al. (2014) and Wu et al. (2013) report that RO membrane fouling behaviour is affected significantly by solid retention time (SRT) and the food to microorganism ratio (F/M) in MBR. Increasing the SRT and the F/M can increase fouling propensity of RO membrane in an MBR-RO system for municipal wastewater treatment. Indeed, the characteristics (size, hydrophobicity, etc.) of organic matters (soluble polysaccharides and transparent exopolymer particles) in MBR permeate strongly depend on the design and operation of the MBR system, and the quality of the effluents from the MBR process is mainly associated with the fouling development of RO membrane in an MBR-RO system for municipal wastewater reuse.

Table 1.6 Summary of the fouling studies of RO membrane for municipal wastewater reuse

Operating conditions	Fouling analysis	Main finding	Reference
Organic matters and inorganic ions are responsible for RO membrane fouling			
Dead-end mode. Operating pressure: 8 bar. Volume reduction factor (VRF) ¹ : from 1 to 4.	<ul style="list-style-type: none"> • Flux decline • SEM ² • Water rinse of the membrane after RO experiments 	<ul style="list-style-type: none"> • For MBR permeate with a low concentration of organic matters and conductivity, a lower flux decline is observed, which is due to a rise of the osmotic pressure. • For MBR permeate with a high level of organic matters and conductivity, a more significant flux decline is observed, which is due to a rise of the osmotic pressure and a cake layer formation. • Transmembrane pressure (range: 6 - 12 bar) has no significant influences on RO performance in terms of flux decline. • The fouling is reversible 	Jacob et al. (2010)
A full-scale plant. Fouled membrane deposit analysis. Desorb deposit with HCl, NaOH and ultrapure water.	<ul style="list-style-type: none"> • Inductively coupled plasma mass spectrometry. • FTIR ³ • Resin fraction of DOM ⁴ 	<ul style="list-style-type: none"> • Organic matters (occupied 75% (dry weight) of the deposit) are a major problem for RO membrane. • The deposit comprises of microbial-derived organic matters and humic-like organics. • Hydrophobic acids and hydrophilic neutrals organics are the largest fractions in deposit. • Inorganic scaling of the RO membrane is mainly due to the presence of element Fe, Ca and Si. 	Tang et al. (2014)
Cross-flow velocity: 41.7 cm s ⁻¹ . No membrane cleaning.	<ul style="list-style-type: none"> • Permeability reduction • Fouled membrane autopsy (SEM-EDS and FTIR) 	<ul style="list-style-type: none"> • Content of organic matters (humic- and protein-like substances) and of inorganic salts in the MBR permeate relates to a severe RO membrane fouling. • RO membrane fouling is a result of compact and homogenous cake layer formation on the RO membrane surface, which comprises of C, O, Mg, Ca, and P. • Humic- and protein-like substances in the MBR permeate are likely responsible for the severe organic fouling of the RO membrane. 	W. Luo et al. (2017)
A full-scale plant	<ul style="list-style-type: none"> • Flux decline • Analysis of fouled RO membrane 	<ul style="list-style-type: none"> • Different bacterial species and their extracellular polymeric substances (EPS) exhibits a strong impact on RO membrane fouling. • EPS with a MW over 10 kDa are major constituents responsible for RO membrane fouling. 	Yu et al. (2018)

Operating conditions	Fouling analysis	Main finding	Reference
Effect of MBR operating conditions on RO membrane fouling potential			
<p>A pilot-scale.</p> <p>SRT⁵ in MBR: 2, 10, and 20 days.</p> <p>HRT⁶ in MBR: 8 h.</p> <p>Cross-flow velocity for RO : 0.15 m s⁻¹.</p> <p>Water recovery⁷: 75%.</p>	Flux decline	<ul style="list-style-type: none"> • Membrane fouling in MBR increases as the SRT decreases • Membrane fouling in RO increases as the SRT increases. • A 10-day SRT is the best for minimizing fouling of the membrane in both MBR and RO. • The increase in RO membrane fouling with increasing SRT cannot be related to water quality of MBR permeate such as DOC, proteins, or carbohydrate. 	Farias et al. (2014)
<p>Synthetic wastewater.</p> <p>Ratio of food to microorganisms in MBR (F/M): ~0.17 and ~ 0.50 g COD/gMLSS day.</p> <p>Cross-flow velocity in RO: 0.1 m s⁻¹.</p>	<ul style="list-style-type: none"> • Analysis of (transmembrane pressure – osmotic pressure). • Characteristics of the fouled RO membrane 	<ul style="list-style-type: none"> • MBR permeate quality affects the development of RO membrane fouling. • MBR permeate produced at a high F/M leads to a higher RO membrane fouling propensity. • Soluble polysaccharides and transparent exopolymer particles on the RO membrane surface relate to RO membrane fouling. • Humic acid-like and microbial by-product-like substances are predominant in RO foulants. • Optimization of MBR operation is a solution to reduce RO membrane fouling. 	Wu et al. (2013)

(1) VRF: RO feed volume/RO retentate volume. (2) SEM: scanning electronic microscopy. (3) FTIR: Fourier transform infrared spectrometer. (4) DOM: dissolved organic matters. (5) SRT: solid retention time. (6) HRT: hydraulic retention time. (7) Ratio of RO permeate flow to RO feed flow

I.2.4 Characteristics and disposal of RO concentrate

RO concentrate contains high levels of inorganic salts, organic substance and trace micropollutants, which may associate to the potential toxicity to receiving bodies. Therefore, it is of great importance to address and to treat RO concentrate.

I.2.4.1 Characteristics of RO concentrate

The main characteristics of municipal RO concentrate reported in various studies are summarized in Table 1.7. From this table, pH value of the RO retentate is in the range of 6.9 - 8.8. There is a large variation in conductivity in RO concentrate, from 2.6 Ms cm⁻¹ to 23.5 Ms cm⁻¹, which is linked with the quality of RO feed, operating condition, etc.. RO concentrate is characterized by a high concentration of inorganic ions, especially for Na⁺, K⁺, Mg²⁺, Ca²⁺, Cl⁻, NO₃⁻ and SO₄²⁻. As compared to other studies, RO concentrate from the findings of Pradhan et al. (2015) and Umar et al. (2016a) show higher values of conductivity and Cl⁻ concentration, which is explained by the infiltration of salty groundwater into the sewer system, further leading to the increase in salinity of RO feedwater.

RO concentrate also contains a high load of organic matters in terms of total organic carbon (TOC) or dissolved organic carbon (DOC). As exhibited in Table 1.7, the concentration of TOC or DOC ranges from 18 mg L⁻¹ to 36 mg L⁻¹. On the other hand, the raw RO concentrate has a relatively low biodegradability, with 13% biodegradable dissolved organic carbon (BDOC) (Liu et al., 2012) and 0.03 BOD₅/COD (Justo et al., 2013), which indicates a high bio-recalcitrant organic matters content.

Table 1.7 Main characteristics of RO concentrate from municipal wastewater treatment

Parameter	Unit	Ref. a	Ref. b	Ref. c	Ref. d	Ref. e	Ref. f	Ref. g	Ref. h
Recovery ¹	%	-	65	-	75	-	-	-	-
pH	-	8.3	8.8	6.9	7.7	7.8	7.4	7.82	7.4 - 7.6
TOC ²	mg L ⁻¹	27.6	-	-	-	18 - 36	-	-	-
DOC ³	mg L ⁻¹	- ⁶	22	23.7	36	-	32	-	20 - 30
COD ⁴	mg L ⁻¹	77	-	61.5	120	-	101	162	-
Conductivity	mS cm ⁻¹	6.0	3.8	7.3	23.5	2.6 - 3.6	23	4.7	2.5 - 3.5
Alkalinity as CaCO ₃	mg L ⁻¹	914	242	308	-	380	710	-	-
TDS ⁵	mg L ⁻¹	-	-	-	16600	-	16587	2684	-
Colour (Pt-Co)	mg L ⁻¹	-	55	-	148	-	157	-	-
Na ⁺	mg L ⁻¹	1065	600	1637	-	376 - 563	-	610	373 - 540
K ⁺	mg L ⁻¹	135	-	90.9	-	48 - 75	-	96	64 - 120
N-NH ₄ ⁺	mg L ⁻¹	2.5	-	29.8	-	-	-	-	-
Mg ²⁺	mg L ⁻¹	145	53	236	-	63 - 84	-	91	45 - 80
Ca ²⁺	mg L ⁻¹	477	47	469	-	73 - 108	-	300	95 - 200
Cl ⁻	mg L ⁻¹	1540	954	1627	7700	478 - 819	8520	601	600 - 900
NO ₃ ⁻	mg L ⁻¹	83.7	-	15.9	-	24 - 75	-	219	97 - 177
SO ₄ ²⁻	mg L ⁻¹	569	207	1200	-	153 - 294	-	361	540 - 900
P-PO ₄ ³⁻	mg L ⁻¹	1.29	8	5.1	28.5	6.9	-	-	9-15

(a) Conventional activated sludge effluents → pre-treatment (coagulation, lamellar setting, disinfection) → UF → RO (Justo et al., 2013). (b) Biological treated effluents from municipal WWTPs → RO (Hurwitz et al., 2014). (c) Municipal RO brines (Justo et al., 2015). (d) Biological treated effluent from municipal WWTPs → UF → RO (Pradhan et al., 2015). (e) From water reclamation plant (Jamil et al., 2016). (f) Effluent of municipal WWTPs → UF → RO (Umar et al., 2016a). (g) Municipal WWTP → RO (H. Luo et al., 2017). (h) Biologically treated effluents → MF → RO (Shanmuganathan et al., 2017).

(1) Recovery (%): the volume ratio of RO permeate to RO feed, or the flow rate ratio of RO permeate to RO feed. (2) TOC: total organic carbon. (3) DOC: dissolved organic carbon. (4) COD: chemical oxygen demand. (5) TDS: total dissolved solids. (6) -: not analysed.

1.2.4.2 Occurrence of PhACs in RO concentrate

The occurrence of PhACs in RO concentrate is reviewed through this study, as summarized in Table 1.8. As can be clearly seen that, the concentration of PhACs in RO concentrate from different researches is in the range of ng L⁻¹ to high µg L⁻¹. Among these micropollutants, atenolol, carbamazepine, caffeine, diclofenac, gemfibrozil, naproxen, and sulfamethoxazole are detected frequently in RO concentrate based on the literature reported. The significant difference in the quantity of PhACs can be attributed to PhACs content in wastewater, the characteristics of a membrane used, organic chemicals structure, and RO operating conditions (Joo and Tansel, 2015; Xu et al., 2005). Moreover, the concentrations of the majority of retained contaminants are found to be several times larger in the retentate than in the feed water, even dozen times (Acero et al., 2016; Benner et al., 2008; Pérez-González et al., 2012; Solley et al., 2010; Urriaga et al., 2013).

Table 1.8 Concentrations of micropollutants in RO concentrate

PhACs ($\mu\text{g L}^{-1}$)	Ref. a	Ref. b	Ref. c		Ref. d	Ref. e	Ref. f	Ref. g
Recovery % ¹	-	-	50%	70%	-	-	80%	-
Atenolol	2.9±0.3	2.634	1.452	2.779	1.028	0.361	-	0.466
Carbamazepine	3.4±0.2	0.134	-	-	1.038	0.098	0.474	2.240
Caffeine	- ²	0.708	33.939	50.000	-	-	0.164	1.410
Diazepam	-	-	-	-	-	0.135	-	-
Diclofenac	1.5±0.1	-	-	-	0.605	0.283	0.142	0.337
Gemfibrozil	-	6.979	5.921	9.868	-	3.443	-	0.344
Ketoprofen	-	-	-	-	-	0.628	-	0.377
Ibuprofen	1.33±0.07	-	10.416	21.250	-	-	-	-
Metoprolol	0.88±0.03	0.470	-	-	-	-	-	-
Naproxen	0.98±0.06	1.416	4.161	9.223	1.080	0.254	0.034	0.443
Ofloxacin	-	0.299	-	2.575	-	-	-	-
Propranolol	1.05±0.02	-	-	-	-	-	-	-
Sulfamethoxazole	1.19±0.05	0.437	-	-	1.638	0.026	0.737	0.144

(a) WWTPs effluents → UF → RO (Benner et al., 2008). (b) 20% trickling water + 80% activated sludge effluents → MF → RO (Abdelmelek et al., 2011). (c) WWTP effluents → UF → RO (Urtiaga et al., 2013). (d) WWTP effluents → coagulation → lamellar setting → UF → RO (Justo et al., 2013). (e) Municipal RO brines (Justo et al., 2015). (f) Water reclamation plant (Jamil et al., 2016). (g) Biologically treated effluents → MF → RO (Shanmuganathan et al., 2017).

(1) Recovery (%): the volume ratio of RO permeate to RO feed, or the flow rate ratio of RO permeate to RO feed. (2) -: not analysed.

Due to containing high levels of inorganic and organic compounds, the direct discharge of RO concentrate might pose potential ecotoxicity risk on receiving water body. By employing the Microtox[®] assay, studies have demonstrated that no apparent toxicity of the raw RO concentrate is noticed for the luminescent marine bacterium *Vibrio fischeri* (Justo et al., 2013; Liu et al., 2012; Lu et al., 2013; Umar et al., 2016b). However, an opposite conclusion is reported by T. Zhou et al. (2011) that raw RO concentrate appears to be toxic, with 62% inhibition for *Vibrio fischeri*. A similar study from Miralles-Cuevas et al. (2017) has found 30.4% inhibition for *V. fischeri* and 100% immobilization for *D. magna* in untreated NF concentrate obtained at a recovery of 80%. This difference in toxicity response is likely to be linked to different characteristics of RO concentrate, the concentration of hazardous substances present in RO concentrate, and the organism used. Overall, it is of importance to establish innovative and cost-effective technologies for RO concentrate management, aiming to enhance the recovery of reclaimed water and to reduce the contents of contaminants entering to the environment.

I.2.4.3 Recirculation of RO concentrate into the biological unit

A possible strategy is proposed to recirculate RO concentrate to a biological system, like MBR. The prolonged biological contact time by RO concentrate recycling might improve biodegradation rate of

some recalcitrants. It should be pointed out that, nonetheless, the recirculation of non-biodegradable organic substances and inorganic species could change the compositions of MBR permeate, which may directly or indirectly accelerate RO membrane fouling. To date, information regarding the recirculation of municipal RO concentrate to MBR is relatively scarce. Several works report the impact of nanofiltration (NF) concentrate to a biological unit on NF performance for wastewater treatment (Kappel et al., 2014; K. Li et al., 2016; Rautenbach and Mellis, 1994; Wang et al., 2015, 2014). Table 1.9 presents the main findings on the NF or RO concentrate recycling to a biological unit.

In an early study, a conventional biological unit combining nanofiltration (NF) process is used to treat dumpsite leachate (Rautenbach and Mellis, 1994). In order to improve the biodegradation of recalcitrant organics through increasing the residence time, recalcitrants rejected in NF concentrate are recycled back to the biological system. The results show that the removal rate of COD (as an indicator to evaluate process efficiency) is increased by 9-17% with NF concentrate recycling.

Kappel et al. (2014) investigate the performance of MBR combining NF process for municipal wastewater treatment with the recirculation of NF concentrate. The combination of MBR and NF unit with NF concentrate recycling is successful in continuously producing reusable water with a relatively low concentration of inorganic/organic compounds. NF membrane fouling behaviour is mainly attributed to precipitation of calcium phosphate, whereas organics like humic acids have not a significant effect on NF fouling. For MBR process, after NF concentrate recirculation, an increased fouling potential is observed and more frequent membrane cleaning is required.

Li et al. (2016) and Wang et al. (2015, 2014) investigate performance of an MBR-NF process for treating antibiotic production wastewater with NF concentrates recirculation into MBR unit. Their results demonstrate that this MBR-NF is effective in producing reusable water with excellent NF permeate quality. It should be noticed that, nonetheless, salinity brought by NF concentrate is a key factor in influencing activity of sludge. Salinity and soluble microbial products (SMPs) brought by NF concentrate recycling are major constituents responsible for fouling of MF membrane in MBR. NF membrane fouling is related to the presence of fulvic acid-like and humic acid-like substances in NF concentrate.

At present, only Joss et al. (2011) and Vu et al. (2017) study RO concentrate recycling to MBR in an MBR-RO system. However, the main focus of Joss et al. (2011) is on the removal efficiency of micropollutants by using this combination. Information on the impacts of organics and inorganic ions brought by RO concentrate on the fouling propensity of the RO membrane is still scarce. The purpose of Vu et al. (2017) is to investigate MBR performance for municipal wastewater treatment in a MBR-RO system with RO concentrate recycling. The results show that the sludge activity and the removal efficiency of global parameter (COD, DOC, etc.,) for water quality are not influenced significantly by RO concentrate recycling. In order to better and comprehensively understand the performance of this combination process with RO concentrate recycling, more works regarding RO performance in this integrated system need to be extended.

Table 1.9 Impacts of NF or RO concentrate recycling to a biological unit on NF or RO performance

Wastewater	Operating conditions	Main Findings	Reference
Dumpsite leachate → activated sludge bioreactor → NF → NF concentrate → activated sludge bioreactor →	-	During the NF concentrate recirculation to the biological unit, the elimination rate of COD is increased by 9 - 17%.	Rautenbach and Mellis (1994)
Municipal wastewater → MBR → NF → NF concentrate → MBR →	Flux of MF membrane in MBR: 6.4 - 7.5 L m ⁻² h ⁻¹ . SRT ¹ in MBR: 16 days. HRT ² in MBR: 4.7 h. NF permeate recovery: 85%. Operating pressure in NF: 11 bar. NF concentrate makes up 15% of the total inflow of MBR.	<ul style="list-style-type: none"> NF concentrate recirculation does not affect the quality of NF permeate. NF membrane fouling is mainly due to inorganics (divalent cations) with NF concentrate recirculation. After NF concentrate recycling, organics (humic acids) do not have a major effect on NF membrane fouling. NF concentrate recycling increases the fouling potential of MF membrane in MBR. 	Kappel et al. (2014)
Antibiotic wastewater → MBR → NF → NF concentrate → MBR →	SRT in MBR: 600 days. HRT in MBR: 36 h. Transmembrane pressure in NF: 7.5 bar. Cross-flow rate: 2.0 m ³ h ⁻¹ . 90% of the total flow of RO concentrate is added to MBR.	<ul style="list-style-type: none"> This process exhibits excellent water quality throughout the entire experimental period. The recirculation of 90% of total volume of RO concentrate produced significantly inhibits the sludge activity. The electric conductivity and soluble microbial products brought by NF concentrate recycling lead to severe membrane fouling in MBR. The accumulation of undegradable organics (fulvic acid – and humic acid-like substances) in NF concentrate increases the fouling potential of NF membrane 	K. Li et al., (2016); and Wang et al. (2015, 2014)
Municipal wastewater → MBR → RO → RO concentrate → ozonation → MBR →	HRT in MBR: 15 h. SRT in MBR: 95 days. Sludge concentration in MBR: 5.8 g TSS L ⁻¹ . transmembrane pressure in RO: 5-6 bar. Cross-flow velocity: 1.9 m ³ h ⁻¹ . 90% of the total flow of RO concentrate is added to MBR.	<ul style="list-style-type: none"> This integrated process produces high-quality water suitable for many reuse purposes. The removal rate of micropollutants is relatively high in this process. The accumulation of inorganic ions in RO concentrate potentially causes RO membrane scaling. 	Joss et al. (2011)
Municipal wastewater → MBR → RO → RO concentrate → MBR →	SRT in MBR: 30 days. Sludge concentration in MBR: 8-9 g L ⁻¹ . Organic load: 0.2 kg COD kg ⁻¹ MLSS d ⁻¹ . RO concentrate represents 15% of the total flow of MBR inflow.	<ul style="list-style-type: none"> RO concentrate recycling causes a significant increase in protein-like substances with 10-100 kDa and 100-1000 kDa in MBR supernatant. The increased contents of protein-like substances relate to MF membrane fouling in MBR. Sludge activity is not affected significantly by RO concentrate recycling. RO concentrate recycling exhibits a minor effect on the quality of MBR permeate. 	Vu et al. (2017)

(1) SRT: solid retention time. (2) HRT: hydraulic retention time. (3) COD: chemical oxygen demand. (4) TSS: total suspended solid. (4) MLSS: mixed liquid suspended solid.

I.2.4.4 Treatment of RO concentrate by advanced oxidation processes

Advanced oxidation processes (AOPs), eco-friendly methods generating $\cdot\text{OH}$ radicals as an oxidant for organics of non-selective degradation, have been known for high versatility and compatibility for removal of contaminants. Electron-rich organics could be undergone hydroxylation or dehydroxylation under $\cdot\text{OH}$ radicals until the formation of carbon dioxide, water and non-toxic small molecules. Various AOPs, such as ozonation, H_2O_2 oxidation, electro-oxidation, photocatalytic oxidation etc., have been reported recently to dispose the RO concentrate generated from municipal wastewater reclamation, (Acero et al., 2016; Bagastyo et al., 2011a; Justo et al., 2013; Pérez et al., 2010; Pérez-González et al., 2012; Radjenovic et al., 2011; Zhou et al., 2011). Figure 1.6 depicts the schematic of RO concentrate treatment by AOPs. Table 2.10 reviews the treatment efficiency of ozonation, UV/ H_2O_2 and electrochemical oxidation for the degradation of organics from RO concentrate based the literature reported recently.

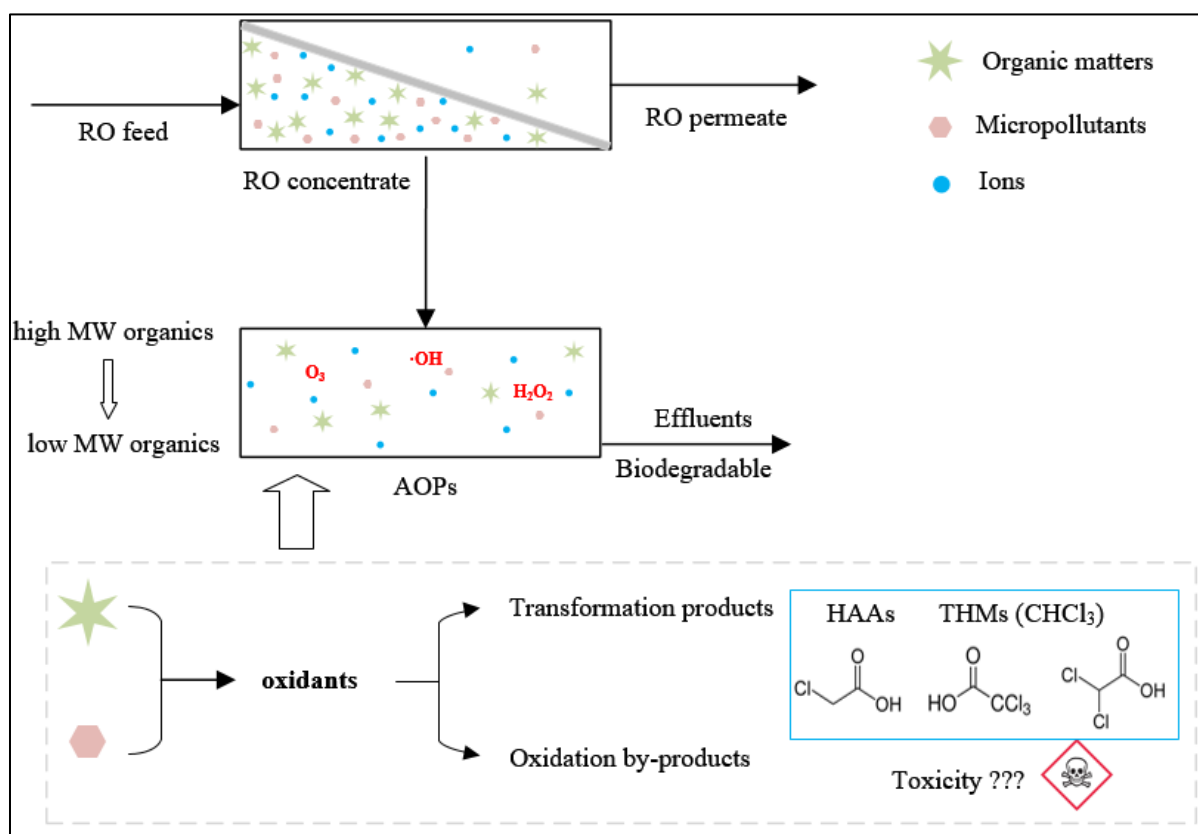


Figure 1.6 Schematic of RO concentrate treatment by AOPs.

Table 1.10 Removal efficiency of organics by AOPs from municipal RO concentrate

Ozonation				
Ozone dose (mg O ₃ L ⁻¹)	Reaction time (min)	DOC removal (%)	Colour removal (%)	Reference
3.0-10.0	20	9.9-24.5	>99	Lee et al. (2009)
Gas flow rate: 1 L min ⁻¹ O ₃ production: 17.6 mg h ⁻¹	60	21.7	83	Zhou et al. (2011)
UV/H ₂ O ₂				
H ₂ O ₂ concentration	Irradiation time (min)	DOC removal (%)	Colour removal (%)	Reference
0.54 mg mg ⁻¹ TOC	61.7	9.6 TOC	-	Justo et al. (2013)
4 mmol L ⁻¹	30	15	50	Lu et al. (2013)
3 mmol L ⁻¹	60	25	>90	Umar et al. (2014)
3 mmol L ⁻¹	30	15	86	Pradhan et al. (2015)
3 mmol L ⁻¹	-	22	94	Umar et al. (2015)
3 mmol L ⁻¹	30	9-12	96	Pradhan et al. (2016)
3 mmol L ⁻¹	60	29	96	Umar et al. (2016a)
Electrochemical oxidation				
Current density (A m ⁻²)	Contact time (min)	DOC removal (%)	COD removal (%)	Reference
Ti/Pt-IrO ₂	-	28	87	Bagastyo et al. (2013)
Ti/SnO ₂ -Sb	-	31	93	Bagastyo et al. (2013)
BDD (200)	300	35	-	Hurwitz et al. (2014)
Co-PbO ₂ (200)	120	-	30	Weng and Pei (2016)

Removal (%) is obtained based on the concentration of the selected parameter before and after oxidation

From Table 1.10, these three AOPs are found to be adequate to remove colour from RO concentrate. Nonetheless, only 9-35% of organics in terms of DOC are mineralized, whatever AOPs are. It should be highlighted that, after AOPs treatments, the biodegradability of RO concentrate effluents is greatly improved due to the degradation of organic matters with bigger MW to smaller MW organic molecular. For instance, Lee et al., (2009) report that only 5.3 - 24.5% of TOC could be removed at different ozone dose (from 3 to 10 mg O₃ L⁻¹) and contact time (10 and 20 min), whereas the biodegradability (BOD₅/TOC) of the RO concentrate increased by 1.8 - 3.5 times. As compared to low biodegradability of raw RO concentrate (BOD₅/COD: 0.03), satisfactory biodegradability ratios (BOD₅/COD) of 0.34 and 0.30 could be achieved after RO concentrate oxidation treatment at the amount of 1.38 mg O₃ mg TOC⁻¹ and 0.54 mg H₂O₂ mg TOC⁻¹, respectively (Justo et al., 2013). These studies suggest that, the application of AOPs to RO concentrate treatment could break down the bigger size organics and produce the smaller size organics. It is proposed that, therefore, implementing a subsequent biological unit after chemical oxidation could decrease the organics load of RO concentrate in a cost-effective way and produce high-quality effluents for an environmentally-friendly discharge (Acero

et al., 2016; Azaïs et al., 2016; Justo et al., 2015).

To date, there are a few studies concerning the oxidation efficiency of AOPs in removing micropollutants from RO concentrate with more complex matrix (Acero et al., 2016; Benner et al., 2008; Justo et al., 2013; Lee et al., 2012; Pérez et al., 2010; Radjenovic et al., 2011). Justo et al. (2013) have studied the mitigation of 11 selected pharmaceuticals in RO retentate by using UV/H₂O₂ and ozonation. Higher than 80% elimination could be obtained for all of pharmaceuticals at the amount of 0.82 mg O₃ per mg TOC (except for atenolol, carbamazepine and diclofenac) and 0.11 mg H₂O₂ per mg TOC (except for codeine, paroxetine and trimethoprim), indicating that the amount of H₂O₂ required to completely degrade the sum of selected micropollutants generally appear to be significantly lower as compared to applied ozone dose needed. The matrix complexity of RO concentrate may be responsible for the difference from expected and observed oxidation kinetics of these six micropollutants with low removal during the oxidation process. Yang et al. (2016) examines the effect of matrix components on UV/H₂O₂ process for trace organic degradation in RO concentrate from municipal wastewater reuse facilities, and the results show that the degradation efficiency of the target micropollutants reduces due to organic matters in RO concentrate scavenging ~75% of ·OH radicals.

It should be highlighted the importance of the salinity of RO concentrate on the efficacy of AOPs technologies, which is described later.

I.3 Ozonation application for decontamination of PhACs

Ozonation, one of the most used AOPs, has been confirmed having a great performance for eliminating a large spectrum of organic chemicals (e.g., pharmaceuticals, pesticides, synthetic compounds) in WWTPs (Benner et al., 2008; Huber et al., 2005). It is therefore widely and increasingly applied for the purification of water or the reclamation of wastewater as a further complement technology or a promising tertiary treatment alternative (Domenjoud et al., 2015; Nebout et al., 2015). The potential efficacy of ozonation for organic micropollutants removal is mainly ascribed to the combination of molecular ozone with selectivity and radical reactions generally involving ·OH radicals with non-selectivity (Beltrán, 2004; F et al., 1991; Prasse et al., 2012; Tizaoui and Grima, 2011), as depicted in Figure 1.7.

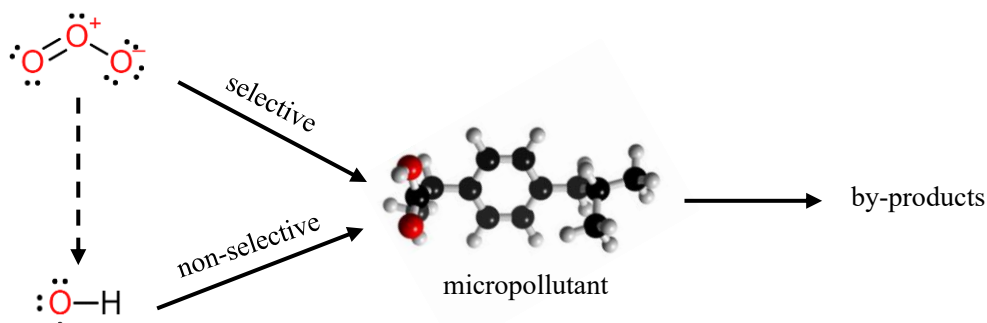


Figure 1.7 Oxidation pathways of micropollutants in water

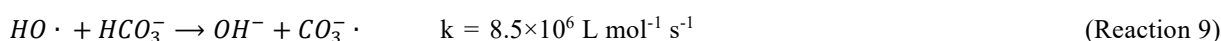
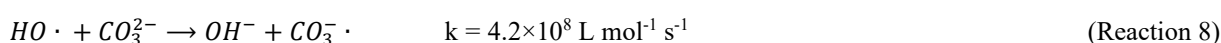
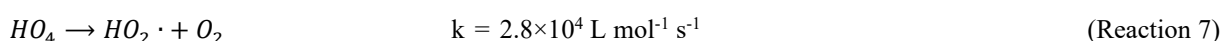
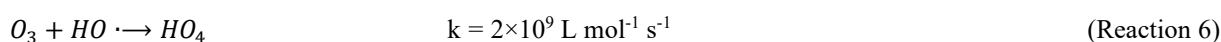
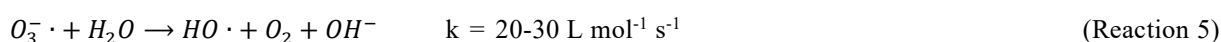
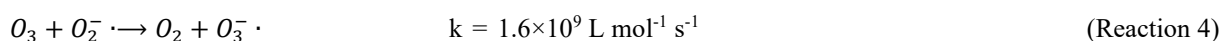
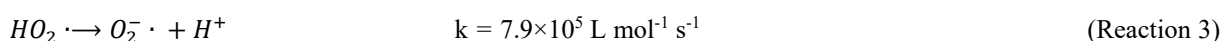
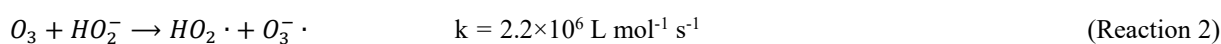
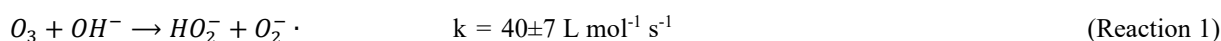
During the ozonation process of micropollutants, the ozonation kinetics of a micropollutant B is the contribution of oxidants, ozone and $\cdot\text{OH}$ radicals, and is expressed in the following form:

$$\ln\left(\frac{[B]}{[B]_0}\right) = -(k_{O_3-B} \int [O_3] + k_{OH-B} \int [\cdot OH]) dt$$

where $[O_3]$ and $[\cdot\text{OH}]$ present the concentration of ozone and $\cdot\text{OH}$ radical, respectively. k_{O_3-B} and k_{OH-B} are second-order reaction rate constants for the reaction of the micropollutant with ozone and $\cdot\text{OH}$ radicals, respectively. A detailed method determining reaction rate constants has been given by several researchers (Hoigné and Bader, 1983; Huber et al., 2003). Based on the literature, the ozone rate constants range from $0.05 \text{ L mol}^{-1} \text{ s}^{-1}$ of diatrizoate (Real et al., 2009a) to $3.8 \times 10^7 \text{ L mol}^{-1} \text{ s}^{-1}$ of triclosan (Lee et al., 2013), varying over many orders of magnitude, which is depending on the different reactivity of micropollutants towards molecular ozone. The rate constants of $\cdot\text{OH}$ radicals towards organic compounds are relatively high and have a variation by a factor of ten ($\sim 10^8$ to $\sim 10^9$) (Dodd et al., 2006; Huber et al., 2005), which also reveals the non-selective nature of $\cdot\text{OH}$ radical for micropollutants.

I.3.1 Ozone decomposition and the formation of hydroxyl radicals

Ozone, is not stable in water phase, and rapidly decomposes via some reactions with substances present in water body to further generate $\cdot\text{OH}$ radicals. A comprehensive study on ozone decomposition and the formation mechanism of $\cdot\text{OH}$ radicals in aqueous medium has been illustrated by Hoigné and Bader (1976). During the transformation of ozone into $\cdot\text{OH}$ radicals process, hydroxide acts as reactants, H_2O_2 ion is initiators, and then superoxide radicals and $\cdot\text{OH}$ radicals are chain carriers. Reactions of initiation (Reaction 1 and 2), prorogation (Reaction 3-7), and inhibition (Reaction 8-9) are involved. It should be pointed that, however, the presence of several undesirable inorganic or organic impurities in natural water or wastewater can directly interrupt radicals' chain by interacting with the non-selective $\cdot\text{OH}$ radicals, such as carbonate alkalinity etc.. The presence of t-butanol and the change of solution pH have an impact on ozone self-decay kinetics (López-López et al., 2007).



I.3.2 Expected attack site of micropollutants towards ozone

At low pH value or in the presence of $\cdot\text{OH}$ radicals' inhibitors such as tertiary butanol, direct electrophilic attack by molecular ozone for organic compounds (cycloaddition reaction and electrophilic substitution reaction), is a predominant mechanism, where ozone is acted as electrophilic agent to react selectively with micropollutants possessing electron-rich functional groups including unsaturated hydrocarbon bonds ($-\text{C}=\text{C}-$, exception for different double bond such as $-\text{C}=\text{N}-$ and $-\text{C}=\text{O}$), activated aromatic system (styrene), phenol, aniline and non-protonated amines (De Vera et al., 2015; Derco et al., 2015; Hoigné and Bader, 1976; Lee and Gunten, 2016). Figure 1.8 displays the expected attack site of four common micropollutants towards molecular ozone.

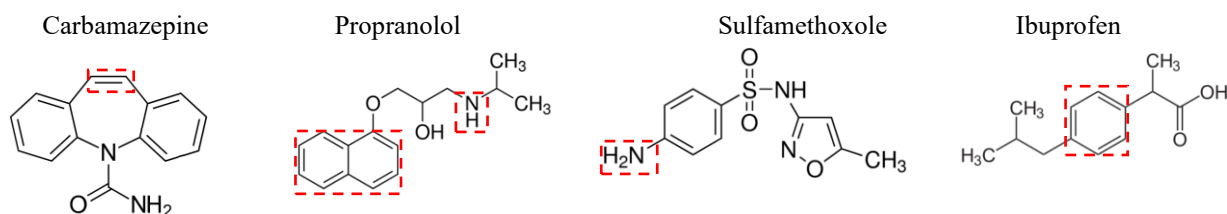


Figure 1.8 Expected attack site of micropollutants towards molecular ozone

According to the reaction rules of ozone, the transformation products of organic micropollutants can be predicted during the ozonation process. Corresponding the formation of oxidation products, possible reaction mechanisms involved are (Benner, 2009; Lee and Gunten, 2016; Sonntag and Gunten, 2012; Sui et al., 2017): (1) ozone attacking carbon double bond of micropollutants can result in the formation of a very unstable five-member ring. And then this ring breaks up to further generate ketone, carboxylic acid, or aldehyde according to Criegee mechanism (Figure 1.9a). For example, carbamazepine, having a high reactivity towards ozone, can be decomposed into several products with quinazoline-based functional groups by ozonation (McDowell et al., 2005). In addition, an epoxide maybe occur via singlet oxygen release during ozonation of olefins (Lee and Gunten, 2016); (2) ozone attacking double bond of an activated aromatic ring can result in the formation of an ozone adduct and the aromatic ring opening, and further generate ketone, carboxylic acid, or aldehyde via cycloaddition and ozonide; (3) ozone is likely to hydroxylate an aromatic ring by electron donating substituents via electrophilic substitution (Figure 1.9b); (4) Reactions between ozone and aromatic amine can occur via ozone attack towards nitrogen or benzene ring (Figure 1.9c).

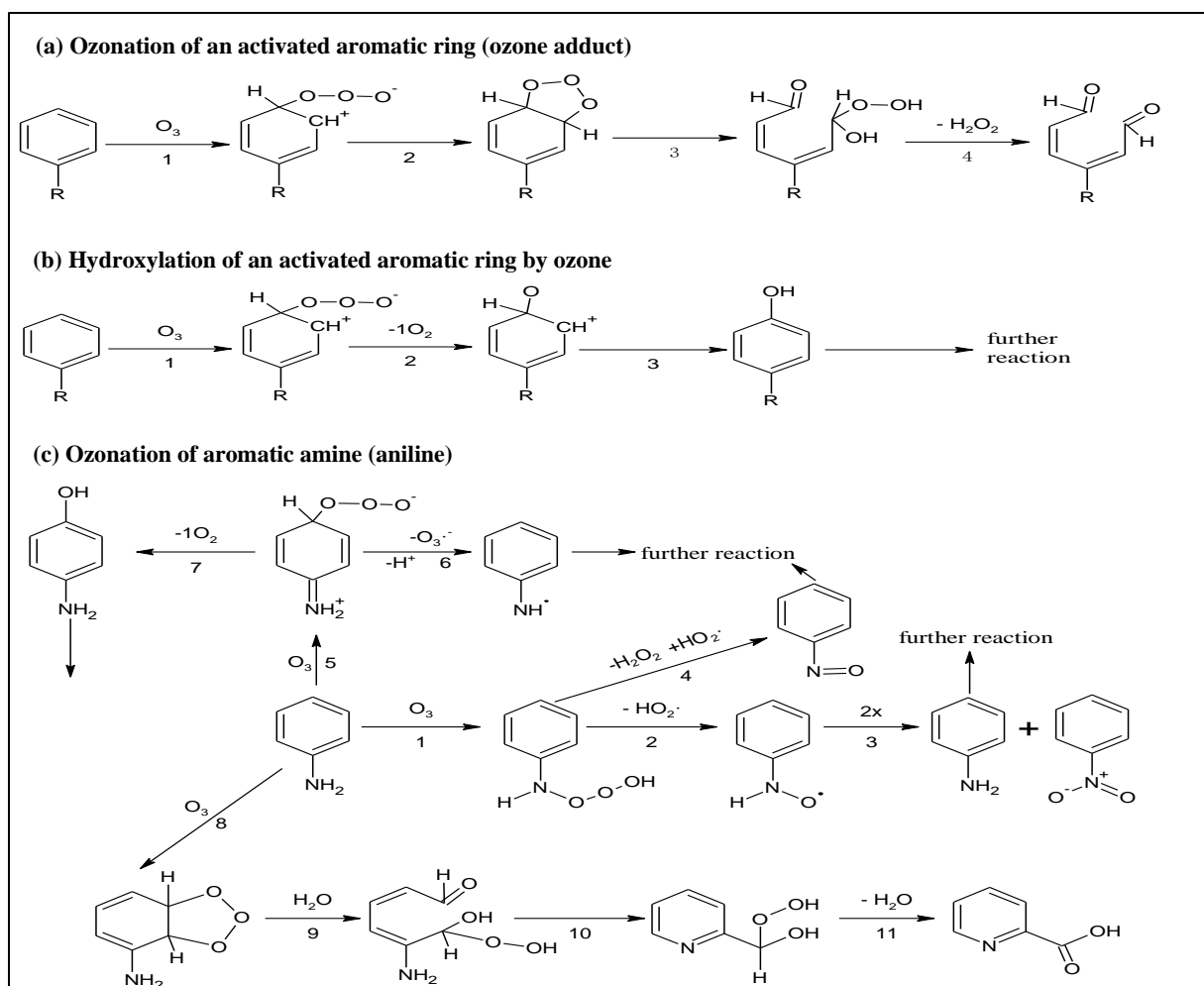


Figure 1.9 Ozonation of specific moiety (aromatic ring and amine) (Benner, 2009; Lee and Gunten, 2016; Sonntag and Gunten, 2012)

I.3.3 Micropollutants decontamination in wastewater by ozonation

The removal efficiency of micropollutants by ozonation in the WWTPs effluents is compiled in Table 1.11. There is a significant difference in the ozonation removal of different micropollutants in wastewater. Amoxicillin, carbamazepine, diclofenac, etc., can be completely abated during the ozonation process. However, bezafibrate, enrofloxacin, iopromide etc. compounds are difficult to be destroyed to undetectable trace levels. This deviation caused can be explained by their reactivity towards molecular ozone.

Table 1.11 Complication of ozonation removal of micropollutants in wastewater effluents

Micropollutants	Operating condition	Removal ¹ %	Reference
Acetaminophen	The concentration of ozone gas-in: 5 mg L ⁻¹ . Initial DOC: 12.3 mg L ⁻¹ . The concentration of micropollutants in effluents (spike): 10 mg L ⁻¹ . pH: 7.7. Reaction time: 14 - 30 min.	>90	Javier Rivas et al. (2011)
Atrazine		~50	
Caffeine		~75	
Diclofenac		>90	
Hydroxybiphenyl		>90	
Metoprolol		>90	
Sulfamethoxazole		>90	
Amoxicillin	Ozone dose: 4 mg L ⁻¹ . The concentration of micropollutants: ambient concentration in raw wastewater, no spike.	100	Lee et al., 2012
Atenolol		98	
Caffeine		90	
Carbamazepine		100	
Meprobamate		81	
Naproxen		100	
Sulfamethoxazole		98	
Trimethoprim	Applied ozone dose ² : 4.86 mg L ⁻¹ . Initial DOC: 16.8 mg L ⁻¹ . The concentration of micropollutants: 5 - 10 µg L ⁻¹ .	92	Hübner et al., 2013
Bezafibrate		41	
Carbamazepine		88	
Ciprofloxacin		85	
Diclofenac		92	
Enrofloxacin		92	
Naproxen		89	
Sulfamethoxazole		91	
Bisphenol A	Transferred ozone dose ³ : 4.4 mg L ⁻¹ .	~100	Singh et al., 2015
Carbamazepine		~100	
Diclofenac		~90	
Erythromycin		~50	
Enrofloxacin		~25	
Ketoprofen		~80	
Norfloxacin		~72	
Caffeine	ozone consumption: 9.31 mg L ⁻¹ . Initial DOC: 10.7 mg L ⁻¹ . The concentration of micropollutants (no spike): <10 µg L ⁻¹ .	70	Knopp et al., 2016
Diatrizoate		27	
Erythromycin		87	
Gabapentin		78	
Iopromide		67	
Iomeprol		56	
Sulfamethoxazole		98	
Tolytriazole		95	

(1) removal (%) is obtained based on the concentration of selected parameter before and after ozonation. (2) applied ozone dose: the total dose of gaseous ozone injected into the reactor. (3) transfer ozone dose: the dose of gaseous transferred from the gaseous to liquid phase.

Sonntag and Gunten (2012) make a complication on micropollutants removal by ozonation based on the previous researches. Compounds from diclofenac to sulfamethoxazole with the ozone kinetic rate constants more than $10^5 \text{ L mol}^{-1} \text{ s}^{-1}$, are completely removed at specific ozone doses of 0.4 g ozone per g DOC_0 . For micropollutants with a middle ozone kinetic rate constant between $2 \times 10^2 \text{ L mol}^{-1} \text{ s}^{-1}$ and $10^4 \text{ L mol}^{-1} \text{ s}^{-1}$, a higher specific ozone dose of 1 g per g DOC_0 is needed to accomplish a full elimination. As for compounds such as iopromide with ozone kinetic rate constants near $100 \text{ L mol}^{-1} \text{ s}^{-1}$ and below, specific ozone dose of 1 g per g DOC_0 can only achieve the removal of 50-90%, where $\cdot\text{OH}$ route will be a dominated pathway. A finding reported by Bahr et al. (2007) agrees well with this complication, i.e., diclofenac and indomethacin can be quickly attacked by ozone. In contrast, the reaction of ozone with bezafibrate or clofibrac acid is relatively low.

Lee et al. (2013) investigate the effect of the structure of micropollutants and of different effluents from biological treated secondary wastewater (dissolved organic matter: 4.7 - 26 mg C L^{-1}) on ozonation potential for micropollutants. In this study, micropollutants are divided into five groups based on their kinetic rate constants with ozone and $\cdot\text{OH}$ radicals. The relationship between ozone dose and the elimination of these micropollutants is depicted in Figure 1.10. It suggests that, when the rate constant of a micropollutant toward ozone is higher, its elimination by ozone is larger and specific ozone dose required is less, vice versa.

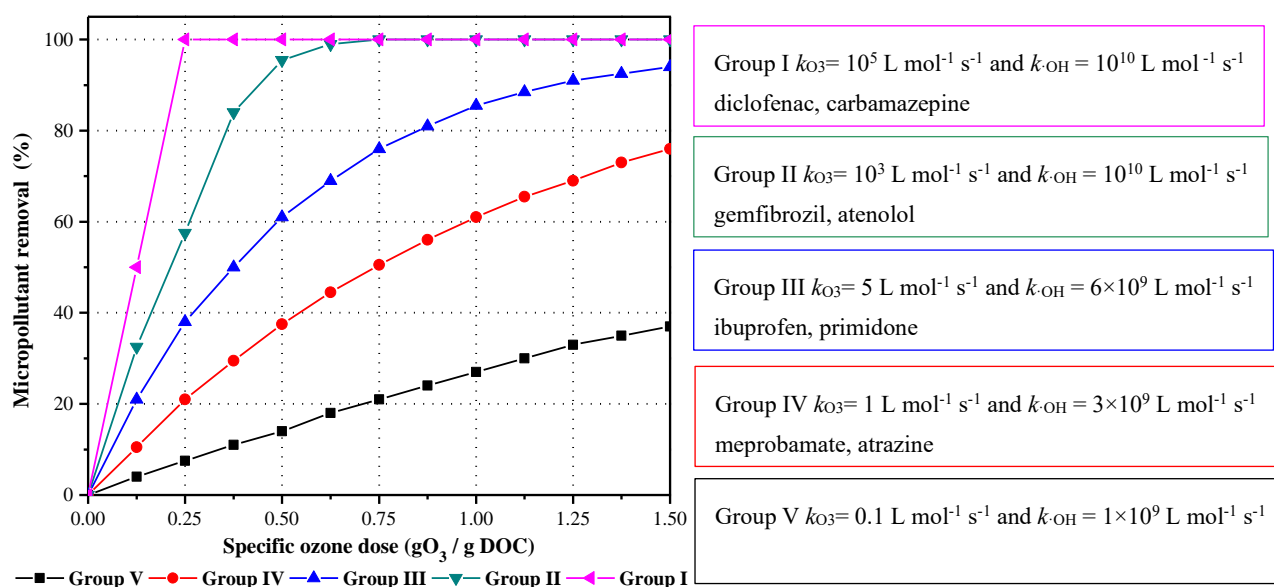


Figure 1.10 Different types of micropollutants and their elimination by ozone. From Lee et al. (2013)

In many cases, the concentrations of target micropollutants are abated dramatically during ozonation processes. It should be highlighted that, nevertheless, a relatively low mineralization in terms of organic matters (DOC or TOC) removal in natural or wastewater after ozonation, only ranging from about 10% to 40%, (Beltrán et al., 2012, 2009; Coelho et al., 2009; de Vera et al., 2016; Huber et al., 2003; Javier Rivas et al., 2011; Papageorgiou et al., 2017; Sadrnourmohamadi and Gorczyca, 2015). It is possibly due to: (1) the formation of intermediates and by-products that are refractory to further ozonation, and

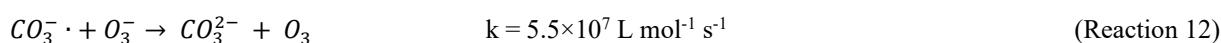
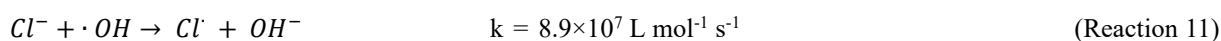
(2) the consumption of oxidants by other substances. Thus, more research efforts should be made to improve the overall ozonation removal of microcontaminants via promoting $\cdot\text{OH}$ radicals formation or enhancing direct reactions.

I.3.4 Impact of water matrix on the degradation of PhACs by ozonation

Besides the reactivity of oxidizing agents (ozone and $\cdot\text{OH}$ radicals) with PhACs and ozone dose, other factors, including inorganic ion concentration (Cl^- , SO_4^{2-} , and HCO_3^-) and organic matters content, might influence the degradation efficiency of PhACs by ozonation.

I.3.4.1 Effect of scavengers

The presence of inorganic constituents in water, such as SO_4^{2-} and Cl^- (Haag and Hoigné, 1983; Miralles-Cuevas et al., 2017), HCO_3^- and CO_3^{2-} (Beltrán, 2004), leads to a reduction in degradation efficiency for micropollutants like atrazine (Javier Rivas et al., 2011), due to their scavenge effect for $\cdot\text{OH}$ radicals, as implied in Reaction 8-11. Among the anions, more attention is paid to HCO_3^- and CO_3^{2-} with the kinetic rate constants with $\cdot\text{OH}$ radicals of $3.9 \times 10^8 \text{ L mol}^{-1} \text{ s}^{-1}$ and $8.5 \times 10^6 \text{ L mol}^{-1} \text{ s}^{-1}$, respectively (Beltrán, 2004). Several attempts have been made to identify the mechanism of CO_3^{2-} species as an inhibitor (Acero and Gunten, 2000; Beltrán, 2004; Nöthe et al., 2009), and a proper description is that two dominant chain carrier radicals, i.e., $\cdot\text{OH}$ radical and ozonide ion, are scavenged by HCO_3^- and CO_3^{2-} (Reaction 8-9, 12).



I.3.4.2 Impact of organic matters and alkalinity on ozone lifetime

The ozone consumption is largely decided by organic load and inorganic content in water, and the contribution of micropollutants towards ozone can be neglected to some extent (Miralles-Cuevas et al., 2017). These results are in agreement with those obtained by Nöthe et al. (2009); Sonntag and Gunten (2012) and von Gunten (2003). Thus, it is essential to discuss the relationship between the nature of water matrix and ozone lifetime in different water. The role of dissolved organic matters (DOM) and alkalinity in ozone stability can be elucidated by: (i) the direct reaction of DOM with ozone, and (ii) $\cdot\text{OH}$ scavenging by DOM and carbonate alkalinity.

Urfer et al. (2001) investigate the ozone stability in various Swiss natural waters with different compositions (DOC and salts) at pH 8 and 15°C (ozone dose 1 mg L⁻¹). Ozone consumption increases in the following order of Lake 3 (DOC: 3.2 mg L⁻¹, carbonate alkalinity: 3.4 mmol L⁻¹) > Lake 2 (DOC: 1.6 mg L⁻¹, carbonate alkalinity: 3.6 mmol L⁻¹) > Lake 1 (DOC: 1.3 mg L⁻¹, carbonate alkalinity: 2.5 mmol L⁻¹) > Spring water (DOC: 0.9 mg L⁻¹, carbonate alkalinity: 5.4 mmol L⁻¹) > Groundwater (DOC: 0.7 mg L⁻¹, carbonate alkalinity: 6.7 mmol L⁻¹), which may be linked to an increasing trend in DOC content and a declining trend in alkalinity concentration. This finding is in good accordance with the results from Huber et al. (2003). The ozone half-lives are 75 min for River Seine with 1.3 mg L⁻¹ of

DOC and 4.1 mmol L⁻¹ of HCO₃⁻ and 4 min for Lake Water with 3.7 mg L⁻¹ of DOC and 0.7 mmol L⁻¹ of HCO₃⁻. An increased DOC can facilitate the transformation of ozone into ·OH radicals, while alkalinity is prone to the stability of ozone. Thus, the oxidation efficiency of organic micropollutants is affected by DOC and alkalinity present in natural water or wastewater (Figure 1.11). Indeed, nearly 100% triclosan (ozone-reactive) removal is obtained at 4 mg L⁻¹ of the ozone dose in the wastewater with 7.5 mg L⁻¹ of DOC and 8.1 mmol L⁻¹ of HCO₃⁻, whereas only 58% triclosan depletion for dosage of 6 mg L⁻¹ can be achieved in the wastewater containing 12.4 mg L⁻¹ of DOC and 0.9 mmol L⁻¹ of HCO₃⁻ (Suarez et al., 2007).

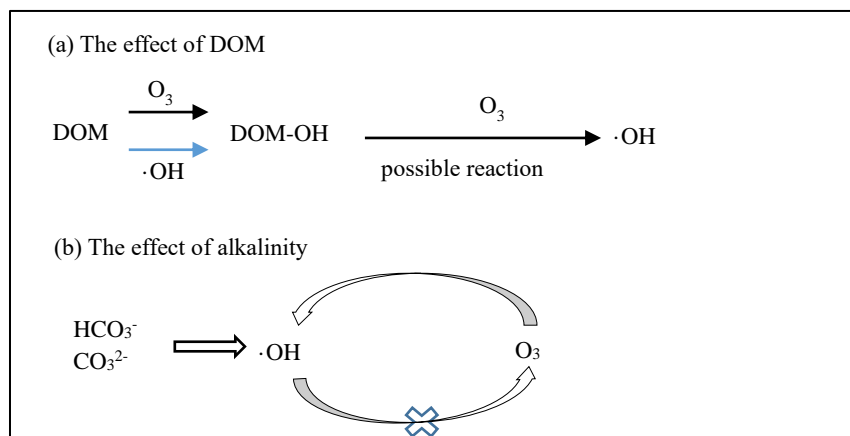


Figure 1.11 Effect of water matrix on the removal efficiency of organic micropollutants

The presence of effluents organic matter (EfOM) has also been proven to pose adverse effects on ozonation process to eliminate micropollutants by consuming ozone and ·OH radical (Cai and Lin, 2016; Lee et al., 2013). However, the composition of EfOM is more complex compared to natural organic matter (NOM), including NOM from water sources, soluble microbial products from the activated sludge treatment, and trace levels of synthetic compounds. The role of EfOM in ozone decay, ·OH radical generation, water matrix scavenging capacity, as well as the abatement of micropollutants should be investigated to fill the knowledge gap for ozonation application.

I.3.5 Formation and toxicity of transformation products

During the ozonation process of micropollutants, intermediate products or by-products are formed, which is consistent with the non-complete mineralization (as discussed above), possibly leading to high toxicity of the treated effluents. As reported by Sui et al. (2017), in terms of bezafibrate, lethal concentration /effective concentration values of two oxidation products are around 2-6 times higher than bezafibrate toxicity for algae, daphnid and fish. The finding obtained from Miralles-Cuevas et al. (2017) also demonstrates that acute toxicity of ozone-treated effluents increases during the ozonation of real municipal wastewater effluents, indicating that by-products are probably more toxic than their precursor micropollutants. However, the treated wastewater by ozonation may be not toxic toward a given specie, which mainly depends on the type of bioassays (acute versus chronic toxicity) and on the species exposed (bacteria, microalgae, invertebrates, fishes, etc.) (Azaïs et al., 2017). Hence, more studies

should be extended to examine the toxic potential after ozonation of wastewater.

I.4 Urine wastewater

It is reported that each person can produce 1~1.5 L urine per day, and a single adult discharges 500 L urine per year (Karak and Bhattacharyya, 2011), indicating that urine stream is a non-negligible part of municipal wastewater. Even if urine stream only represents one percent of the total flow of municipal wastewater, ~50% of P, 80% of N, 90% of K, and a large fraction of non-desirable micropollutants (pharmaceuticals and natural hormones) present in municipal wastewater mainly originate from urine (Dodd et al., 2008). In the 1990s, some researchers in Europe start focusing on the separation of urine at source, which could promote the sustainability of wastewater management (Kirchmann and Pettersson, 1994; Larsen and Gujer, 1996). Separating and treating urine at the source, not only reduce energy costs required by downstream WWTPs for nutrients removal, but also minimize the related ecotoxicity concern due to the excreted pharmaceuticals (Maurer et al., 2006). By the Tool for the Reduction and Assessment of Chemical and Other Environmental Impacts (TRACI) method, Landry and Boyer (2016) observe that the separation of urine at the source could have less environmental impacts as compared to centralized wastewater treatment, mainly resulting from the reduction of electricity use at the wastewater treatment plant and from nutrient recovery from urine. Therefore, separation and treatment of urine at the source might be a feasible and attractive solution for the production of urine- based fertilizer (Ikehata et al., 2006).

I.4.1 Characteristics of source-separated urine

Based on the literature reported previously, the general compositions of urine have been compiled in Table 1.12 (Kirchmann and Pettersson, 1994; Pronk et al., 2007; Ronteltap et al., 2003; Tettenborn et al., 2007; Udert and Wächter, 2012). There is a significant difference in the compositions between fresh and hydrolysed urine. The reason for this is that the hydrolysis of urea in fresh urine by urease- positive bacterial results in a strong pH increase and in the formation of ammonia and bicarbonate species, as shown in Reaction 12. As illustrated in Table 1.12, NH_4^+ , Na^+ , K^+ , Cl^- , HCO_3^- , SO_4^{2-} and P-PO_4^{3-} are seven main ionic species in hydrolysed urine, with the concentration at least higher than 100 mg L⁻¹.



Table 1.12 Compositions of fresh and hydrolysed urine

Parameter	Unit	Household ^a	School ^a	Workplace ^b	Workplace ^c	Library ^d	Hydrolysed urine ^e	Fresh urine ^e
pH	-	9	8.9	8.7	9	8.7	9.3	6.0
N-NH ₄ ⁺	mgN L ⁻¹	1691	2499	2390	4347	2900	7000	-
Na ⁺	mg L ⁻¹	982	938	1740	1495	1600	2391	1701
K ⁺	mg L ⁻¹	875	1150	1410	3284	1400	1560	1950
Mg ²⁺	mg L ⁻¹	1.63	1.5	<5	-	-	-	97
Ca ²⁺	mg L ⁻¹	15.75	13.34	16	-	-	-	160
Cl ⁻	mg L ⁻¹	2500	2235	3210	2112	3000	3545	3545
S-SO ₄ ²⁻	mgS L ⁻¹	225	175	778	273	700	481	321
PO ₄ ³⁻ -P	mg L ⁻¹	210	200	208	154	180	421	619
TIC ¹	mg C L ⁻¹	- ⁴	-	1210	-	-	3000	-
DOC ²	mg C L ⁻¹	-	-	1830	-	-	-	-
COD ³	mg L ⁻¹	-	-	4500	6000	3600	-	-

(a) from Kirchmann and Pettersson (1994). (b) from Udert and Wächter (2012). (c) from Ronteltap et al. (2003). (d) from Pronk et al. (2007). (e) from O'Neal and Boyer (2013).

(1) TIC: total inorganic carbon. (2) DOC: dissolved organic carbon. (3) COD: chemical oxygen demand. (4) -: not analysed.

I.4.2 Occurrence of PhACs in source-separated urine

Due to a non-complete metabolization in the liver or kidney, an important excretion pathway for PhACs and their metabolites is via urine, and finally reaches wastewater collection system (Ikehata et al., 2006; Karak and Bhattacharyya, 2011; Maurer et al., 2006). It is reported by Lienert et al. (2007) that about two-thirds of micropollutants from human metabolism are discharged into the environment via urine, and 33% via faeces. The residual of PhACs in urine, with the level of $\mu\text{g L}^{-1}$, has been reported by Tettenborn et al. (2007), as presented in Table 1.13. It is observed that the concentration of PhACs in urine is significantly higher than that in municipal wastewater. To date, knowledge regarding the elimination of pharmaceuticals and their metabolites from urine is still scarce (Zhang et al., 2015).

Table 1.13 Concentration of PhACs found in urine from a public toilet (from Tettenborn et al. (2007))

PhACs ($\mu\text{g L}^{-1}$)	Hamburg			Berlin		
	March 5	May 5	December 5	May 6	October 5	November 5
Ibuprofen	411	511	417	442	398	794
Bezafibrate	202	192	230	495	846	207
β -Sitosterol	31	52	18	40	30	22
Diclofenac	27	17	17	14	9	45
Carbamazepine	23	29	20	4	11	13
Phenacetin	23	<1	2	1	<1	1
Pentoxifylline	8	9	7	6	<1	3
Phenazone	<3	<1	4	2	<1	2
Ketoprofen	<LOD ¹	<LOD	<LOD	<LOD	<LOD	<LOD

(1) LOD: limit of detection

I.4.3 Urine valorisation and treatment of source-separated urine

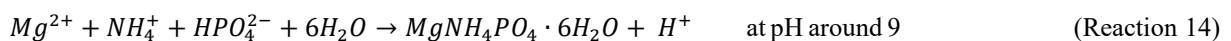
As mentioned above, urine contains large proportions of nutrients including N, P and K. Therefore, urine-based products as fertilizers have also been gaining popularities in the agricultural farming throughout the world (Pronk et al., 2006). Nonetheless, due to the presence of micropollutants, the farming application of urine could pose a threat and risk on receiving bodies via transfer into aqueous environment and accumulation in soils (Karak and Bhattacharyya, 2011). The removal of excreted and unwanted micropollutants must be established for the production and application of multi-nutrient urine fertilizers. Maurer et al. (2006) provide a comprehensive review on the treatment process of source-separated urine based on this main purposes, including P-recovery (struvite formation), N-recovery (ion-exchange, ammonia stripping), micropollutants removal (electrodialysis, nanofiltration, ozonation), etc.. In the present thesis, struvite precipitation, RO and ozonation are investigated for urine valorisation.

Table 1.14 Treatment processes of source-separated urine (from Maurer et al. (2006))

Purpose	Treatment processes
Volume reduction	evaporation, freeze-thaw, ro
Stabilization	acidification, partial nitrification
P-recovery	struvite formation
N-recovery	ion-exchange, ammonia stripping, isobutyraldehyde-diurea precipitation
Nutrient removal (P and N)	anammox process
Micropollutants removal	electrodialysis, nanofiltration, ozonation, advanced oxidation

I.4.3.1 Struvite precipitation

Struvite precipitation, a fast and undemanding process regarding energy and Mg required, has gained a lot of attention regarding P-nutrient recovery from urine at the source over the past decades (Ganrot et al., 2007; Ronteltap et al., 2003; Triger et al., 2012). Magnesium ammonium phosphate, also known as struvite ($MgNH_4PO_4 \cdot 6H_2O$), a slow release fertilizer composed of magnesium, ammonium and phosphorus at a molar ratio of 1:1:1, is a white crystalline substance (Doyle and Parsons, 2002). With the addition of extra magnesium chemicals, hydrolysed urine solution (pH around 9) is supersaturated, leading to more than 93% phosphorus recovery in the form of struvite (Reaction 14) (Barbosa et al., 2016; Ronteltap et al., 2007; Triger et al., 2012; Wilsenach et al., 2007). It should be noted that, nevertheless, higher than 98% of micropollutants still remain in the urine supernatant (Ronteltap et al., 2007). Thus, subsequent treatment units should be established to reduce efficiently these non-desirable micropollutants load for a urine valorisation purpose.



I.4.3.2 Reverse osmosis process

In an early report, reverse osmosis (RO) membrane has been used to recover NH_4^+ , P and K from acidified stored urine (pH around 7.1) by retaining these nutrients in the RO retentate (Dalhammar, 1997). In more recent years, works concerning the removal of PhACs from urine by RO process cannot be found, which is likely to be due to the relatively complicated compositions (highly concentrated ions and organics).

Only Pronk et al. (2006) assess the potential of nanofiltration membrane (NF) for the separation of organic compounds from nutrients in the source-separated urine, where NF could produce permeate effluents with a major part of ammonia and a small number of model micropollutants.

I.4.3.3 Ozonation process

As already mentioned above, struvite precipitation and membrane filtration are considered as feasible options to separate nutrients and micropollutants in the source-separated urine, whereas degradation of urine-derived micropollutants are achieved mainly through advanced oxidation processes (AOPs) (ozonation, UV, UV/H₂O₂, etc.) (Dodd et al., 2008; Escher et al., 2006; Giannakis et al., 2017; Larsen et al., 2004; Pronk et al., 2007).

Studies have evidenced that ozonation process is a well-accepted technology for wastewater reclamation, resulting from high reactivity of molecular ozone and ·OH radicals from ozone self-decomposition or reactions with organic matters towards most of micropollutants (Benner, 2009; El-taliawy et al., 2017; Marce et al., 2016). However, works that have focused on the elimination of excreted pharmaceuticals from urine by ozonation process are relatively scarce. To the best of our knowledge, to date, only four studies report the degradation of micropollutants from real urine by ozonation process (Dodd et al., 2008; Escher et al., 2006; Gajurel et al., 2007; Tettenborn et al., 2007). Escher et al. (2006) observe that 0.6-1.3 g L⁻¹ ozone dose is effective in the removal of 17 α -ethynylestradiol, propranolol, diclofenac, carbamazepine and ibuprofen from urine, whereas algal toxicity only reduces by 50-60% at the ozone dose of 1.1 g L⁻¹. Dodd et al. (2008) find that a relatively large dose of ozone is required to achieve a satisfactory oxidation efficiency for target micropollutants in the hydrolysed urine, which is likely attributed to the presence of ozone-consuming reactive components with high levels of concentration, such as amino acids and aromatic organic compounds. Indeed, after N depletion in urine, less ozone dose (4.8 g O₃ per litre urine) is needed to remove effectively most of micropollutants as compared to untreated urine with ozone dose of 6.6 g O₃ per litre urine (Tettenborn et al., 2007). It seems that the nature of urine matrix plays an important role in ozone consumption and in elimination of micropollutants during the ozonation process of real urine. In fact, the ozonation behaviour and oxidation efficiency of organic compounds are determined by the compositions of wastewater tested including organic matter, bicarbonate, ammonia, etc. (Marce et al., 2016).

I.5 Summary of literature review

The presence of PhACs in the environmental media, with the concentration ranging from ng L⁻¹ to μ g L⁻¹ even up to mg L⁻¹, has received great attention, as these substances and their metabolites exhibit negative impacts on the health of aquatic ecosystems. The excretion via urine and the discharge of MWWTPs effluents are two important pathways for PhACs entering into the environment.

Reverse osmosis (RO) technology has gained worldwide acceptance for the reclamation of wastewater due to its high efficiency in rejecting a wide spectrum of organic pollutants, bacteria, dissolved organic matter and inorganic salts. However, the application of RO process for wastewater reuse could generate RO concentrate which is generally characterized by a high concentration of ions, organic matters and PhACs, a low biodegradability (low ratio of BOD₅/COD), and potential ecotoxicity.

Untreated or improper discharge of RO concentrate might result in a potentially serious threat to water receiving body. It should therefore be further disposed or treated by effective technologies in a cost-effective way, aiming to minimize the potential environmental risk associated with its disposal or reuse.

Recently, several studies have investigated the recirculation of NF concentrate to the MBR in an MBR-NF system, and the results obtained demonstrate this system is successful to produce high-quality water. To date, there are a few information on the impact of RO concentrate recycling to MBR on RO performance. In addition, further research on the elimination of PhACs from RO concentrate is also needed to be developed.

Ozonation has been demonstrated as a well-established technology to degrade micropollutants from municipal wastewater through a synergism of ozone and $\cdot\text{OH}$ radicals. Actually, the ozonation reaction becomes complex due to the presence of different reactive micropollutants as well as other impurities and numerous running reactions in parallel. However, information regarding which constituent is more pronounced to affect ozonation efficiencies of micropollutants is scarce, especially for a complicated wastewater matrix (such as urine containing ions, ammonia and organics). In addition, the combination of RO process and ozonation for PhACs removal from urine has not yet been investigated.

Chapter II Materials and Methods

In this chapter, the first section gives information on the relevant properties of the model micropollutants. The second and third section describe the configuration and operation of dead-end RO cell, cross-flow RO pilot, and ozonation pilot. The last section presents the analytical method of chemicals as indicators for treatment efficiencies of the processes used in this thesis.

II.1 Target micropollutants

II.1.1 Properties of the target micropollutants

In this thesis, 10 target PhACs are involved, including 2-hydroxyibuprofen (2OH-IBP), caffeine (CAF), carbamazepine (CBZ), diclofenac (DIF), ibuprofen (IBP), ketoprofen (KET) ofloxacin (OFL), oxazepam (OXA), propranolol (PRO), and sulfamethoxazole (SMX). These model PhACs are ubiquitous in the surface water and wastewater. It should be pointed out that, even though the occurrence of CAF in wastewater is mainly due to the consumption of coffee, the chemical is a central nervous system and metabolic stimulant (Nikolaou et al., 2007). Thus, CAF, as a PhACs, is also investigated in this thesis. The key properties of the target PhACs are summarized in Table 2.1. These model PhACs have different properties (e.g., molecular weight, charge and hydrophobicity), which are important factors in determining their removal efficiency during the wastewater treatment.

Table 2.1 Relevant properties of the target PhACs

PhACs	Caffeine (CAF)	Carbamazepine (CBZ)	Diclofenac (DIF)	Ibuprofen (IBP)	Ketoprofen (KET)
CAS	58-08-2	298-46-4	15307-86-5	15687-27-1	22071-15-4
Family group	stimulant	antiepileptic	anti-inflammatory	anti-inflammatory	anti-inflammatory
Formula	C ₈ H ₁₀ N ₄ O ₂	C ₁₅ H ₁₂ N ₂ O	C ₁₄ H ₁₁ Cl ₂ NO ₂	C ₁₃ H ₁₈ O ₂	C ₁₆ H ₁₄ O ₃
Molar mass g mol ⁻¹	194.2	236.3	296.2	206.3	254.3
Water solubility mg L ⁻¹ b	2.16×10 ⁴ (25 °C)	17.7 (25 °C)	2.37 (25 °C)	21 (25 °C)	52 (20 °C)
pKa ^a	0.6, 14	2.3, 13.9 ^b	4.2	4.4	3.12
LogKow ^a	-0.07 (hydrophilic)	2.45 (hydrophobic)	4.51 (hydrophobic)	4.0 (hydrophobic)	4.23 (hydrophobic)
PhACs	Ofloxacin (OFL)	Oxazepam (OXA)	Propranolol (PRO)	Sulfamethoxazole (SMX)	2 hydroxyibuprofen (2OH-IBP)
CAS	82419-36-1	604-75-1	525-66-6	723-46-6	51146-55-5
Family group	antibiotic	anxiolytic	beta blocker	antibiotic	ibuprofen metabolite
Formula	C ₁₈ H ₂₀ FN ₃ O ₄	C ₁₅ H ₁₁ ClN ₂ O ₂	C ₁₆ H ₂₁ NO ₂	C ₁₀ H ₁₁ N ₃ O ₃ S	C ₁₃ H ₁₈ O ₃
Molar mass g mol ⁻¹	361.4	286.7	259.3	253.3	222.3
Water solubility mg L ⁻¹ b	2.83×10 ⁴ (25 °C)	179 (drugbank)	61.7 (25 °C)	610 (37 °C)	not found
pKa ^a	6.05, 8.22 ^b	1.7, 11.6	9.5	1.6, 5.6	not found
LogKow ^a	-0.4 ^b (hydrophilic)	2.24 (hydrophobic)	3.48 ^b (hydrophobic)	0.9 (hydrophilic)	not found

(a) from Moffat et al., (2011). (b) Data from PubChem

Negative charge: solution pH > pKa; A compound is hydrophobic when logKow > 2 (Taheran et al., 2016)

Figure 2.1 shows the expected attack site of the target PhACs towards molecular ozone. Based on the second-order rate constant of ozone reaction with PhACs ($k_{O_3\text{-PhACs}}$ at pH 7) reported in the literature, target PhACs are classified into three groups in this thesis, i.e., Group I: ozone-reactive PhACs ($k_{O_3\text{-PhACs}} > 10^5 \text{ L mol}^{-1} \text{ s}^{-1}$), Group II: PhACs with moderate reactivity towards molecular ozone ($10 \text{ L mol}^{-1} \text{ s}^{-1} < k_{O_3\text{-PhACs}} < 10^5 \text{ L mol}^{-1} \text{ s}^{-1}$), and Group III: ozone-refractory PhACs ($k_{O_3\text{-PhACs}} < 10 \text{ L mol}^{-1} \text{ s}^{-1}$).

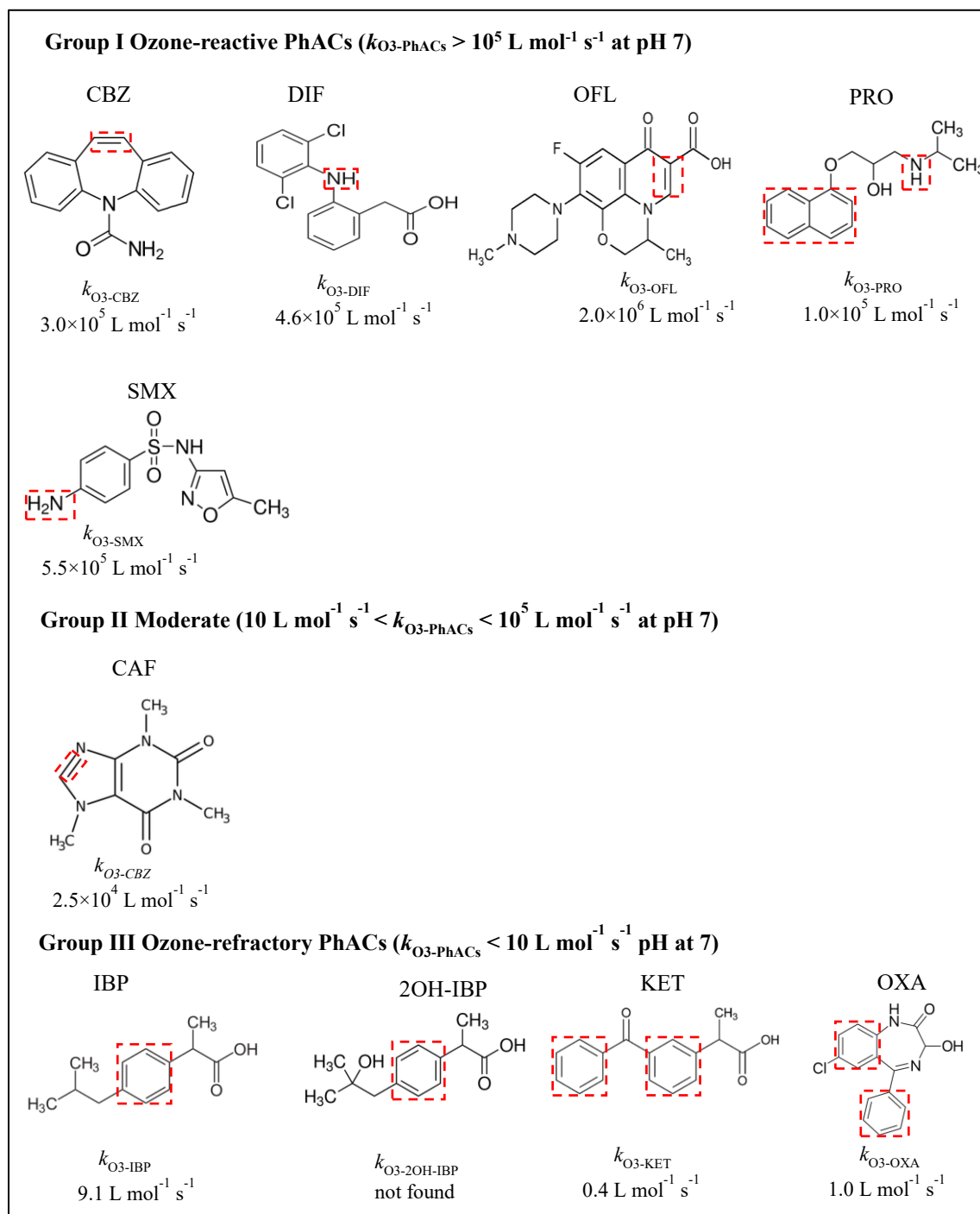


Figure 2.1 Expected attack site of PhACs towards molecular ozone and their ozone kinetic rate constant. (Benner et al., 2008; Huber et al., 2003; Lee et al., 2014; Rosal et al., 2009; Tay and Madehi, 2015; Zeng et al., 2018)

II.1.2 Preparation of stock solution of the target micropollutants

For municipal MBR permeate studied in Chapter III, no micropollutants were spiked before RO process or ozonation treatment.

In Chapter IV (Effect of water matrix on ozonation efficiencies), considering the effect of solvents (such as methanol or ethanol) on ozone consumption, both CBZ and KET were directly dissolved with ultrapure water, saline solution and synthetic urine at a working concentration of 10 mg L⁻¹.

In Chapter V (Treatment of urine-based wastewater treatment), a concentrated mother solution was first prepared by dissolving the target micropollutants with pure methanol as solvent, stored at -20°C and used for further experiments. Table 2.2 shows the concentration of each tested micropollutant in the stock solution. Then a mixture of these PhACs was spiked to synthetic urine and hydrolysed urine. Their working concentration with µg L⁻¹ level was shown in Chapter V. The final concentration of methanol added in the working solution was 0.3% (v/v).

Table 2.2 Concentration of target micropollutants in the stock solution

PhACs	CAF	CBZ	DIF	IBP	OFL
Concentration (mg L ⁻¹)	105.5-714.9	6.8-10.0	12.7-16.5	657.0-704.9	15.0-56.8
PhACs	OXA	PRO	SMX	2OH-IBP	-
Concentration (mg L ⁻¹)	5.4-72.4	2.9-40.7	2.3-111.0	302.9-343.8	-

II.2 Description of RO process

II.2.1 RO membrane used

The previous work has proved that ESPA2 membrane (negative charge, Polyamide) exhibited not only an excellent retention for organic and inorganic ions present in wastewater, but also a low fouling level, as compared to NF membrane (loose and tight membrane) (Jacob et al., 2010). Therefore, ESPA2 membrane was employed in this thesis. The membrane characteristics are given in Table 2.3. This membrane with the higher salt rejection presents a lower water permeability. RO module is operated in dead-end mode or in cross-flow mode.

Table 2.3 Characteristics of ESPA2 RO membrane (from Alturki et al. (2010))

Manufacturer	Hydranautics
Material	Polyamide
Average pore diameter (nm)	Not applicable
Na ⁺ rejection (%)	96.5
MWCO (g mol ⁻¹) ¹	<100
Surface roughness (nm)	30.0
Membrane charge	Negative
Surface charge (mV)	~20
Water permeability at 20°C (L h m ⁻² bar) (from our experiment)	~2.0

(1) from the manufacturer

II.2.2 Dead-end RO cell configuration

Dead-end RO filtration is performed in a stirred stainless-steel batch cell (total volume: 0.5 L) at the room temperature, as depicted in Figure 2.2. RO permeate is forced through the ESPA2 membrane (membrane area: 0.00418 m²) by nitrogen gas. The mass of RO permeate is recorded continuously by an electronic balance along with the RO filtration process. For each experiment, RO permeate and RO concentrate produced are collected and then stored for subsequent experiment or analysis.

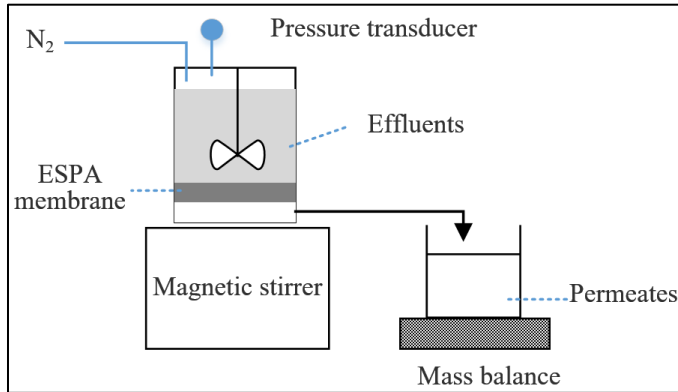


Figure 2.2 Device for RO filtration with dead-end mode

II.2.3 Cross-flow RO pilot

A lab-scale cross-flow RO pilot consists of a storage tank with the useful volume of 50 L, a feed pump, a rectangular stainless steel filtration cell with the effective membrane surface of 0.051 m², a recirculation loop with the volume of 0.8 L, a pressure-regulating valve and several digital flowmeter, as shown in Figure 2.3. During the filtration process, the flow rate of both RO concentrate and RO permeate is recorded continuously by a digital flowmeter that connected to a PC.

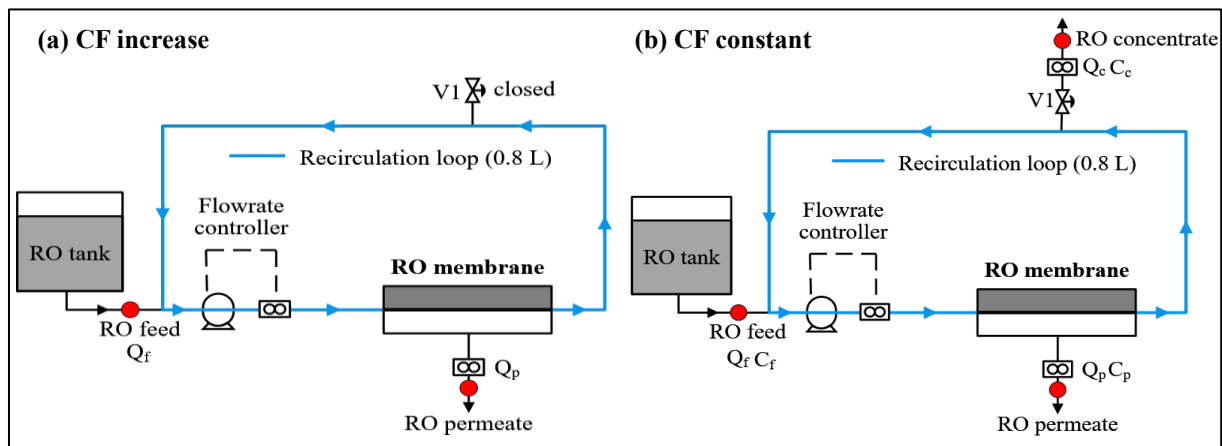


Figure 2.3 Schematic of cross-flow RO pilot. Q_f , Q_p and Q_c are flow rate of RO feed, RO permeate and RO concentrate, respectively. C_f , C_p and C_c are the concentration of a selected parameter in RO feed, RO permeate and RO concentrate, respectively. Red cycle represents the sampling point.

For this pilot, during the filtration process, two modes with respect to concentration factor (CF) are involved, i.e., CF increase, and CF constant. Firstly, due to a closed valve V_1 , as shown in Figure 2.4a,

solutes inside the recirculation loop are forced continuously to the RO entrance cell, leading to a continuous accumulation of solutes on the RO membrane surface. During this period, CF increases with operating time, and is followed based on the conductivity in both RO feed and bulk RO concentrate (Equation 1). When a required CF is reached, the regulation of RO concentrate flow rate (Q_c) by a valve (V1) could enable RO pilot to run at this fixed CF, as shown in Figure 2.4b.

$$CF = \frac{C_{\text{conductivity-RO concentrate}}}{C_{\text{conductivity-RO feed}}} \quad (\text{Equation 1})$$

where $C_{\text{conductivity-RO feed}}$ and $C_{\text{conductivity-RO concentrate}}$ are the conductivity in RO feed and bulk RO concentrate ($\mu\text{S cm}^{-1}$), respectively.

The volume reduction factor (VRF) is defined as the volume ratio of the total RO feed (V_f) to RO concentrate collected (V_c), as expressed in Equation 2.

$$\text{VRF} = \frac{V_f}{V_c} = \frac{Q_p}{Q_c} + 1 \quad (\text{Equation 2})$$

where Q_c and Q_p are the flow rate of RO feed, RO concentrate and RO permeate (L h^{-1}), respectively.

If the rejection of RO membrane (R) for the solutes is 100%, CF is equal to VRF, as expressed as $CF = (\text{VRF})^R$ (Field et al., 2017).

During the period of CF increase, the flow rate of RO feed (Q_f) is equal to that of RO permeate (Q_p). When RO is performed at a constant CF, the flow rate of RO feed (Q_f) is the sum of both RO permeate (Q_p) and RO concentrate (Q_c).

II.2.4 RO process parameters

Prior to RO experiments, ESPA membrane should be first immersed in the ultra-pure water overnight, then is compressed and stabilized at an operating pressure of 10 bar for at least 2 h until a stable flux achieved.

RO process is operated at a constant transmembrane pressure. The permeate flux (J), the permeate flow through one square meter of RO membrane surface, is measured by Equation 3. The permeability (L_p) of the RO membrane is calculated from Equation 4:

$$J = \frac{Q_p}{A_m} \quad (\text{Equation 3})$$

$$L_p = \frac{J}{\Delta P - \Delta \pi} \quad (\text{Equation 4})$$

where J is the permeate flux of the RO membrane ($\text{L h}^{-1} \text{m}^{-2}$). A_m is the specific surface of the RO membrane (m^2). L_p represents the permeability of the RO membrane ($\text{L h}^{-1} \text{m}^{-2} \text{bar}^{-1}$). ΔP is the transmembrane pressure (bar), and which acts as the driving force for RO process. $\Delta \pi$ is the osmotic pressure difference between RO feed side and RO permeate side (Pa). In membrane filtration processes, the more common unit for pressure is bar instead of Pa. One bar is equal to 10^5 Pa.

$$\Delta P = P_f - P_p \quad \text{for dead-end RO cell} \quad (\text{Equation 5})$$

$$\Delta P = \frac{P_f + P_c}{2} - P_p \quad \text{for cross-flow RO pilot} \quad (\text{Equation 6})$$

where P_f , P_c and P_p are the pressure on the side of RO feed, concentrate and permeate, respectively (bar). Note that, for cross-flow RO pilot, P_f is the pressure before RO feed entering into the membrane.

The water recovery, indicating the overall production of RO permeate, describes the relationship between RO permeate and RO feed, as shown in Equation 7. For example, a recovery of 70% means that 70% of RO feed flow is produced as RO permeate, and VRF is equal to 3.3.

$$\text{water recovery (\%)} = \frac{V_p}{V_f} \times 100 = \frac{Q_p}{Q_f} \times 100 = \left(1 - \frac{1}{VRF}\right) \times 100 \quad (\text{Equation 7})$$

Retention/rejection indicates the amount of solutes rejected by RO membrane. The observed retention of an indicator (R_{obs}) can be calculated based on its concentration in both RO permeate (C_p , mg L⁻¹ or µg L⁻¹) and bulk RO concentrate (C_c , mg L⁻¹ or µg L⁻¹) (Liu et al., 2014), as shown in the following equation:

$$R_{obs} (\%) = \frac{C_c - C_p}{C_c} \times 100 \text{ for organic matters (NPOC), conductivity, and ions, etc.} \quad (\text{Equation 8})$$

II.2.5 Saturation index calculation

Scaling can occur when an ionic product of a sparingly soluble product exceeds its equilibrium solubility product (supersaturation). Supersaturation is estimated by the saturation index (SI). The SI value of mineral salt (A_aB_b) could be obtained by Equation 9 and Equation 10. In this work, PHREEQC software (Parkhurst and Appelo, 1999) was used to quantify the SI values of selected mineral salts. The positive SI value related to the risk of inorganic scaling, while the negative one showed the solution was undersaturated (Joss et al., 2011).

$$SI = \log \left(\frac{IAP}{K_{sp}} \right) \quad (\text{Equation 9})$$

$$IAP = [A]^a [B]^b \quad (\text{Equation 10})$$

where the ionic activity product (IAP) is the product of ionic activity. K_{sp} is the solubility product constant of related salts.

II.3 Semi-batch ozonation

II.3.1 Description of ozonation pilot

Ozonation pilot in a lab-scale consists of an ozone generator, a glass vessel with the useful volume of 2 L, a 6-blades turbine (Rushton) for totally mixing, an ozone gas analyser, a dissolved ozone analyser, a pH sensor, a temperature monitor, ozone residual destruction, a peristaltic pump and several valves, as depicted in Figure 2.4. Ozone as a feed gas at a desired concentration, generated from pure oxygen by using an ozone generator (BMT Messtechnik GMBH 802N, Germany), is introduced from the bottom of the reactor through a porous diffuser (diameter: 2.5 cm). A complete and continuous mixing of the bulk liquid phase could be achieved by using a turbine with 6-blades at a rate of 470 rpm. Gaseous ozone concentration is measured by a UV absorbance spectrophotometer (Trailgaz Uvozon model TLG 200, France). An online ozone analyser (Orbisphere Laboratories model 410, Germany) with polarography

probe (Orbisphere Laboratories model 31330.15, Germany), mounted on a recirculation loop, is used to detect the concentration of dissolved ozone based on indigo method proposed by Bader and Hoigne (1981). This sensor allows measuring the concentration of dissolved ozone in the range of 0 - 50 mg L⁻¹. A circulation rate of 500 rpm adjusted by a peristaltic pump (Masterflex, USA) is required to assure the solution containing dissolved ozone pass through polarographic membrane. Both excess gas and gas-out flows are forced into an ozone destruction unit before releasing into the atmosphere. During the ozonation experiment, the solution in the reactor is kept at a constant temperature by circulating water from a thermostatic bath through the reactor jacket. The solution pH is monitored by a pH analyser (Consort R305, Belgium) with a combination electrode (SI Analytics GmbH H 8481HD, Germany). The values corresponding to the concentration of ozone gas-in, gas-out and dissolved ozone, solution pH and temperature are recorded continuously by a software in PC.

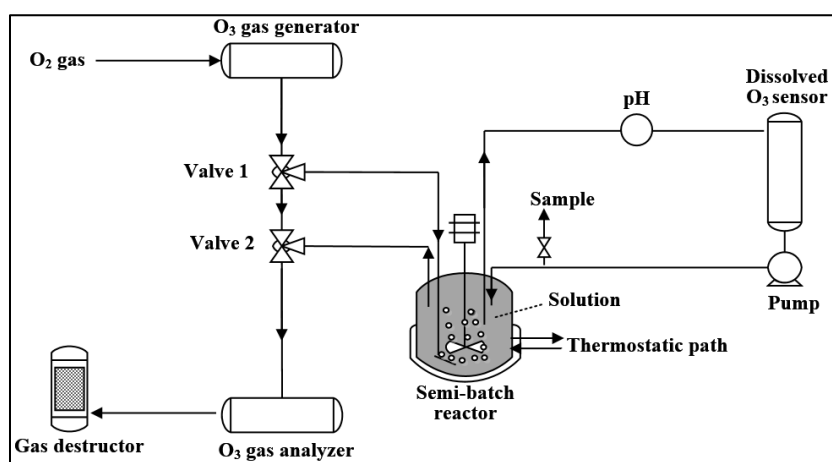


Figure 2.4 Ozonation pilot with a semi-batch reactor

II.3.2 Concentration profile of ozone in ultra-pure water and mass balance of ozone

Figure 2.5 presents the concentration profile of ozone in the gaseous phase and liquid phase during the ozonation of ultra-pure water. From Figure 2.5, two stages are distinguished:

- The left side of Figure 2.5 represents a transient regime where the concentration of both ozone gas-out and dissolved ozone gradually increases over time. During this period, the quantity of ozone transferred from the gaseous phase to the liquid phase is greater than the quantity of ozone that breaks down in the liquid phase, thus leading to an accumulation of ozone in the liquid phase.
- The right part exhibits a steady state where these concentrations maintain almost unchangeable, and the concentration of ozone gas-out ($[O_3]_{\text{gas-out}}$) and the concentration of dissolved ozone ($[O_3]_L$) take the particular values $[O_3]_{\text{gas-out}}^{\infty}$ and $[O_3]_L^{\infty}$, respectively. During this period, the amount of ozone transferred is equal to that of ozone decomposed.

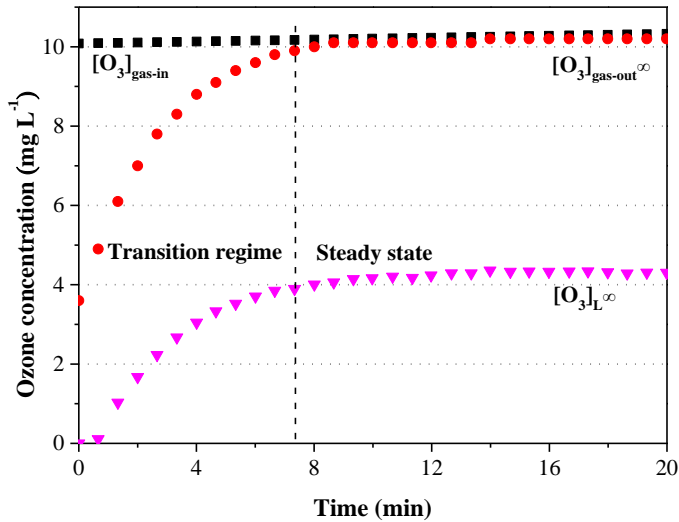


Figure 2.5 Typical ozone concentration profiles.

II.3.2.1 Mass balance of ozone in the gaseous and liquid phase

In a semi-batch reactor, several assumptions should be made to write ozone mass balance equation: (1) both liquid and gas phases are considered as perfectly mixed; (2) the flow of gas remains constant in the reactor; (3) the gas hold-up is small and the volume of the liquid reaction mixture is assimilated to the volume of liquid.

Corresponding to the gaseous phase, the mass balance is written as Equation 11, where the quantity of ozone gas-in over a range of time (dt) is normally equal to the sum of the quantity of ozone gas-out, of ozone transferred and of ozone gas accumulated. Since the steady state is reached for the gaseous phase, the accumulation of ozone gas could be negligible. Thus, Equation 11 is rewritten as Equation 12.

$$Q_g [O_3]_{gas-in} dt = Q_g [O_3]_{gas-out} dt + T_{O_3} dt + V_g d[O_3]_{gas} \quad (\text{Equation 11})$$

$$Q_g [O_3]_{gas-in} dt = Q_g [O_3]_{gas-out} dt + T_{O_3} dt \quad (\text{Equation 12})$$

where $[O_3]_{gas-in}$ and $[O_3]_{gas-out}$ are the concentration of ozone gas-in and gas-out (mg L^{-1} or mol L^{-1}), respectively. $[O_3]_{gas}$ refers to the concentration of gaseous ozone (mg L^{-1} or mol L^{-1}). Q_g is the ozone gas flow rate (L h^{-1}). V_g is the volume of gas in the reactor (L). t is the contact time (s, min or h). T_{O_3} is the rate of ozone transfer from the gaseous phase to the liquid phase (mg s^{-1} or mol s^{-1}).

In the liquid phase, the amount of ozone transferred over a time interval (dt) is equal to the sum of the amount of decomposed ozone (including self-decomposition and chemical reactions) and ozone accumulated in the liquid, as shown in Equation 13.

$$E k_L a V_{Liq} ([O_3]_L^* - [O_3]_L) dt = r_{appO_3} V_{Liq} dt + V_{Liq} d[O_3]_L \quad (\text{Equation 13})$$

where E is the enhancement factor. $k_L a$ is the volumetric mass transfer coefficient (s^{-1}). V_{Liq} is the volume of liquid in the reactor (L). $[O_3]_L$ and $[O_3]_L^*$ are the concentration of dissolved ozone in the liquid phase and at the equilibrium (mg L^{-1} or mol L^{-1}), respectively. r_{appO_3} is the apparent consumption rate of ozone ($\text{mol L}^{-1} \text{s}^{-1}$ or $\text{mg L}^{-1} \text{s}^{-1}$), which involves the self-decomposition into $\cdot\text{OH}$ radicals in the ultra-pure water.

II.3.2.2 Rate constant of ozone self-decomposition

In the case of ultra-pure water, ozone consumption is mainly due to the self-decomposition of ozone in the liquid phase. In addition, the dissolved ozone concentration is quickly closed to the saturation value, where enhancement factor E is assumed to be equal to the value 1. Therefore, Equation 13 can be rewritten as Equation 14.

$$k_L a V_{Liq} ([O_3]_L^* - [O_3]_L) dt = k_c [O_3]_L V_{Liq} dt + V_{Liq} d[O_3]_L \quad (\text{Equation 14})$$

where k_c is the self-decomposition rate constant of the ozone (s^{-1}).

In order to obtain the parameter of ozone decomposition (k_c), the steady period is considered, where the concentration of ozone in both gas and liquid phase no longer varies. During this period, the accumulation of ozone ($d[O_3]_{gas}$ and $d[O_3]_L$) is equal to zero. Therefore, based on Equation 12 and Equation 14, the k_c parameter is easily obtained from the following Equation 15:

$$k_c = \frac{Q_g([O_3]_{gas-in} - [O_3]_{gas-out})}{[O_3]_L^\infty V_{Liq}} \quad (\text{Equation 15})$$

II.3.2.3 Volumetric mass-transfer coefficient

At nonstationary condition, Equation 14 could be rearranged as Equation 16.

$$\frac{d[O_3]_L}{dt} = k_L a [O_3]_L^* - (k_L a + k_c) [O_3]_L \quad (\text{Equation 16})$$

After intergradation, Equation 16 can be rewritten as follows:

$$[O_3]_L = [O_3]_L^* \frac{k_L a}{k_L a + k_c} (1 - \exp(-(k_L a + k_c) t)) \quad (\text{Equation 17})$$

Considering a sufficiently long time, $[O_3]_L^*$ trends towards $[O_3]_L^\infty$. Thus, Equation 18 could be obtained.

$$[O_3]_L^\infty = [O_3]_L^* \frac{k_L a}{k_L a + k_c} \quad (\text{Equation 18})$$

By combining Equation 17 and Equation 18, we can write Equation 19, as shown below:

$$\ln([O_3]_L^\infty - [O_3]_L) = -(k_L a + k_c) t + \ln[O_3]_L^\infty \quad (\text{Equation 19})$$

The value of $k_L a + k_c$ is given by the slope of straight line obtained by plotting the left side of Equation 19 against ozonation contact time. In this work, the volumetric transfer coefficient $k_L a$ obtained is $0.0052 s^{-1}$, which is similar to the values reported by Aboussaoud (2014) with the $k_L a$ of 0.0053 and $0.0064 s^{-1}$ for different diffusers.

II.3.3 Ozone dose

Three different ozone dose, applied ozone dose, transferred ozone dose, and consumed ozone dose, are involved during the ozonation process in a semi-batch reactor. Applied ozone dose (mg) refers to the total amount of gaseous ozone introduced throughout the experiment, as shown in Equation 20. Transferred ozone dose (mg) represents the accumulated amount of ozone effectively transferred from the gaseous phase to the liquid phase (Equation 21). Consumed ozone dose (mg) reflects the amount of ozone required to finish chemical reactions (Equation 22).

$$O_3 \text{ applied} = \int_0^t [O_3]_{\text{gas-in}} Q_g dt \quad (\text{Equation 20})$$

$$O_3 \text{ transferred} = \int_0^t T_{O_3} dt = \int_0^t [O_3]_{\text{gas-in}} Q_g dt - \int_0^t [O_3]_{\text{gas-out}} Q_g dt \quad (\text{Equation 21})$$

$$O_3 \text{ consumed} = \left(\int_0^t [O_3]_{\text{gas-in}} Q_g dt - \int_0^t [O_3]_{\text{gas-out}} Q_g dt \right) - [O_3]_{L(t)} V_{Liq} \quad (\text{Equation 22})$$

II.3.4 Ozone solubility in the ionic solution

Ozone solubility, a fundamental parameter in the ozonation kinetic study, is involved for the discussion of impacts of matrix on ozone kinetic regimes in Chapter IV. The solubility parameter of ozone in pure water is 0.31 (López-López et al., 2007). The effect of salts presence on the solubility of ozone in a concentrated aqueous solution is usually described by the Sechenov equation (Beltrán, 2004; Rischbieter et al., 2000).

$$\log\left(\frac{m_0}{m}\right) = \sum (h_i + h_G) C_i \quad (\text{Equation 23})$$

$$h_G = h_{G,0} + h_T(T - 298.15) \quad (\text{Equation 24})$$

where m_0 and m are the solubility parameter of ozone in pure water and in the salt solution, respectively. C_i is the molar concentration of ion i . h_i is an ionic-specific parameter. h_G , $h_{G,0}$ and h_T are the gas-specific parameters. The relevant values of h_i , $h_{G,0}$ and h_T are from the finding of Beltrán (2004), which are given in Appendix 3.

II.4 Analysis of chemicals

II.4.1 pH and conductivity

pH of solution samples is recorded by a pH 539 microprocessor meter (WTW, Germany). Conductivity is obtained by an LF538 conductivity meter (WTW, Germany).

II.4.2 Dissolved organic carbon and dissolved inorganic carbon

The measurement of dissolved organic carbon (DOC) in samples is performed by a Shimadzu TOC- V_{CSH} total organic carbon analyser, using non-purgeable organic carbon (NPOC) method. Firstly, a small amount of acid solution (HCl and H₃PO₄) is added to acidify the samples. Next, the samples are sparged with purified air. The purpose for this is to remove inorganic carbon. After that, the samples are heated at 680 °C in a combustion column packed with a platinum catalyst. After combustion, NPOC compounds convert to CO₂, which is detected using a non-dispersive infrared gas analyser (NDIR).

Dissolved inorganic carbon (DIC), including carbonate and bicarbonate, is also quantified in TOC- V_{CSH} analyser. After sample acidification, CO₂ from DIC is directly detected by the NDIR detector.

Prior to NPOC or DIC analysis, samples require filtration using a 0.45 µm PES filter which is rinsed with ultra-pure water, aiming to remove bigger particles. The analytical deviation of both NPOC and DIC is 2%.

II.4.3 Chemical oxygen demand

Chemical oxygen demand (COD), a global indicator of water quality, represents the amount of oxygen required to oxidize substances (organics and some salts) in wastewater. In this thesis, COD test vials (HACH), containing dichromate reagent as a chemical oxidant, are used to measure COD with a low range of 0 - 150 mg L⁻¹ and a high range of 0 - 1500 mg L⁻¹. 2 mL of samples are added to the vial with a clean pipet, which is then digested in a preheated reactor (HACH Co., USA) at 150 °C for 2 h. COD of samples after heating is determined with a direct reading UV spectrophotometer (DR/2000, HACH Co., USA) at a wavelength of 420 nm for the low range and of 620 nm for the high range, respectively. In the case of real urine, before COD analysis, the solutions should be diluted, and the dilution times are depending on the COD content in the real urine. The analytical uncertainty for this method is ±2 mg L⁻¹ (0 - 150 mg L⁻¹) and ±10 mg L⁻¹ (0 - 1500 mg L⁻¹), respectively.

II.4.4 Ions analysis

The concentrations of cations (Na⁺, K⁺, N-NH₄⁺, Mg²⁺ and Ca²⁺) and anions (Cl⁻, N-NO₂⁻, N-NO₃⁻, SO₄²⁻ and P-PO₄³⁻) is determined with an ionic chromatography (IC) system (IC 25 and ICS-2000, Dionex, USA). Prior to sample analysis, the IC system is calibrated with a standard solution. Ions in the sample can be identified and quantified by comparing the data from samples and from the known standard. Before analysis, samples should be passed through a 0.2 µm PES filter which is rinsed with ultra-pure water. The analytical deviation for this method is 10%.

II.4.5 Ultraviolet absorbance

Ultraviolet absorbance at 254 nm and 280 nm (UV₂₅₄ and UV₂₈₀), important parameters for water quality, provide indications of organic matters content in water. UV₂₅₄ is linked to organic compounds containing aromatic ring or unsaturated bonds, such as humic substances. UV₂₈₀ relates to amino acids with aromatic rings, such as tryptophan. Ultraviolet absorbance (UVA) measurement of samples filtered with 0.45 µm PES filter is carried out by using a UV/Visible V-530 spectrophotometer (Shimadzu, Japan) at a given wavelength (254 nm and 280 nm). A quartz cell with the path length of 1 cm is used. The analytical uncertainty for UV₂₅₄ and UV₂₈₀ is ±0.002 cm⁻¹.

II.4.6 Size-exclusion high performance liquid chromatography

Size-exclusion high performance liquid chromatography (HPLC-SEC) analysis is performed using an AKTA Purifier system (GE Healthcare, USA), which is equipped with a fluorescence detector (excitation/emission: 280/380 nm). A Shodex Protein KW804 column (particle size: 7 µm), with an exclusion limit of 1000 kDa, is used in this thesis. The system is operated at a flow rate of 1.0 mL min⁻¹ with mobile phase prepared with 25 mmol Na₂SO₄ and a phosphate buffer at pH 6.8 (2.4 mmol NaH₂PO₄ and 1.6 mmol Na₂HPO₄). To determine the distribution of protein-like substances in wastewater, several standard proteins (provided by GE healthcare) with different molecular weight are used, i.e., aldolase (158 kDa), conalbumin (75 kDa), ovalbumin (43 kDa), carbonic anhydrase (29 kDa), ribonuclease A (13.7 kDa), and aprotinin (6.5 kDa). Prior to analysis, samples should be passed through a 0.45 µm PES

filter already rinsed with ultra-pure water.

II.4.7 Polysaccharides and proteins

The concentration of polysaccharides in wastewater is determined by Anthrone method (Dreywood, 1946). The mixture of 0.5 mL samples and 1 mL anthrone solution (0.2 g anthrone in 100 mL sulfuric acid) is heated at 105 °C for 15 min. During the heating process, polysaccharides are hydrolysed in the presence of sulfuric acid, and then monosaccharides are dehydrated by anthrone (green colour). The absorbance is measured at 620 nm. There is a linear relationship between the absorbance and the content of polysaccharides in wastewater. Glucose is used as a standard. The analytical uncertainty for this method is 10%.

The bicinchoninic acid assay (BCA) is used to quantify the concentration of total proteins in wastewater (Olson and Markwell, 2007). The principle of this method is that cysteine, cystine, tryptophan, tyrosine and peptide bond in proteins could reduce Cu^{2+} to Cu^+ under alkaline conditions, and Cu^+ react with BCA to form a purple-coloured complex (BCA- Cu^+) which strongly adsorbs at a wavelength 570 nm. The mixture of 0.05 mL samples and 1 mL solutions containing BCA and CuSO_4 is heated at 60 °C for 15 min in the thermostatic bath. The amount of Cu^{2+} reduction is proportional to the protein content. The concentration of proteins in wastewater is obtained by comparing with a calibration curve which is prepared with bovine serum albumin protein standard. The analytical uncertainty for this method is 20% for the protein concentration of $\leq 25 \text{ mg L}^{-1}$ and 10% for the concentration of $\geq 25 \text{ mg L}^{-1}$.

II.4.8 Micropollutants

The analytical determination of carbamazepine (CBZ) and ketoprofen (KET) with mg L^{-1} range in the aqueous solution is performed using reverse phase-HPLC (Agilent LC 1200, USA) equipped with a UV diode-array detector. Separation is carried out with ZORBAX Eclipse XDB-C 18 column (4.6×150 mm, 5 μm) in the isocratic mode with water of 55% and ethanol of 45% (v/v). The injection volume of samples and the flow rate are set as 20 μL and 1 mL min^{-1} , respectively. The system is operating at 40 °C. CBZ and KET are detected at the UV wavelength of 285 nm and 260 nm, respectively. The retention time of KET and CBZ are 1.7 min and 2.9 min, respectively. The limit of detection for CBZ and KET is 5 $\mu\text{g L}^{-1}$ and 10 $\mu\text{g L}^{-1}$, respectively.

The concentration of target PhACs ($\mu\text{g L}^{-1}$ range) in the municipal effluents and in the urine-based solution is performed using UHPLC/MS/MS at the Chemistry Institute of Toulouse in France with a QuEChERS (Quick, Easy, Cheap, Effective, Rugged, Safety) method (Cavallé et al., 2017).

**Chapter III Combining RO and ozonation process for municipal
wastewater reuse: RO membrane fouling and emerging
micropollutants removal**

Introduction

At present, MBR followed by an RO process (MBR-RO) has gained worldwide acceptance as a most promising technology for municipal wastewater reclamation to produce high-quality reclaimed water (Cartagena et al., 2013; Dialynas and Diamadopoulos, 2009; Dolar et al., 2012; Jacob et al., 2010; Sahar et al., 2011). However, RO membrane fouling and the disposal of RO concentrate are two main challenges in the sustainable application of this integrated system for municipal wastewater reuse.

RO membrane fouling is a complicated phenomenon, which is prone to occur in different forms (scaling, organic fouling, biofilm and colloidal fouling) (Jiang et al., 2017). MBR permeate constituents, including inorganic ions and organic matters, are mainly associated with how fouling develops in the RO membrane (Jacob et al., 2010; Kimura et al., 2016; Lee et al., 2006; Moreno et al., 2013).

On the other hand, the application of RO process in an MBR-RO system inevitably generates a concentrated waste stream. RO concentrate is characterized by a broad range of inorganic and organic substances at elevated concentrations, such as salts, organic matters, and refractory organic compounds (Bagastyo et al., 2011a; Pérez-González et al., 2012). Several studies have shown that the direct discharge of RO concentrate to the environment may be associated with a risk of toxicity for aquatic organisms (Tang et al., 2013; Zhou et al., 2011). Therefore, it is of importance to establish beneficial reuse strategies for RO concentrate management.

To reduce the quantities of untreated RO concentrate discharge into the natural water environment and to improve the overall water recovery rate, a possible strategy is to recycle RO concentrate back to the preceding MBR unit in an MBR-RO system. It should be pointed out that, however, the recirculation of RO concentrate to the MBR possibly change the compositions of both MBR permeate and RO concentrate, further affecting the fouling propensity of the RO membrane in an MBR-RO system.

In addition, the concentration of the majority of micropollutants in RO concentrate is found to be several times larger than in the wastewater treatment plants (WWTPs) effluents as RO feed water (Benner et al., 2008; Justo et al., 2013; Urtiaga et al., 2013). In order to reduce the environmental effects of RO concentrate, advanced treatment process, such as ozonation, should be used to eliminate these micropollutants from RO concentrate.

In this context, the first objective of the present study was to investigate the effect of RO concentrate recycling to MBR on the RO performance with respect to RO membrane fouling and the retention capacity for the global water quality parameters. The MBR performance was presented in another Ph.D. thesis. The second one was to evaluate the removal efficiency of trace PhACs by the RO process followed by ozonation.

III.1 Experimental protocols

For these purposes, RO pilot in cross-flow mode and semi-batch ozonation pilot were used to treat municipal MBR permeate. Detailed information on the operation of both RO pilot and ozonation process

has been given in Chapter II.2 and Chapter II.3, respectively. MBR permeate was first treated by the RO process. During the treatment of MBR permeate by the RO process, RO permeate was discharged directly, while RO concentrate was disposed through: (1) continuously recycling back to MBR unit to reduce the quantity of RO concentrate (Set 1); and (2) ozonation to eliminate micropollutants present in RO concentrate (Set 2), as depicted in Figure 3.1.

In this study, ESPA2 RO membrane was used, and whose characteristics are shown in Table 2.3 (see Chapter II.2).

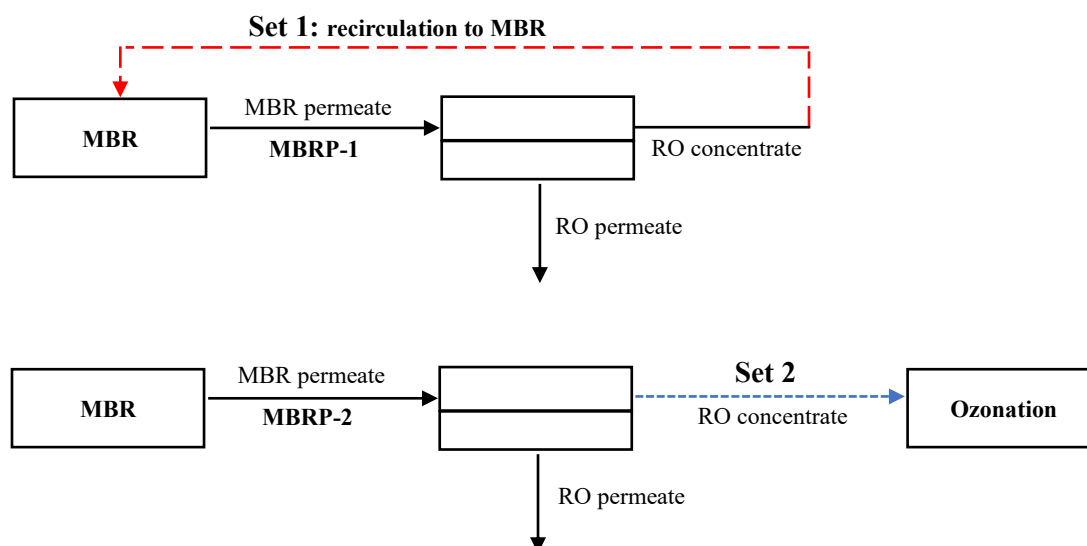


Figure 3.1 Treatment schema of MBR permeate

In Set 1, RO concentrate produced in the MBR-RO system was recirculated continuously to the MBR. Before and during RO concentrate recycling, RO performance was addressed in terms of RO membrane fouling potential and the retention capacity of the RO membrane for the solutes. RO membrane fouling was studied by analysing the reduction in RO permeate flux, osmotic pressure effect of the retained ions, saturation index (SI) of common scalants, as well as the organic load in the bulk RO concentrate. RO permeate flux was determined by Equation 3 (see Chapter II.2). The retention capacity of the RO membrane for the global water quality parameters was estimated using Equation 8 (see Chapter II.2). More details regarding RO process operating conditions were given in Section III.3.

In Set 2, RO concentrate, produced during the treatment of MBR permeate by the RO process without RO concentrate recycling, was treated by a followed ozonation process to remove trace PhACs. The removal efficiency of the target PhACs by ozonation was calculated based on their concentration before and after ozonation process. More details regarding RO process operating conditions were given in Section III.4.

III.2 Characteristics of MBR permeate

Prior to the collection of MBR permeate, a lab-scale MBR system for municipal wastewater treatment has been operated for six weeks to achieve stable performance. Table 3.1 shows the main

characteristics of two tested MBR permeates (MBRP-1 and MBRP-2). The two MBR permeate had a similar conductivity, $1268 \pm 26 \mu\text{S cm}^{-1}$ for MBRP-1 and $1330 \pm 26 \mu\text{S cm}^{-1}$ for MBRP-2. The quantity of organic matters (NPOC) was 2.3 times higher in MBRP-1 than MBRP-2. Moreover, in MBR permeate, the presence of pharmaceutically active compounds (PhACs), including carbamazepine (CBZ), diclofenac (DIF), ibuprofen (IBP), propranolol (PRO) and ketoprofen (KET), was mainly due to the spike of target PhACs in MBR influents. Their concentration varied from $0.12 \mu\text{g L}^{-1}$ of KET to $16.1 \pm 0.9 \mu\text{g L}^{-1}$ of DIF. The key properties of these target PhACs are given in Table 2.1 in Chapter II.1.

Table 3.1 Characteristics of two tested MBR permeate (as RO feed)

Parameter	Unit	MBRP-1 for Set 1	MBRP-2 for Set 2
pH	-	8.1	8.4
Conductivity	$\mu\text{S cm}^{-1}$	1268 ± 26	1330 ± 26
NPOC ¹	mg L^{-1}	5.8 ± 0.1	2.5 ± 0.1
Proteins	mg L^{-1}	6.5 ± 1.3	- ⁵
Polysaccharide	mg L^{-1}	1.0 ± 0.1	-
COD ²	mg L^{-1}	21 ± 2	10 ± 2
UV ₂₈₀	cm^{-1}	0.152 ± 0.002	0.040 ± 0.002
UV ₂₅₄	cm^{-1}	0.118 ± 0.002	0.047 ± 0.002
DIC ³	mg L^{-1}	6.5 ± 0.1	88 ± 2
Cl ⁻	mg L^{-1}	127 ± 13	189 ± 19
N-NO ₂ ⁻	mg L^{-1}	n.d. ⁴	0.33 ± 0.03
N-NO ₃ ⁻	mg L^{-1}	5.0 ± 0.5	0.27 ± 0.03
HCO ₃ ⁻	mg L^{-1}	27 ± 3	445 ± 9
SO ₄ ²⁻	mg L^{-1}	43 ± 4	10 ± 1
P-PO ₄ ³⁻	mg L^{-1}	0.90 ± 0.09	1.2 ± 0.1
Na ⁺	mg L^{-1}	176 ± 18	108 ± 11
N-NH ₄ ⁺	mg L^{-1}	n.d.	0.36 ± 0.04
K ⁺	mg L^{-1}	12 ± 1	9.3 ± 0.9
Mg ²⁺	mg L^{-1}	5.7 ± 0.6	2.7 ± 0.3
Ca ²⁺	mg L^{-1}	70 ± 7	92 ± 9
Carbamazepine	$\mu\text{g L}^{-1}$	0.43	4.2 ± 0.1
Diclofenac	$\mu\text{g L}^{-1}$	0.84	16.1 ± 0.9
Ibuprofen	$\mu\text{g L}^{-1}$	-	0.54 ± 0.16
Ketoprofen	$\mu\text{g L}^{-1}$	0.12	-
Propranolol	$\mu\text{g L}^{-1}$	-	1.6 ± 0.1

(1) NPOC: non-purgeable organic carbon. (2) COD: chemical oxygen demand. (3) DIC: dissolved inorganic carbon. (4) n.d. : not detected. (5) - : not analysed.

III.3 RO performance with RO concentrate recirculation to MBR (Set 1)

This section presented the impacts of RO concentrate continuous recycling to MBR on the RO performance. The experimental approach was first presented. The influences of RO concentrate recycling on the retention capacity of the RO membrane for global water quality parameters (ions and organic matters) and for the target micropollutants and on the RO permeate quality were then discussed. At last, RO membrane fouling potential was studied before and during RO concentrate recycling.

III.3.1 MBR-RO process with RO concentrate recycling

Figure 3.2 depicts the pilot-scale MBR-RO system with RO concentrate recirculation to the MBR. The MBR system was equipped with an anoxic reactor (5.4 L) and an aerobic reactor (12.6 L). A flat-sheet MF membrane (0.2 μm pore size, 0.1 m^2 surface area, Kubota, Japan) was submerged in the aerobic tank. The solid retention time (SRT) and hydraulic retention time (HRT) were 45 days and 18.4 h, respectively. MBRP-1, produced at a flow rate of 23.6 L d^{-1} , was first stored in a tank for RO tests. The principal operating conditions of the MBR pilot are summarized in Table 3.2.

In this work, the RO process was operated at a cross-flow velocity of 0.18 m s^{-1} and a temperature of 22 ± 1 $^{\circ}\text{C}$. The transmembrane pressure (ΔP) was around 7 bar. CF was set to around 3, where the first 5 hours were required to increase CF to 3. During the treatment of MBR permeate by the RO process, the actual CF was around 2.8. Operation of RO pilot at a fixed CF has been described in detail in Chapter II.2. RO experiment of MBR permeate lasted 17 days. The MBRP-1 produced in MBR was fed continuously to the RO process at an average flow rate of 16.8 L d^{-1} . RO concentrate produced (6.0 L d^{-1}) was collected in a tank. From the first 3 days on, RO concentrate started to be recycled to the MBR unit at a flow rate of 4.8 L d^{-1} , which represented 20% of MBR inflow (RO concentrate + wastewater). To prevent inorganic scaling on the RO membrane surface, the solution pH of MBR permeate as RO feed was adjusted to ~ 6 by using 1 mol L^{-1} HCl. At the end of the test, the recirculation loop was deconcentrated with distilled water as RO feed under the same operating conditions (velocity: 0.18 m s^{-1} and ΔP : 7 bar), aiming to remove substances accumulated at the RO membrane surface. The principal operating conditions of RO process are also presented in Table 3.2.

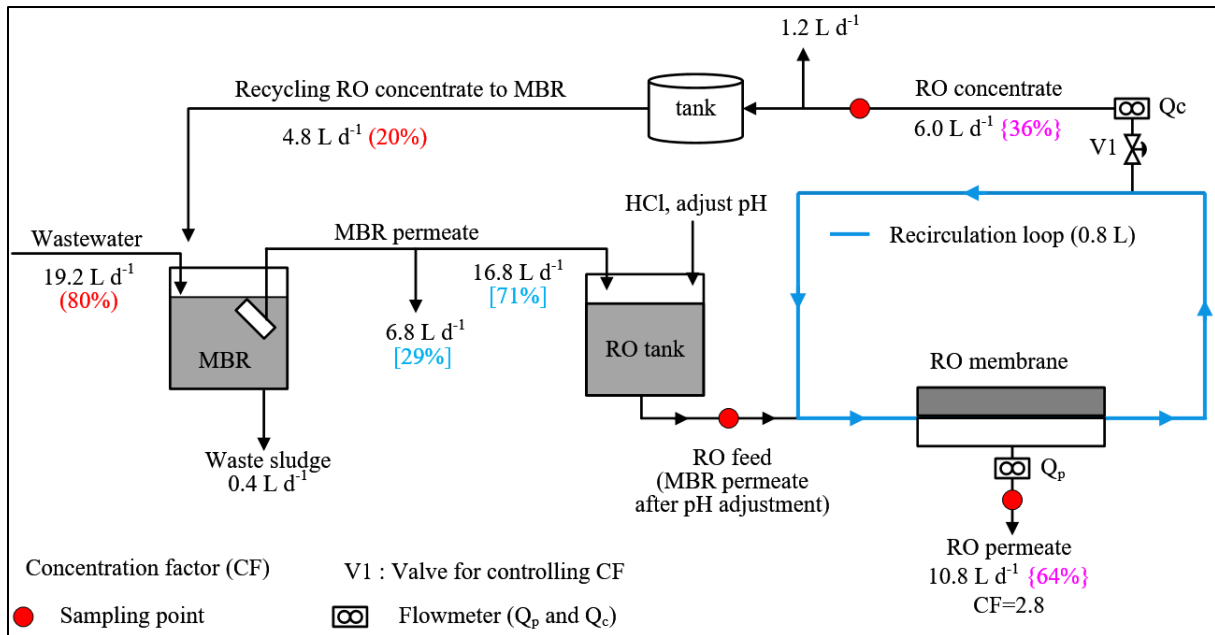


Figure 3.2 Schematic of cross-flow RO pilot with recirculation of RO concentrate to the MBR unit. (%): MBR influent consisted of 80% wastewater and 20% RO concentrate. [%]: 71% of the total flow of MBR permeate was used as RO feed water. {%}: RO permeate represent 64% of RO feed flow, and the rest (36%) of RO feed flow formed the RO concentrate stream.

Table 3.2 Operating conditions of MBR pilot and RO process

MBR unit		RO process	
Net flux of MBR permeate	9.8 L h ⁻¹ m ⁻²	Membrane	ESPA2
Filtration/relaxation cycles	8 min / 4 min	Cross-flow velocity	0.18 m s ⁻¹
Solid retention time (SRT)	45 day	ΔP	~7 bar
Hydraulic retention time (HRT)	18.4 h	pH of RO feed	~6
Aerobic MLSS	7.7 ± 0.8 g L ⁻¹	Temperature	22 ± 1 °C
Aeration	With big air bubbles at a flow rate of 1.5 L min ⁻¹	CF	~ 3

If the treated water was used for non-potable reuse, e.g., industrial use or landscape irrigation, the water recovery of the MBR-RO process (R_{MBR-RO}) was defined in Equation 25, and the value was around 92%.

$$R_{MBR-RO} (\%) = \frac{(Q_{MBR \text{ permeate discharged}} + Q_{RO \text{ permeate}})}{Q_{wastewater}} \times 100 \quad (\text{Equation 25})$$

Where $Q_{MBR \text{ permeate discharged}}$ refers to the flow rate of MBR permeates that are not used as RO feed water (6.8 L d⁻¹) (See Figure 3.2). $Q_{RO \text{ permeate}}$ is the flow rate of RO permeates produced, and the value is around 10.8 L d⁻¹. $Q_{wastewater}$ is the flow rate of MBR inflow (19.2 L d⁻¹).

If high-quality water was used for specific reuse, the water recovery of the process (R_{RO}) was around 64%.

$$R_{RO} (\%) = \frac{Q_{RO \text{ permeate}}}{Q_{RO \text{ feed}}} \times 100 \quad (\text{Equation 26})$$

III.3.2 Characteristics of MBR permeate produced before and during RO concentrate recycling

The characteristics of municipal wastewater and of the permeate produced by the MBR first without and then with RO concentrate recirculation are given in Table 3.3. It was observed that, the MBR was effective in removing organic matters, with a removal around 97% for NPOC. As expected, the elimination of inorganic salts by MBR was relatively poor, which meant that most of the ionic salts passed through MF membrane in MBR and were present in MBR permeate. A higher Cl^- concentration in MBR permeate than wastewater was explained by the addition of HCl for pH adjustment during the RO process. On the other hand, after the recirculation of RO concentrate to the MBR, the concentration of inorganic and organic substances present in MBR permeate increased with the recirculation of RO concentrate, as discussed later.

Table 3.3 Compositions of wastewater and MBR permeate (RO feed) without and with RO concentrate recycling to MBR

Parameters	Unit	Wastewater	MBR permeate					
			before recycling (MBRP-1)	after 2 d of recycling	after 4 d of recycling	after 9 d of recycling	after 11 d of recycling	14 d after recycling
Operating time for RO	day	-	3	5	7	12	14	17
pH	-	- ¹	8.1	7.4	6.8	6.5	6.3	6.9
Conductivity	$\mu\text{S cm}^{-1}$	-	1268 \pm 26	1728 \pm 35	2055 \pm 41	2230 \pm 45	2285 \pm 46	2240 \pm 45
NPOC ²	mg L^{-1}	231 \pm 5	5.8 \pm 0.1	7.7 \pm 0.2	8.7 \pm 0.2	9.7 \pm 0.2	11.1 \pm 0.2	12.6 \pm 0.3
Proteins	mg L^{-1}	33.4 \pm 3.3	6.5 \pm 1.3	8.0 \pm 1.6	-	-	12.1 \pm 2.4	-
Polysaccharide	mg L^{-1}	7.4 \pm 0.7	1.0 \pm 0.1	2.0 \pm 0.2	-	-	1.7 \pm 0.2	-
COD ³	mg L^{-1}	830 \pm 10	21 \pm 2	27 \pm 2	25 \pm 2	34 \pm 2	32 \pm 2	34 \pm 2
UVA ₂₅₄ ⁴	cm^{-1}	-	0.152 \pm 0.002	0.204 \pm 0.002	0.226 \pm 0.002	0.245 \pm 0.002	0.251 \pm 0.002	0.260 \pm 0.002
UVA ₂₈₀	cm^{-1}	-	0.118 \pm 0.002	0.151 \pm 0.002	-	-	0.198 \pm 0.002	-
DIC ⁵	mg L^{-1}	-	6.5 \pm 0.1	7.9 \pm 0.2	8.6 \pm 0.2	9.7 \pm 0.2	10.1 \pm 0.2	11.2 \pm 0.2
Cl ⁻⁶	mg L^{-1}	64 \pm 6	127 \pm 13	-	357 \pm 36	-	505 \pm 51	-
N-NO ₃ ⁻	mg L^{-1}	0.20 \pm 0.02	5.0 \pm 0.5	-	6.4 \pm 0.6	-	7.1 \pm 0.7	-
HCO ₃ ⁻	mg L^{-1}	-	27 \pm 3	-	34 \pm 3	-	26 \pm 3	-
SO ₄ ²⁻	mg L^{-1}	42 \pm 4	43 \pm 4	-	75 \pm 8	-	81 \pm 8	-
P-PO ₄ ³⁻	mg L^{-1}	3.0 \pm 0.3	0.90 \pm 0.09	-	0.70 \pm 0.07	-	1.5 \pm 0.2	-
Na ⁺	mg L^{-1}	174 \pm 17	176 \pm 18	-	293 \pm 29	-	406 \pm 41	-
K ⁺	mg L^{-1}	14 \pm 1	12 \pm 1	-	20 \pm 2	-	25 \pm 3	-
Mg ²⁺	mg L^{-1}	8.4 \pm 0.8	5.7 \pm 0.6	-	10 \pm 1	-	12 \pm 1	-
Ca ²⁺	mg L^{-1}	124 \pm 12	70 \pm 7	-	114 \pm 11	-	118 \pm 12	-

(1) -: not analysed. (2) NPOC: non-purgeable dissolved organic carbon. (3) COD: chemical oxygen demand. (4) UV: ultra-violet absorbance. (5) DIC: dissolved inorganic carbon. (6): for MBR permeate, the amount of Cl⁻ introduced by RO feed pH control was also included

III.3.3 Influence of RO concentrate recycling on RO retention capacity for NPOC, COD and ions

Dissolved organic carbon (NPOC), chemical oxygen demand (COD), and ions were considered as indicators to evaluate RO performance in terms of RO retention capacity in the MBR-RO system with RO concentrate recycling. The observed retention for such parameters was calculated based on their concentration measured in the bulk RO concentrate and RO permeate, as shown in Equation 8 (see Chapter II.2).

Figure 3.3a displays the concentration of organic matters in terms of NPOC in the three flows, including MBR permeate, RO permeate and RO concentrate, before and during RO concentrate recirculation. The recirculation of RO concentrate induced an increase up to a factor of 2.2 in the concentration of NPOC in MBR permeate after two weeks. There were two reasons for this increase of organic matters in MBR permeate: one was the recirculation of poorly biodegradable organics with small molecular weight (MW) from RO concentrate to MBR influents; and the other was that the continuous addition of salts into the MBR may decrease the microbial activity for the degradation of low MW organics in the MBR or increase the release of SMPs. Indeed, the amount of low MW acid and neutral type substances increased in MBR effluents when salt concentration increased from 0 to 35 g NaCl L⁻¹ in MBR (Johir et al., 2013). Regarding RO concentrate, after only 2 days of RO concentrate recycling, the concentration of NPOC rose rapidly from 20.4 ± 0.4 mg L⁻¹ before RO concentrate recycling to 25.6 ± 0.5 mg L⁻¹ and then maintained a relatively constant level over the following 7 days. After 9 days of RO concentrate recycling, the concentration of NPOC in RO concentrate increased sharply, and finally reached 35.0 ± 0.6 mg L⁻¹ in the next 5 days. The rapid increase of NPOC in RO concentrate mainly resulted from the increase in organic matters in MBR permeate and the excellent rejection (>98%) of organic matters (NPOC) by the RO membrane. During the period of RO concentrate recycling, the concentration ratio of NPOC in RO concentrate and MBR permeate was around 2.7, which was consistent with the studied CF of 3. Despite RO concentrate recirculation, the concentration of NPOC in RO permeate remained constant, at a value below 0.57 ± 0.01 mg L⁻¹.

The concentration profile of chemical oxygen demand (COD) was similar to the NPOC curve, as can be seen in Figure 3.3b. After 14 days of RO concentrate recirculation to the MBR, the concentration of COD increased by a factor of 1.4 in MBR permeate (from 25 ± 2 mg L⁻¹ to 34 ± 2 mg L⁻¹), of 1.7 in RO concentrate (from 61 ± 2 mg L⁻¹ to 105 ± 2 mg L⁻¹). In RO permeate, the concentration of COD remained almost constant throughout the experiment, near to the detection limit, which also matched a fact of the overall retention capacity remaining above 94% over the entire filtration experiment.

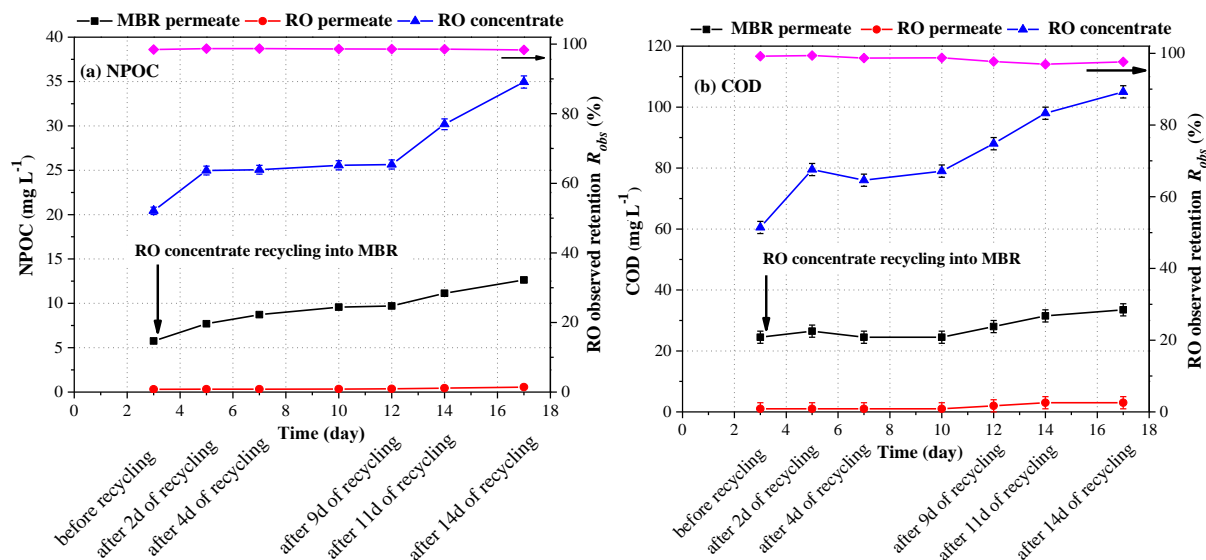


Figure 3.3 Variation of NPOC (a) and COD (b) in RO flows with the recirculation of RO concentrate. MBRP-1. Cross-flow velocity: 0.18 m s^{-1} . ΔP : $\sim 7 \text{ bar}$. CF : ~ 3 .

One of the important constituents that affected the RO membrane fouling was inorganic salts in the RO feed water. Thus, after RO concentrate recycling to the MBR, the concentration of inorganic salts in the RO system was also addressed. Figure 3.4 plots the conductivity variation in RO flows versus the operation time. RO concentrate injection into the MBR unit elevated significantly the conductivity in MBR permeate and in RO concentrate until Day 7 (4 days after start of RO concentrate recycling). After that, the curve showed a plateau for the next 10 days. The conductivity of RO concentrate was approximately 3-fold higher than that of MBR permeate, which revealed that the RO filtration was carried out with a nearly constant CF of 3 in terms of conductivity. In contrast, variation in the conductivity of RO permeate was less significant, with values ranging only between $176 \pm 4 \mu\text{S cm}^{-1}$ and $290 \pm 6 \mu\text{S cm}^{-1}$. Throughout the experiment, the observed retention of conductivity was around 95%.

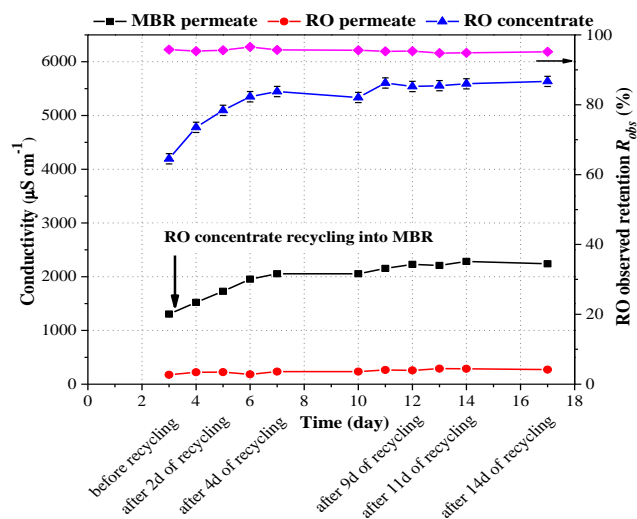


Figure 3.4 Variation of conductivity in RO flows as a function of operation time. MBRP-1. Cross-flow velocity: 0.18 m s^{-1} . ΔP : $\sim 7 \text{ bar}$. CF : ~ 3 .

Table 3.4 displays the retention capacities of the RO membrane for anions and cations before and during RO concentrate recirculation. Firstly, as expected, before RO concentrate recycling, the RO membrane presented the retention rate higher than 86% for every ion not including P-PO₄³⁻. Hence, the recirculation of RO concentrate to MBR did not influence the retention capacities of the RO membrane for most of the ions. The abnormal trend of the retention of the RO membrane for P-PO₄³⁻ is possibly related to the variation in concentration of P-PO₄³⁻ in the bulk RO concentrate and the changed pH of RO concentrate. Pinto et al. (2011) pointed out that, when solution pH increased more basic values, calcium phosphate becomes increasingly insoluble. As illustrated in Table 3.4, it was also noticed similar retention capacities of the RO membrane for all monovalent or divalent ions, suggesting that other mechanisms were also responsible for the rejection of the RO membrane for the tested ions, in addition to the hydrated ion sizes and the charge effect.

Table 3.4 RO membrane retention capacities for anions and cations

R_{obs} (%) ¹	Hydrated radius (nm) ^a	before recycling	after 4d of recycling	after 11d of recycling
pH of RO concentrate	-	7.40	7.14	6.90
Cl ⁻	0.332	96	95	95
N-NO ₃ ⁻	0.335	86	89	88
HCO ₃ ⁻	- ^b	95	97	97
SO ₄ ²⁻	0.379	98	98	99
P-PO ₄ ³⁻	- ^b	77	90	93
Na ⁺	0.358	95	95	93
K ⁺	0.331	97	95	93
Mg ²⁺	0.428	97	98	98
Ca ²⁺	0.412	96	97	98

(1) R_{obs} is calculated by Equation 9. (a) values from Tansel (2012). (b) not found in the literature.

Figure 3.5 shows the variation of ionic concentration before and during RO concentrate recirculation. Since almost all the cations and anions passed through the MF membrane in MBR, the continuous recirculation of RO concentrate with a high load of ionic salts led to a significant rise in the concentration of ionic salts in both MBR permeate and RO concentrate, as indicated in Figure 3.5. After 11 days of RO concentrate recirculation, the ion concentration in MBR permeate was 4.0 times higher for Cl⁻, 1.4 times higher for N-NO₃⁻, 1.9 times higher for SO₄²⁻, 1.7 times higher for P-PO₄³⁻, 2.3 times higher for Na⁺, 2.0 times higher for K⁺, 2.1 times higher for Mg²⁺, and 1.7 times higher for Ca²⁺ than that obtained before RO concentrate recycling. With respect to RO concentrate, as compared to the initial results (without RO concentrate recycling), 11 days of RO concentrate recirculation also increased the concentration of these ions, 2.9 times for Cl⁻, 1.2 times for N-NO₃⁻, 1.4 times for SO₄²⁻, 4.1 times for P-PO₄³⁻, 1.1 times for Na⁺, 1.5 times for K⁺, 1.8 times for Mg²⁺, and 1.5 times for Ca²⁺, respectively.

The different increased level of Cl^- in MBR permeate (4.0 times higher) and RO concentrate (2.9 times higher) was associated with the addition of HCl for controlling RO membrane scaling.

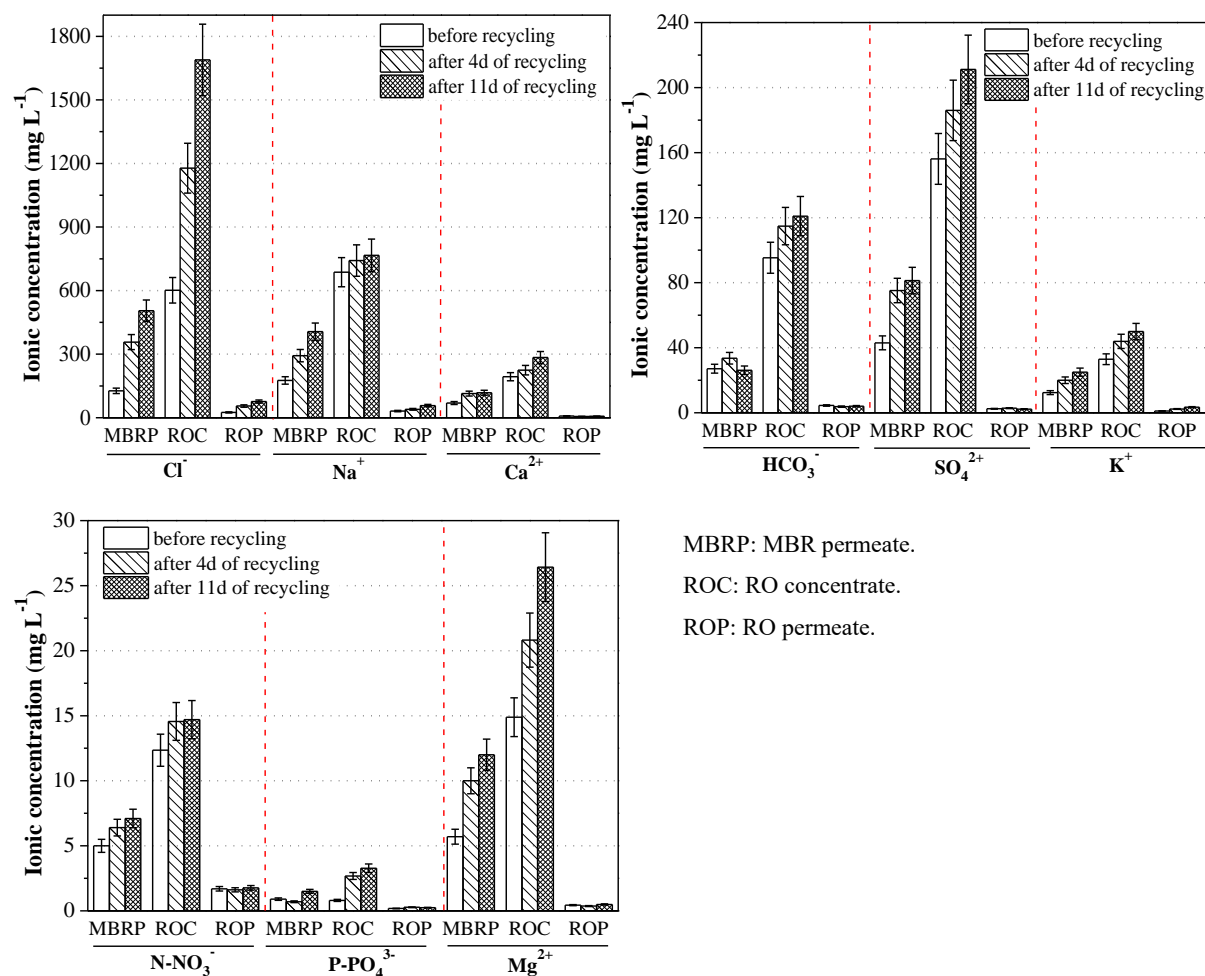


Figure 3.5 Effect of RO concentrate recycling on the concentration of ionic salts in the RO flows. MBRP-1. Cross-flow velocity: 0.18 m s^{-1} . ΔP : $\sim 7 \text{ bar}$. CF: ~ 3 .

To sum up, the recirculation of RO concentrate to the MBR did not influence significantly the global performance of the RO system in terms of RO permeate quality or the retention capacities of the most common monitoring parameters. The RO permeate produced without and with RO concentrate recirculation could meet the standard for reclaimed water reuse in several industrial processes or for indirect potable reuse (Asano and Metcalf & Eddy, Inc., 2007).

III.3.4 Influence of RO concentrate recycling on RO membrane fouling propensity

As discussed above, the recirculation of RO concentrate, containing salinity and non-degradable organics to the MBR in the MBR-RO system, led to a significant increase in the concentration of inorganic or organic substances in MBR permeate. However, such components in MBR permeate were almost totally retained by the following RO membrane. Consequently, the continuous accumulation of solutes on the RO membrane surface possibly affected RO membrane fouling potential. In this section, the fouling behaviour of the RO membrane was examined through the variation of the RO permeate flux

versus operating time, osmotic pressure model, saturation index (SI) and the analysis of the concentration of protein-like substances in the RO flows.

III.3.4.1 RO membrane fouling in terms of RO permeate flux decline

Figure 3.6 shows the RO permeate flux behaviour before and after the start of RO concentrate recirculation to the MBR under the operating conditions investigated. Three different stages were identified in Figure 3.6: Stage 1 (0 - Hour 5, CF increase, no RO concentrate recycling), Stage 2 (Hour 5 - Day 3, CF kept constant at 3, no RO concentrate recycling), and Stage 3 (Day 3 - Day 17, CF kept constant at 3, RO concentrate recycling). In Stage 1, a rapid decline in permeate flux was observed, with a reduction of approximately 30% of the initial permeate flux when CF reached 3. This remarkable loss in RO permeate flux could be linked to a rapid accumulation of solutes (inorganic ions and organic matters) on the RO membrane surface with CF increase. In the following 3 days (Stage 2), RO permeate flux remained almost constant. Once RO concentrate was added into the MBR from Day 3 (Stage 3), RO permeate flux started to decrease slowly over the next 14 days, and an additional 19% reduction in RO permeate flux was noted, from $8.9 \text{ L h}^{-1} \text{ m}^{-2}$ to $6.5 \text{ L h}^{-1} \text{ m}^{-2}$.

At the end of the experiment, MBR permeate was replaced by distilled water as RO feed. After 3.5 hours' deconcentration of the recirculation loop with distilled water at the same cross-flow velocity of 0.18 m s^{-1} , around 35% of the initial RO permeate flux could be recovered, indicating that the accumulation of some solutes was removable. This removal fouling mechanism related to concentration polarization (CP) or the precipitation of retained ions. On the other hand, the incomplete recovery of the flux (around 16% of initial RO permeate flux) may be associated with a colloidal cake layer or adsorption of organic matters on the RO membrane surface.

To better understand the impact of RO concentrate recycling on RO fouling behaviour, deeper analysis was developed below regarding the role of inorganic salts and organics in the reduction of RO permeate flux.

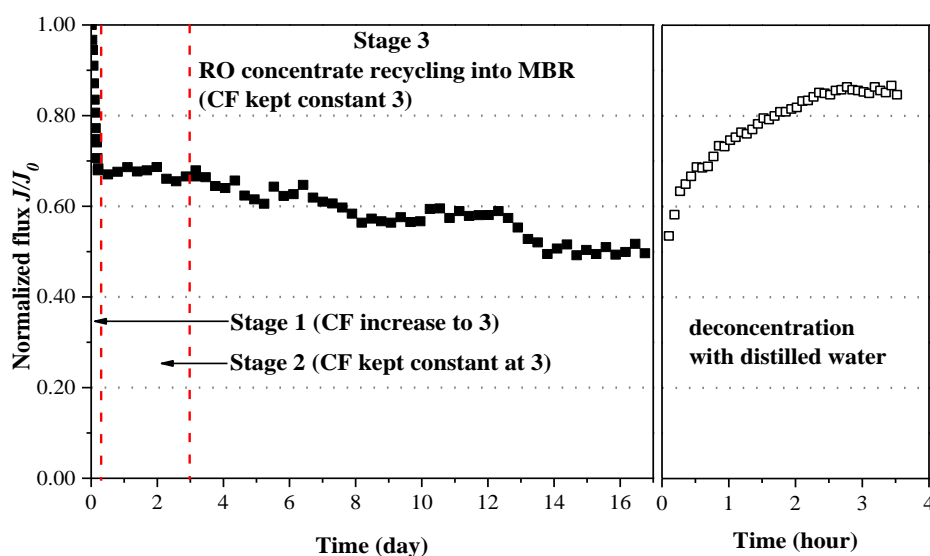


Figure 3.6 RO permeate flux behaviour throughout the operating time. MBRP-1. Cross-flow velocity: 0.18 m s^{-1} . initial permeate flux: $12.5 \text{ L h}^{-1} \text{ m}^{-2}$. ΔP : $\sim 7 \text{ bar}$. operating temperature: $22 \pm 1 \text{ }^\circ\text{C}$. uncertainty of J/J_0 : ± 0.08 .

III.3.4.2 Impact of osmotic pressure gradient of salts on RO permeate flux decline

The continuous recirculation of RO concentrate caused a high ionic concentration at the RO membrane surface, so it could be possible that the increased osmotic pressure of the ions retained at the membrane surface affected the RO permeate flux. To address this point, the osmotic pressure model (Equation 27) was used to study the effect of the increased osmotic pressure of the ions retained at the membrane surface on the RO permeate flux through the RO membrane.

$$J_{model} = Lp_0(\Delta P - \Delta\pi) \quad (\text{Equation 27})$$

where J_{model} refers to the RO permeate flux that is calculated with the osmotic pressure model ($\text{L h}^{-1} \text{m}^{-2}$). Lp_0 is the permeability of the RO membrane with distilled water ($1.9 \text{ L h}^{-1} \text{m}^{-2} \text{bar}^{-1}$). $\Delta\pi$ is the osmotic pressure difference (bar) of ionic salts between the membrane surface and the RO permeate side, which can be calculated with the Van't Hoff equation (Akbari et al., 2002):

$$\Delta\pi = \pi_m - \pi_p = \sum C_{m,i} z_i RT - \sum C_{p,i} z_i RT \quad (\text{Equation 28})$$

where π_m and π_p are the osmotic pressure of ions at the RO membrane surface and in the RO permeate (Pa), respectively. The unit of both π_m and π_p is converted to bar ($1 \text{ bar} = 10^5 \text{ Pa}$). z_i is the valency of ion i . T is the absolute temperature (K). R is the ideal gas constant, $8.3145 \text{ J mol}^{-1} \text{K}^{-1}$ or $8.3145 \text{ m}^3 \text{ Pa mol}^{-1} \text{K}^{-1}$. $C_{p,i}$ is the concentration of ion i in RO permeate (mol L^{-1}), which can be obtained from the experimental data (see Figure 3.5). $C_{m,i}$ represents the concentration (mol L^{-1}) of ion i at the RO membrane surface, which cannot be measured directly but can be estimated by Equation 29.

$$\ln \frac{C_{m,i} - C_{p,i}}{C_{c,i} - C_{p,i}} = \frac{J_{exp}}{k_i} \quad (\text{Equation 29})$$

where $C_{c,i}$ represents the concentration of ion i in the bulk RO concentrate (mol L^{-1}), the value of which is found from the experiment (see Figure 3.5). J_{exp} is the RO permeate flux from experiments (see Figure 3.6). k_i refers to the mass transfer coefficient of ion i (m s^{-1}), which can be estimated by the following equations (Hoek et al., 2008).

$$k_i = \text{Sh} \frac{D_i}{d_H} = 0.065 \text{Re}^{0.875} \text{Sc}^{0.25} \frac{D_i}{d_H} \quad (\text{Equation 30})$$

$$\text{Re} = \frac{\rho U d_H}{\mu} \quad (\text{Equation 31})$$

$$\text{Sc} = \frac{\mu}{\rho D_i} \quad (\text{Equation 32})$$

$$d_H = 2\varepsilon_{sp}H \quad (\text{Equation 33})$$

where Sh is the Sherwood number. Re is the Reynolds number. Sc is the Schmidt number. D_i is the diffusivity of ion i in water ($\text{m}^2 \text{s}^{-1}$). U is the tangential velocity, equal to 0.18 m s^{-1} . ρ is the volumetric mass density (998 kg m^{-3} at $22 \text{ }^\circ\text{C}$). d_H is the hydraulic diameter of a rectangular channel. μ is the viscosity of the solution (0.9544 mPa s at $22 \text{ }^\circ\text{C}$). H is the spacer thickness (0.00063 m). ε_{sp} is the spacer porosity (0.8). Throughout the RO process, the operating temperature was kept at $22 \pm 1 \text{ }^\circ\text{C}$, so the viscosity, density, and diffusivity of the feed solution were constant here. The k_i values of ion i are summarized in Table 3.5.

Table 3.5 Diffusion coefficient, Reynolds Number, Schmidt Number, Sherwood Number, and transfer coefficient of different ions.

Re=191	Cl ⁻	N-NO ₃ ⁻	HCO ₃ ⁻	SO ₄ ²⁻	P-PO ₄ ³⁻	Na ⁺	K ⁺	Mg ²⁺	Ca ²⁺
$D_i \times 10^{10} \text{ m}^2 \text{ s}^{-1}$ ^a	20.32	19.02	11.85	10.65	8.24	13.34	19.57	7.06	7.92
Sc	471	503	807	898	1161	717	489	1355	1207
Sh	29.8	30.3	34.1	35.0	37.4	33.1	30.1	38.8	37.7
$k_i \times 10^5 \text{ m s}^{-1}$	6.01	5.72	4.01	3.70	3.05	4.38	5.84	2.72	2.96

(a) the diffusion coefficients of ionic species were obtained from Lide, (2005) and Hille, (1992).

Based on the k_i value and the ionic concentration measured in both the RO permeate (C_p) and bulk RO concentrate (C_c), the concentration of each ion at the RO membrane surface (C_m) was calculated before and after RO concentrate recycling, as shown in Table 3.6. The C_m value of each ion increased with RO concentrate recycling. Moreover, the C_m value of each ion was slightly higher than C_c , which confirmed that concentration polarization occurred. The ratio of the ionic concentration between at the RO membrane surface and in the bulk RO concentrate (C_m/C_c) kept almost constant before or during RO concentrate recycling. The average C_m/C_c ratio of different ions is also listed in Table 3.6, ranging from 1.03 times for N-NO₃⁻ to 1.08 times for SO₄²⁻.

Table 3.6 Ionic concentration at the RO membrane surface before and during RO concentrate recirculation

Ions	before recycling				during recycling (Stage 3)				average C_m/C_c ¹
	Hour 5 (end of Stage 1)		Day 3 (end of Stage 2)		Day 7 (after 4 d of recycling)		Day 14 (after 11 d of recycling)		
	C_m	C_c	C_m	C_c	C_m	C_c	C_m	C_c	
Cl ⁻	556	534	627	602	1220	1178	1740	1689	1.04
N-NO ₃ ⁻	13	12	13	12	15	15	15	15	1.03
HCO ₃ ⁻	95	89	101	95	121	115	126	121	1.05
SO ₄ ²⁻	164	154	170	156	201	186	226	211	1.08
P-PO ₄ ³⁻	0.89	0.84	0.85	0.80	2.9	2.7	3.5	3.3	1.06
Na ⁺	688	651	725	687	777	742	797	766	1.05
K ⁺	34	32	34	33	45	44	51	50	1.03
Mg ²⁺	16	15	16	15	22	21	28	26	1.07
Ca ²⁺	203	187	209	193	240	225	301	284	1.07

(1) the average ratio of the ionic concentration at the membrane surface and in the bulk RO concentrate

Figure 3.7 shows the osmotic pressure gradient of inorganic salts and the RO permeate flux decline from both the test (J_{exp}) and the model (J_{model}). During the period of CF increase (Stage 1), the osmotic pressure gradient of inorganic salts increased, from the initial 0.37 bar (CF=1) to 1.51 bar when CF

reached 3. The increase of osmotic pressure gradient led to a reduction of 18% in permeate flux from the model, which was lower than the reduction in permeate flux found in the experiment, with a value around 30%, revealing that other fouling behaviour, such as the precipitation of salts, adsorption or a cake layer caused by smaller colloids at the RO membrane surface, took place in this stage. In the following 3 days (Stage 2), the osmotic pressure gradient and RO permeate flux stayed almost constant. However, when RO concentrate was recycled to the MBR from Day 3 (Stage 3), the osmotic pressure gradient of inorganic salts increased gradually, reaching 2.58 bar after 11 d of RO concentrate recycling (Day 14). Correspondingly, the RO permeate flux from the model decreased continuously. In addition, comparing the behaviour of flux in the test and the model (Stage 3), a similar slope as a function of operating time revealed that the increased osmotic pressure caused by RO concentrate recirculation was mainly responsible for the additional 19% decline in RO permeate flux during this stage.

In conclusion, except Stage 1 at the beginning, the RO permeate flux decrease was due to the increased osmotic pressure of retained ions. At the first stage of the operation, adsorption phenomena or colloidal cake layer could happen, which represented 15% of the RO permeate flux decline. This point was confirmed by the reversibility of the fouling by the deconcentration of the recirculation loop with distilled water.

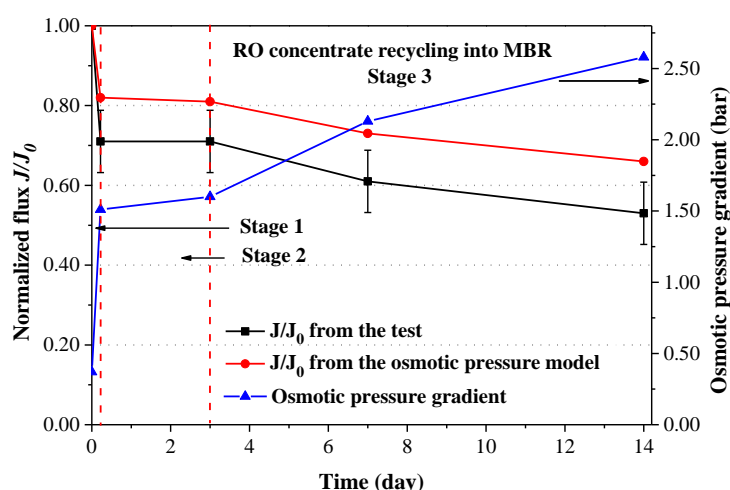


Figure 3.7 Variation of the osmotic pressure gradient of retained ions and RO permeate flux as a function of operation time. MBRP-1. Cross-flow velocity: 0.18 m s^{-1} . ΔP : $\sim 7 \text{ bar}$. initial permeate flux for both the test and the model: $12.5 \text{ L h}^{-1} \text{ m}^{-2}$.

III.3.4.3 Scaling potential analysis based on saturation index model

To confirm a minor effect of inorganic scaling (the precipitation of ionic salts) on the RO permeate flux decline, the most common scalants, hydroxyapatite ($\text{Ca}_5(\text{PO}_4)_3\text{OH}$), calcite (CaCO_3) and gypsum ($\text{CaSO}_4 \cdot 2\text{H}_2\text{O}$) (Jiang et al., 2017), were used to predict the calcium-based salt scaling behaviour on the RO membrane surface. The ionic concentration near the membrane surface was quite similar in RO concentrate, as implied in Table 3.6. Thus, the ionic concentration in RO concentrate was used to estimate the SI value with PHREEQC model. Table 3.7 summarizes the SI values of three scalants in the bulk RO concentrate before and during RO concentrate recirculation. Before or during RO

concentrate recirculation, SI values of alkaline calcite and non-alkaline gypsum were lower than zero, indicating that the corresponding ionic salts were undersaturated. Their lower SI values can be explained by their high k_{sp} : 2.80×10^{-9} for calcite and 4.93×10^{-5} for gypsum. Moreover, with RO concentrate recirculation, a decreasing trend of the SI values for calcite and hydroxyapatite could be explained by the different pH values of RO concentrate at the different operating time. Compared to calcite and gypsum, the SI values of hydroxyapatite, with a relatively low k_{sp} of 2.34×10^{-59} , were above 0 during the entire process, which meant that non-alkaline hydroxyapatite occurred on the RO membrane surface. However, the concentration of $P-PO_4^{3-}$ in MBR permeate was low, with a value of around 0.90 mg L^{-1} . Thus, inorganic precipitation may have become less pronounced for RO membrane fouling potential in this work.

Table 3.7 Saturation index of three common scalants before and after RO concentrate recirculation

SI value (PHREEQC model)		k_{sp}^a	CF around 3		
			Before recycling	after 4 d of recycling	after 11 d of recycling
pH of RO concentrate	-	-	7.4	7.1	6.9
Calcite	$CaCO_3$	2.80×10^{-9}	-0.06	-0.21	-0.38
Gypsum	$CaSO_4 \cdot 2H_2O$	4.93×10^{-5}	-1.29	-1.21	-1.10
Hydroxyapatite	$Ca_5(PO_4)_3OH$	2.34×10^{-59}	6.76	4.53	3.93

(a) from Ball and Nordstrom (1991)

III.3.4.4 Organic fouling potential analysis

The continuous accumulation of MBR effluent organic matters (EfOM) on the RO membrane surface over time also induced RO permeate flux reduction. In this context, protein-like and polysaccharide-like substances, the main organic components in MBR permeate, have been identified as two non-negligible contributors to RO membrane fouling (Wu et al., 2013). Peldszus et al. (2011) and Kimura et al. (2004) reported that the accumulation of protein-like and polysaccharide-like substances on the membrane surface was responsible for the development of irreversible fouling. To better understand the role of EfOM in RO membrane fouling and flux decline during RO concentrate recycling to the MBR system, the molecular size distribution of protein-like substances, proteins concentration, and polysaccharides concentration in RO were addressed before and during RO concentrate recirculation.

The molecular size distribution of protein-like substances in RO was recorded by HPLC-SEC-fluorescence with excitation/emission wavelengths of 280/350 nm, as depicted in Figure 3.8. It can be clearly seen that, before RO concentrate recirculation, HPLC-SEC analysis of both MBR permeate and RO concentrate showed two distinct peaks, i.e., a high peak for 10 - 100 kDa protein-like substances and a small peak for protein-like molecules smaller than 10 kDa, respectively (Figure 3.8a). In contrast, a negligible response to fluorescence in RO permeate indicated that these two groups of protein-like substances were retained totally on the RO membrane surface. After 13 days of

RO concentrate recycling, the concentration of both <10 kDa and 10 - 100 kDa protein-like substances increased significantly, as indicated in Figure 3.8b. For example, for protein-like molecules with 10 - 100 kDa, an increase of 80% in peak height for MBR permeate and of 40% for RO concentrate was found. These results appeared to demonstrate that the continuous accumulation of these protein-like substances on the RO membrane surface may be related to the reduction of RO permeate flux.

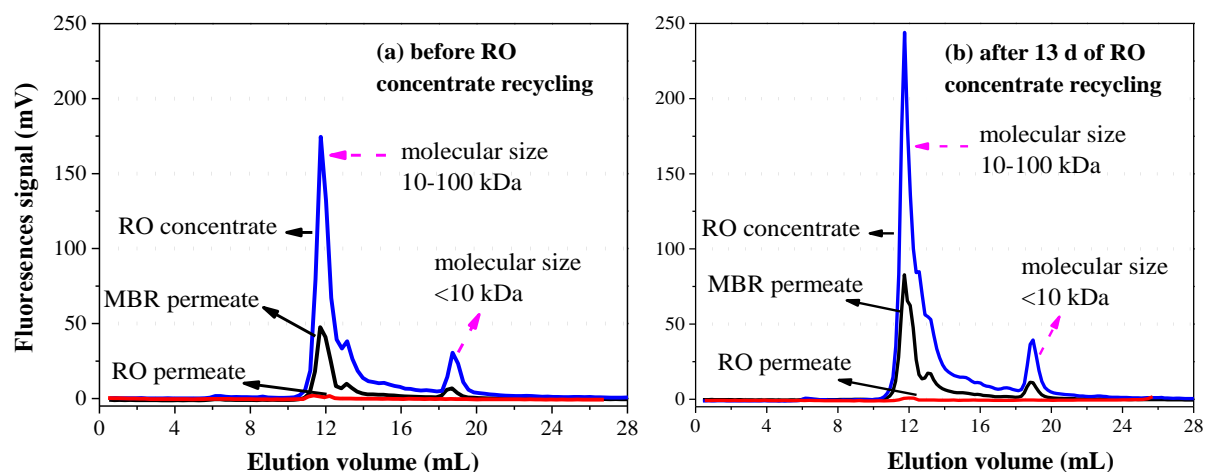


Figure 3.8 HPLC-SEC analysis of RO flows before and after RO concentrate recirculation to MBR unit. MBRP- 1. Cross-flow velocity: 0.18 m s^{-1} . ΔP : $\sim 7 \text{ bar}$. CF: ~ 3 .

To obtain further insight into the importance of extracellular polymeric substances (EPS) for RO membrane fouling potential, the concentration of proteins and polysaccharides in RO solutions was examined, as shown in Figure 3.9. It appeared that only 2 days after RO concentrate recycling caused an increase by a factor of 1.2 for proteins and of 2.0 for polysaccharides in MBR permeate. After 11 days of RO concentrate recycling, in MBR permeate, the concentration of proteins reached $12.1 \pm 2.4 \text{ mg L}^{-1}$, and the concentration of polysaccharides was $1.7 \pm 0.2 \text{ mg L}^{-1}$. With respect to RO concentrate, before RO concentrate recycling, the concentration of proteins and of polysaccharides was around $24.0 \pm 4.8 \text{ mg L}^{-1}$ and $3.5 \pm 0.4 \text{ mg L}^{-1}$, respectively. After 11 days of RO concentrate recycling, the concentration of proteins was 1.5 times higher compared to before RO concentrate recycling, and 1.7 times higher for polysaccharides. A continuous increase in the concentration of both proteins and polysaccharides in MBR permeate was possibly due to: (1) the recirculation of non-biodegradable proteins and polysaccharides in MBR-RO with RO concentrate recycling; (2) the high load of salts in the MBR improving the solubility of proteins and polysaccharides (Johir et al., 2013; Sun et al., 2010); and (3) the release of proteins and polysaccharides by microorganism because of the presence of toxic compounds brought by RO concentrate recycling. Indeed, the high salinity could promote the endogenous respiration of microorganisms in activated sludge, further leading to the enhancement of the secretion of organic cellular substances (Reid et al., 2006). These organics, which passed through the MF membrane in the MBR, were effectively rejected in RO concentrate, with larger than 90% observed retention for both protein and polysaccharide. These could possibly induce RO membrane

fouling by their interactions with the RO membrane (Jiang et al., 2017) and calcium present in RO concentrate (Lee et al., 2006).

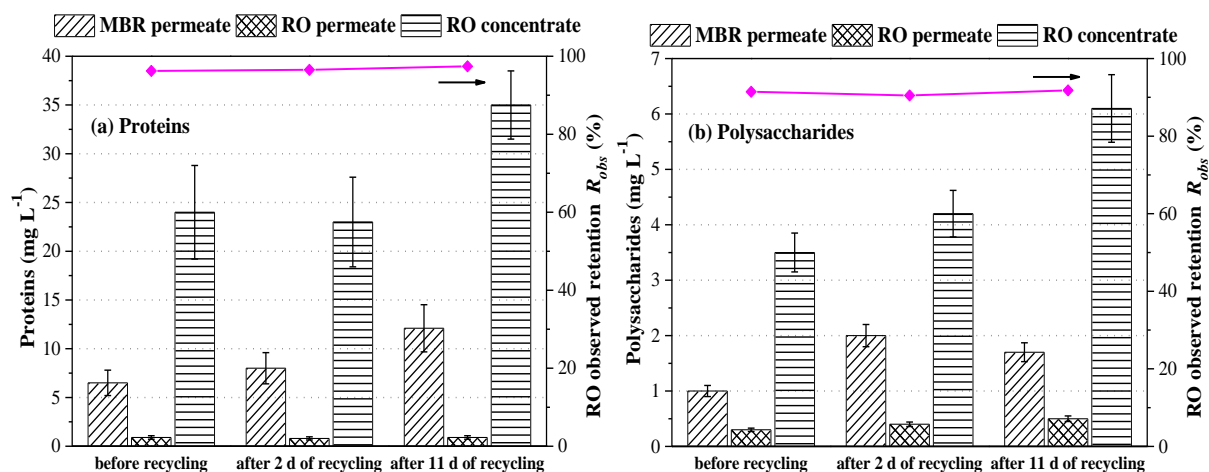


Figure 3.9 Concentration of proteins and polysaccharides in RO flows before and after RO concentrate recirculation. MBRP-1. Cross-flow velocity: 0.18 m s^{-1} . ΔP : $\sim 7 \text{ bar}$. CF: ~ 3 .

In order to better identify the major foulants (e.g., P, Ca, proteins, etc.) responsible for the flux decline in the MBR-RO system with RO concentrate recirculation, autopsies of the fouled RO membrane should be implemented in future work through scanning electron microscopy with energy dispersive X-ray spectroscopy (SEM-EDX) and fourier-transform infrared spectroscopy (FTIR).

III.3.5 Influence of RO concentrate recycling on the retention capacity for PhACs

Besides organic matters and inorganic ions, the fate of trace PhACs in RO was also examined before and during RO concentrate recycling. In this work, carbamazepine (CBZ), diclofenac (DIF) and ketoprofen (KET) were the target micropollutants. Figure 3.10 presents their concentration in RO flows before and during RO concentrate recirculation.

It can be clearly seen that from Figure 3.10, for CBZ and DIF, their concentration increased in MBR permeate and RO concentrate with RO concentrate recycling. After 11d of recycling, their concentration in both RO feed and RO concentrate increased by a factor of 1.3 as compared to before recycling. In contrast, there was no significant change in the concentration of KET. The reason for this was due to an effective removal for KET in MBR but a poor removal for both CBZ and DIF in MBR. Indeed, MBR is found to be insufficient to remove trace hydrophilic and biologically persistent trace organic constituents (such as CBZ, etc.) from municipal wastewater, due to their low biodegradation efficiency and their low adsorption capacity to sludge (Dolar et al., 2012; Li et al., 2015).

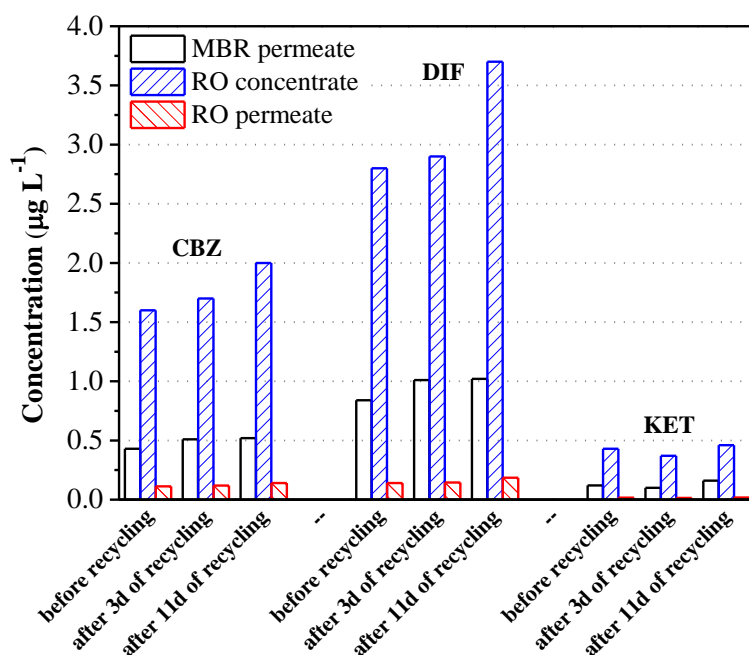


Figure 3.10 Concentration of the target PhACs in RO flows before and during RO concentrate recirculation. MBRP-1. Cross- flow velocity: 0.18 m s^{-1} . ΔP : $\sim 7 \text{ bar}$. CF: ~ 3 .

Table 3.8 lists the retention rate of the three tested PhACs by the RO membrane before and during RO concentrate recirculation. Before RO concentrate recycling, $>92\%$ of the target PhACs were retained by the RO membrane. A detailed information on the rejection mechanism of the RO membrane for these micropollutants were given in next section. During RO concentrate recycling, their retention capacity remained almost constant, which meant that RO concentrate recycling did not significantly affect the retention capacity of the RO membrane for the target PhACs.

Table 3.8 The retention rate of the tested PhACs before and during RO concentrate recycling

PhACs	Carbamazepine	Diclofenac	Ketoprofen
Retention (%)	~ 93	~ 95	~ 96

Overall, RO concentrate recycling to MBR resulted in an increase of the amount of both carbamazepine and diclofenac in the MBR-RO system. In order to reduce the load of these PhACs in this integrated system, other technologies, such as ozonation, should be followed.

III.3.6 Conclusions on the impacts of RO concentrate recycling to MBR on RO performance

RO concentrate, produced by the RO process at a fixed CF around 3, was added continuously to the MBR, representing 20% of the total MBR inflow. The results obtained suggested that, regardless of RO concentrate recycling to the MBR unit, the RO membrane in the MBR-RO system still maintained a relatively stable and effective retention capacity for the global water quality parameters, for instance, $>98\%$ for organic matters (NPOC) and $>95\%$ for conductivity. Moreover, RO process in this integrated system also exhibited an excellent retention rate for the three tested PhACs, with the value higher than 92%.

Since the recirculation of RO concentrate changed the characteristics of MBR permeate and RO concentrate, the fouling propensity of the RO membrane was enhanced, which was mainly due to an increase in the osmotic pressure of retained ions at the RO membrane surface. In addition, over the entire process, a reduction of approximately 15% of the initial RO permeate flux was linked to adsorption or a colloidal fouling layer at the RO membrane surface.

Overall, the MBR-RO process with the recirculation of RO concentrate could minimize the quantity of the RO concentrate waste stream. In view of the RO permeate flux decline mainly due to the increased osmotic pressure of retained ions, the amount of inorganic ions brought to the MBR by RO concentrate recirculation should be reduced by using capacitive deionisation process. In addition, PhACs at a higher concentration in RO concentrate should be further treated.

III.4 Removal of micropollutants by RO process combining ozonation (Set 2)

These trace organic constituents are excellently rejected by RO process, resulting in a removal >95% for a wide range of trace organic compounds (Alturki et al., 2010; Dolar et al., 2012; Jacob et al., 2012; Mamo et al., 2018). Micropollutants in RO concentrate usually multiplied by a factor of 2-7 compared to RO feed water (Bagastyo et al., 2011b; Pérez-González et al., 2012), which may associate with the toxic risk on the aquatic organism (Zhou et al., 2011). Therefore, it is of importance to establish beneficial reuse strategies to minimize the environmental impact of RO concentrate by the reduction of these unwanted contaminants.

In Set 2, the retention capacity of the RO membrane for trace micropollutants was first examined. After that, ozonation was used to reduce the amount of the micropollutants that were retained in RO concentrate.

III.4.1 RO retention capacity for micropollutants

In Set 2, MBRP-2 was treated by RO process, and the characteristic of MBRP-2 was given in Table 3.1. RO process was conducted at a constant CF 3 and at a cross-flow velocity of 0.18 m s^{-1} without RO concentrate recycling to MBR. RO concentrate and RO permeate were collected for the analysis of RO performance with respect to RO retention capacity for the solutes. The observed retention of each solute was calculated based on its average concentration in RO concentrate mixture and RO permeate mixture at the end of tests (see Equation 8 in Chapter II.2). Figure 3.11 presents the observed retention of 4 model PhACs (CBZ, DIF, IBP and PRO) by the RO process.

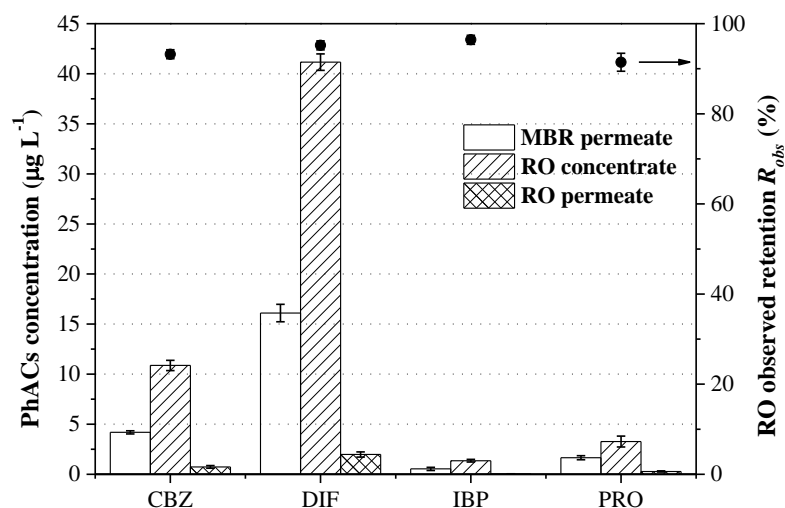


Figure 3.11 Observed retention of PhACs during the RO process of MBRP-2. ΔP : ~ 5.8 bar. MBRP-2, cross-flow velocity: 0.18 m s^{-1} . RO feed pH: ~ 6 . temperature: $21 \pm 1 \text{ }^\circ\text{C}$. CF: ~ 3 .

It was expected that, the RO process with ESPA2 membrane exhibited a high removal, greater than 90%, for the target PhACs, which was consistent with the finding obtained from the experiment with RO concentrate recycling (see Section 3.5 in this chapter). This meant that the model PhACs were well retained in RO concentrate by the ESPA2 membrane. The high rejection rates for micropollutants were in agreement with the previous finding where RO process was used to treat municipal MBR permeate (Alturki et al., 2010; Dolar et al., 2012; Jacob et al., 2012; Mamo et al., 2018; Sahar et al., 2011). Mamo et al. (2018) found that the RO process with ESPA2 membrane resulted in a removal efficiency above 99% for all the compounds tested including CBZ and DIF. Alturki et al. (2010) proved that ESPA2 RO membrane could complement MBR treatment very well, leading to a removal $>99\%$ for 40 trace organic compounds including CBZ, DIF, and IBP. Dolar et al. (2012) reported that most of emerging micropollutants including CBZ and PRO were rejected by the RO membrane to below the detection limit from municipal MBR permeate. The high rejection rate of emerging PhACs by the RO membrane was attributed to complex interactions between solutes, solvent and the RO membrane.

The membrane used in this study, ESPA2 membrane, was a negative membrane with the molecular weight cut-off (MWCO) of 100 g mol^{-1} . The molecular weight (MW) of the selected PhACs was ranging between 206.3 g mol^{-1} (IBP) and 296.2 g mol^{-1} (DIF) (see Table 2.1 in Chapter II.1), which was greater than MWCO of the RO membrane. It was clear that, therefore, size exclusion was a primary rejection mechanism for all the target PhACs rejection.

Among these 4 target PhACs, the observed retention of DIF and IBP ($>95\%$) was found to be a bit higher than that of CBZ (93%) and PRO (91%), which can be explained by their highly hydrophobic nature ($\text{LogKow} > 4$) and the negatively charged fraction at pH around 7 (see Table 2.1 in Chapter II.1). Except for size exclusion, other rejection mechanisms, hydrophobic adsorption to RO membrane polymeric matrix and electrostatic repulsion were likely to be responsible for the removal of DIF and IBP by the RO membrane. For less hydrophobic and neutral CBZ, RO membrane showed observed

retention of 93%, where the size exclusion was the main rejection mechanism. Regarding hydrophobic PRO ($\text{LogKow} > 3.48$), a bit lower observed retention (91%) was found compared to the other three PhACs. One of the possible rejection mechanisms involved for PRO was the hydrophobic adsorption of the positively charged PRO (at pH around 7) to the negatively charged RO membrane (Pronk et al., 2006). In addition, the lower rejection for hydrophobic PRO related to the diffusion through the dense polymeric matrix after the adsorption to RO membrane (Alturki et al., 2010).

III.4.2 Removal efficiency of PhACs from RO concentrate by ozonation

RO concentrate contained a high concentration of constituents including inorganic and organic substances (see Table 3.9). In this work, the model PhACs were concentrated by a factor of 2.0 - 2.6 over the RO feed. Thus, the additional ozonation was used to remove the target PhACs from RO concentrate, aiming to minimize the environmental impacts of RO concentrate.

Table 3.9 Concentration of the selected indicators and their observed retention by the RO membrane

MBRP-2	Unit	RO feed ¹	RO permeate	RO concentrate	Retention % ²	C_c / C_f ³
pH	-	6.1	6.8	7.3	-	-
Conductivity	$\mu\text{S cm}^{-1}$	1500 ± 70	46 ± 20	3810 ± 190	87.8	2.5
NPOC ⁴	mg L^{-1}	2.45 ± 0.05	0.39 ± 0.01	6.23 ± 0.12	93.8	2.5
DIC ⁵	mg L^{-1}	32 ± 1	8.81 ± 0.18	70 ± 1	87.3	2.2
COD ⁶	mg L^{-1}	13 ± 2	4 ± 2	25 ± 2	84.0	1.9
UV ₂₈₀	cm^{-1}	0.040 ± 0.002	0.007 ± 0.002	0.110 ± 0.002	93.3	2.8
UV ₂₅₄	cm^{-1}	0.047 ± 0.002	0.012 ± 0.002	0.180 ± 0.002	95.2	3.8
Cl ⁻	mg L^{-1}	433 ± 43	122 ± 12	1005 ± 100	87.8	2.3
N-NO ₂ ⁻	mg L^{-1}	0.93 ± 0.09	0.23 ± 0.02	n.d. ⁷	-	-
N-NO ₃ ⁻	mg L^{-1}	0.37 ± 0.04	0.15 ± 0.02	0.92 ± 0.09	83.7	2.5
HCO ₃ ⁻	mg L^{-1}	59 ± 1	32 ± 1	315 ± 6	89.8	5.4
SO ₄ ²⁻	mg L^{-1}	14 ± 1	2.02 ± 0.02	36 ± 4	94.5	2.7
P-PO ₄ ³⁻	mg L^{-1}	2.85 ± 0.29	0.72 ± 0.07	1.74 ± 0.17	58.7	0.6
Na ⁺	mg L^{-1}	153 ± 15	61 ± 6	323 ± 32	81.2	2.1
N-NH ₄ ⁺	mg L^{-1}	0.47 ± 0.05	0.23 ± 0.02	0.91 ± 0.09	75.1	2.0
K ⁺	mg L^{-1}	13 ± 1	5.48 ± 0.55	28 ± 3	80.2	2.1
Mg ²⁺	mg L^{-1}	3.64 ± 0.36	0.61 ± 0.06	9.23 ± 0.92	93.4	2.5
Ca ²⁺	mg L^{-1}	150 ± 15	30 ± 3	318 ± 32	90.5	2.1
Carbamazepine (CBZ)	$\mu\text{g L}^{-1}$	4.19 ± 0.03	0.74 ± 0.01	10.87 ± 0.51	93.2	2.6
Diclofenac (DIF)	$\mu\text{g L}^{-1}$	16.10 ± 0.87	1.98 ± 0.26	41.16 ± 0.82	95.2	2.6
Ibuprofen (IBP)	$\mu\text{g L}^{-1}$	0.54 ± 0.16	0.04 ± 0.01	1.36 ± 0.03	96.4	2.5
Propranolol (PRO)	$\mu\text{g L}^{-1}$	1.64 ± 0.02	0.28 ± 0.02	3.27 ± 0.55	91.4	2.0

(1) RO feed: after pH addition of MBRP-2. (2) the observed retention was calculated by Equation 8 in Chapter II. (3) C_m/C_f : the ratio of the concentration of an indicator in the bulk RO concentrate and RO feed. (4) NPOC: dissolved organic carbon. (5) DIC: dissolved inorganic carbon. (6) COD: chemical oxygen demand. (7) n.d.: not detected.

After RO experiment of MBRP-2, each 2 L RO concentrate were further treated by ozonation. The principal operating conditions of ozonation process are summarized in Table 3.10.

Table 3.10 Operating conditions of ozonation process for RO concentrate

$[O_3]_{\text{gas-in}}$	8 - 11 mg L ⁻¹	Gas flow rate	30 L h ⁻¹
Temperature	20 ± 1 °C	Reaction time	180 min

At present, there was no information on a specific requirement for PhACs removal for wastewater reuse. Azaïs et al. (2016) proposed 90% disappearance of the concentration of the selected indicator compound. Thus, in this work, 90% removal of PhACs by ozonation was considered as criteria to assess the ozonation efficiency of RO concentrate. The removal efficiency of micropollutants was calculated based on its residual concentration before and after ozonation. Consumed ozone dose involved in this section reflected the ozone dose required by chemical reactions, was defined in Equation 22 (see Chapter II.3).

Residual concentration of CBZ, DIF, IBP, and PRO in RO concentrate as a function of cumulated consumed ozone dose is plotted in Figure 3.12. The degradation of micropollutants by ozonation was achieved through two mechanisms: reactions with molecular ozone (direct reaction) and reactions with hydroxyl radicals ($\cdot OH$ radicals) that were generated from ozone decomposition. A detailed information has been given in Chapter I.3. In this work, due to the presence of highly concentrated bicarbonate and chloride (as $\cdot OH$ radicals scavengers) in RO concentrate (see Table 3.9), direct reactions through molecular ozone, not $\cdot OH$ radicals route, were believed to be responsible for the degradation of organic compounds in RO concentrate by ozonation.

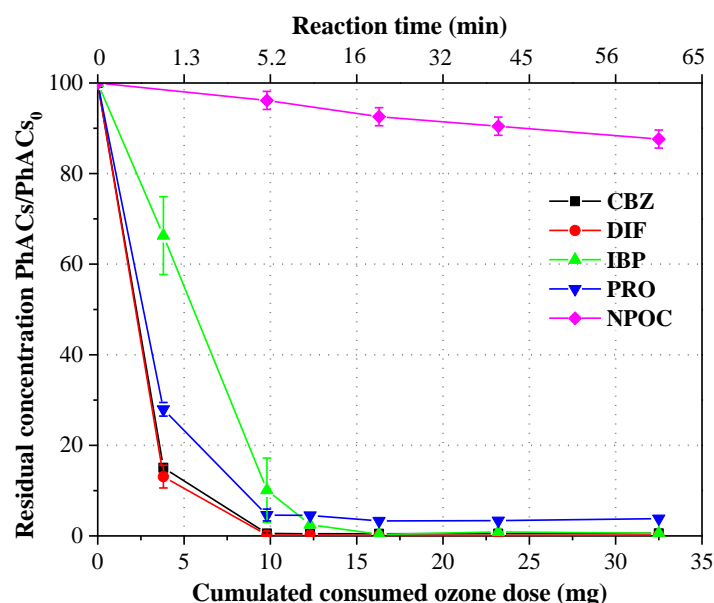


Figure 3.12 Residual concentration of PhACs selected during the ozonation of RO concentrate from the RO process of MBRP-2. ozone gas-in concentration: 8 - 11 mg L⁻¹. gaseous ozone flow rate: 30 L h⁻¹. liquid volume: 2 L. temperature: 20±1 °C. initial concentration of PhACs in RO concentrate: 10.5 µg L⁻¹ for CBZ, 38.0 µg L⁻¹ for DIF, 1.4 µg L⁻¹ for IBP, and 3.2 µg L⁻¹ for PRO. the initial NPOC: 6.2 ± 0.1 mg L⁻¹.

It was observed that, at a cumulated consumed ozone dose of 9.8 mg corresponding to 0.79 mg consumed O_3 per mg initial NPOC ($NPOC_0$), 90% removal for the four target PhACs can be achieved by ozonation, indicating that ozonation was sufficient in removing trace micropollutants from municipal RO concentrate. This observation was similar with finding from Joss et al. (2011), where an ozone dose of 0.85 mg O_3 per mg DOC_0 effectively eliminated most of micropollutants from RO concentrate with the initial DOC of 19 mg L^{-1} . Justo et al. (2013) noticed that >90% removal for CBZ and DIF was achieved at a 1.38 mg consumed O_3 per mg initial TOC during the ozonation of RO concentrate (the initial TOC: 27.6 mg L^{-1}). Based on our results and the reported literature, a comparison on the percentage removal of four target PhACs from RO concentrate by ozonation was made, as presented in Table 3.11. It can be seen that, there is no good agreement for ozone dose for a higher than 90% elimination of the four PhACs, which was mainly associated with nature matrix of RO concentrate including organic matters load and ionic concentration. A detailed discussion regarding the impacts of water matrix on ozonation efficiency of micropollutants was done in the next chapter.

Table 3.11 Removal of four PhACs by ozonation from RO concentrate

Parameter	Our experimental data		Joss et al. (2011) ⁶		Justo et al. (2013) ⁷	
Initial pH	7.3		6.8		8.3	
Initial DOC (mg L^{-1}) ¹	6.23		19		27.6 (TOC ³)	
Initial DIC (mg L^{-1}) ²	70		360 (TIC ⁴)		-	
Initial Cl^- (mg L^{-1})	1005		930		1540	
Cumulated consumed ozone dose (mg) ⁵	3.8	9.8	-	-	-	-
Consumed O_3 per mg DOC_0 (or TOC_0)	0.31	0.79	0.25	0.85	0.82	1.38
CBZ removal	85 ± 1 %	>99%	62 ± 15 %	>94%	~60%	>95%
DIF removal	87 ± 3 %	>99%	86 ± 10 %	>98%	~70%	>95%
IBP removal	34 ± 9 %	90 ± 7 %	<20%	58 ± 30 %	-	-
PRO removal	72 ± 2 %	92 ± 1 %	63 ± 28 %	>86%	-	-

(1) DOC : dissolved organic carbon. (2) DIC : dissolved inorganic carbon. (3) TOC : total organic carbon. (4) TIC : total inorganic carbon. (5) consumed ozone dose was calculated by Equation 23 in Chapter II.3. (6) Initial micropollutant concentration: 0.2 - 8 $\mu g L^{-1}$. (7) Initial micropollutant concentration: 1.0 $\mu g L^{-1}$ for CBZ and 0.6 $\mu g L^{-1}$ for DIF

On the other hand, prior to ozonation, the initial concentration of IBP (1.6 $\mu g L^{-1}$) in RO concentrate was the lowest compared to other PhACs (10.5 $\mu g L^{-1}$ for CBZ, 38.0 $\mu g L^{-1}$ for DIF, and 3.2 $\mu g L^{-1}$ for PRO. Nonetheless, before a >90% reduction was achieved, the removal rate of IBP was lower than that of three PhACs at the same consumed ozone dose. For example, within 1 min ozonation, ozone consumption of 3.8 mg (0.31 mg consumed O_3 per mg $NPOC_0$) could remove 87% of DIF, 85% of CBZ,

and 72% of PRO, whereas only 34% of IBP was reduced. This observation was in good accordance with the result from Joss et al. (2011), as implied in Table 3.11. The different elimination efficiency by ozonation was mainly related to their different ozone kinetic rate constants (order of magnitude: $>10^5$ L mol⁻¹ s⁻¹ for CBZ, DIF, and PRO, whereas ~ 9.1 L mol⁻¹ s⁻¹ for IBP) (see Figure 2.1 in Chapter II.1).

III.4.3 Removal efficiency of organic matters from RO concentrate by ozonation

Figure 3.13 plots the residual concentration of organic matters in terms of NPOC as a function of cumulated consumed ozone dose. Even if an elimination $>90\%$ of the target PhACs could be achieved at a low consumed ozone dose of 9.8 mg, only 4% organic matters in terms of NPOC was mineralized at the same ozone dose. After 180 min ozonation process, the consumption of 120.3 mg ozone dose only achieved around 17% elimination for NPOC in RO concentrate. This low mineralization of organics by ozonation was quite close to the finding with the organic removal efficiency of 22% (Zhou et al., 2011).

Even though ozonation process was not successful in completely degrading organic matters in RO concentrate, the previous studies have provided evidence that the biodegradability of RO concentrate was greatly improved, due to the degradation of organic matters with bigger MW to smaller MW organic molecular (Lee et al., 2009; Treguer et al., 2010; Zhou et al., 2011). Thus, in future works, RO concentrate treated by ozonation should be recycled to MBR for municipal wastewater reuse.

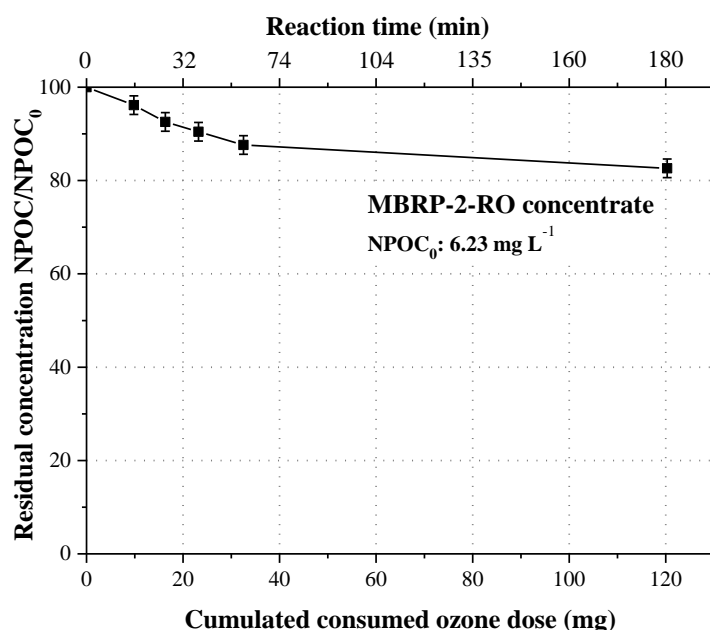


Figure 3.13 Residual concentration of NPOC during the ozonation of RO concentrate from the RO process of MBRP-2. ozone gas-in concentration: 8-11 mg L⁻¹. gaseous ozone flow rate: 30 L h⁻¹. liquid volume: 2 L. temperature: 20 ± 1 °C.

III.4.4 Conclusions on performance of RO process + ozonation for PhACs removal

RO membrane used in this work was proven to be effective in rejecting the four PhACs from municipal MBR permeate, with a removal higher than 91%. Ozonation exhibited a high performance in

the elimination of the target PhACs from RO concentrate produced from the treatment of MBR permeate by the RO process. An ozone dose of 0.79 mg consumed O_3 per mg $NPOC_0$ could achieve 90% removal for the four target PhACs .

III.5 Conclusions of this chapter

In this study, cross-flow RO process and ozonation were applied for municipal wastewater reuse. The first objective of the present study was to investigate the effect of RO concentrate recycling to MBR on the RO performance in the MBR-RO system. In this part, RO concentrate produced in this integrated system was recirculated continuously to MBR. Before and during RO concentrate recycling, RO membrane fouling potential and the retention capacity of the RO membrane for the global water quality parameters were investigated to evaluate RO performance. The second objective of this study was to examine the efficiency of trace PhACs removal by the RO process followed by ozonation. In this part, MBR permeate was first treated by the RO process without RO concentrate recycling. After that, RO concentrate produced was treated by ozonation to remove trace PhACs.

The continuous recirculation of RO concentrate to the MBR unit elevated significantly the concentration of the solutes in both MBR permeate and RO concentrate. For example, after two weeks of RO concentrate recycling, the concentration of $NPOC$ and conductivity increased by a factor of 1.7 and 1.3, respectively. However, the RO membrane in the MBR- RO system still maintained a relatively stable and effective retention capacities for the solutes, for instance, >98% for $NPOC$, >95% for conductivity and >92% for the tested PhACs. After RO concentrate recycling, the fouling propensity of the RO membrane was enhanced in terms of RO permeate flux decline, which was mainly due to an increase in the osmotic pressure of retained ions at the RO membrane surface. In addition, adsorption of organic matters and a colloidal layer could happen to reduce RO permeate flux over the entire RO process.

RO process and ozonation can complement each other very well to remove trace organic micropollutants from MBR permeate. RO process exhibited an excellent rejection for the target PhACs present in MBR permeate, with a >91% retention for four target PhACs. The followed ozonation was proved to be effective in degrading the target PhACs retained in RO concentrate at a low ozone dose. A consumed ozone dose of 9.8 mg, corresponding to 0.79 mg consumed O_3 per mg $NPOC_0$, could achieve a satisfactory elimination (>90%) for the tested PhACs from municipal RO concentrate. After 180 min ozonation, only a minority of organic matters (17%) were eliminated from RO concentrate at a consumed ozone dose of 120.3 mg.

To sum up, the combination of MBR-RO process with RO concentrate recirculation is successful to reduce the unwanted discharge of RO concentrate. The trace micropollutants present in MBR permeate was removed effectively by the RO process combining ozonation. Nonetheless, to avoid a fast and large reduction in RO permeate flux caused by RO concentrate recycling, more studies should be extended with the objective of improving RO concentrate disposal. For example, prior to RO concentrate

recycling to MBR, ozonation could be proposed to break down non- biodegradable organics responsible for RO membrane fouling. Capacitive deionisation process should be applied to control the amount of inorganic ions brought to the MBR by RO concentrate recirculation. The mitigation of membrane fouling in the MBR-RO process with RO concentrate recirculation could be the aim of further studies.

**Chapter IV Effect of water matrix on the mechanisms and
performance of ozonation for micropollutants removal**

Introduction

To date, only four research works regarding ozonation as a powerful barrier against excreted PhACs in real urine have been reported (Dodd et al., 2008; Escher et al., 2006; Gajurel et al., 2007; Tettenborn et al., 2007). Their findings highlight that relatively high doses of ozone are required to reach a satisfactory oxidation degree for model micropollutants in hydrolysed urine, which is mainly due to the presence of ozone-consuming reactive components at high concentrations, such as ammonia and aromatic organic compounds.

Nevertheless, at present, very little information is available regarding the influence of real urine compositions, including bicarbonate, ammonia and organic matters, on the elimination rates of PhACs by the ozonation process, possibly because of the complexity of real urine. In order to improve the efficiency of urine ozonation, it is necessary to understand the competitive reactions between molecular ozone and micropollutants + ionic salts + ammonia + organic matters.

To this end, ozonation experiments with different compositions, including (1) ultra-pure water (PWM), (2) saline solution (SAM, ionic salts), (3) synthetic urine (simulating hydrolysed urine compositions) with ionic salts and ammonia (SUM), and (4) hydrolysed urine containing ionic salts, ammonia and organic matters (HUM), were performed in a semi-batch ozonation reactor. A comparison between the efficiency of micropollutant ozonation in PWM, SAM, SUM and HUM was helpful to better understand the mechanism and the behaviour of PhACs ozonation in source-separated urine.

IV.1 Experimental protocols

Carbamazepine (CBZ) was selected to represent ozone-reactive PhACs ($k_{O_3-PhACs} > 10^5 \text{ L mol}^{-1} \text{ s}^{-1}$), and ketoprofen (KET) to represent ozone-resistant PhACs ($k_{O_3-PhACs} \ll 10^5 \text{ L mol}^{-1} \text{ s}^{-1}$). Their key properties have been described in Table 2.1 and Figure 2.1 (see Chapter II.1). The experimental protocols applied for the determination of the impacts of water matrix on the ozonation of these two PhACs are presented in Figure 4.1.

- Firstly, in order to determine the oxidation pathway of these two PhACs at the solution pH of 8-9 (similar to pH of hydrolysed urine). Two experiments with ultrapure water (PWM) was conducted at the initial solution pH of 4.5 (PWM-1) and 8.4 (PWM-2).
- The results from PWM-2 and SAM were then used to demonstrate the effect of salts (HCO_3^- , Cl^- , SO_4^{2-} , etc.).
- The effects of ammonia on ozonation behaviour of micropollutants were investigated by comparing the ozonation behaviour of SAM and SUM.
- At last, the experiments of real urine ozonation were carried out to study the effect of organic matters on ozonation behaviour of micropollutants.

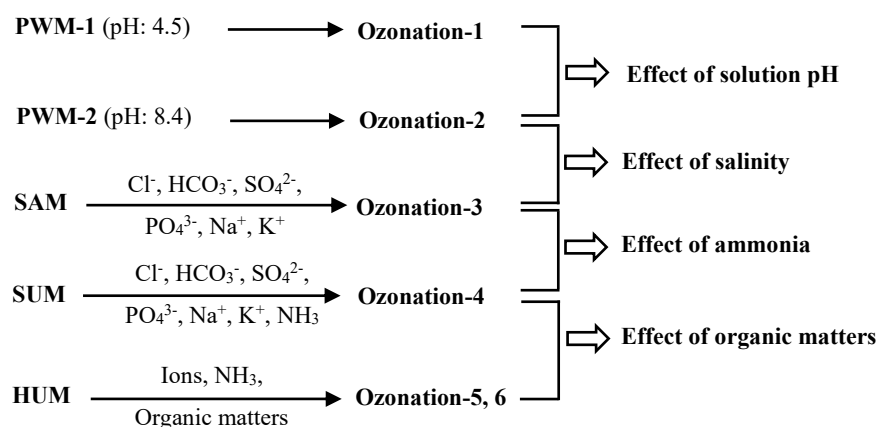


Figure 4.1 Experimental protocols applied to study the impact of water matrix on the ozonation of PhACs

IV.1.1 Preparation of organic matter-free solutions spiked with CBZ and KET

Working solutions containing target PhACs with a desired concentration of around 10 mg L⁻¹ were prepared with ultra-pure water (PWM), saline solution (SAM) and synthetic urine (SUM). The compositions of these solutions are listed in Table 4.1. The difference between PWM-1 and PWM-2 was the pH adjustment. Synthetic urine was prepared based on the recipe from a previous study (Triger, 2012), in which the addition of HCO₃⁻ and NH₃ was intended to simulate hydrolysed urine, due to the hydrolysis of urea in fresh urine to bicarbonate and ammonium after several weeks storage (see Reaction 13 in Chapter I.4). To investigate the effect of ammonia/ammonium on ozonation performance with respect to PhACs removal, a saline solution was prepared without ammonia, and where the ammonium salts of synthetic urine were replaced by sodium salts. In order to understand and compare the behaviour of ozone in hydrolysed urine with a pH of 8 - 9, the solution pH of PWM (PWM-2) and SAM were adjusted to a similar level by using 0.1 mol L⁻¹ NaOH.

IV.1.2 Real urine collection and pre-treatment

Two different types of urine effluents were collected: one from a urine biological treatment unit (HU-1) and one from a urine collection system (HU-2). Storage of HU-2 for several weeks ensured the hydrolysis of urea in fresh urine into bicarbonate and ammonia. Firstly, an ultrafiltration membrane was applied to remove gross organics from the two urine effluents. Then, a mixture of target PhACs, including 2-hydroxyibuprofen (2OH-IBP), caffeine (CAF), carbamazepine (CBZ), diclofenac (DIF), ibuprofen (IBP), ofloxacin (OFL), oxazepam (OXA), propranolol (PRO), and sulfamethoxazole (SMX), was used to spike two urine effluents (HUM-1 and HUM-2). The concentration of the PhACs was set at a very low value, with the range that could be found in real urine. This work focused only on CBZ. Subsequently, precipitation with the addition of MgCl₂ was performed to recover P-PO₄³⁻. After that, the ozonation experiments of real urine solutions were performed. Table 4.1 presents the

compositions of the urine solutions before ozonation. The concentration of CBZ in HUM-2 was lower than that in HUM-1. However, the concentrations of dissolved organic carbon (NPOC), chemical oxygen demand (COD), dissolved inorganic carbon (DIC), and N-NH_4^+ were higher in HUM-2 than in HUM-1.

Table 4.1 Characteristics of the tested solutions before ozonation

Parameter	Unit	PWM-1	PWM-2	SAM	SUM	HUM-1 (after bio-treatment) ¹	HUM-2 (hydrolysed urine) ²
CBZ	mg L ⁻¹	~10	~10	~10	~10	0.022	0.0004
KET	mg L ⁻¹	~10	~10	~10	~10	-	-
NPOC ³	mg L ⁻¹	-	-	-	-	88 ± 2	415 ± 8
COD ⁴	mg L ⁻¹	-	-	-	-	361 ± 10	1215 ± 10
DIC ⁵	mg L ⁻¹	-	-	3879 ± 78	2973 ± 60	2.9 ± 0.1	396 ± 8
Cl ⁻	mg L ⁻¹	-	-	3720 ± 372	4148 ± 415	199 ± 20	419 ± 42
N-NO ₃ ⁻	mg L ⁻¹	-	-	-	-	0.86 ± 0.09	7.5 ± 0.8
SO ₄ ²⁻	mg L ⁻¹	-	-	1560 ± 156	1555 ± 156	342 ± 34	121 ± 12
P-PO ₄ ³⁻	mg L ⁻¹	-	-	199 ± 20	442 ± 44	1.5 ± 0.2	1.6 ± 0.2
Na ⁺	mg L ⁻¹	-	-	8660 ± 866	1665 ± 167	93 ± 9	188 ± 19
N-NH ₄ ⁺	mg L ⁻¹	-	-	-	8934 ± 893	123 ± 12	516 ± 52
K ⁺	mg L ⁻¹	-	-	1466 ± 147	2286 ± 229	73 ± 7	185 ± 19
Mg ²⁺	mg L ⁻¹	-	-	-	-	13 ± 1	39 ± 4
Ca ²⁺	mg L ⁻¹	-	-	-	-	1.9 ± 0.2	5.8 ± 0.6
pH	-	4.5	8.4	8.1	9.1	7.0	8.9
NaOH ⁶	mg L ⁻¹	-	5.2	11.8	-	-	-

(1) after 20 times dilution. (2) after 10 times dilution. (3) NPOC: non-purgeable organic carbon. (4) COD: chemical oxygen demand. (5) DIC: dissolved inorganic carbon. (6) to adjust the pH of solutions (0.1 mol L⁻¹ NaOH: 1.3 mL L⁻¹ for PWM-1, 2.95 mL L⁻¹ for SAM)

IV.1.3 Ozonation operating conditions

Ozonation pilot has been described in detail in Chapter II.3. Ozonation experiments were conducted at a gas flow rate of 30 L h⁻¹ and at 20 ± 1 °C. Table 4.2 shows the principal operating conditions of ozonation of the tested 6 solutions. For organic matter-free solutions (PWM, SAM and SUM), the concentration of ozone gas-in was set to 10 mg L⁻¹. For real urine (HUM), prior to ozonation, several times dilution was done, i.e., 20 times for HUM-1 and 10 times for HUM-2. In addition, a higher ozone gas-in concentrate was used, i.e., 50 mg L⁻¹ for HUM-1 and 60 mg L⁻¹ for HUM-2. The purpose of several times dilution and a higher ozone gas-in concentration for HUM was to shorten the ozonation time.

Table 4.2 Operating conditions of ozonation for different solution matrix

Parameter	PWM-1	PWM-2	SAM	SUM	HUM-1	HUM-2
$[O_3]_{\text{gas-in}} \text{ (mg L}^{-1}\text{)}$	10	10	10	10	50	60
Dilution times	1	1	1	1	20	10
Reaction time (min)	120	120	540	540	300	450

IV.2 Ozonation kinetic regime and ozone mass transfer

IV.2.1 Mass transfer with chemical reactions

Double film theory was used to explain the mass transfer of ozone with chemical reactions in an ozone-liquid system, as represented in Figure 4.2 (Beltrán, 2004; Levenspiel, 1999). Since ozone is only slightly soluble in water, the concentrations of ozone in the gas phase ($[O_3]_{\text{gas}}$) and that at the gas interface ($[O_3]_{\text{gas}}^i$) are the same, and the concentration of ozone at the liquid interface ($[O_3]_{\text{L}}^i$) is equal to that at equilibrium with the bulk of the gas phase ($[O_3]_{\text{L}}^*$). Thus, when direct reactions between compound B and ozone take place in a reactor (Reaction 15), the rate of ozone transfer from the gas phase to the liquid phase can be expressed by Equation 34. The enhancement factor (E) involved in Equation 34 describes the enhancement of ozone mass transfer in the presence of chemical reactions, as defined in Equation 35. ($[O_3]_{\text{L}}^*$) can be obtained by Equation 36.

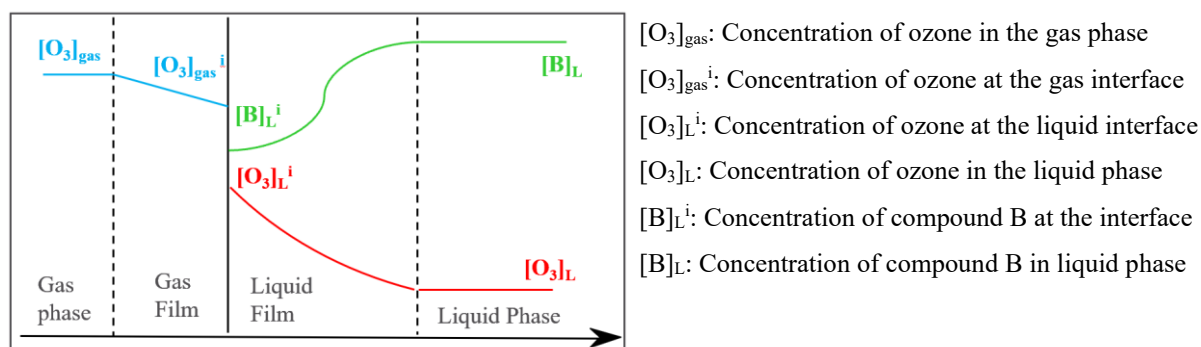


Figure 4.2 Mass transfer with chemical reactions in the case of ozone of low solubility



where γ is the apparent stoichiometric ratio of compound B reacting with ozone, defined as the moles of ozone consumed per mole of compound B removed.

$$T_{O_3} = Ek_L a V_{\text{Liq}} ([O_3]_{\text{L}}^* - [O_3]_{\text{L}}) \quad (\text{Equation 34})$$

$$E = \frac{\text{the actual rate of ozone mass transfer with chemical reactions}}{\text{the rate of maximum physical absorption without chemical reactions}} \quad (\text{Equation 35})$$

$$[O_3]_{\text{L}}^* = m [O_3]_{\text{gas-out}} \quad (\text{Equation 36})$$

where T_{O_3} is the rate of ozone transfer from the gaseous phase to the liquid phase (g s^{-1} or mol s^{-1}). E is the enhancement factor. $k_L a$ is the volumetric mass transfer coefficient (s^{-1}), which is 0.0052 s^{-1} based on our experimental result in pure water. $[O_3]_{\text{L}}$ and $[O_3]_{\text{L}}^*$ are the

concentration of dissolved ozone in the liquid phase and at equilibrium (mg L^{-1} or mol L^{-1}), respectively. V_{liq} is the liquid volume (L). $[O_3]_{gas-out}$ is the concentration of ozone in the outlet stream (mg L^{-1} or mol L^{-1}). m is the solubility parameter of ozone in water or aqueous salt solution.

The enhancement factor is a function of the Hatta number (Ha) and the enhancement factor of an infinitely fast reaction (also known as instantaneous enhancement factor, E_i). The Hatta number (Ha) is often used as a criterion to demonstrate whether chemical reactions between ozone and the solute B develop in the liquid film, in the bulk of the solution, or in both zones (Table 4.3). A value higher than 3 relates to a fast kinetic regime that occurs in the liquid film, whereas a value lower than 0.3 indicates that a slow kinetic regime exists in the liquid bulk. If ozone reacts with two or more compounds through an irreversible second-order reaction in a complex parallel reaction system, the Ha is expressed as follows (Benítez et al., 1997):

$$Ha = \frac{(\sum_i \gamma_i k_{O_3-i} [i]) \times D_{O_3}}{k_L}^{0.5} \quad (\text{Equation 37})$$

where k_{O_3-i} is the kinetic rate constant of molecular ozone reaction with compound i ($\text{L mol}^{-1} \text{s}^{-1}$). $[i]$ is the concentration of compound i in the bulk liquid (mol L^{-1}). D_{O_3} is the diffusivity of ozone in water at 20 °C ($\text{m}^2 \text{s}^{-1}$), taken as $1.3 \times 10^{-9} \text{m}^2 \text{s}^{-1}$ (Beltrán, 2004). k_L represents the mass transfer coefficient of ozone (m s^{-1}), with the value of $2 \times 10^{-5} \text{m s}^{-1}$ for a reactor with a bubble tube at 20 °C (Beltrán, 2004).

Table 4.3 Hatta number and the kinetic regime

Hatta value	$[O_3]_L$	Enhancement factor	Kinetic regime	Reaction occurring	Rate controlling step
> 3	= 0	minimum (Ha, E_i)	fast	in the film layer	mass transfer
0.3 - 3	-	$1 < E < Ha$	moderate	partially in the film	both
< 0.3	$\neq 0$	≈ 1	slow	in the liquid bulk	chemical reaction
$\ll 0.01$	$\neq 0$	≈ 1	very slow	in the liquid bulk	chemical reaction

Taking the contribution of the stoichiometric ratios and the solute mixture into account, for a film theory, E_i is estimated by the following expression (Equation 38) (Benítez et al., 1997).

$$E_i = 1 + \frac{\sum_i \gamma_i [i] D_i}{[O_3]_L^* D_{O_3}} \quad (\text{Equation 38})$$

where D_i is the diffusivity of compound i in water ($\text{m}^2 \text{s}^{-1}$). The diffusivity of CBZ, KET and NH_3 is $7.50 \times 10^{-10} \text{m}^2 \text{s}^{-1}$ (Lu and Li, 2016), $7.56 \times 10^{-11} \text{m}^2 \text{s}^{-1}$ (Chi and Jun, 1991), and $1.96 \times 10^{-9} \text{m}^2 \text{s}^{-1}$ (Lide, 2005), respectively.

IV.2.2 Mass balance of ozone with chemical reactions

In the presence of chemical reactions, the mass balance of gaseous ozone is defined by Equation 11 (see Chapter II.3), which can be rewritten as Equation 39.

$$V_g \frac{d[O_3]_{gas}}{dt} = Q_g ([O_3]_{gas-in} - [O_3]_{gas-out}) - T_{O_3} \quad (\text{Equation 39})$$

where $[O_3]_{gas-in}$ is the concentration of ozone in the inlet stream (mg L^{-1} or mol L^{-1}). Q_g is the ozone gas flow rate (L h^{-1}). V_g is the volume of gas in the reactor (L) and, normally, the value remains constant.

Since the steady state is reached rapidly for the gaseous phase, the accumulation of ozone gas could be negligible. Combining Equation 34 and Equation 39, the enhancement factor from experimental results (E_{exp}) is obtained by Equation 40.

$$E_{exp} = \frac{Q_g ([O_3]_{gas-in} - [O_3]_{gas-out})}{k_L a V_{Liq} ([O_3]_L^* - [O_3]_L)} \quad (\text{Equation 40})$$

In the liquid phase with chemical reactions, the mass balance of ozone is written as the following equation:

$$\frac{d[O_3]_L}{dt} = Ek_L a ([O_3]_L^* - [O_3]_L) - r_{appO_3} \quad (\text{Equation 41})$$

where r_{appO_3} is the apparent consumption rate of ozone ($\text{L mol}^{-1} \text{s}^{-1}$), which involves the self-decomposition into $\cdot\text{OH}$ radicals, and the direct reactions of ozone towards reactants and intermediate compounds ($\sum \gamma_i k_{O_3-i} [O_3]_L [i]$).

IV.3 Investigation of the oxidation mechanism of CBZ and KET

As a general rule, the removal of organic compounds by ozonation is a result of direct reactions involving molecular ozone and indirect reactions via secondary oxidants, such as $\cdot\text{OH}$ radicals (Beltrán, 2004; Derco et al., 2015). The former is a true ozone reaction, i.e., molecular ozone selectively reacts with organic compounds containing electron-rich moieties, such as olefins, phenols, and amine. The indirect reactions are oxidation through $\cdot\text{OH}$ radicals without selectivity, which is more favourable at solution pH above 7 (Beltrán, 2004). To investigate the pathway of CBZ and KET oxidation by ozone, the experiments with PWM were performed at the initial pH of 4.5 (PWM-1) and 8.4 (PWM-2). Figure 4.3a and 4.3b present the PhACs residuals versus cumulated consumed ozone dose and the concentration profile of ozone gas-out and dissolved ozone during the ozonation of PWM-1 and PWM-2.

It can be seen that, no dissolved ozone was detected during the first 3 min of ozonation for PWM-1 and during the first 10 min for PWM-2, demonstrating that the chemical reactions of ozone with reactants were fast, and mass transfer of ozone had to be considered as a limiting step. During this period with the absence of dissolved ozone, elimination of CBZ was nearly complete, whereas that of KET was only partial. This suggested that the fast reactions observed at the beginning of experiments could be attributed to CBZ removal. During the following ozonation, the detection of dissolved ozone indicated that chemical reactions took place in the bulk of liquid phase at a slow rate, which related to the oxidation of both KET and intermediates.

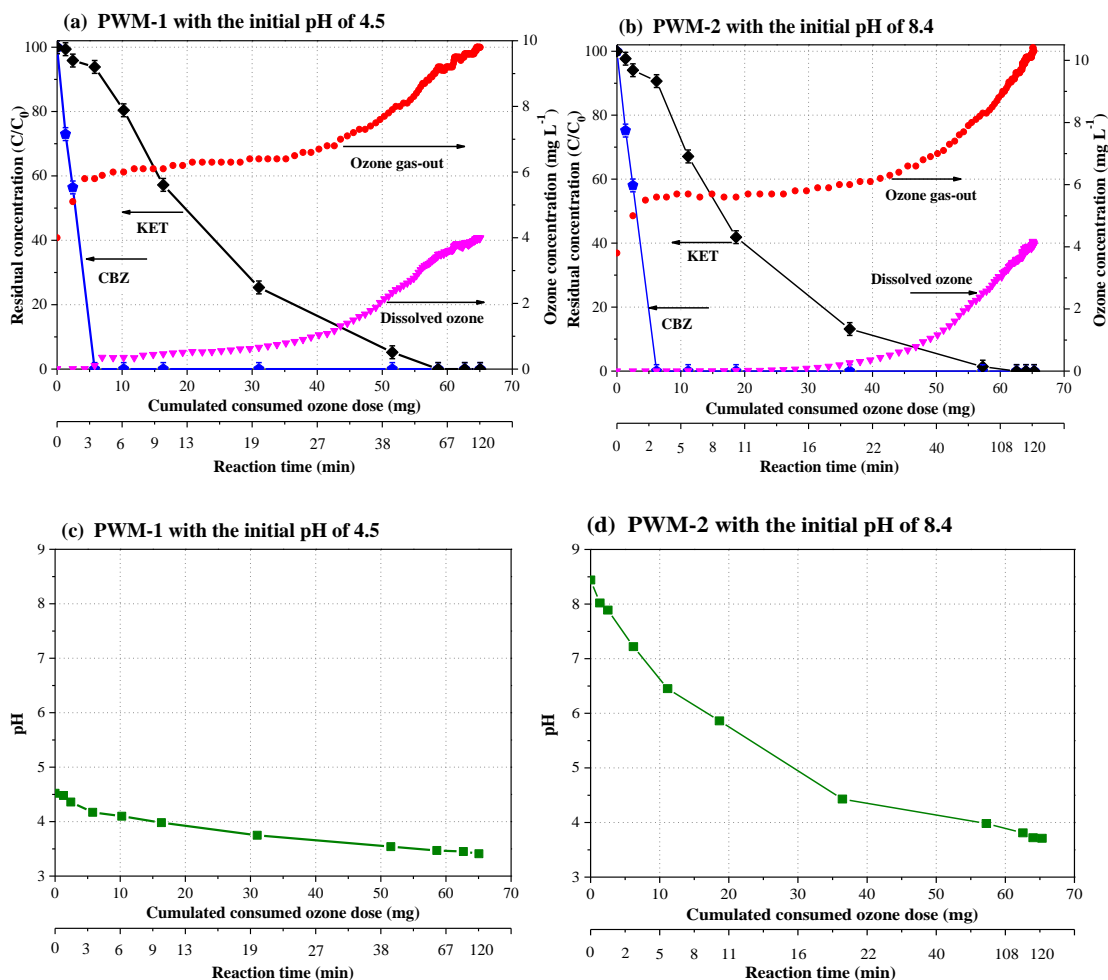


Figure 4.3 PhACs residual, pH and concentration of ozone gas-out and of dissolved ozone as a function of cumulated consumed ozone dose during the ozonation of PWM-1 and PWM-2. ozone gas-in concentration: $\sim 10 \text{ mg L}^{-1}$ for PWM-1 and PWM-2. gaseous ozone flow rate: 30 L h^{-1} . initial PhACs concentration: $\sim 10 \text{ mg L}^{-1}$ of CBZ and of KET. liquid volume: 2 L , temperature: $20 \pm 1 \text{ }^\circ\text{C}$.

For ozone-resistant KET, once the gaseous ozone was introduced into the reactor, the concentration of KET decreased gradually. Around 58 mg of cumulated consumed ozone dose ($\sim 1 \text{ h}$ reaction time) was required to reduce the concentration of KET to below the detection limit in PWM-1, as shown in Figure 4.3a. For this experiment with an initial pH of 4.5, molecular ozone was thought to be the main oxidant decomposing KET. When the initial pH of solutions was adjusted to 8.4 (PWM-2, Figure 4.3b), similar removal of KET was observed at the same cumulated consumed ozone dose in PWM-2 as in PWM-1, indicating that molecular ozone, rather than $\cdot\text{OH}$ radicals, was responsible for the degradation of KET in PWM-2.

With respect to ozone-reactive CBZ, less ozone consumption, around 7 mg , could result in the rapid and complete disappearance of CBZ from either PWM-1 or PWM-2, as indicated in Figure 4.3a and 4.3b. In addition, CBZ removal was achieved through a direct pathway by molecular ozone.

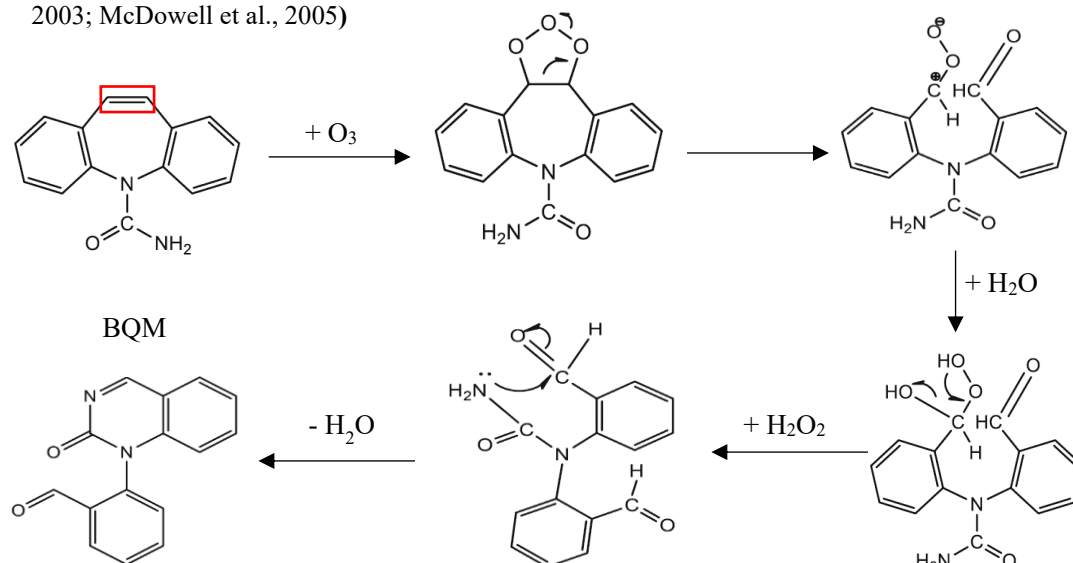
In this study, the difference in the amount of ozone consumed to achieve complete removal

for CBZ and KET, i.e., the fact that the ozone consumption for >95% removal of KET was approximately 9 times higher than that for >95% removal of CBZ, can be explained by their different ozone kinetic rate constants: $3 \times 10^5 \text{ L mol}^{-1} \text{ s}^{-1}$ for CBZ (Huber et al., 2003) and $0.4 \text{ L mol}^{-1} \text{ s}^{-1}$ for KET (Real et al., 2009b), respectively.

Figure 4.3c and 4.3d show pH variation during the ozonation of PWM-1 and PWM-2. For PWM-1, pH decreased from 4.5 to 3.4 during 120 min ozonation, which was related to the oxidation of the target PhACs. In the case of PWM-2, a faster pH reduction ranging from 8.4 to 5.9 was noticed during the first 10 min, which was linked to the formation of a small part of $\cdot\text{OH}$ radicals. Indeed, as compared to PWM-1, the removal rate of KET in PWM-2 was higher at the beginning of ozonation, as implied in Figure 4.3b. After 60 min ozonation, solution pH decreased to around 3.7, which was close to the value obtained in PWM-1.

As discussed above, the direct molecular ozone reaction, not $\cdot\text{OH}$ radicals oxidation pathway, was mainly responsible for the degradation of ozone-reactive CBZ and ozone-refractory KET, even at the initial pH of around 8.4. Based on the literature reported above, the primary reaction between molecular ozone and CBZ or KET was proposed, as displayed in Figure 4.4. 1-(2-benzaldehyde)-4-hydro-(1H,3H)-quinazoline-2-one (BQM) was considered as a primary intermediate for the oxidation of carbamazepine by ozone ($k_{\text{O}_3\text{-BQM}} = 3 \times 10^5 \text{ L mol}^{-1} \text{ s}^{-1}$) (Huber et al., 2003; McDowell et al., 2005). Regarding the reaction of molecular ozone towards ketoprofen, four primary transformation products have been reported, associated to different degradation mechanisms (hydroxylation of aromatic ring or decarboxylation) (Illés et al., 2014; Zeng et al., 2018).

(a) Proposed mechanism for the formation of primary product of CBZ by ozone (Huber et al., 2003; McDowell et al., 2005)



(b) Proposed mechanism for the formation of primary product of KET by ozone (Illés et al., 2014; Zeng et al., 2018)

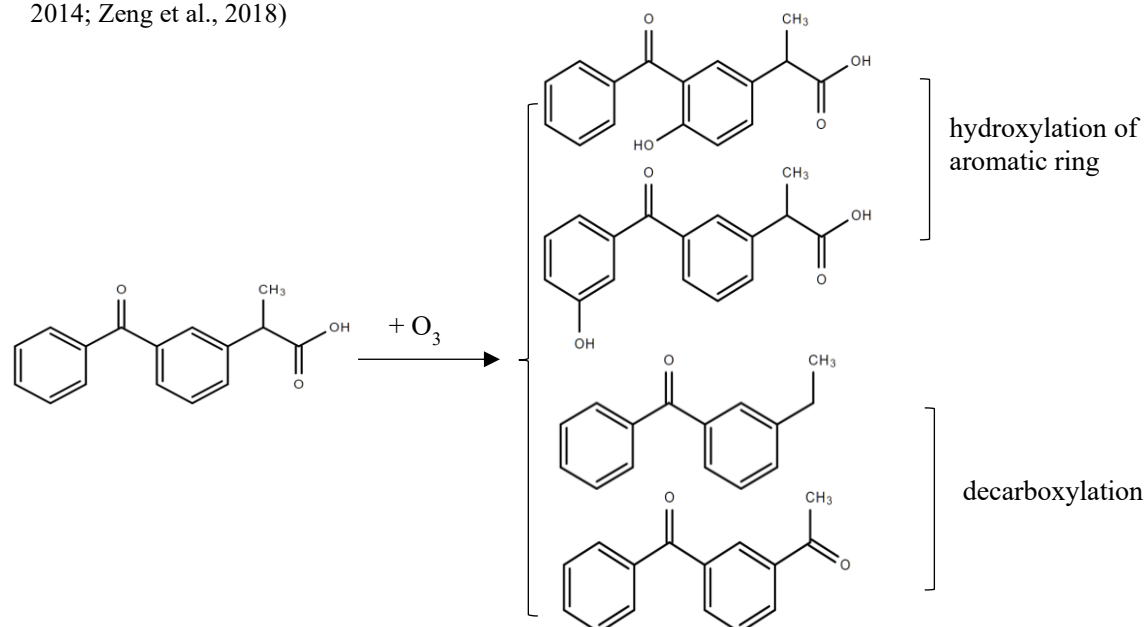


Figure 4.4 Proposed primary reaction products of molecular ozone towards CBZ and KET

IV.4 Impacts of solution matrix on the efficiency of PhACs removal by ozonation

IV.4.1 Ozonation of CBZ and KET in saline solution and synthetic urine

Figure 4.5a and 4.5b present the measured losses of CBZ and KET, which had an initial concentration around 10 mg L^{-1} , as a function of the cumulated consumed ozone dose in SAM with ionic salts, and in SUM containing both ionic salts and ammonia.

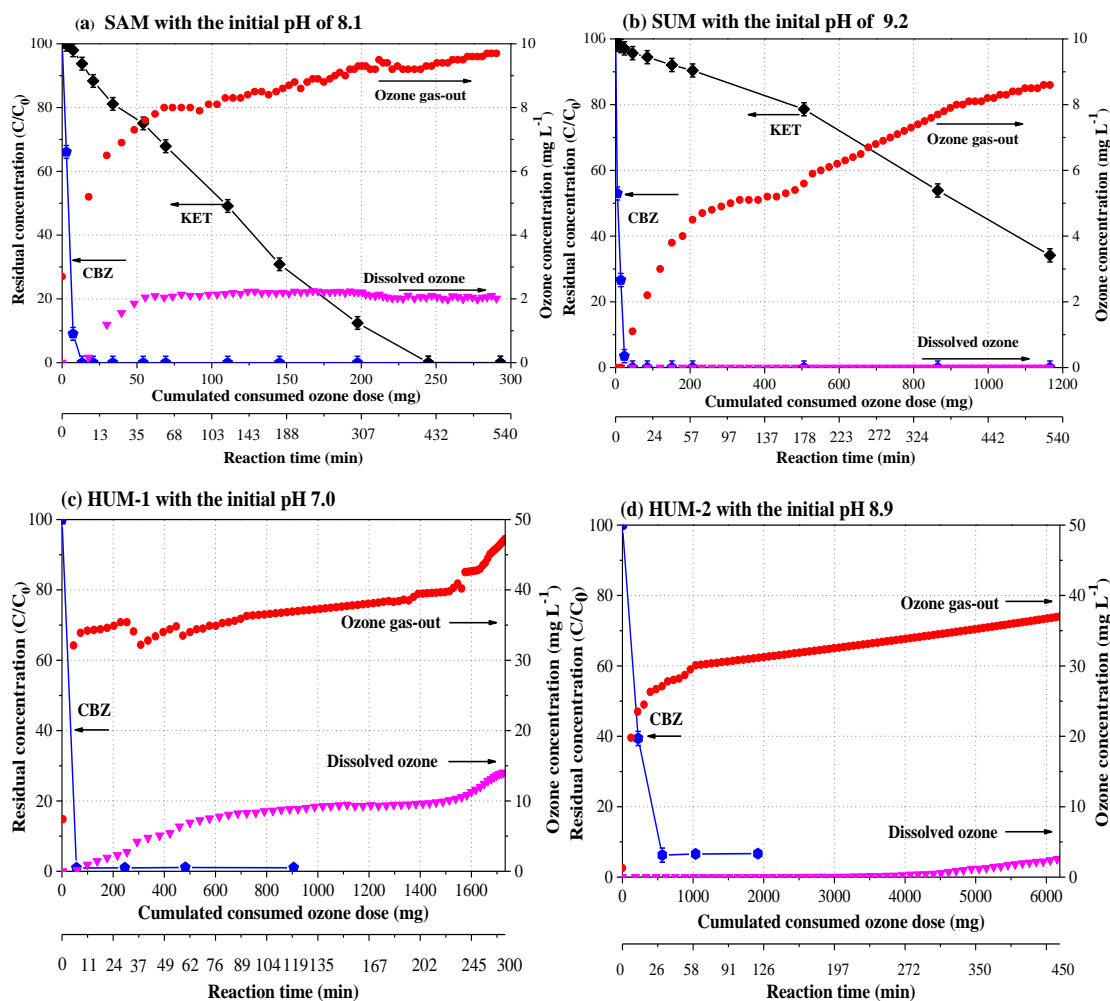
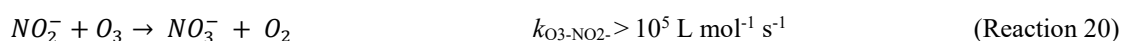
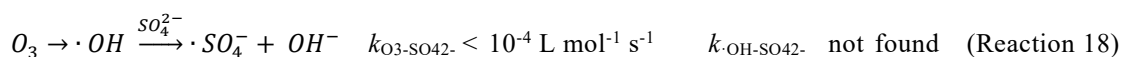
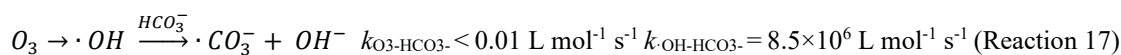
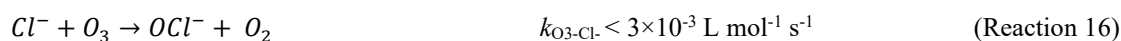


Figure 4.5 PhACs residual, concentration of ozone gas-out and of dissolved ozone as a function of cumulated consumed ozone dose during the ozonation of SAM, SUM and HUM. ozone gas-in concentration: $\sim 10 \text{ mg L}^{-1}$ for SAM and SUM; $\sim 60 \text{ mg L}^{-1}$ for HUM. initial PhACs concentrations: $\sim 10 \text{ mg L}^{-1}$ of CBZ and of KET in SAM and SUM; $3.5 \pm 0.2 \mu\text{g L}^{-1}$ of CBZ in HUM. liquid volume: 2 L. temperature: $20 \pm 1 \text{ }^\circ\text{C}$.

As can be seen from Figure 4.5a and 4.5b, the concentration variation of CBZ in both SAM and SUM was quite similar to that for ozonation in PWM-2 (see Figure 4.3b). Before dissolved ozone was detected, a fast and complete disappearance of CBZ could be achieved at the low cumulated consumed ozone dose of 7.3 mg for SAM (within 3 min) and 23.7 mg for SUM (within 6 min). A minor difference in ozone consumption to achieve an equivalent elimination of CBZ from different organic matters-free solutions was noticed, demonstrating that the presence of a high load of ionic salts and ammonia slightly inhibited the degradation of ozone-reactive CBZ by ozonation.

On the other hand, while CBZ was completely removed by ozonation within the first 3 min for both PWM-2 and SAM, and within 6 min for SUM, at the same cumulated consumed ozone dose, 91%, 98% and 97% of ozone-refractory KET still remained in PWM-2, SAM and SUM, respectively. The reason for this was a much lower ozone kinetic rate constant for KET than for

CBZ. In the case of SAM, KET was almost linearly degraded. To reduce the concentration of KET to below the detection limit, an ozone dose of 245 mg was consumed, which was higher than the 57.3 mg required for PWM-2. The different KET oxidation efficiency by ozonation between PWM-2 and SAM was due to the competition of ionic salts (Cl^- , SO_4^{2-} , HCO_3^-) for molecular ozone (Reaction 16 - 18). It can be observed that the oxidation of KET was much less effective in SUM than in SAM, with only 66% removal at quite a high cumulated consumed ozone dose of 1166 mg, corresponding to 540 min reaction time, which was linked to the reaction of ammonia with molecular ozone in SUM (Reaction 19 - 20). A comparison of KET removal efficiency in these three organic matters-free matrices supports the idea that ozone preferably attacked other substances (such as ammonia) rather than ozone-resistant KET in the presence of high concentrations of ionic salts and free ammonia.



The competition of ionic salts and ammonia for molecular ozone can be evidenced through the comparison of the reaction rates. Considering that the kinetics has partial orders 1 with respect to ozone and 1 with the compound i and a kinetic constant k_{O_3-i} , the values of $k_{\text{O}_3-i} \times [i]$ were calculated, where $[i]$ was the concentration before ozonation (for CBZ, KET, Cl^- , HCO_3^- , SO_4^{2-} and NH_3). Table 4.4 gives the relevant $k_{\text{O}_3-i} \times [i]$ values. It appeared that the $k_{\text{O}_3-i} \times [i]$ value decreased in the order $\text{CBZ} > \text{NH}_3 \gg \text{HCO}_3^- > \text{Cl}^- > \text{KET} > \text{SO}_4^{2-}$, indicating that the consumption of molecular ozone was mainly due to its reactions with CBZ and NH_3 . In addition, the fact that $k_{\text{O}_3\text{-CBZ}} \times [\text{CBZ}]$ had the largest value was evidence that the participation of ionic salts and ammonia had no significant influence on the ozonation of ozone-reactive CBZ. In contrast, due to a relatively low $k_{\text{O}_3\text{-KET}} \times [\text{KET}]$, there was significant inhibition of the abatement of ozone-recalcitrant KET when ionic salts and ammonia were present in the solutions, especially for NH_3 and HCO_3^- . It should be pointed out that, even though the related ozone kinetic rate constants of these ions were also low like KET, below $20 \text{ L mol}^{-1} \text{ s}^{-1}$, as reported by Hoigné et al. (1985), their concentration in SAM and SUM was around three orders of magnitude higher than that of selected KET (see Table 4.1). Therefore, it was easy to understand that the removal efficiency of KET at the same ozone consumption was largest in PWM-2, intermediate in SAM with ionic salts, and lowest in SUM with ionic salts and ammonia.

Table 4.4 $k_{O_3-i} \times [i]$ values of the different compounds before ozonation

<i>i</i>	$k_{O_3-i} (\text{L mol}^{-1} \text{s}^{-1})^a$	$k_{O_3-i} \times [i] (\text{s}^{-1})$		
	-	PWM-2	SAM	SUM
CBZ	3×10^5	12.70	12.70	12.70
KET	0.4	1.57×10^{-5}	1.57×10^{-5}	1.57×10^{-5}
Cl ⁻	0.003	-	3.14×10^{-4}	3.50×10^{-4}
HCO ₃ ⁻	0.01	-	3.19×10^{-3}	2.47×10^{-3}
SO ₄ ²⁻	0.0001	-	1.62×10^{-6}	1.62×10^{-6}
NH ₃	20	-	-	6.31
Total	-	12.70	12.70	19.01

(a) k_{O_3-ion} values were taken from Hoigné et al. (1985)

With respect to pH variation during the ozonation of SAM, a slight increase in pH, from 8.1 to 9.2, was observed, which was possible due to the presence of high contents of bicarbonate. However, the effect of bicarbonate on pH remained unclear during the ozonation. For SUM, the solution pH was quite constant over the entire process, which was associated with ammonia as buffer.

IV.4.2 Ozonation of CBZ in real urine

Besides ionic salts and ammonia, organic matters in real urine had a non-negligible influence on the transformation of micropollutants by ozonation. To evaluate the role of organic matters in the degradation efficiency of micropollutants and ozone consumption, the ozonation experiment was carried out with real urine containing ionic salts, ammonia and organic matter. Note that only the ozonation efficiency with respect to ozone-reactive CBZ was discussed here. Figure 4.5c and 4.5d show plots of the observed CBZ removal against cumulated consumed ozone dose during the ozonation of two urine effluents (HUM-1 and HUM-2), and Figure 4.6 plots the residual concentration of organic carbon (NPOC), organic carbon from CBZ and COD.

Regarding ozonation of HUM-1 (NPOC₀: 88 mg L⁻¹, N-NH₄⁺: 123 mg L⁻¹) (Figure 4.5c), at a cumulated consumed ozone dose of 56.8 mg, the concentration of CBZ declined drastically from the initial $21.8 \pm 1.5 \mu\text{g L}^{-1}$ to around $0.2 \mu\text{g L}^{-1}$, i.e., >95% depletion (0.043 mg CBZ eliminated). At the same time, the removal of NPOC was only 2.6 mg (i.e. 1.5% removal), as implied in Figure 4.6a, which corresponded to a specific ozone dose of 0.3 mg transferred ozone per mg NPOC₀. When ozonation was further applied up to 300 min, the removal of NPOC reached 82% corresponding to 145 mg NPOC removed for 1731 mg ozone consumed.

For HUM-2 (NPOC₀: 415 mg L⁻¹, N-NH₄⁺: 516 mg L⁻¹), a higher ozone dose, of 564 mg was consumed to achieve a removal >90% of CBZ (0.007 mg CBZ eliminated) (Figure 4.5d) and of 50 mg NPOC (Figure 4.6b), which corresponded to a specific ozone dose of 0.7 mg

transferred ozone per mg NPOC₀. When the experiment was extended up to 450 min, the removal of NPOC gained 568 mg (i.e. 68% removal) for a total ozone consumption of 6191 mg.

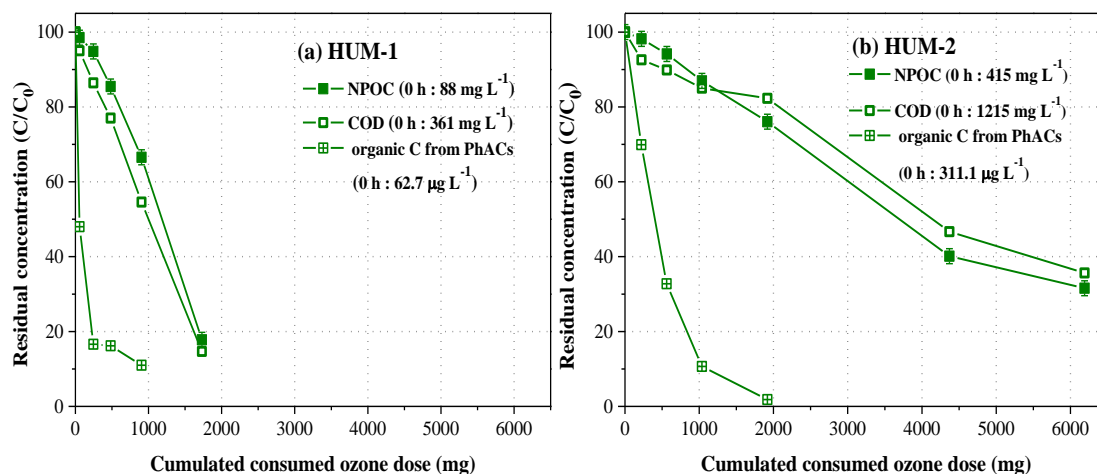


Figure 4.6 Residuals of organic carbon and COD as a function of cumulated consumed ozone dose. (a) HUM-1 (300 min), (b) HUM-2 (450 min). gas flow rate: 30 L h⁻¹. initial pH: 7.0 for HUM-1, and 8.9 for HUM-2.

Even though the concentration of CBZ in both HUM-1 and HUM-2 (see Table 4.1) was much lower than that in SUM, the ozonation efficiency on real urine in terms of CBZ removal was much less than that on SUM without organic matters (23.39 mg CBZ removal at a 23.7 mg ozone consumption, see Figure 4.5b). These results demonstrated that the degradation rates of micropollutants were influenced significantly by the reactions of organic matters with molecular ozone.

Figure 4.7 presents the pH evolution as a function of cumulated consumed dose. For both hydrolysed urine, as expected, the solution pH decreased during the ozonation process, from 7.0 to 4.0 in HUM-1, and from 8.9 to 7.7 in HUM-2, which was related to the oxidation of organic matters to form carboxylic acid, aldehyde and ketone as end products. In addition, a strong decrease of pH was found in HUM-1, which indicated that organic matters in HUM-1 was more easily degraded as compared to HUM-2.

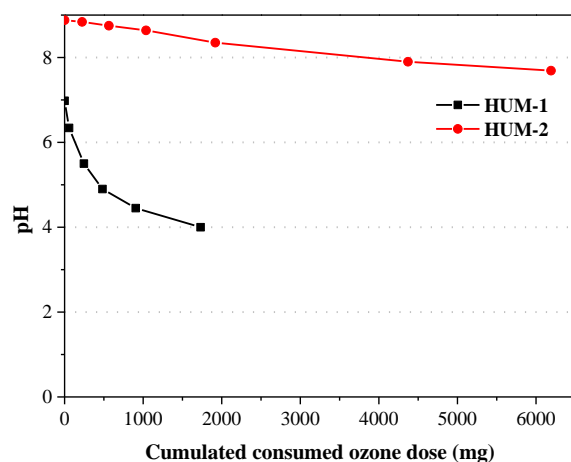


Figure 4.7 pH variation as a function of cumulated consumed ozone dose.

IV.4.3 Variation of the concentration of ionic salts and N-NH₄⁺

As discussed above, the presence of ionic salts, ammonia and organic matters could consume molecular ozone to a certain extent, so the efficiency of micropollutant degradation was influenced significantly. To better understand this point, the removal of ions after the ozonation process is depicted in Figure 4.8.

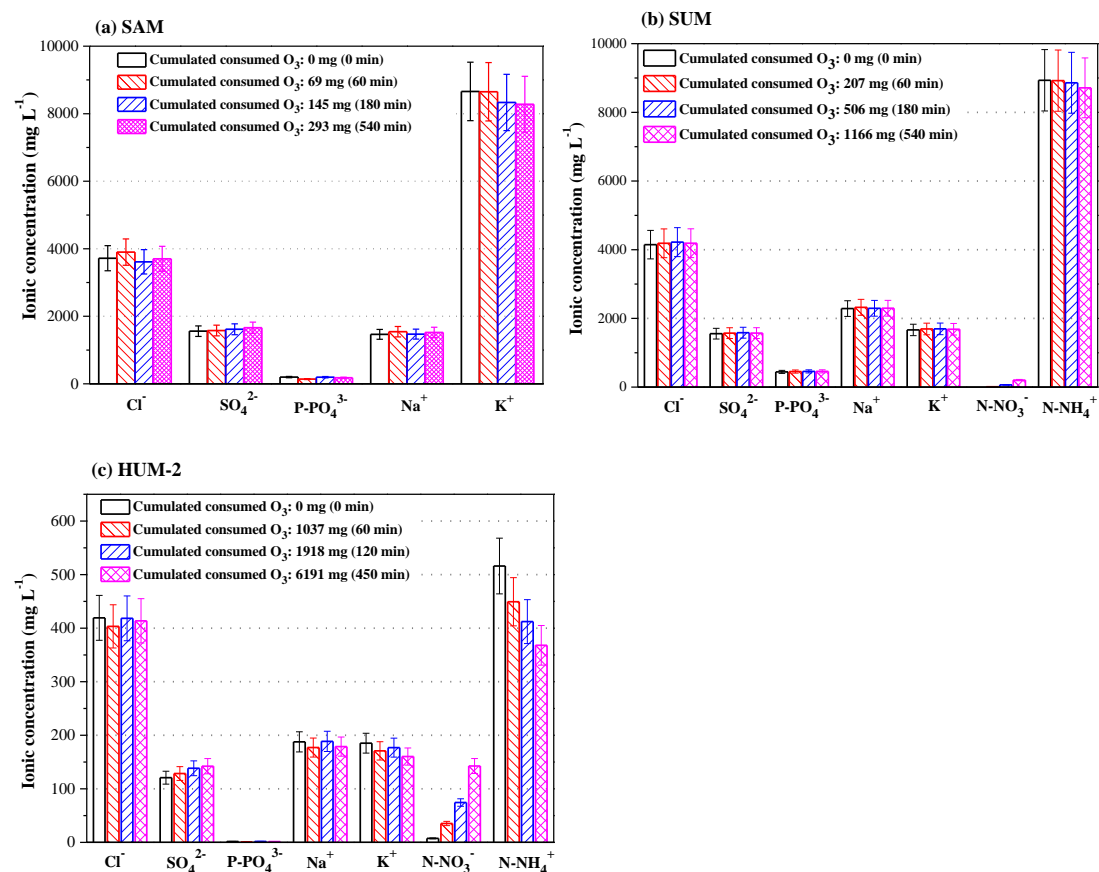


Figure 4.8 Variation of ionic concentration during the ozonation of SAM, SUM and HUM-2.

After ozonation of SAM, SUM and HUM, for the tested ions, not including N-NO₃⁻ and N-NH₄⁺, no significant difference in their concentration was expected.

During the ozonation of urine-based solutions containing ammonia, the depletion of N-NH₄⁺ by ozonation could lead to the yield of nitrate (see Reaction 19-20). For the ozonation of SUM (pH 9.1) and HUM-2 (pH 8.9), the yield of nitrate production was almost same as the rate of ammonia reduction. It was interesting to note, however, that the high yield of N-NO₃⁻ was inconsistent with the reduced amount of N-NH₄⁺ after HUM-1 (pH 7.0) ozonation, probably indicating that other nitrogen-containing compounds contained in urine were also oxidized, such as creatinine or unprotonated amino acids (cysteine, tyrosine, tryptophan, etc.) (Eichelsdörfer and Jandik, 1985). Moreover, molecular ozone preferably attacked NH₃ (electrophilic species) rather than NH₄⁺, thus the lower the pH value, such as in HUM-1 (pH 7.0), the lower the ratio NH₃/NH₄⁺, and the slower the degradation rate of ammoniacal species.

During the ozonation process, N-NO_2^- was not found in significant amounts, which was in good agreement with the observation from Hoigne and Bader (1978).

IV.4.4 Comparison of removal efficiencies of CBZ and KET in the different matrix

Table 4.5 compares the removal efficiencies of CBZ and KET in the different matrix.

For ozone-reactive CBZ, the presence of highly concentrated ions and ammonia affect slightly the amount of ozone consumption for an equivalent elimination of CBZ from different organic matters-free solutions. However, when organic matters were involved (in HUM-2), a large ozone dose, around 564 mg, was consumed to achieve a satisfactory removal rate for CBZ, which was due to the competitive reactions of organic matters with molecular ozone. These findings indicated that organic matter was more pronounced in affecting elimination efficiencies of CBZ by ozonation as compared to other constituents in real urine.

Regarding the ozonation of ozone-refractory KET, when ions and ammonia were present, the amount of ozone consumption to achieve an equivalent elimination increased significantly, from 57.3 mg in PWM-2 to 1166 mg in SUM (only 66% removal for KET), demonstrating water matrix had a strong impact on the removal efficiencies of KET.

Table 4.5 Variation of PhACs, organic carbon and ionic salts after ozonation

Solutions	PWM-2		SAM		SUM		HUM-1	HUM-2
	0-99% CBZ removal	0-maxmum KET removal	0-99% CBZ removal	0-maxmum KET removal	0-99% CBZ removal	0-maxmum KET removal	0-99% CBZ removal	0-99% CBZ removal
Parameters								
Time (min)	3	40	3	420	6	540	5	30
Cumulated consumed O ₃ (mg)	6.2	57.3	7.3	245	23.7	1166	56.8	564
CBZ eliminated (mg)	20.55	-	18.92	-	23.39	-	0.043	0.007
KET eliminated (mg)	1.89 (9% removal)	20.24 (>95% removal)	0.41 (2% removal)	19.96 (>95% removal)	0.66 (3% removal)	14.95 (66% removal)	-	-
NPOC eliminated (mg)	1.04 (3% removal)	7.02 (24% removal)	1.09 (3% removal)	10.36 (24% removal)	0.34 (1% removal)	3.72 (10% removal)	2.64 (1.5% removal)	48.6 (6% removal)
N-NH ₄ ⁺ eliminated (mg)	-	-	-	-	9	441	10	78
Consumed O ₃ / (NPOC + N-NH ₄ ⁺) eliminated (mol/mol)	1.5	2.0	1.7	5.9	0.7	0.8	1.3	1.2

-: not analysed

IV.5 Effect of water matrix on ozonation consumption and kinetic regimes

IV.5.1 Hatta number and enhancement factor

The Hatta number and the theoretical enhancement factor in the different solution matrices were calculated to elucidate the corresponding kinetic regimes, and compared to the experimental enhancement factor, as listed in Table 4.6. The reactions of intermediate products were not considered here. Moreover, on account of the complexity of the organic matters in real urine, it was not possible to estimate the reaction kinetic regime in terms of the theoretical Hatta number and the instantaneous enhancement factor during the ozonation of HUM-1 and HUM- 2.

Table 4.6 Hatta number, instantaneous enhancement factor (E_i) and enhancement factor from the experimental result (E_{exp}) in PWM-2, SAM, SUM and HUM

Parameter	At the initial time of ozonation					When dissolved ozone was detected			
	PWM-2	SAM	SUM	HUM-1	HUM-2	PWM-2	SAM	HUM-1	HUM-2
Diffusivity of ozone at 20 °C ($m^2 s^{-1}$) ^a	1.3×10 ⁻⁹					1.3×10 ⁻⁹			
k_L ($m s^{-1}$) ^a	2.0×10 ⁻⁵					2.0×10 ⁻⁵			
Ozone solubility parameter	0.31 ^b	0.25 ^c	0.25 ^c	0.31 ^c	0.30 ^c	0.31	0.25	0.31	0.30
Hatta number ^d	6.4	6.4	11.1	-	-	0.005	0.007	-	-
E_i ^e	1.4	1.4	42466	-	-	~1	~1	-	-
$E_{theoretical}$ ^f	1.4	1.4	11.1	-	-	~1	~1	-	-
E_{exp} ^g	3.8	7.8	100.3	12.9	97.7	1.7	2.6	1.5	2.6

(a): from Beltrán (2004). (b): from López-López et al. (2007). (c): the solubility of ozone in salt solution was calculated based on the Sechenov equation (see Chapter II.3.4). (d): calculated by Equation 37. (e): calculated by Equation 38. (f): $E_{theoretical}$ = minimum (Ha , E_i) for a fast kinetic regime (Levenspiel, 1999). (g): calculated by Equation 40.

For PWM-2, SAM and SUM, at the initial time of ozonation, as the Hatta number was found to be higher than 3, indicating that a fast kinetic regime existed and that the reactions occurred near the gas-liquid interface, and not in the liquid bulk. The theoretical enhancement factors were found equal to 1.4 and 11.1, respectively, and the experimental values ranged from 3.8, 7.8 and 100.3. These figures indicate that the overall rate of ozone consumption was limited by mass transfer of ozone. Moreover, no dissolved ozone was detected during the first 10 min for PWM-2 (Figure 4.3b), during the first 3 min for SAM (Figure 4.5a), and over the entire ozonation process for SUM (Figure 4.5b), which supported this conclusion. It should be emphasized that, in the case of SUM, the instantaneous enhancement factor (E_i) was much higher than $5Ha$ ($E_i > 5Ha$), demonstrating that the pseudo-first order reaction regime occurred

in the liquid film where the theoretical enhancement factor ($E_{theoretical}$) was almost equal to the Hatta number ($E_{theoretical} = Ha$) (Levenspiel, 1999). For HUM-1 and HUM-2, the experimental enhancement factor was found equal to 12.9 and 97.7 respectively, also suggesting the occurrence of a fast kinetic regime, as confirmed by the absence of dissolved ozone during the first 5 min of ozonation for HUM-1 (Figure 4.5c) and the first 120 min for HUM-2 (Figure 4.5d).

Since the concentration of ozone-reactive compound, such as CBZ, decreased with the reaction time, the Hatta number also decreased with the ozonation process, and mass transfer limitation was progressively reduced, leading to the increase of dissolved ozone concentration. When dissolved ozone was detected in PWM-2 and SAM, the concentration of CBZ was reduced to the detection limit. Consequently, the ozonation reaction for PWM-2 and SAM changed from the fast kinetic regime of the beginning to slow reaction with respect to mass transfer, with the Hatta number value of 0.005 for PWM-2 and 0.007 for SAM. A bit higher Hatta number in SAM than in PWM-2 was linked to the high salinity in SAM. Another “blank” ozonation experiment on the saline solution not spiked with PhACs (SA) (see Appendix 4) demonstrated that dissolved ozone was observed as soon as the experiment started. This indicated that the absence of dissolved ozone during the first 3 min ozonation in SAM was attributed to the fast oxidation of CBZ and not to the salts themselves.

It was thus concluded that for PWM-2 and SAM a fast kinetic regime in PWM-2 and SAM occurred at the beginning of the experiment, due to the presence of CBZ, highly reactive with ozone. Once CBZ was completely eliminated, dissolved ozone started to accumulate in the liquid solution and the kinetic regime became slow compared to mass transfer. With respect to SUM, in addition to CBZ, highly concentrated ammonia also rapidly reacted with molecular ozone in the liquid film, leading to the absence of dissolved ozone, and thus mass transfer limitation, during the entire ozonation process. For the ozonation of real urine, the absence of dissolved ozone and the experimental enhancement factor (E_{exp}) >1, showed that fast reactions were also taking place between molecular ozone and various compounds. Here again the overall ozonation kinetics was mass transfer controlled.

IV.5.2 Ozone effectiveness yield

In order to determine the effectiveness of micropollutant elimination by ozone, it was relatively important to know the rate of ozone consumption by the wastewater matrix (Nöthe et al., 2009). Figure 4.9 shows the cumulated consumed ozone dose versus applied ozone dose during the ozonation process in PWM-2, SAM, SUM, HUM-1 and HUM-2. Note that, the ozonation reaction time of PWM was only 120 min, where CBZ and KET have disappeared completely. However, for SAM, SUM and HUM, a longer ozonation time was required to reduce organic compounds. Applied ozone dose was defined in Equation 20 in Chapter II.3.

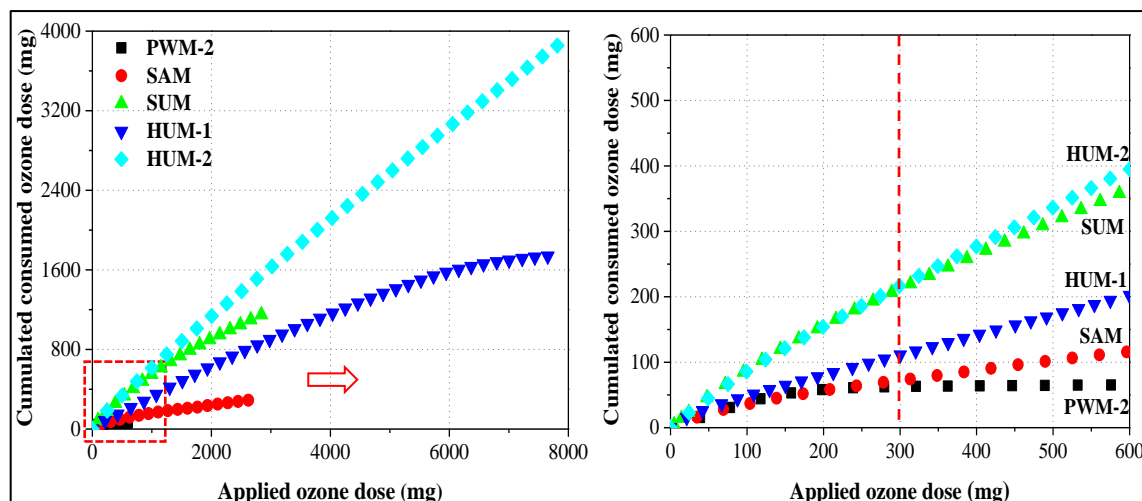


Figure 4.9 Cumulated consumed ozone dose as a function of applied ozone dose during the ozonation of 5 solution matrices. Reaction time: 120 min for PWM-2, 540 min for both SAM and SUM, 300 min for HUM-1, and 450 min for HUM-2.

From Figure 4.9, before 300 mg of applied ozone dose, the slope of the curve of cumulated consumed ozone dose against the applied ozone dose followed an order of $\text{PWM-2} \approx \text{SAM} < \text{HUM-1} \ll \text{SUM} \approx \text{HUM-2}$. The similar tendency for PWM-2 and SAM indicated that the reaction of salts with ozone did not much affect the global ozone consumption rate. On the other hand, the presence of ammonia and/or organic matters has led to an increase of the slope with an intermediate value for HUM-1, less concentrated, and the highest slope for highly concentrated SUM and HUM-2. These findings also confirmed the competitive influence of ammonia and organic matters on the model micropollutants' decomposition by ozone.

After 300 mg of applied ozone dose, ozone-consumption seemed to be constant for PWM-2, with a value of around 64 mg consumed ozone, revealing that all oxidation reactions had finished this including CBZ and KET, as shown in Figure 4.3b, but also their oxidation by-products. This was confirmed by the value gained by the liquid/gas ratio around 0.35 (approximately equal to dissolved ozone saturation: 0.31). On the contrary, the consumed ozone dose of SAM, SUM, HUM-1 and HUM-2 continued to increase until the final moment of ozonation, reflecting that the relevant reactions were continuing due to the presence of highly concentrated ionic species. In addition, even if the concentration of ammonia in SUM was around 17 times greater than in HUM-2, the rate of ozone consumption in HUM-2 was slightly higher than that in SUM, indicating the important influence of organic matters present in real urine on ozone consumption.

Table 4.7 presents the ozone transferred yield and the ratio of consumed ozone dose to transferred ozone dose at the end of ozonation experiment. The ozone transferred yield was defined as: $(\text{transferred ozone dose} / \text{applied ozone dose}) \times 100$. Transferred ozone dose was expressed by Equation 21 in Chapter II.3.

For all the ozonation experiments, the transferred yield was less than 46%, whereas the ratio of consumed ozone dose to transferred ozone dose was higher than 89%. These observations provided implication that mass transfer was a limiting step.

Table 4.7 Transferred ozone yield and ratio of consumed ozone dose to transferred ozone dose at the end of reaction time

Parameter	Unit	PWM-2	SAM	SUM	HUM-1	HUM-2
[O ₃] gas-in	mg L ⁻¹	~10 mg L ⁻¹	~10 mg L ⁻¹	~10 mg L ⁻¹	~50 mg L ⁻¹	~60 mg L ⁻¹
Reaction time	min	120	540	540	300	450
Applied ozone	mg	591.4	2657.9	2900.4	7500.2	13504.3
Transferred ozone	mg	73.6	297.0	1165.9	1759.2	6195.8
Consumed ozone	mg	65.3	293.0	1165.9	1731.1	6190.7
Transferred yield	-	12%	11%	40%	24%	46%
Consumed ozone / Transferred ozone	-	89%	99%	100%	98%	100%

IV.6 Conclusions of this chapter

In the present study, a series of experiments on the ozonation of CBZ and KET in ultrapure water (PWM-1, PWM-2), saline solution without ammonia (SAM), synthetic urine containing salts and ammonia (SUM), and finally hydrolysed urine containing ionic salts, ammonia and organic matters (HUM-1 and HUM-2) were performed in a stirred semi-batch reactor, with the aim of investigating and evaluating the influence of the effects of solution matrices on the micropollutant elimination efficiency, ozone consumption and ozonation kinetic regimes. Most of the findings noted below were useful for the understanding micropollutants' ozonation process in solutions with highly concentrated ions and organic matters.

- The degradation of both CBZ and KET at the studied pH (between 8 and 9), was mainly achieved by molecular ozone. The oxidation of CBZ was fast, whereas the reaction between ozone and KET was slow;
- When the solution contained highly concentrated ions and ammonia, they exhibited a slight influence on the removal efficiency of ozone-reactive CBZ. However, once organic matters were involved (as in hydrolysed urine), the degradation of CBZ was strongly inhibited due to the competition for molecular ozone;
- The presence of ionic salts and ammonia significantly reduced the removal efficiency of ozone-refractory KET by ozonation;
- The occurrence of fast kinetic regimes, responsible for mass transfer limitation, was observed at the beginning of all experiments. This was attributed to the reaction of molecular ozone with CBZ, ammonia and organic matters;

- The oxidation degree of micropollutants, the ozone consumption and the ozone kinetic regimes were strongly matrix-dependent.

When both the amount of ozone consumed and the elimination degree of PhACs, especially ozone-refractory PhACs, are taken into account, it appears that the quantity of ammonia and organic matters should be reduced from real urine by available technologies prior to the ozonation process, in the aim of improving the oxidation degree of micropollutants at a lower ozone consumption.

**Chapter V A combination process of struvite precipitation,
reverse osmosis and ozonation for the reclamation of
source- separated urine: nutrient valorisation and
micropollutants removal**

Introduction

Urine, a small but highly concentrated stream, is a major source of unwanted contaminants including emerging micropollutants (pharmaceuticals and natural hormones) and nutrient salts (P, N, and K) in the municipal wastewater (Abdel-Shafy and Mohamed-Mansour, 2013; Dodd et al., 2008). In the context of wastewater reclamation, separation and treatment of urine at the source, a sustainable wastewater management, have received increasing attention. Separation and treatment of urine at the source not only allows nutrients valorization but also prevents potentially hazardous urine-derived micropollutants from releasing into wastewater streams (Maurer et al., 2006; Pronk et al., 2006; Pronk and Koné, 2009).

Over the past two decades, many researchers have investigated the recovery of P nutrients as struvite from real urine (Ganrot et al., 2007; Pronk and Koné, 2009; Ronteltap et al., 2010). Their results demonstrate that struvite precipitation of urine is successful in producing a solid P fertilizer. A large quantity of micropollutants still remained in the urine solutions (Ronteltap et al., 2007). On the other hand, information on the removal of micropollutants from real urine is still scarce.

The main objectives of the present study were to recover P nutrients and eliminate urine-derived micropollutants from real urine. For these purposes, an integrated treatment process, which consisted of struvite precipitation, low-pressure RO process and ozonation, was proposed for urine reclamation with respect to the recovery of P nutrients and the elimination of unwanted micropollutants. The findings obtained in this study could provide useful information on the reclamation of highly concentrated wastewater.

V.1 Description of the treatment line

Figure 5.1 displays the treatment line of urine valorisation. Before struvite precipitation test, UF as a pre-treatment was to remove bigger particles from real urine solutions. Struvite precipitation was performed to recover P nutrients from urine-based solutions (see Reaction 14 in Chapter I.4). The removal of P before the RO system also avoided RO membrane scaling caused by the P-based crystals (such as hydroxyapatite). Subsequently, the RO filtration process was used to retain micropollutants from the tested solutions to a higher concentration. At last, the application of ozonation unit was to degrade micropollutants present in the tested solutions.

Five solutions, including ultrapure water with PhACs (PWM) as a blank control, synthetic urine with PhACs (SUM), and three hydrolysed urine with PhACs (HUM-1, HUM-2, and HUM-3) were investigated. The residual of the target PhACs, dissolved organic carbon (NPOC), chemical oxygen demand (COD), dissolved organic carbon (DIC), as well as ionic analysis was addressed along with the treatment line.

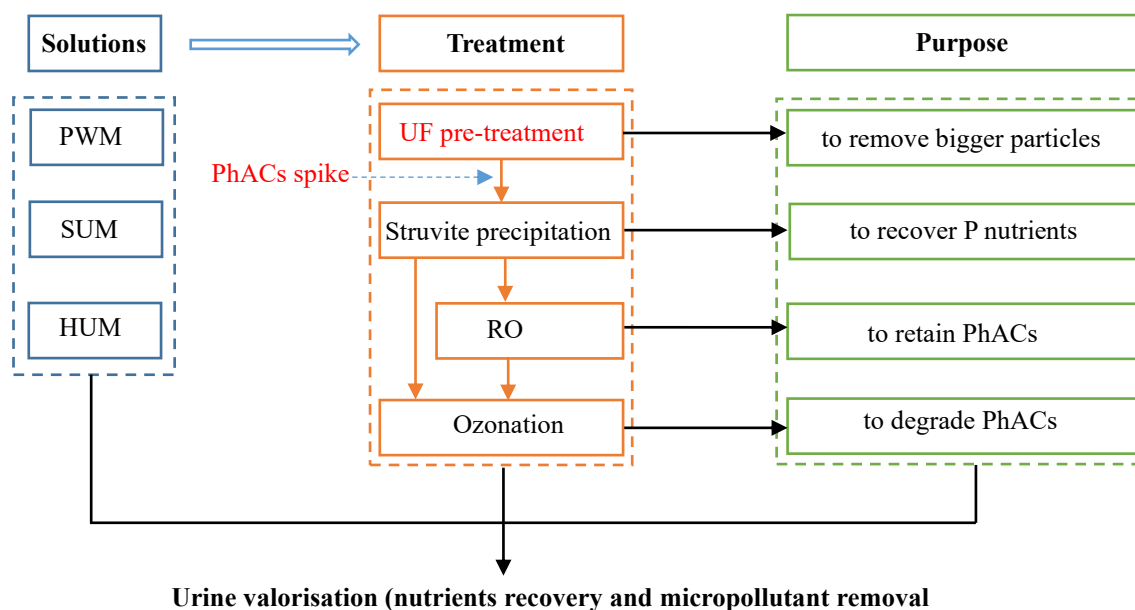


Figure 5.1 Experimental treatment line of urine valorisation

Five scenarios were performed in this work, as depicted in Figure 5.2.

- **Scenario 1:** a blank experiment was performed with ultrapure water containing PhACs (PWM). Due to the absence of P-PO_4^{3-} , only RO and ozonation were used. RO permeate and RO concentrate collected were further treated by ozonation.
- **Scenario 2:** SU with PhACs (SUM) was treated by struvite precipitation + RO process + ozonation.
- **Scenario 3 and 4:** for HU-1 and HU-2 containing PhACs (HUM-1 and HUM-2), a similar treatment line was run. After UF treatment, PhACs mixture was spiked into urine solutions. Subsequently, precipitation test was run. After that, two steps, RO and ozonation, were conducted to treat urine effluents.
- **Scenario 5:** the treatment line of HUM-3 was almost similar to that of SUM.

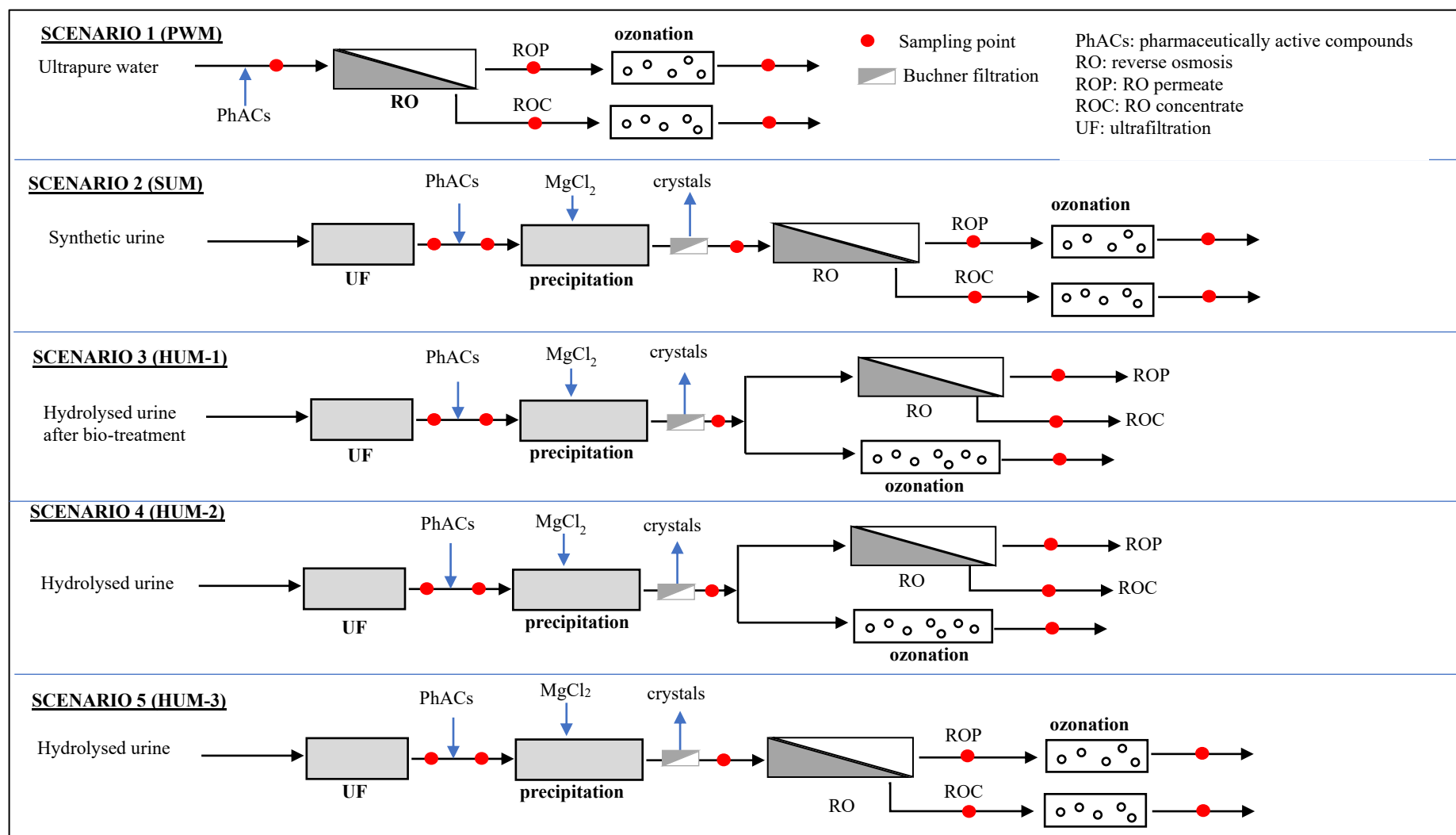


Figure 5.2 Treatment of urine-based solutions by precipitation, RO and ozonation

V.1.1 Characteristics of urine-based solutions and the target PhACs spike

The composition and preparation of synthetic urine mixture (SU) has been introduced in Chapter IV (see Table 4.1).

Three types of hydrolysed urine wastewater (HU-1, HU-2 and HU-3) were investigated in this work. HU-1 was collected after bio-treatment of real urine. HU-2 and HU-3 were collected from a storage tank connected to a urine collecting system. Prior to precipitation experiments, these urine solutions were settled, and then permeated through an ultrafiltration (UF) membrane with a pore size of 0.1 μm , aiming to remove precipitates matters or the other bigger particles. The main characteristics of urine-based solutions after UF filtration are displayed in Table 5.1. It was observed that there was a significant difference in the concentration of constituents present in three HU solutions. For example, the concentration of NPOC in HU-1 collected after bio-treatment, was 9.6 times and 3.6 times lower than that in HU-2 and HU-3, respectively. The N-NH_4^+ concentration exhibited the following order of $\text{HU-1} < \text{HU-3} < \text{HU-2}$.

Table 5.1 Characteristics of synthetic urine and of hydrolysed urine after UF pre-treatment

Parameter	Unit	SU	HU-1 (after bio-treatment)	HU-2 (hydrolysed urine)	HU-3 (hydrolysed urine)
pH	-	9.3	8.6	9.2	9.3
Conductivity	mS cm^{-1}	41.6 ± 0.83	27.10 ± 0.54	31.20 ± 0.62	24.40 ± 0.49
NPOC ¹	mg L^{-1}	- ⁴	321 ± 6	3089 ± 62	1164 ± 33
DIC ²	mg L^{-1}	3024 ± 302	261 ± 5	3919 ± 79	1661 ± 33
COD ³	mg L^{-1}	-	1475 ± 10	8017 ± 10	2900 ± 10
Cl^-	mg L^{-1}	4135 ± 414	2678 ± 268	2747 ± 275	2116 ± 212
N-NO_3^-	mg L^{-1}	-	11 ± 1	99.76 ± 10	n.d. ⁵
SO_4^{2-}	mg L^{-1}	1506 ± 151	7100 ± 710	1440 ± 144	600 ± 60
P-PO_4^{3-}	mg L^{-1}	407 ± 41	442 ± 44	499 ± 50	362 ± 36
Na^+	mg L^{-1}	1396 ± 140	1882 ± 188	1964 ± 196	1066 ± 107
N-NH_4^+	mg L^{-1}	7694 ± 769	2500 ± 250	7272 ± 727	3907 ± 397
K^+	mg L^{-1}	1868 ± 187	1469 ± 147	2013 ± 201	935 ± 94
Mg^{2+}	mg L^{-1}	-	111 ± 11	311 ± 31	10.34 ± 1.03
Ca^{2+}	mg L^{-1}	-	75 ± 8	172 ± 17	242 ± 24

(1) NPOC : dissolved organic carbon. (2) DIC : dissolved inorganic carbon. (3) COD : chemical oxygen demand. (4) - : not analysed. (5) n.d. : not detected.

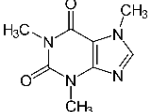
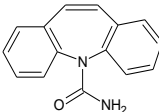
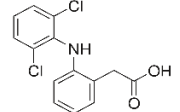
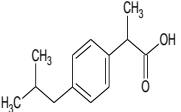
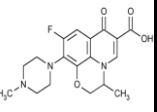
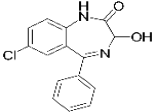
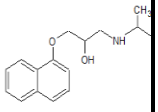
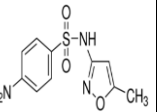
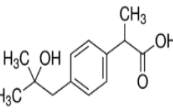
After UF pre-treatment, a mixture of 9 PhACs, prepared with methanol solvent, was spiked into the target solutions, where the concentration of PhACs was at the trace level. Methanol concentration was 0.3% (v/v) in the tested solutions. Table 5.2 shows the final concentration of the target PhACs in the tested solutions. Note that, due to the presence of methanol, PhACs spike led to a significant increase in the load of both NPOC and COD. The key physicochemical properties of the target PhACs are listed in Table 5.3.

Table 5.2 Concentration of target PhACs in the tested solutions before precipitation or RO process

PhACs $\mu\text{g L}^{-1}$		PWM	SUM	HUM-1	HUM-2	HUM-3
2OH-ibuprofen	2OH-IBP	n.d. ¹	n.d.	154	1237.0 \pm 67.4	977.0 \pm 58.7
Caffeine	CAF	320.5 \pm 3.5	316.5 \pm 9.8	1139	575.2 \pm 10.2	2306.0 \pm 18.2
Carbamazepine	CBZ	27.7 \pm 0.1	30.1 \pm 0.1	425.6	33.0 \pm 1.0	21.8 \pm 0.2
Diclofenac	DIF	46.7 \pm 0.4	49.4 \pm 1.9	13.3	45.8 \pm 4.2	47.6 \pm 0.1
Ibuprofen	IBP	2196.4 \pm 44.9	2114.6 \pm 15.4	336.0	2364.0 \pm 17.8	2235.9 \pm 54.0
Ofloxacin	OFL	85.7 \pm 0.1	170.3 \pm 1.9	87.0	54.1 \pm 0.8	112.6 \pm 4.9
Oxazepam	OXA	257.0 \pm 1.7	217.1 \pm 5.6	2.5	19.3 \pm 0.8	208.4 \pm 2.2
Propranolol	PRO	125.5 \pm 0.2	122.2 \pm 3.5	24.4	10.5 \pm 0.1	70.7 \pm 1.1
Sulfamethoxazole	SMX	336.3 \pm 7.6	333.0 \pm 13.4	46.2	8.3 \pm 0.4	217.3 \pm 1.5
NPOC (mg L^{-1}) ²	-	839 \pm 17	907 \pm 18	2081 \pm 42	4170 \pm 83	2066 \pm 41
COD (mg L^{-1}) ²	-	- ³	-	8000 \pm 10	12983 \pm 10	6600 \pm 10

(1) n.d. : not detected. (2) after PhACs spike. (3) - : not analysed

Table 5.3 Relevant properties of the target PhACs

PhACs	Caffeine (CAF)	Carbamazepine (CBZ)	Diclofenac (DIF)	Ibuprofen (IBP)	Ofloxacin (OFL)	Oxazepam (OXA)	Propranolol (PRO)	Sulfamethoxazole (SMX)	2 hydroxyibuprofen (2OH-IBP)
Family group	stimulant	antiepileptic	anti-inflammatory	anti-inflammatory	antibiotic	anxiolytic	beta blocker	antibiotic	ibuprofen metabolite
Structure									
Formula	C ₈ H ₁₀ N ₄ O ₂	C ₁₅ H ₁₂ N ₂ O	C ₁₄ H ₁₁ Cl ₂ NO ₂	C ₁₃ H ₁₈ O ₂	C ₁₈ H ₂₀ FN ₃ O ₄	C ₁₅ H ₁₁ ClN ₂ O ₂	C ₁₆ H ₂₁ NO ₂	C ₁₀ H ₁₁ N ₃ O ₃ S	C ₁₃ H ₁₈ O ₃
Molar mass g mol ⁻¹	194.2	236.3	296.2	206.3	361.4	286.7	259.3	253.3	222.28
pK _a ^a	0.6, 14	2.3, 13.9 ^b	4.2	4.4	6.05, 8.22 ^b	1.7, 11.6	9.5	1.6, 5.6	not found
LogK _{ow} ^a	-0.07 (hydrophilic)	2.45 (hydrophobic)	4.51 (hydrophobic)	4.0 (hydrophobic)	-0.4 ^b (hydrophilic)	2.24 (hydrophobic)	3.48 ^b (hydrophobic)	0.9 (hydrophilic)	not found
Expected O ₃ attack	double bond	carbon double bond	aromatic amine	benzene ring	tertiary amine	benzene ring	secondary amine and naphthalene	aromatic amine	benzene ring
k _{O₃-PhACs} pH=7 L mol ⁻¹ s ⁻¹	2.5×10 ⁴ ^c	3×10 ⁵ ^d	4.6×10 ⁵ ^c	9.1 ^d	2.0×10 ⁶ ^e	1 ^f	1×10 ⁵ ^g	5.5×10 ⁵ ^d	not found
k _{O₃-PhACs} pH=7 L mol ⁻¹ s ⁻¹	not found	8.8×10 ⁹ ^h	7.5×10 ⁹ ^h	7.4×10 ⁹ ^h	4.2×10 ⁹ ⁱ	9.1×10 ⁹ ^f	not found	5.5×10 ⁹ ^h	not found
Species (pH=5.5)	uncharged, slightly basic	uncharged, neutral	negative, acidic	negative, acidic	OFL ⁺ > OFL ⁰	-	positive, basic	SMX ⁰ = SMX ⁻	negative, acidic
Species (pH=9.2)	uncharged, slightly basic	uncharged, neutral	negative, acidic	negative, acidic	OFL ⁻ > OFL ⁰	-	PRO ⁰ = PRO ⁺	negative, acidic ⁻	negative, acidic

(a) from Moffat et al. (2011). (b) Data from PubChem. (c) from Javier Rivas et al. (2011). (d) from Lee et al. (2013). (e) from Javier Benitez et al. (2015). (f) from Lee et al. (2014). (g) from Benner et al. (2008). (h) from Huber et al. (2005). (i) from Márquez et al. (2013).

Negative charge: solution pH > pK_a; Hydrophobic (high sorption): logK_{ow} > 3; hydrophilic (low sorption): logK_{ow} < 2

V.1.2 Struvite precipitation

In the case of SUM and HUM, prior to RO filtration and ozonation process, struvite precipitation tests were run in a double-wall glass reactor with a maximum volume of 2 L (as displayed in Figure 5.3). Since the Mg^{2+} concentration was low in the urine solution compared to P and $N-NH_4^+$, $MgCl_2$ with a concentration of 2.75 mol L^{-1} , as Mg^{2+} source, was added to the reactor, aiming to recover all the P through struvite formation. The initial molar $Mg^{2+} : P$ ratio was between 1.8:1 and 2.5:1. These solutions were mixed by a magnetic stirrer for 5 mins to reach equilibrium at a stirring speed of 300 rpm and at $20 \text{ }^\circ\text{C}$. Subsequently, precipitated crystals were separated through $0.45 \text{ }\mu\text{m}$ and $0.2 \text{ }\mu\text{m}$ filters (Sartorius Stedim Biotech). Urine filtrates obtained were kept at $4 \text{ }^\circ\text{C}$ for further RO filtration and ozonation. The crystals were dried in the oven at $110 \text{ }^\circ\text{C}$ and then weighted.

Before and after the precipitation test, solution samples were withdrawn for the analysis of nutrient recovery. The removal efficiency of compound i was calculated by Equation 42.

$$\text{Removal (\%)} = \frac{m_{ini} - m_{fil}}{m_{ini}} \times 100 \quad (\text{Equation 42})$$

where m_{ini} (mg) and m_{fil} (mg) represent the mass of the selected parameter in the initial urine solution and filtrate (after Buchner filtration), respectively.

In order to identify struvite crystals, SEM-EDX analysis of the crystals was conducted at the INSA Department Genie Physique from Toulouse (France).



1: Reactor (total volume 2 L)
2: Stirrer
3: Temperature control

Figure 5.3 Device for precipitation reactor

V.1.3 Dead-end RO filtration

The RO filtration trials of different solutions were conducted in a stirred dead-end batch cell at a low operating pressure and at room temperature. The RO process in dead-end mode has been described in Chapter II.2. ESPA2 RO membrane was used in this work, whose properties are listed in Table 2.3 (see Chapter II.2). The mass of RO permeate was recorded by an electrical balance along with the RO filtration process. For each experiment, RO permeate and RO concentrate produced during the filtration process were collected, and then stored for the subsequent ozonation experiment or the analysis of RO

performance in terms of the retention of constituents. The operating conditions for different solutions are given in Table 5.4.

Table 5.4 Operating conditions of the dead-end RO process for different solutions

Parameter	PWM	SUM	HUM-1	HUM-2	HUM-3
Dilution times	1	1	5 ¹	5 ¹	1
Volume of RO feed (mL)	460	459	500	500	466
ΔP (bar) ²	7	7	4	4	7
pH of RO feed	5.48	9.23	5.20 ³	5.10 ³	9.25
VRF ⁴	~2	~2	~2	~1.4	~2
The permeability of the RO membrane in pure water at 20 °C (L h ⁻¹ m ² bar ⁻¹)	~2.4	~3.1	~1.9	~2.6	~2.9

(1) urine solutions were diluted 5 times with the ultrapure water. (2) ΔP : pressure difference across the membrane. (3) solution pH was adjusted to ~5 with 5 mol L⁻¹ HCl, 0.15 mL for HUM-1 and 1.6 mL for HUM-2. (4) VRF: volumetric reduction factor (volume ratio of RO feed to RO concentrate). Note that, for each solution, several membranes were used, depending on VRF achieved.

V.1.4 Ozonation experiment

Solutions, which were collected after precipitation, RO process or both, were treated by ozonation in a stirred thermostatic semi-batch reactor with a useful volume of 2 L liquid. During the ozonation process, several samples were withdrawn from the reactor at desired intervals and analysed quickly. The operating conditions of ozonation for different solutions are listed in Table 5.5.

It should be mentioned that, before ozonation, hydrolysed urine solutions, containing a high level of organic matters and inorganic ions, were diluted 20 or 10 times with ultra-pure water, aiming to shorten the operation time.

Table 5.5 Operating conditions of semi-batch ozonation for different solutions

Parameter	PWM-ROC	PWM-ROP	SUM-ROC	SUM-ROP
Ozone gas-in (mg L ⁻¹)	1.9-4.8	2.0-4.2	2.1-15.0	2.4-24.4
Dilution times	2	1	1	1
Reaction time (h)	6.0	6.0	8.0	9.0
Parameter	HUM-1	HUM-2	HUM-3-ROC	HUM-3-ROP
Ozone gas-in (mg L ⁻¹)	50	60	~55	~55
Dilution times	20	10	10	10
Reaction time (h)	5.0	7.5	8.0	8.0

ROC : RO concentrate. ROP : RO permeate

V.2 Recovery of P nutrient from urine-based solutions as struvite crystals

V.2.1 Identification of crystals

Batch precipitation experiments of four urine-based solutions containing target micropollutants (SUM, HUM-1, HUM-2, and HUM-3) were performed for 5 mins. To identify the characteristics of the crystals produced, SEM-EDX analysis was conducted for the precipitates obtained from SUM and HUM-3 experiments, as shown in Figure 5.4. The SEM images presented in Figure 5.4a and Figure 5.4c showed that: (1) two crystals collected from SUM and HUM-3 exhibited fern leaf-like and needle-like shape, which were typical shapes for struvite (Prywer et al., 2012; Wilsenach et al., 2007); and (2) the crystal size was irregular. On the other hand, it was clearly observed that O, P and Mg were the main constituents for these two crystals, with high peaks in the EDX spectrum, as indicated in Figure 5.4b and 5.4d. Their content in terms of weight% and atomic% is given in Table 5.6. The crystals from SUM mainly contained 68.78% O, 16.89% Mg, and 13.79% P (atomic%). A quite similar composition was noticed in the crystals from HUM-3. The significant presence of O, Mg, and P in the EDX spectrum has been reported frequently in the literature (Table 5.6). And the characteristic peaks of the precipitates in the XRD analysis matched well with the database model for struvite (Huang et al., 2010; Kwon et al., 2018; Le Corre et al., 2005; Zhang et al., 2009). Thus, the precipitates produced in this work were recognized as struvite crystals.

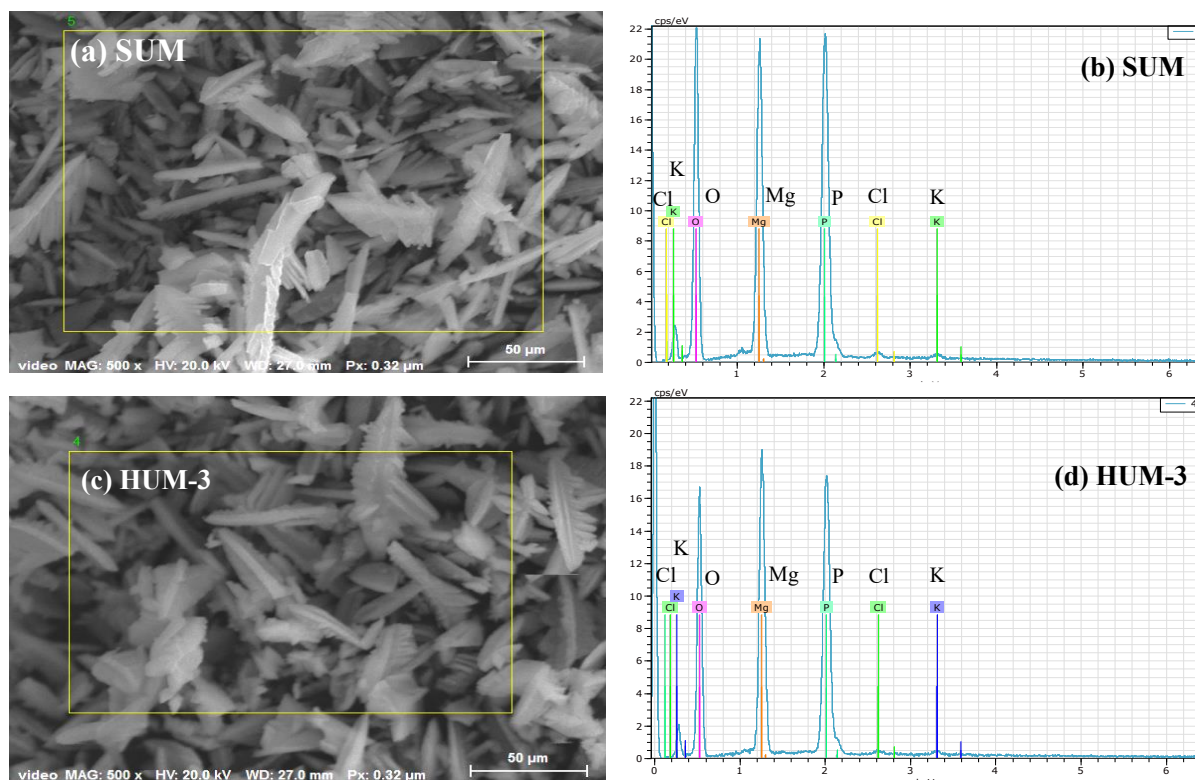


Figure 5.4 SEM image and EDX spectrum of the crystals from the precipitation of SUM and HUM-3 with MgCl_2 as Mg^{2+} source.

Table 5.6 Compositions of crystals from this study and the elements of struvite reported by the previous literature

Parameter	SUM		HUM-3		Reference 1		Reference 2	Reference 3
	weight%	atomic%	weight%	atomic%	weight%	atomic%	weight%	weight%
O	56.21	68.78	53.41	66.20	43.40	46.85	52.39	50.01
Mg	20.97	16.89	23.16	18.90	15.03	10.67	13.26	19.88
P	21.82	13.79	22.43	14.36	17.38	9.69	10.90	27.26
Cl	0.63	0.35	0.46	0.26	0.64	0.31	0.66	- ¹
K	0.37	0.18	0.54	0.28	-	-	3.08	-
N	-	-	-	-	-	-	-	0.82
C	-	-	-	-	21.61	31.07	11.00	-
Atomic ratio Mg :P	-	1.2 :1	-	1.3 :1	-	1.1 :1	-	-

Reference 1: from Huang et al. (2010). Reference 2 : from Kwon et al. (2018). Reference 3 : from Kumar and Pal (2013).

(1) -: not analysed

V.2.2 Removal of P by struvite precipitation

The removal efficiencies of global parameters including P and N-NH₄⁺ were calculated based on their measured mass before and after precipitation (see Equation 40), and the results are presented in Table 5.7. Almost all the P-PO₄³⁻ was removed from the four urine-based solutions, with a removal rate ranging from 92% in HUM-2 to 98% in SUM. Similar observations have been reported in the literature (Kemacheevakul et al., 2015; Ronteltap et al., 2010; Wilsenach et al., 2007). With respect to N-NH₄⁺, only 7%~48% removal was achieved by the struvite precipitation, which related to the relatively high load of N-NH₄⁺ in the urine solutions, at least 2600 mg L⁻¹. In addition to P-PO₄³⁻ and N-NH₄⁺, other ions, such as Mg²⁺ and Ca²⁺, were eliminated during the precipitation process to a certain extent. The removal of Mg²⁺ was due to the struvite precipitation. The elimination of Ca²⁺ from real urine solutions was possibly related to the formation of calcium-based precipitates. Nonetheless, the EDX spectrum analysis of the crystals from HUM-3 displayed the absence of Ca²⁺, as implied in Figure 5.4d. The reason for this was a quite low quantity of Ca²⁺ in the real urine compared to other ions (see Table 5.1).

Table 5.7 Removal efficiencies of global parameters from urine-based solutions during the struvite precipitation

Solutions		HUM-1			HUM-2			HUM-3			SUM		
Parameter	Unit	before precipitation	after precipitation	mass loss (%) ¹	before precipitation	after precipitation	mass loss (%)	before precipitation	after precipitation	mass loss (%)	before precipitation	after precipitation	mass loss (%)
Volume	mL	270	~270	-	676	~680	-	618	~622	-	3000	~3000	-
pH	-	8.6	7.2	-	9.2	9.1	-	9.4	9.3	-	9.3	9.2	-
conductivity	mS cm ⁻¹	-	-	-	31.20 ± 0.62	-	-	24.50 ± 0.49	25.50 ± 0.51	-	41.60 ± 0.83	43.00 ± 0.86	-
DIC	mg L ⁻¹	225 ± 5	57 ± 1	74.6	4092 ± 81	3956 ± 80	2.7	1680 ± 34	1565 ± 31	6.9	3024 ± 60	3003 ± 60	0.7
COD	mg L ⁻¹	8000 ± 10	6700 ± 10	16.3	12983 ± 10	12150 ± 10	5.9	6600 ± 10	6500 ± 10	1.5	-	-	-
Cl ⁻	mg L ⁻¹	2689 ± 269	4944 ± 494	-	2766 ± 277	4118 ± 412	9.0	2107 ± 211	3477 ± 348	-	4135 ± 414	5322 ± 532	1.9
N-NO ₃ ⁻	mg L ⁻¹	n.d.	n.d.	-	118 ± 12	105 ± 11	10.4	n.d.	n.d.	-	n.d.	n.d.	-
SO ₄ ²⁻	mg L ⁻¹	-	-	-	1447 ± 145	1068 ± 107	25.8	200 ± 20	186 ± 19	7.1	1506 ± 151	1459 ± 146	3.1
P-PO ₄ ³⁻	mg L ⁻¹	389 ± 39	19 ± 2	95.0	458 ± 46	36 ± 4	92.0	331 ± 33	25 ± 3	92.4	407 ± 41	6.4 ± 0.6	98.4
Na ⁺	mg L ⁻¹	1996 ± 200	1028 ± 103	48.5	1902 ± 190	1680 ± 168	11.2	1073 ± 107	980 ± 98	8.7	1396 ± 140	1291 ± 129	7.6
N-NH ₄ ⁺	mg L ⁻¹	2623 ± 262	1361 ± 136	48.1	7051 ± 705	6166 ± 617	12.0	3826 ± 383	3367 ± 337	12.0	7694 ± 769	7164 ± 716	6.9
K ⁺	mg L ⁻¹	1583 ± 158	835 ± 84	47.3	1976 ± 198	1732 ± 173	11.8	942 ± 94	849 ± 85	9.9	1868 ± 187	1683 ± 168	9.9
Mg ²⁺	mg L ⁻¹	114 ± 11	152 ± 15	74.9 ²	298 ± 30	379 ± 38	58.0 ²	9.0 ± 0.9	169 ± 17	63.4 ²	n.d.	168 ± 17	62.0 ²
Ca ²⁺	mg L ⁻¹	68 ± 7	21 ± 2	69.2	149 ± 15	84 ± 8	43.3	236 ± 34	74 ± 7	68.8	n.d.	n.d.	-
MgCl ₂ added	mL	2.0			6.1			4.2			20		
Mole ratio Mg : P (initial)	-	2.0 : 1			2.5 : 1			1.8 : 1			2.0 : 1		

(1) mass loss (%) = (the concentration of a compound before precipitation × solution volume before precipitation) - (the concentration after precipitation × solution volume after precipitation) / (the concentration of a compound before precipitation × solution volume before precipitation) × 100

(2) The calculation of Mg²⁺ removal needed to consider the amount of Mg²⁺ due to the addition of MgCl₂.

Based on the removed mass of P-PO_4^{3-} , Mg^{2+} , and N-NH_4^+ after the precipitation, the molar ratio of $\text{Mg} : \text{P} : \text{N}$ and the theoretical mass of struvite crystals can be estimated, as shown in Table 5.8. The molar ratio of $\text{Mg} : \text{P} : \text{N}$ was between 0.9:1:2.9 for SUM and 1.6:1:7.6 for HUM-1, which was not consistent with the stoichiometric ratio of 1mol Mg per 1 mole P per 1 mole N in the struvite. The removed quantities of N-NH_4^+ (molar) was higher than that of Mg and of P, which was possibly linked to air stripping of volatile N-NH_4^+ during the precipitation process.

Table 5.8 Mass of crystals from a test and a theoretical calculation

Parameter	Unit	HUM-1	HUM-2	HUM-3	SUM
P- PO_4^{3-} removed	mg	99.79	284.84	189.06	1201
P- PO_4^{3-} removed	mmol	3.22	9.20	6.10	38.77
Mg^{2+} removed	mg	122.57	351.73	181.45	825
Mg^{2+} removed	mmol	5.04	14.47	7.47	33.92
N-NH_4^+ removed	mg	340.73	573.34	269.81	1589
N-NH_4^+ removed	mmol	24.34	40.95	19.27	113.48
Molar ratio $\text{Mg} : \text{P} : \text{N}$ removed	-	1.6 : 1 : 7.6	1.6 : 1 : 4.5	1.2 : 1 : 3.2	0.9 : 1 : 2.9
$\text{MgNH}_4\text{PO}_4 \cdot 6\text{H}_2\text{O}$ in theory	mg	790.7	2256.8	1508.6	9513.5
MgNH_4PO_4 in theory	mg	443.0	1264.0	839.0	5326.8
Crystal mass from the test	mg	408.0	1899.8	857.5	5461.1

In addition, the molar ratio of $\text{Mg} : \text{P}$, 1.2:1 for HUM-3 and 0.9:1 for SUM, was quite close to the atomic ratio of $\text{Mg} : \text{P}$, 1.3:1 for HUM-3 and 1.2:1 for SUM (see Table 5.6). These observations confirmed that P- PO_4^{3-} present in the real urine can be recovered as struvite.

Comparing the mass of crystals collected from the tests and the theoretical expected mass of anhydrous struvite (MgNH_4PO_4), in addition to HUM-2, the results obtained from the other three urine- based solutions were similar. In HUM-2, a higher mass of crystals from the tests may be due to the formation of other precipitates such as bobierrite ($\text{Mg}_3(\text{PO}_4)_2 \cdot 8\text{H}_2\text{O}$).

V.2.3 Removal of organic compounds during struvite precipitation

Table 5.9 shows the concentration of the target PhACs before and after struvite precipitation of urine-based solutions. As can be seen that, after struvite precipitation, most of the micropollutants tested still remained in the solution, which meant that only a relatively small fraction of the tested PhACs was attached to struvite precipitates. This result is in good agreement with the finding from Ronteltap et al. (2007), where more than 98% of the hormones and pharmaceuticals spiked in urine stilled remained in the solution after precipitation. It can be observed that from Table 5.9, the removal rate of several PhACs was negative, which meant that PhACs concentration was higher after precipitation than before precipitation. The reason for this abnormal finding was possible linked to the effect of real urine complexity on quantification of micropollutants or transformation of micropollutants during treatment.

Table 5.9 Residual concentration of organic compounds before and after the precipitation experiments

Solutions		HUM-1			HUM-2			HUM-3			SUM		
Parameter	Unit	before precipitation	after precipitation	mass loss (%) ¹	before precipitation	after precipitation	mass loss (%)	before precipitation	after precipitation	mass loss (%)	before precipitation	after precipitation	mass loss (%)
Volume	mL	270	~270	-	676	~680	-	618	~622	-	3000	~3000	-
NPOC	mg L ⁻¹	2081 ± 42	1720 ± 34	17.4	4170 ± 83	4147 ± 83	-0.05	2066 ± 41	1919 ± 38	7.1	907 ± 18	861 ± 17	5.0
2OH-IBP	µg L ⁻¹	154.0	168.2	-9.3	1237.0 ± 67.4	1471.5 ± 88.5	-	977.0 ± 58.7	938.5 ± 51.1	3.3	n.d.	n.d.	n.d.
CAF	µg L ⁻¹	1139.0	1063.6	6.6	575.2 ± 10.2	704.3 ± 5.5	-24.3	2306.0 ± 18.2	2151.7 ± 38.0	6.1	316.5 ± 9.8	318.2 ± 15.3	-0.6
CBZ	µg L ⁻¹	425.6	435.3	-2.3	33.0 ± 1.0	35.4 ± 0.4	-9.0	21.8 ± 0.2	21.1 ± 0.6	2.8	30.1 ± 0.1	28.5 ± 0.4	5.3
DIF	µg L ⁻¹	13.3	10.3	22.7	45.8 ± 4.2	43.8 ± 0.1	3.0	47.6 ± 0.1	39.2 ± 3.6	17.0	49.4 ± 1.9	46.7 ± 1.3	5.4
IBP	µg L ⁻¹	336.0	245.2	27.1	2364.0 ± 17.8	2140.7 ± 51.7	8.1	2235.9 ± 54.0	2060.3 ± 15.5	7.3	2114.6 ± 15.4	2124.9 ± 64.9	-0.5
OFL	µg L ⁻¹	87.0	84.0	3.5	54.1 ± 0.8	58.8 ± 2.6	-10.4	112.6 ± 4.9	105.8 ± 1.5	5.4	170.3 ± 1.9	160.8 ± 1.1	5.6
OXA	µg L ⁻¹	2.5	8.3	-	19.3 ± 0.8	18.3 ± 0.2	3.6	208.4 ± 2.2	197.5 ± 8.6	4.6	217.1 ± 5.6	214.8 ± 1.6	1.0
PRO	µg L ⁻¹	24.4	23.8	2.6	10.5 ± 0.1	11.3 ± 0.2	-9.2	70.7 ± 1.1	65.9 ± 0.7	6.2	122.2 ± 3.5	115.2 ± 0.1	5.7
SMX	µg L ⁻¹	46.2	41.2	10.7	8.3 ± 0.4	9.6 ± 0.1	-17.9	217.3 ± 1.5	198.6 ± 9.1	8.0	333.0 ± 13.4	312.5 ± 14.0	6.2

(1) mass loss (%) = (concentration of a compound before precipitation × solution volume before precipitation) - (concentration after precipitation × solution volume after precipitation) / (concentration of a compound before precipitation × solution volume before precipitation) × 100

Overall, after treatment, a high recovery for P from urine and most of micropollutants still remaining in urine solutions demonstrated that struvite crystallization of real urine could provide an opportunity to reuse micropollutants-free phosphate nutrients for agricultural purposes. Nonetheless, due to the presence of non-desirable micropollutants, the urine effluent remaining after precipitation must be further treated by other technologies.

V.3 RO performance for urine treatment

V.3.1 Retention capacity of RO membrane for target micropollutants

As stated earlier, struvite precipitation was effective in removing P nutrients from urine solutions, but almost all the PhACs still remained in urine-based solutions. Therefore, the followed RO process was used to concentrate these PhACs from these urine solutions. Due to the presence of highly concentrated ions, urine-based solutions were only filtrated at a water recovery of 50% corresponding to volumetric reduction factor (VRF) of 2, not including HUM-2 (VRF = 1.3). PWM was also done as a blank control (VRF = 2). Figure 5.5 and Table 5.10 exhibit the concentration of target PhACs in RO solutions (RO feed, RO permeate, and RO concentrate) and their observed retention. The observed retention of an indicator was calculated based on its concentration in the RO concentrate and RO permeate, as expressed by Equation 8 in Chapter II.2.

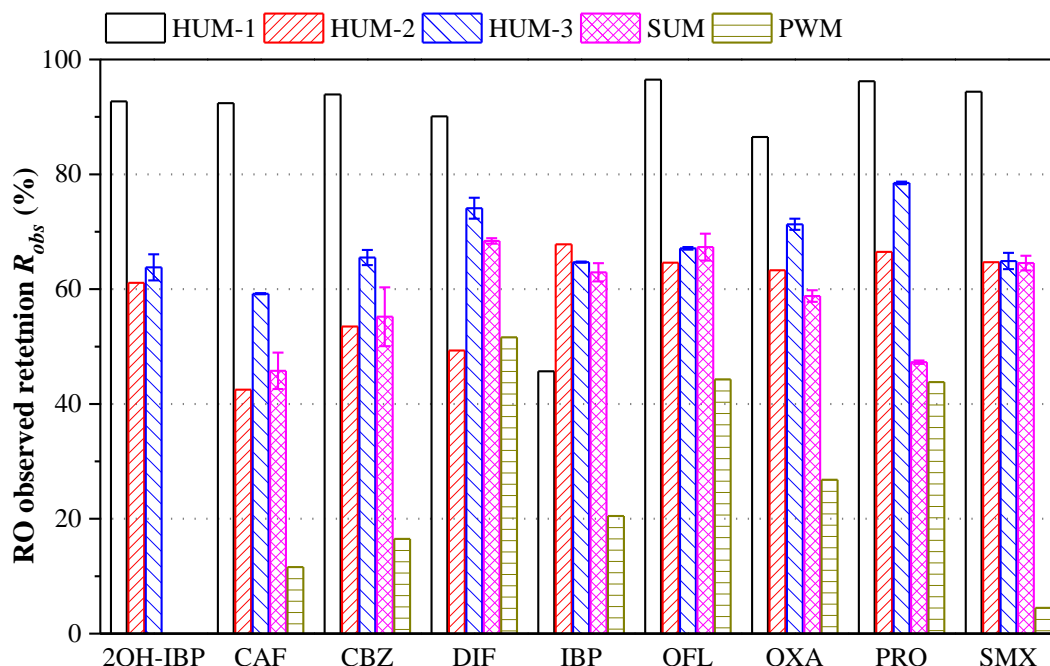


Figure 5.5 Observed retention of the target PhACs by the RO membrane in different solutions

From Figure 5.5, the ESPA2 membrane used in this work showed a moderate and high rejection for all the target PhACs in the real urine solutions (HUM-1, HUM-2 and HUM-3), varying from the lowest 43% of CAF in HUM-2 to the biggest 97% of OFL in HUM-1. On the other hand, for the same PhACs, its retention efficiency in real urine almost followed an order of HUM-1 > HUM-3 > HUM-2, except

IBP. For example, 90%, 49% and 74% retention capacities were observed for DIF in HUM- 1, HUM-2 and HUM- 3, respectively. This difference in rejection rate for the same PhACs was likely to be linked to the complicated constituents of real urine solutions, PhACs load in RO feed, as well as operating conditions including VRF and the RO feed pH.

At present, there was a few information regarding the selective rejection of membrane for trace organic compounds in real or synthetic urine. Only Pronk et al. (2006) mentioned that variations of salts concentration in feedwater could influence the adsorption behaviour of micropollutants by NF membrane.

With respect to HUM-3 (containing ions and organic matters), SUM (with ions) and PWM, at the same operating conditions (ΔP of 7 bar and VRF of 2), the ESPA2 membrane had a highest rejection rate for the same PhACs in HUM-3 (see Table 5.10c), the intermediate in SUM (see Table 5.10d), and the lowest in PWM (see Table 5.10e). For instance, the observed rejection of PRO in HUM-3 was 79%, whereas 47% in SUM and 44% in PWM. This observation suggested the interactions between micropollutants, complex organics, and ions in real urine. Indeed, the presence of organic matters in HUM could be conducive to form a secondary layer at the membrane surface (Pronk et al., 2006). A higher retention rate of PhACs in SUM than PWM mainly related to a concentrated layer caused by a high concentration of ions present in SUM on the membrane surface.

Surprisingly, the ESPA2 membrane exhibited a relatively low rejection capacity for the tested PhACs present in PWM, ranging from 4.5% for SMX to 51.6% for DIF, which was not consistent with the previous findings where this membrane could well retain most of micropollutants with the rejection rate above 80% (Jacob, 2011). A plausible explanation was associated with the presence of methanol as solvent to dissolve the target micropollutants. Indeed, only around 14% of organic carbon (methanol as a main contributor to organic carbon) was retained by the used membrane, as implied in Table 5.10e.

Table 5.10 Concentration of organic compounds in RO solutions and their observed retention

Solutions		(a) HUM-1: Dilution times: 5. ΔP: 4 bar. VRF: ~2.					(b) HUM-2: Dilution times: 5. ΔP: 4 bar. VRF: ~1.3.				
Parameter	Unit	RO feed (C _f) ¹	RO permeate (C _p) ¹	RO concentrate (C _c) ¹	Observed retention (%) ²	C _c /C _f ³	RO feed (C _f) ¹	RO permeate (C _p) ¹	RO concentrate (C _c) ¹	Observed retention (%) ²	C _c /C _f ³
Volume	mL	500	265	235	-	-	500	140	360	-	-
pH	-	5.20	3.35	5.05	-	-	5.20	6.21	5.25	-	-
NPOC	mg L ⁻¹	344 ± 7	276 ± 6	428 ± 9	35.5	1.3	829 ± 17	645 ± 13	924 ± 18	30.22	1.1
2OH-IBP	μg L ⁻¹	33.6	3.9	53.1	92.7	1.6	294.3	141.9	246.9	61.1	0.8
CAF	μg L ⁻¹	212.7	29.5	388.0	92.4	1.8	140.9	75.7	162.7	42.5	1.2
CBZ	μg L ⁻¹	87.1	9.6	157.7	93.9	1.8	7.1	4.3	8.5	53.5	1.2
DIF	μg L ⁻¹	2.1	0.3	2.7	90.1	1.3	8.8	3.8	11.9	49.3	1.4
IBP	μg L ⁻¹	49.0	22.2	41.0	45.7	0.8	428.1	168.6	476.5	67.8	1.1
OFL	μg L ⁻¹	16.8	1.0	28.9	96.5	1.7	11.8	4.6	12.4	64.6	1.1
OXA	μg L ⁻¹	1.7	0.2	1.2	86.5	0.7	3.7	1.5	4.4	63.3	1.2
PRO	μg L ⁻¹	4.8	0.3	8.1	96.2	1.7	2.3	0.9	2.5	66.5	1.1
SMX	μg L ⁻¹	8.2	0.8	14.0	94.4	1.7	1.9	0.9	1.9	64.7	1.0
Observed retention order		OFL > PRO > SMX > CBZ > 2OH-IBP > CAF > DIF > OXA > IBP					IBP > PRO > SMX > OFL > OXA > 2OH-IBP > CBZ > DIF > CAF				
Solutions		(c) HUM-3: Dilution times: 1. ΔP: 7 bar. VRF: ~2.					(d) SUM: Dilution times: 1. ΔP: 7 bar. VRF: ~2.				
Parameter	Unit	RO feed (C _f)	RO permeate (C _p)	RO concentrate (C _c)	Observed retention (%) ¹	C _c /C _f	RO feed (C _f)	RO permeate (C _p)	RO concentrate (C _c)	Observed retention (%) ¹	C _c /C _f
Volume	mL	466	235	231	-	-	4044	2076	1968	-	-
pH	-	9.25	9.11	8.97	-	-	9.23	9.14	9.01	-	-
NPOC	mg L ⁻¹	1919 ± 38	1385 ± 28	2330 ± 47	40.57	1.21	861 ± 17	893 ± 18	905 ± 18	1.26	1.05
2OH-IBP	μg L ⁻¹	938.5 ± 51.1	505.1 ± 47.8	1396.4	63.8 ± 2.3	1.5	n.d. ⁴	n.d.	n.d.	-	-
CAF	μg L ⁻¹	2151.7 ± 38.0	1226.4 ± 19.6	3004.2 ± 44.4	59.2 ± 0.1	1.4	318.2 ± 15.3	229.7 ± 1.4	423.5 ± 8.8	45.8 ± 3.2	1.33
CBZ	μg L ⁻¹	21.1 ± 0.6	10.1	29.4 ± 2.3	65.5 ± 1.3	1.4	28.5 ± 0.4	17.8 ± 1.7	39.8 ± 0.1	55.2 ± 5.1	1.40
DIF	μg L ⁻¹	39.2 ± 3.6	15.8 ± 0.8	60.9 ± 0.2	74.1 ± 1.8	1.6	46.7 ± 1.3	22.7 ± 0.9	71.8 ± 5.1	68.4 ± 0.5	1.54

Parameter	Unit	RO feed (C _f)	RO permeate (C _p)	RO concentrate (C _c)	Observed retention (%) ¹	C _c /C _f	RO feed (C _f)	RO permeate (C _p)	RO concentrate (C _c)	Observed retention (%) ¹	C _c /C _f	
IBP	µg L ⁻¹	2060.3 ± 15.5	1059.6 ± 5.9	2997.9 ± 127.0	64.7 ± 0.1	1.5	2124.9±64.9	1132.7 ± 2.1	3055.9 ± 30.2	62.9 ± 1.6	1.44	
OFL	µg L ⁻¹	105.8 ± 1.5	52.0 ± 0.5	158.1 ± 10.9	67.1 ± 0.2	1.5	160.8±1.1	81.8 ± 4.3	250.4 ± 4.3	67.3 ± 2.3	1.56	
OXA	µg L ⁻¹	197.5 ± 8.6	66.4 ± 1.0	231.5 ± 2.4	71.3 ± 1.0	1.2	214.8±1.6	106.5 ± 3.0	258.5 ± 1.2	58.8 ± 1.0	1.20	
PRO	µg L ⁻¹	65.9 ± 0.7	17.8 ± 0.2	82.8 ± 4.9	78.5 ± 0.2	1.3	115.2±0.1	75.0 ± 0.4	142.2 ± 1.1	47.3 ± 0.3	1.23	
SMX	µg L ⁻¹	198.6 ± 9.1	102.6 ± 2.0	292.2 ± 5.0	64.9 ± 1.4	1.5	312.5±14.0	174.2 ± 11.6	491.2 ± 5.1	64.5 ± 1.3	1.57	
Observed retention order	PRO > DIF > OXA > OFL > CBZ > SMX > IBP > 2OH-IBP > CAF						DIF > OFL > SMX > IBP > OXA > CBZ > PRO > CAF					
Solutions		(e) PWM: Dilution times: 1. ΔP: 7 bar. VRF: ~2.										
Parameter	Unit	RO feed (C _f)	RO permeate (C _p)	RO concentrate (C _c)	Observed retention (%) ¹	C _c /C _f						
Volume	mL	5.97	5.43	5.87	-	-						
pH	-	455	245	210	-	-						
NPOC	mg L ⁻¹	839±17	737±15	858±17	14.4	1.2						
2OH-IBP	µg L ⁻¹	n.d.	n.d.	n.d.	-	-						
CAF	µg L ⁻¹	320.5 ± 3.5	294.0 ± 18.2	332.3 ± 33.4	11.6	1.0						
CBZ	µg L ⁻¹	27.7 ± 0.1	25.3 ± 1.5	30.3 ± 0.5	16.5	1.1						
DIF	µg L ⁻¹	46.7 ± 0.4	23.8 ± 1.2	49.1 ± 1.2	51.6	1.0						
IBP	µg L ⁻¹	2196.4 ± 44.9	1798.2 ± 9.7	2261.6 ± 33.7	20.5	1.0						
OFL	µg L ⁻¹	85.7 ± 0.1	53.5 ± 4.3	96.1 ± 6.1	44.3	1.1						
OXA	µg L ⁻¹	257.0 ± 1.7	217.9 ± 15.0	297.7 ± 3.9	26.8	1.2						
PRO	µg L ⁻¹	125.5 ± 0.2	64.9 ± 7.4	115.5 ± 10.4	43.8	0.9						
SMX	µg L ⁻¹	336.3 ± 7.6	328.4 ± 14.2	343.8 ± 0.1	4.5	1.0						
Observed retention order	DIF > OFL > PRO > OXA > IBP > CBZ > CAF > SMX											

(1) C_f, C_p, and C_c are the concentration of each parameter in RO feed, RO permeate and RO concentrate. (2) the observed retention was calculated by Equation 9 (see Chapter II.2). (3) C_c/C_f: concentration ratio of a parameter in RO concentrate and RO feed. (4) n.d.: not detected.

V.3.2 Retention efficiencies for ionic species

The retention efficiencies of ions by the ESPA2 membrane from urine-based solutions was also studied, as listed in Table 5.11. It was observed that the ESPA2 membrane could retain ions to a certain degree. Among these ions, at least half of SO_4^{2-} was rejected by the RO membrane for all the cases, which was higher than the rejection for other ions. This can be explained by the membrane with negative charge preferring to reject multivalent anions like SO_4^{2-} based on Donnan exclusion (Chen et al., 2017). As compared to the filtration of SUM, a higher observed retention value for all the parameters could be also noticed in the real urine solutions, e.g., for Mg^{2+} , 40% in HUM-3 and 29% in SUM, which was consistent with the results of the target PhACs.

It can be concluded that, at the studied conditions, the RO process with a low pressure was proven to not exhibit a good separation performance for unwanted micropollutants and ions from urine solutions, in the view of their high detection in both RO permeate and RO concentrate. It was proposed that, therefore, both RO concentrate and RO permeate should be treated by the subsequence ozonation, aiming to reduce the PhACs to an acceptable level. In addition, the RO process should be optimized, including the selection of RO membrane and operating conditions, to retain effectively trace micropollutants from urine wastewater in future studies.

Table 5.11 Concentration of global parameters in RO solutions and their observed retention

Solutions		(a) HUM-1: Dilution times: 5. ΔP: 4 bar. VRF: ~2.					(b) HUM-2: Dilution times: 5. ΔP: 4 bar. VRF: ~1.3.				
Parameter	Unit	RO feed (C _f)	RO permeate (C _p)	RO concentrate (C _c)	Observed retention (%)	C _c /C _f	RO feed (C _f)	RO permeate (C _p)	RO concentrate (C _c)	Observed retention (%)	C _c /C _f
Volume	mL	500	265	235	-	-	500	140	360	-	-
Conductivity	mS cm ⁻¹	-	-	-	-	-	-	-	-	-	-
DIC	mg L ⁻¹	11.4 ± 0.2	2.6 ± 0.1	28.4 ± 0.6	HCl addition	-	791 ± 16	5.0 ± 0.1	81 ± 2	HCl addition	-
COD	mg L ⁻¹	1340 ± 10	1113 ± 10	1635 ± 10	31.9	1.22	2430 ± 10	1850 ± 10	2700 ± 10	31.5	1.11
Cl ⁻	mg L ⁻¹	989 ± 99	209 ± 21	1455 ± 146	HCl addition	-	824 ± 82	1707 ± 171	3781 ± 378	HCl addition	-
SO ₄ ²⁻	mg L ⁻¹	-	-	-	-	-	213 ± 21	96 ± 10	276 ± 28	65.2	1.29
Na ⁺	mg L ⁻¹	206 ± 21	60 ± 6	639 ± 64	90.6	3.11	336 ± 34	192 ± 19	3976 ± 398	51.5	1.18
N-NH ₄ ⁺	mg L ⁻¹	272 ± 27	84 ± 8	702 ± 70	88.0	2.58	1233 ± 123	699 ± 70	1384 ± 138	49.5	1.12
K ⁺	mg L ⁻¹	167 ± 17	49 ± 5	489 ± 49	90.0	2.93	346 ± 35	174 ± 17	386 ± 39	54.7	1.11
Mg ²⁺	mg L ⁻¹	30 ± 3	4.8 ± 0.5	97 ± 10	95.0	3.18	76 ± 8	30 ± 3	78 ± 8	61.5	1.03
Ca ²⁺	mg L ⁻¹	4.2 ± 0.4	1.5 ± 0.2	13.4 ± 1.3	88.6	3.18	17 ± 2	7.1 ± 0.7	18 ± 2	59.9	1.05
Solutions		(c) HUM-3: Dilution times: 1. ΔP: 7 bar. VRF: ~2.					(d) SUM: Dilution times: 1. ΔP: 7 bar. VRF: ~2.				
Parameter	Unit	RO feed (C _f)	RO permeate (C _p)	RO concentrate (C _c)	Observed retention (%)	C _c /C _f	RO feed (C _f)	RO permeate (C _p)	RO concentrate (C _c)	Observed retention (%)	C _c /C _f
Volume	mL	466	235	231	-	-	4044	2076	1968	-	-
Conductivity	mS cm ⁻¹	25.50 ± 0.51	18.60 ± 0.37	30.70 ± 0.61	41.2	1.20	43.00 ± 2.15	34.30 ± 1.72	47.80 ± 2.39	28.2	1.11
DIC	mg L ⁻¹	1565 ± 31	962 ± 19	1917 ± 38	49.8	1.23	3003 ± 60	2572 ± 51	4086 ± 82	37.1	1.36
COD	mg L ⁻¹	6500 ± 10	4750 ± 10	7400 ± 10	35.8	1.14	-	-	-	-	-
Cl ⁻	mg L ⁻¹	3477 ± 348	2730 ± 273	4115 ± 412	33.7	1.18	5322 ± 532	4873 ± 487	5798 ± 580	16.0	1.09
SO ₄ ²⁻	mg L ⁻¹	558 ± 56	309 ± 31	831 ± 83	62.9	1.49	1459 ± 150	872 ± 87	2074 ± 207	58.0	1.42
Na ⁺	mg L ⁻¹	980 ± 98	687 ± 69	1241 ± 124	44.7	1.27	1291 ± 129	1006 ± 101	1589 ± 159	36.7	1.23
N-NH ₄ ⁺	mg L ⁻¹	3367 ± 337	2380 ± 24	3762 ± 376	36.7	1.12	7164 ± 716	5788 ± 579	8271 ± 827	30.0	1.15
K ⁺	mg L ⁻¹	849 ± 85	604 ± 60	1078 ± 108	44.0	1.27	1683 ± 168	1333 ± 133	2088 ± 209	36.2	1.24
Mg ²⁺	mg L ⁻¹	169 ± 17	125 ± 13	207 ± 21	39.5	1.23	168 ± 17	134 ± 13	188 ± 19	28.6	1.12
Ca ²⁺	mg L ⁻¹	74 ± 7	36 ± 4	31 ± 3	-15.0	0.42	n.d.	n.d.	n.d.	-	-

V.3.3 Variation of RO permeate flux versus RO permeate volume

During the dead-end filtration of PWM, SUM and HUM-3, the flux variation was plotted along with the RO permeate volume, as presented in Figure 5.6. Note that, for the RO filtration of HUM-3, several membranes were used to make VRF equal to 2 corresponding to around 230 mL RO permeate, whereas one membrane was available for both PWM and SUM to produce around 230 mL RO permeate.

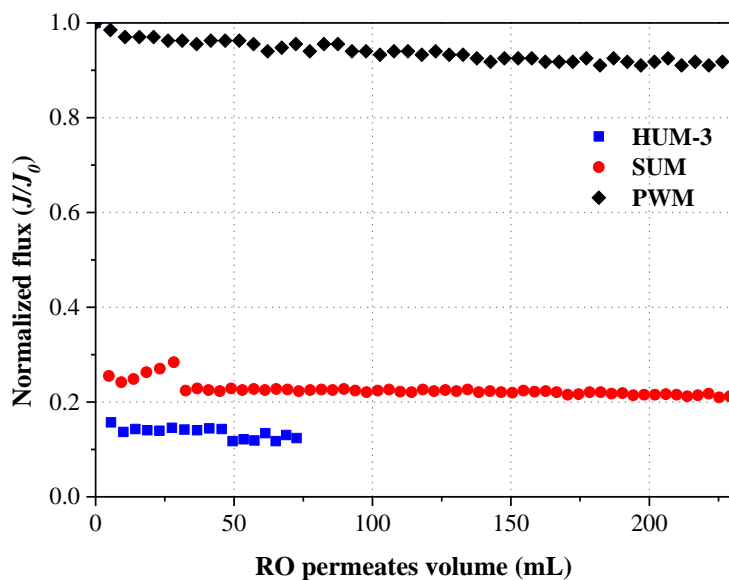


Figure 5.6 Variation of permeate flux over RO permeate volume during the filtration of PWM, SUM and HUM- 3. ΔP : 7 bar. room temperature. Note that, the first point of RO permeate flux in SUM and HUM-3 related to the flux obtained with distilled water.

In the case of HUM-3, at the first moment of the RO process, the RO permeate flux was relatively low, but which remained almost constant until 75 mL RO permeate was produced. This phenomenon was associated with the accumulation of highly concentrated inorganic and organic species. On the other hand, the flux in HUM-3 was lower than that in SUM over the entire filtration process, which was likely to be linked to the accumulation of organic matters. This finding was in good agreement with the result reported by Pronk et al. (2006). In addition, there was only a slight reduction (<10%) in RO permeate flux for PWM. This observation demonstrated that the low flux for HUM-3 at the beginning was caused by the presence of salts and organic matters with a high concentration in real urine solutions.

Moreover, the flux could be recovered completely after a clean with ultra-pure water by hands, confirming that the low RO permeate flux was mainly due to a concentrated layer on the RO membrane surface.

As not expected, during the treatment of SUM by the RO process, a significant increase in RO permeate flux was noticed. A detailed reason for this remained unclear. A possible reason was related to the change of the charge of both solutes and the membrane. Nilsson et al. (2008) mentioned that the salt-membrane interaction was quite complex, where the presence of salts could decrease or increase membrane permeability due to the changes in the membrane structure.

As discussed above, organic matters and salts at a high concentration were main factors responsible for the decline of RO permeate flux during the treatment of urine by RO process. Therefore, in order to improve RO performance in terms of membrane fouling, RO process should be further optimized, including RO membrane selection, operating conditions and the application of pre-treatment, etc..

V.4 Ozonation of the urine-based solutions

After the treatment by struvite precipitation alone or combining RO process, the solutions were further oxidized by ozonation at a desired ozone gas-in concentration and at a gas flow rate of 30 L h⁻¹. Prior to ozonation, to shorten ozonation time, several times dilution for solutions were done (See Table 5.5). In this section, the main focuses were on: (1) the oxidation efficiencies of the target PhACs by ozonation; (2) the possible ozone kinetic regimes based on the concentration profile of dissolved ozone versus reaction time; and (3) the role of organic matters (NPOC) and ammonia on ozone consumption.

V.4.1 Ozonation efficiencies of real urine

V.4.1.1 Ozonation of HUM-1

Table 5.12 presents the residual concentration of the target PhACs and cumulated consumed ozone dose during the ozonation of HUM-1. Consumed ozone dose reflected the amount of ozone required to react with compounds, as defined in Equation 22 (see Chapter II.3). To better understand the ozonation behaviour of micropollutants, the target PhACs were categorized into three groups based on their ozone kinetic rate constants ($k_{O_3-PhACs}$): Group I: ozone-reactive PhACs with $k_{O_3-PhACs} > 10^5 \text{ L mol}^{-1} \text{ s}^{-1}$ (CBZ, DIF, OFL, PRO and SMX); Group II: PhACs with $k_{O_3-PhACs} \sim 10^4 \text{ L mol}^{-1} \text{ s}^{-1}$, like CAF; and Group III: ozone-refractory PhACs with $k_{O_3-PhACs} < 10 \text{ L mol}^{-1} \text{ s}^{-1}$ (IBP and OXA). For 2OH-IBP, its kinetic rate constant was not reported in the literature. Considering its similar structure with IBP, thus, 2OH-IBP was also thought as an ozone-refractory compound in this work.

It was clearly seen that almost complete abatement for ozone-reactive PhACs, including CBZ, DIF, OFL, PRO and SMX, was achieved at a consumed ozone dose of 56.8 mg, corresponding to 0.3 mg consumed ozone per mg NPOC₀. For CAF and ozone-refractory 2OH-IBP, a higher ozone dose, 482.1 mg ozone consumption (2.7 mg consumed ozone per mg NPOC₀), was required for a satisfactory removal from HUM-1. However, a relatively high consumed ozone dose, with the value of 905.4 mg, removed only 31% of ozone-refractory IBP from HUM-1. This significant difference in ozone consumption for a satisfactory removal of the PhACs was mainly linked to the kinetic rate constants for the direct reaction of molecular ozone with the target micropollutants (see Figure 2.1 in Chapter II.1). In addition, a higher elimination of 2OH-IBP by ozone than that of IBP was likely to be attributed to the presence of the -OH functional group of 2OH-IBP structure.

Table 5.12 Residual concentration of PhACs, carbon compounds and N compounds and cumulated consumed ozone dose during the ozonation of HUM-1 (20 times dilution)

Time	h	0.0	0.083	0.50	1.0	2.0	5.0
Cumulated consumed O ₃	mg	0.0	56.8	245.7	482.1	905.4	1731.1
Cumulated consumed O ₃	mg L ⁻¹	0.0	28.4	122.9	241.1	452.7	865.5
mg consumed ozone per mg NPOC ₀		0.0	0.3	1.4	2.7	5.1	9.8
2OH-IBP	µg L ⁻¹	8.4	6.7	1.5	0.3	0.1	-
CAF	µg L ⁻¹	53.2	32.5	0.4	0.2	0.2	-
CBZ	µg L ⁻¹	21.8	0.2	0.2	0.2	0.2	-
DIF	µg L ⁻¹	0.5	0.3	0.3	0.3	0.1	-
IBP	µg L ⁻¹	12.3	11.7	11.4	12.2	8.5	-
OFL	µg L ⁻¹	4.2	0.0	0.2	0.2	0.1	-
OXA	µg L ⁻¹	n.d.	n.d.	n.d.	n.d.	n.d.	-
PRO	µg L ⁻¹	1.2	0.0	0.0	0.0	0.0	-
SMX	µg L ⁻¹	2.1	0.2	0.2	0.4	0.2	-
Total organic C from PhACs	µg L ⁻¹	62.7	30.1	10.4	10.2	6.9	
NPOC	mg L ⁻¹	88 ± 2	87 ± 2	84 ± 2	75 ± 2	59 ± 1	15.7 ± 0.3
COD	mg L ⁻¹	361 ± 10	343 ± 10	312 ± 10	278 ± 10	197 ± 10	53 ± 10
N-NO ₃ ⁻	mg L ⁻¹	0.86 ± 0.09	0.59 ± 0.06	100 ± 10	101 ± 10	101 ± 10	98 ± 10
N-NH ₄ ⁺	mg L ⁻¹	123 ± 12	118 ± 12	120 ± 12	115 ± 12	115 ± 12	106 ± 11
pH	-	6.98	6.34	5.50	4.90	4.45	4.00
DIC	mg L ⁻¹	2.85 ± 0.06	1.48 ± 0.03	0.98 ± 0.02	1.12 ± 0.02	0.63 ± 0.01	0.72 ± 0.01

As already discussed in Chapter IV, solution matrix, such as organic matters and ammonia, had significantly influences on the removal efficiencies of micropollutant by ozonation. Table 5.11 also shows the residual concentration of both organic carbon and ammonia, and the yield of N-NO₃⁻ during the experiment.

Figure 5.7a plots the consumed ozone dose, organic carbon and COD during the ozonation process of HUM-1. A quite linear disappearance was noticed for both NPOC and COD during the entire ozonation experiment. During the first 2 h ozonation, the removal of the carbon from the target PhACs reached about 89%, whereas the removal of COD and of NPOC was only 45% and 33%, respectively. During this stage, 58 mg NPOC (including 0.1 mg from PhACs) were removed for a consumed ozone

dose of 905.4 mg (5.1 mg consumed ozone per mg NPOC₀). After 5 h ozonation (9.8 mg consumed ozone per mg NPOC₀), 1731 mg ozone were consumed for the removal of 144.6 mg NPOC (82% removal), and COD removal reached 85%.

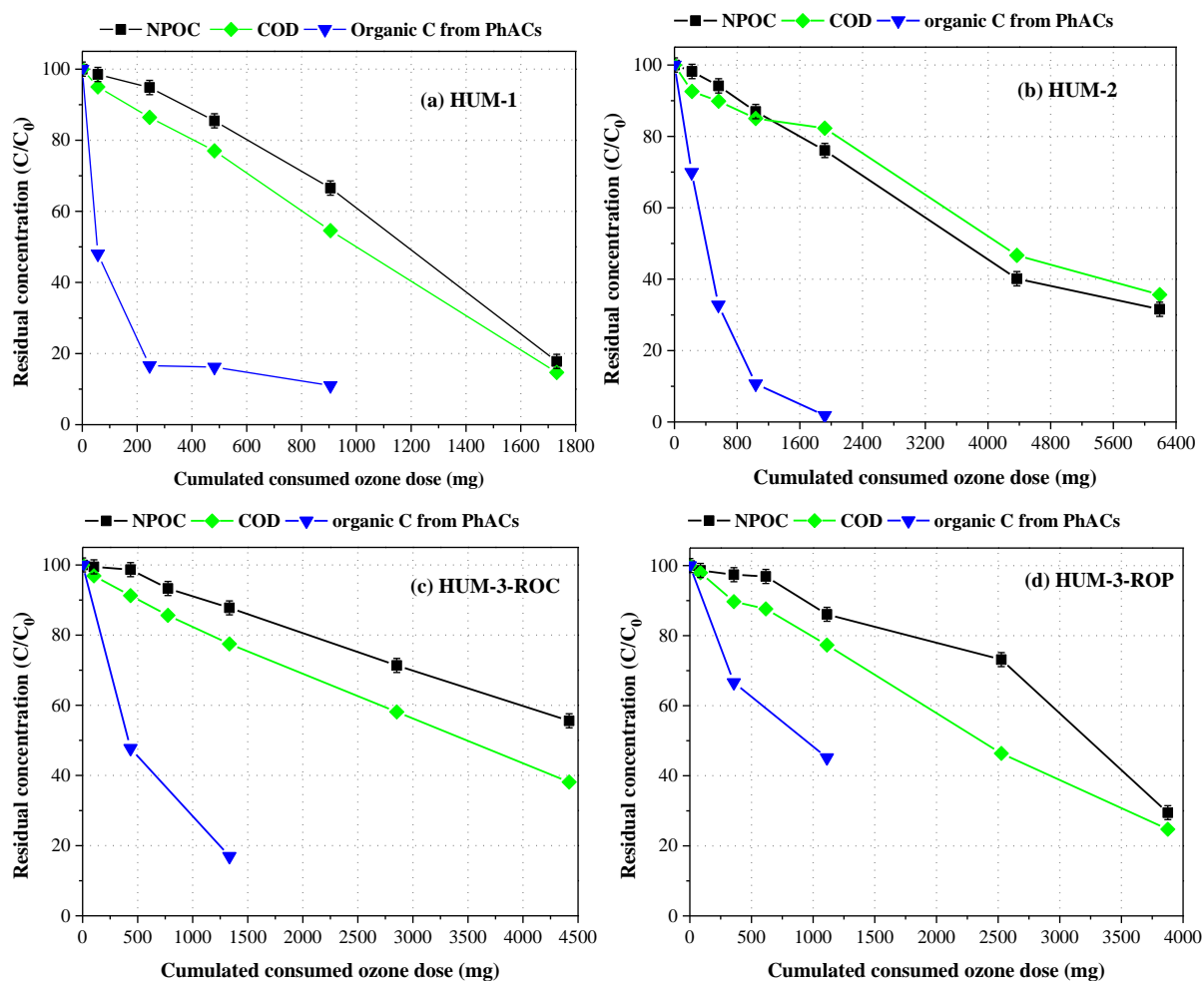


Figure 5.7 Variation of organic C residual and COD as a function of cumulated consumed ozone dose.

From Table 5.12, a slight decrease of 17 mg L⁻¹ in N-NH₄⁺ was found, whereas 97 mg L⁻¹ N-NO₃⁻ was obtained after 5 h ozonation. The conversion of ammonia into nitrate can be described by Reaction 19 and Reaction 20 (see Chapter IV). However, the high value of nitrate production was inconsistent with the expected stoichiometry for the ozonation of ammonia. This probably indicated that other nitrogen-containing compounds contained in urine were also oxidized, such as creatinine or unprotonated amino acids (cysteine, tyrosine, tryptophan, etc) (Eichelsdörfer and Jandik, 1985).

A strong pH reduction ranging from 7.0 to 4.0 should be noticed due to the formation of carboxylic acid, aldehyde and ketone as end products during the oxidation of wastewater matrix. Over the entire ozonation, the concentration of DIC decreased with the ozonation, demonstrating that the indirect reactions of inorganic carbon (as ·OH radical scavenger) with ozone (see Reaction 12 in Chapter I.3) took place to a certain extent.

V.4.1.2 Ozonation of HUM-2

Table 5.13 presents the residual concentration of the target PhACs and cumulated consumed ozone dose during the ozonation of HUM-2.

Similar to HUM-1, 0.3 mg consumed ozone per mg NPOC₀ could effectively reduce the amount of ozone-reactive micropollutants (CBZ, DIF, OFL, PRO and SMX) in HUM-2. A higher ozone dose was consumed to achieve a higher removal for CAF and ozone-refractory micropollutants (2OH-IBP, IBP and OXA) from HUM-2.

Table 5.13 Residual concentration of PhACs, carbon compounds and N compounds and cumulated consumed ozone dose during the ozonation of HUM-2 (10 times dilution)

Time	h	0.0	0.17	0.5	1.0	2.0	5.0	7.5
Cumulated consumed O ₃	mg	0.0	222.8	563.7	1036.5	1917.9	4370.2	6190.7
Cumulated consumed O ₃	mg L ⁻¹	0.0	111.4	281.9	518.2	958.9	2185.1	3095.3
mg consumed ozone per mg NPOC ₀		0.0	0.3	0.7	1.2	2.3	5.3	7.5
2OH-IBP	µg L ⁻¹	147.1	114.3	63.0	23.0	1.2	-	-
CAF	µg L ⁻¹	70.4	60.1	25.6	8.4	0.3	-	-
CBZ	µg L ⁻¹	3.5	1.4	0.2	0.2	0.2	-	-
DIF	µg L ⁻¹	4.4	1.7	0.1	0.2	0.1	-	-
IBP	µg L ⁻¹	214.1	137.0	58.3	16.3	6.5	-	-
OFL	µg L ⁻¹	5.9	1.0	0.0	0.1	0.1	-	-
OXA	µg L ⁻¹	1.8	1.4	0.8	0.1	0.0	-	-
PRO	µg L ⁻¹	1.1	0.2	0.0	0.0	0.0	-	-
SMX	µg L ⁻¹	1.0	0.6	0.3	0.3	0.5	-	-
Total organic C from PhACs	µg L ⁻¹	311.1	217.5	101.9	33.2	5.7		
NPOC	mg L ⁻¹	415 ± 8	407 ± 8	390 ± 8	361 ± 7	315 ± 6	166 ± 3	131 ± 3
COD	mg L ⁻¹	1215 ± 10	1125 ± 10	1092 ± 10	1033 ± 10	1000 ± 10	567 ± 10	433 ± 10
N-NO ₃ ⁻	mg L ⁻¹	7.5 ± 0.8	8.1 ± 0.8	11 ± 1	35 ± 4	45 ± 5	74 ± 7	143 ± 14
N-NH ₄ ⁺	mg L ⁻¹	516 ± 52	490 ± 49	477 ± 48	449 ± 45	434 ± 43	412 ± 41	368 ± 37
pH	-	8.88	8.84	8.75	8.64	8.35	7.90	7.69
DIC	mg L ⁻¹	396 ± 8	362 ± 7	366 ± 7	344 ± 7	315 ± 6	263 ± 5	155 ± 3

During the ozonation of HUM-2, NPOC concentration and COD decreased linearly (Figure 5.7b). After 2 h ozonation (2.3 mg consumed ozone per mg NPOC₀), the removal of the carbon from micropollutants reached about 98%, whereas only 24 % of NPOC and 18% of COD were reduced. During this stage, 1917.9 mg ozone was consumed for the removal of 200 mg NPOC (including 0.6 mg from PhACs). After 7.5 h ozonation (7.5 mg consumed ozone per mg NPOC₀), 568 mg NPOC (93%

removal) was removed at a relatively high consumed ozone dose of 6190.7 mg. And COD removal was 64%.

In this work, the amount of N-NH_4^+ removal (148 mg L^{-1}) was quite close to the N-NO_3^- production (143 mg L^{-1}) after 5 h ozonation, which was similar to the finding from synthetic urine (described in Chapter IV), but different from the finding obtained in HUM-1. A reason for this was associated with the matrix of urine-based solutions. As presented above, HUM-1 was collected after a bio-treatment, while HUM-2 was obtained directly from a storage tank.

Figure 5.8 shows the consumed ozone dose, N-NH_4^+ and N-NO_3^- during the ozonation process for HUM-2. It was clearly seen that, an almost linear decrease in the concentration N-NH_4^+ was found throughout the ozonation process, whereas the concentration of N-NO_3^- was produced gradually, confirming that N-NH_3 reacted with oxidants to generate NO_3^- compound.

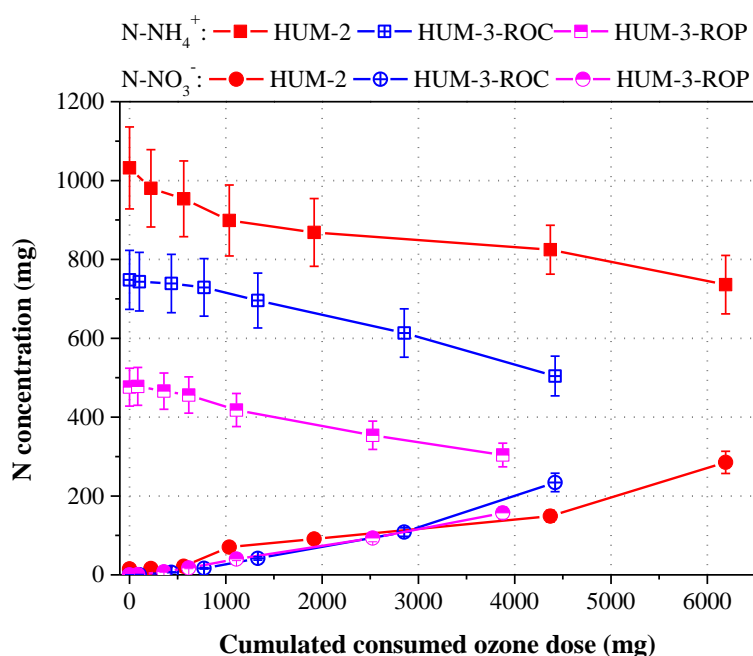


Figure 5.8 Conversion of N-NH_4^+ to N-NO_3^- during the ozonation of HUM-based solutions with 10 times dilution. ozone inlet: $\sim 60 \text{ mg L}^{-1}$. flow rate: 30 L h^{-1} . initial pH: ~ 9 . temperature: $20 \pm 1 \text{ }^\circ\text{C}$. solution volume: 2 L . reaction time: 7.5 h for HUM-2, 8 h for both HUM-3-ROC and HUM-3-ROP.

During the ozonation of HUM-2, solution pH and DIC concentration decreased with the ozonation, as described above.

V.4.1.3 Ozonation of HUM-3 RO concentrate and HUM-3 RO permeate

Table 5.14 and Table 5.15 shows the residual concentration of target PhACs and cumulated consumed ozone dose during the ozonation of HUM-3 RO concentrate (HUM-3-ROC) and HUM-3 RO permeate (HUM-3-ROP), respectively.

In these two cases, for ozone-reactive PhACs, an excellent removal was observed at an ozone dose of 435.7 mg in HUM-3-ROC (1.0 mg consumed ozone per mg NPOC_0) and of 357.4 mg in HUM-3-ROP (1.3 mg consumed ozone per mg NPOC_0). As expected, a large amount of ozone dose

was consumed to reduce effectively CAF and ozone-refractory PhACs. In the case of HUM-3-ROC, after 2 h ozonation (2.9 mg consumed ozone per mg NPOC₀), 19% of 2OH-IBP and 30% of IBP still remained in the solution. Regarding HUM-3-ROP, 4.0 mg consumed ozone per mg NPOC₀ only removed 45% of 2OH-IBP and 20% of IBP. These observation suggested that the removal efficiency of PhACs (particularly for ozone-recalcitrant PhACs) appeared to be higher in RO concentrate than in RO permeate, which was mainly related to the matrix of these two solutions, such as organic matters. Pocostales et al. (2010) mentioned that ozone-resistant micropollutants could be oxidized to some extent by ozonation due to the yield of ·OH radicals from the attack of ozone towards organic matter in wastewater.

Table 5.14 Residual concentration of PhACs, carbon compounds and N compounds and cumulated consumed ozone dose during the ozonation of HUM-3-ROC (10 times dilution)

Time	h	0.00	0.08	0.50	1.00	2.00	5.00	8.00
Cumulated consumed O ₃	mg	0.0	102.7	435.7	774.7	1333.6	2853.0	4419.6
Cumulated consumed O ₃	mg L ⁻¹	0.0	51.4	217.9	387.4	666.8	1426.5	2209.8
mg consumed ozone per mg NPOC ₀		0.0	0.2	1.0	1.7	2.9	6.2	9.6
2OH-IBP	µg L ⁻¹	139.6	-	84.2 ± 9.0	-	26.2	-	-
CAF	µg L ⁻¹	300.4 ± 4.4	-	126.6 ± 8.4	-	6.2	-	-
CBZ	µg L ⁻¹	2.9 ± 0.2	-	0.3	-	n.d.	-	-
DIF	µg L ⁻¹	6.1 ± 0.02	-	0.4	-	n.d.	-	-
IBP	µg L ⁻¹	299.8 ± 12.7	-	159.0 ± 10.0	-	88.8	-	-
OFL	µg L ⁻¹	15.8 ± 1.1	-	0.8	-	n.d.	-	-
OXA	µg L ⁻¹	23.1 ± 0.2	-	9.3 ± 0.6	-	n.d.	-	-
PRO	µg L ⁻¹	8.3 ± 0.5	-	0.7 ± 0.1	-	n.d.	-	-
SMX	µg L ⁻¹	29.2 ± 0.5	-	2.5	-	n.d.	-	-
Total organic C from PhACs	µg L ⁻¹	522.9	-	249.7	-	88.6		
NPOC	mg L ⁻¹	229 ± 5	228 ± 5	226 ± 5	213 ± 4	201 ± 4	163 ± 3	127 ± 3
pH	-	8.80	8.77	8.67	8.56	8.33	7.74	7.53
DIC	mg L ⁻¹	210 ± 4	208 ± 4	207 ± 4	199 ± 4	197 ± 4	181 ± 4	110 ± 2
COD	mg L ⁻¹	800 ± 10	775 ± 10	730 ± 10	685 ± 10	620 ± 10	465 ± 10	305 ± 10
N-NO ₃ ⁻	mg L ⁻¹	-	0.20±0.02	3.25 ± 0.33	8.27 ± 0.83	21 ± 2	54 ± 5	112 ± 11
N-NH ₄ ⁺	mg L ⁻¹	374 ± 37	372 ± 37	369 ± 37	365 ± 37	348 ± 35	307 ± 31	252 ± 25

Table 5.15 Residual concentration of PhACs, carbon compounds and N compounds and cumulated consumed ozone dose during the ozonation of HUM-3-ROP (10 times dilution)

Time	h	0.00	0.08	0.50	1.00	2.00	5.00	8.00
Cumulated consumed O ₃	mg	0.0	86.3	357.4	616.1	1111.6	2526.0	3875.9
Cumulated consumed O ₃	mg L ⁻¹	0.0	43.2	178.7	308.1	555.8	1263.0	1937.9
mg consumed ozone per mg NPOC ₀		0.0	0.3	1.3	2.2	4.0	9.1	13.9
2OH-IBP	µg L ⁻¹	50.5 ± 4.8	-	46.6	-	27.6	-	-
CAF	µg L ⁻¹	122.6 ± 2.0	-	32.4	-	5.1	-	-
CBZ	µg L ⁻¹	1.0	-	0.03	-	n.d.	-	-
DIF	µg L ⁻¹	1.6 ± 0.08	-	n.d.	-	n.d.	-	-
IBP	µg L ⁻¹	106.0 ± 0.6	-	102.6	-	85.3	-	-
OFL	µg L ⁻¹	5.2 ± 0.05	-	n.d.	-	n.d.	-	-
OXA	µg L ⁻¹	6.6 ± 0.1	-	1.6	-	n.d.	-	-
PRO	µg L ⁻¹	1.8	-	0.04	-	n.d.	-	-
SMX	µg L ⁻¹	10.3 ± 0.2	-	0.2	-	n.d.	-	-
Total organic C from PhACs	µg L ⁻¹	191.3		127.5		86.4		
NPOC	mg L ⁻¹	139 ± 3	137 ± 3	135 ± 3	135 ± 3	120 ± 2	102 ± 2	41 ± 1
COD	mg L ⁻¹	485 ± 10	475 ± 10	435 ± 10	425 ± 10	375 ± 10	225 ± 10	120 ± 10
N-NO ₃ ⁻	mg L ⁻¹	n.a.	0.30 ± 0.03	3.85 ± 0.39	8.70 ± 0.87	20 ± 2	47 ± 5	78 ± 8
N-NH ₄ ⁺	mg L ⁻¹	238 ± 24	239 ± 24	233 ± 23	228 ± 23	209 ± 21	177 ± 18	152 ± 15
pH	-	8.90	8.83	8.69	8.55	8.19	7.36	7.06
DIC	mg L ⁻¹	112 ± 2	110 ± 2	109 ± 2	106 ± 2	106 ± 2	81 ± 2	44 ± 1

The concentration profile of NPOC and COD in HUM-3 based solutions (Figure 5.7c and 5.7d) was similar to that in HUM-1 and HUM-2, where NPOC and COD reduced linearly with ozonation. At the end of 8 h ozonation, 9.6 mg consumed ozone dose per mg NPOC₀ removed 204 mg NPOC (45% removal) from HUM-3-ROC, and 13.9 mg consumed ozone dose per mg NPOC₀ removed 196 mg NPOC (71% removal) from HUM-3-ROP.

During the ozonation process of HUM-3-ROC and HUM-3-ROP, COD, solution pH and DIC concentration decreased gradually, like HUM-1 and HUM-2.

The concentration profile of N-NH₄⁺ and N-NO₃⁻ in both HUM-3-ROC and HUM-3-ROP was similar to that in HUM-2.

V.4.1.4 Ozonation of SUM-RO concentrate and -RO permeate

Table 5.16 and Table 5.17 shows the residual concentration of target PhACs and cumulated consumed ozone dose during the ozonation of SUM-RO concentrate (SUM-ROC) and SUM-RO permeate (SUM-ROP). In this work, NPOC was mainly attributed to the presence of methanol as a solvent.

Even though the concentration of most of the target PhACs was at least 10 times larger in SUM-based solutions than in real urine due to solution dilution, less ozone dose was required to effectively remove the target PhACs from SUM-based solutions. This finding indicated the important role of organic matters in real urine on removal efficiency of micropollutants by ozonation, which was described in Chapter IV.

Table 5.16 Residual concentration of PhACs, carbon compounds and N compounds and cumulated consumed ozone dose during the ozonation of SUM-ROC

Time	h	0.0	0.017	0.167	0.5	1.0	3.0	8.0
Cumulated consumed O ₃	mg	0.0	1.1	11.9	44.8	116.2	678.6	2563.1
Cumulated consumed O ₃	mg L ⁻¹	0.0	0.5	6.0	22.4	58.1	339.3	1281.6
2OH-IBP	µg L ⁻¹	n.d.	n.d.	n.d.	n.d.	n.d.	-	-
CAF	µg L ⁻¹	423.5	403.6	337.8	287.3	175.4	-	-
CBZ	µg L ⁻¹	39.8	29.5	0.0	0.0	n.d.	-	-
DIF	µg L ⁻¹	71.8	46.6	0.6	0.7		-	-
IBP	µg L ⁻¹	3055.9	3044.9	2312.9	2058.9	1832.9	-	-
OFL	µg L ⁻¹	250.4	105.9	n.d.	n.d.	n.d.	-	-
OXA	µg L ⁻¹	258.5	227.2	197.3	156.8	135.5	-	-
PRO	µg L ⁻¹	142.2	103.2	0.7	0.3	n.d.	-	-
SMX	µg L ⁻¹	491.2	316.8	10.5	5.4	0.9	-	-
Total organic C from PhACs	µg L ⁻¹	3241.4	2983.6	2045.8	1800.6	1558.3		
NPOC	mg L ⁻¹	939 ± 19	940 ± 19		932 ± 19	929 ± 19	915 ± 18	829 ± 17
pH	-	9.01	-	-	-	-	8.99	8.97
DIC	mg L ⁻¹	4017 ± 80	4017 ± 80		3951 ± 79	3993 ± 80	3921 ± 78	3351 ± 67
COD	mg L ⁻¹	-	-	-	-	-	-	-
N-NO ₃ ⁻	mg L ⁻¹	0	-	-	-	-	30 ± 3	92 ± 9
N-NH ₄ ⁺	mg L ⁻¹	8271 ± 827	-	-	-	-	7953 ± 795	7974 ± 797

Table 5.17 Residual concentration of PhACs, carbon compounds and N compounds and cumulated consumed ozone dose during the ozonation of SUM-ROP

Time	h	0.0	0.017	0.167	0.5	1.0	4.0	9.0
Cumulated consumed O ₃	mg	0.0	1.2	12.5	40.7	90.9	1517.2	4870.8
Cumulated consumed O ₃	mg L ⁻¹	0.0	0.6	6.3	20.4	45.4	758.6	2435.4
2OH-IBP	µg L ⁻¹	n.d.	n.d.	n.d.	n.d.	n.d.	-	-
CAF	µg L ⁻¹	229.7	205.6	189.5	135.7	90.9	-	-
CBZ	µg L ⁻¹	17.8	3.7	0.0	0.0	n.d.	-	-
DIF	µg L ⁻¹	22.7	4.4	0.2	0.2	n.d.	-	-
IBP	µg L ⁻¹	1157.5	1029.9	815.8	647.6	607.5	-	-
OFL	µg L ⁻¹	81.8	14.0	n.d.	n.d.	n.d.	-	-
OXA	µg L ⁻¹	106.5	93.8	81.4	63.0	55.8	-	-
PRO	µg L ⁻¹	75.0	15.8	0.1	0.1	n.d.	-	-
SMX	µg L ⁻¹	174.2	36.3	2.3	0.9	n.d.	-	-
Total organic C from PhACs	µg L ⁻¹	1269.1	981.9	763.1	597.0	539.4	-	-
NPOC	mg L ⁻¹	879 ± 18	-	-	851 ± 17	845 ± 17	827 ± 17	819 ± 16
COD	mg L ⁻¹	-	-	-	-	-	-	-
N-NO ₃ ⁻	mg L ⁻¹	0	-	-	-	-	46 ± 5	331 ± 33
N-NH ₄ ⁺	mg L ⁻¹	5788 ± 579	-	-	-	-	5741 ± 574	5396 ± 540
pH	-	9.14	-	-	9.09	9.02	8.99	8.91

V.4.2 Ozone kinetic regimes and ozone consumption during the ozonation of real urine

The concentration profile of ozone in synthetic urine and ultra-pure water has been described in Chapter IV. Thus, this work only focused on the concentration profile of ozone in the HUM-based solutions. Figure 5.9 plots the concentration of ozone in the gaseous and liquid phase as a function of reaction time.

For the ozonation of HUM-based solutions with several times dilution, a rapid increase in the concentration of ozone gas-out was observed at the early 10 min ozonation. In the following ozonation, the concentration of ozone gas-out increased gradually so that the gap between ozone gas-in and -out became more and more narrow. The more narrow curve gap with the reaction time revealed chemical reactions enhancing the gas-liquid ozone transfer diminished along with the ozonation process (Domenjoud et al., 2011). At the end of ozonation, ozone gas-out curve of HUM-1 was close to that of ozone gas-in (Figure 5.9a), implying that the chemical reactions had finished. However, for the three

other HUM-based solutions (Figure 5.9b, 5.9c, and 5.9d), a significant gap between ozone gas-in and gas-out suggested that the reactions of urine matrix towards ozone were not complete, but relatively slow.

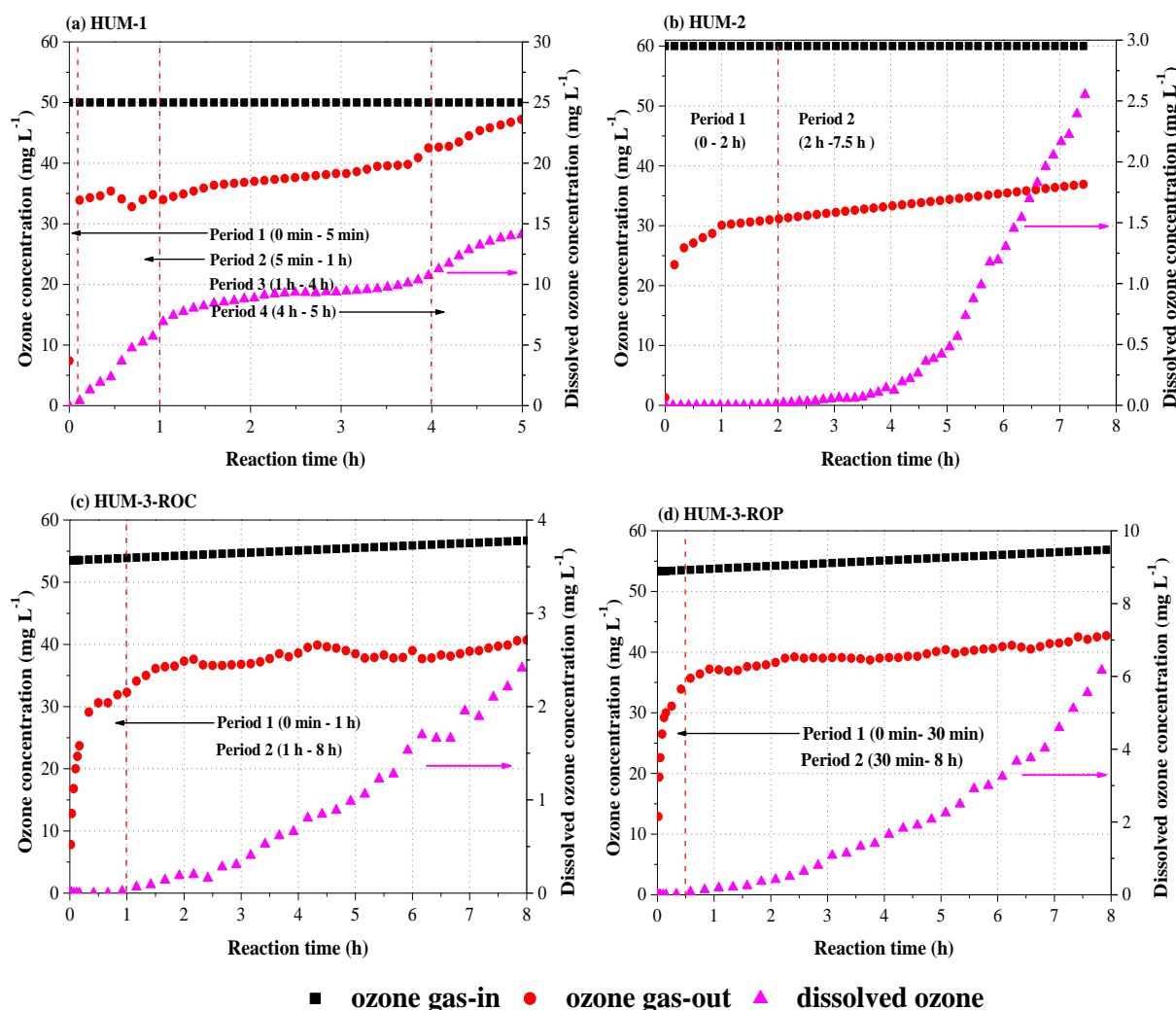


Figure 5.9 Concentration profile of ozone in either gaseous phase or liquid solution as a function of reaction time during the ozonation of the real urine solutions. gas flow rate: 30 L h^{-1} . temperature: $20 \pm 1 \text{ }^\circ\text{C}$. solution volume: 2 L. dilution: 20 times for HUM-1, 10 times for HUM-2, HUM-3-ROC and HUM-3-ROP.

Based on the concentration profile of dissolved ozone, in this work, four distinctive periods can be identified, i.e., Period 1 with the absence of dissolved ozone, Period 2 where the concentration of dissolved ozone ($[\text{O}_3]_{\text{L}}$) raised rapidly, Period 3 where $[\text{O}_3]_{\text{L}}$ increased slowly, and Period 4 where $[\text{O}_3]_{\text{L}}$ almost reached a plateau, corresponding to four different kinetic regimes (instantaneous, fast, moderate, and slow reaction rate, respectively). Regarding the ozonation of HUM-1 (Figure 5.9a), the four different kinetic regimes were experienced, quite fast reactions (0-5 min), fast reactions (5 min-1 h), moderate kinetic regime (1 h-4 h), and the reactions with a slow rate (4 h-5 h). However, only two periods (Period 1 and Period 2) were observed for the ozonation of HUM-2, HUM-3-ROC and HUM-3-ROP, as indicated in Figure 5.9b, 5.9c and 5.9d, respectively. These results provide evidence that the ozone kinetic regimes were strongly matrix- and concentration-dependent.

To further evaluate the ozonation kinetic regimes of the tested solutions, the enhancement factor from the experimental result (E_{exp} , see Equation 40 in Chapter IV) was estimated. Table 5.18 gives the E_{exp} values at the first moment of the HUM-based solutions ozonation. All the E_{exp} values were above one, confirming very fast chemical reactions taking place in the film layer, which matched well with the absence of dissolved ozone (see Figure 5.9). On the other hand, the E_{exp} value increased in the following order of HUM-2 > HUM-3-ROC > HUM-3-ROP > HUM-1, which was mainly linked to the ozone-consuming constituents in the tested solutions, such as organic matters and ammonia. Indeed, during the ozonation process, the amount of organic matters and ammonia decreased gradually, as discussed above.

The immediate/initial ozone demand (IOD), defined as the minimum amount of gaseous ozone transferred to the liquid solution when dissolved ozone was detected in the liquid phase, is a useful parameter for disinfection, elimination of trace organic compounds and ozonation process design (Marce et al., 2016). The calculation of transferred ozone dose is given in Equation 21 in Chapter II.3. IOD increased from 30.0 mg L⁻¹ in HUM-1 to 958.9 mg L⁻¹ in HUM-2 (Table 5.18), which was consistent with the increase of the E_{exp} values. Once IOD was satisfied, dissolved ozone began to accumulate until a plateau was achieved, and the kinetic regime was shifted to moderate or to slow (Marce et al., 2016).

Table 5.18 Initial E_{exp} values and initial ozone demand (IOD) during the ozonation of HUM-based solutions

Solutions	Initial E_{exp} value ¹	Dissolved ozone absence	IOD ²
HUM-1	7.9	the first 5 min	30.0
HUM-2	97.7	the first 2 h	958.9
HUM-3-ROC	16.4	the first 1.0 h	387.4
HUM-3-ROP	10.5	the first 30 min	178.7

(1) calculated by Equation 40 in Chapter IV. (2) IOD is the maximum dose of transferred ozone before dissolved ozone was detected

To understand better the ozonation behaviour of the real urine solutions, it was necessary to check the ozone consumption rate. Figure 5.10 shows the cumulated consumed ozone dose as a function of applied ozone dose (calculated by Equation 20 in Chapter II.3) during the ozonation of synthetic urine and real urine. As can be clearly seen that, the consumption rate by urine-based matrix followed an order of SUM-ROC = SUM-ROP > HUM-2 > HUM-3-ROC > HUM-3-ROP > HUM-1, demonstrating the effect of water matrix mainly referring to N-NH₄⁺ and organic matters (NPOC) on ozone consumption. On the other hand, during 8 h ozonation time, the ratio of cumulated consumed ozone dose to applied ozone dose in SUM-based solutions was quite close 1, indicating all the applied ozone dose was consumed by constituents present in SUM-based solutions.

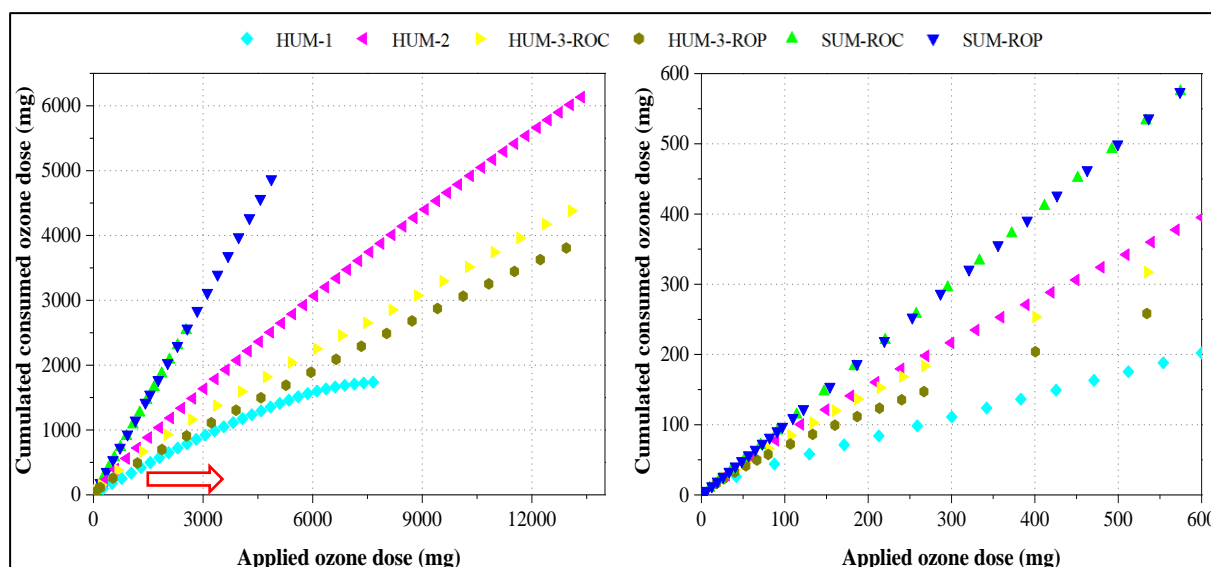


Figure 5.10 Cumulated consumed ozone dose versus applied ozone dose.

V.5 Comparison of P recovery and PhACs removal from source-separated urine by the combination process

In this section, the overall performance of the combination process consisting of struvite precipitation, RO process and ozonation for real urine treatment (HUM-2 and HUM-3) was evaluated in terms of P recovery and PhACs selected removal.

Almost all the P-PO_4^{3-} can be recovered from two kinds of hydrolysed urine in the form of struvite (See Table 5.7). Moreover, the model micropollutants completely remained in the HUM-based solutions, as indicated in Table 5.8. These results indicated that P-PO_4^{3-} recovery as struvite was a recommended technology for urine valorisation.

After struvite precipitation, the ESPA2 membrane showed a moderate rejection for the target PhACs between 43% for CAF and 79% for PRO (see Table 5.10). In future study, therefore, works, including membrane selection, tests with higher transmembrane pressure, etc., needed to be extended, aiming to improve the retention rate of the PhACs by RO membrane.

With respect to the ozonation of the real urine solutions, whatever the solution matrix was, less ozone was consumed to effectively remove ozone-reactive PhACs (CBZ, DIF, OFL, PRO, and SMX) than ozone-refractory PhACs (2OH-IBP, IBP and OXA). Table 5.19 summarizes the removal efficiencies of organic C from ozone-reactive PhACs and ozone-refractory PhACs by ozonation. For these three real urine solutions, at a consumed ozone dose of 1.3 mg per mg NPOC_0 , a full elimination of ozone-reactive PhACs was almost accomplished. It may be pointed out that, however, more ozone dose, at least higher than 1000 mg, was required to achieve a satisfactory degradation degree for the ozone-refractory PhACs, which was mainly due to the competition of highly concentrated organic matters and ammonia for oxidants.

Table 5.19 Removal efficiencies of organic C from PhACs by ozonation

Solutions	HUM-2			HUM-3-ROC			HUM-3-ROP		
Cumulated consumed ozone dose (mg)	0.0	563.7 (0.5 h)	1917.9 (2 h)	0.0	435.7 (0.5 h)	1333.6 (2 h)	0.0	357.4 (0.5 h)	1111.6 (2 h)
mg cumulated consumed ozone dose / mg NPOC ₀	-	0.7	2.3	-	1.0	2.9	-	1.3	4.0
Removed organic C from PhACs (µg)	0.0	418.5	610.9	0.0	546.4	868.6	0.0	127.8	209.9
Organic C from PhACs removal	0%	67%	98%	0%	52%	83%	0%	33%	55%
Removed Organic C from O ₃ -reactive PhACs (µg)	0.0	19.2	18.8	0.0	66.4	70.2	0.0	21.6	21.9
Organic C from O ₃ -reactive PhACs removal	0%	96%	94%	0%	95%	100%	0%	99%	100%
Removed organic C from CAF (µg)	0.0	44.3	69.4	0.0	171.9	290.9	0.0	89.2	116.2
Organic C from CAF removal	0%	64%	100%	0%	58%	98%	0%	74%	96%
Removed organic C from O ₃ -refractory PhACs (µg)	0.0	355.0	522.8	0.0	308.1	507.4	0.0	16.9	71.7
Organic C from O ₃ -refractory PhACs removal	0%	67%	98%	0%	45%	75%	0%	7%	30%

As mentioned above, the presence of organic matters and ammonia had significant influences on the ozone consumption during the ozonation of real urine solutions. To find a relationship between these two substances and ozone consumption, the molar ratio between the consumed ozone dose, the amount of organic matters removal and of ammonia removal was estimated during each period and over the entire ozonation process. The results are listed in Table 5.20.

It was found that, over the entire ozonation process, the molar ratio of consumed O₃/ (NPOC + N- NH₄⁺) eliminated was similar for the four real urine solutions, between 1.9 in HUM-2 and 2.8 in HUM-3-ROP, which also confirmed that a relatively high consumed ozone dose was a result of the reactions of both organic matters and ammonia towards molecular ozone.

Table 5.20 Ozone consumption and the elimination of carbon and N-NH₄⁺ during the ozonation of the real urine solutions

Solutions		HUM-1				HUM-2		HUM-3-ROC		HUM-3-ROP	
Periods		Period 1	Period 2	Period 3	Period 4	Period 1	Period 2	Period 1	Period 2	Period 1	Period 2
Entire the ozonation process	Time	0 -5 min	5 min - 1 h	1 h – 4 h	4 h – 5 h	0 - 2 h	2 h – 7.5 h	0 - 1 h	1 h – 8 h	0 - 30 min	30 min – 8 h
	Cumulated consumed O ₃ (mg)	56.8	482.1	1583.0	1731.1	1917.9	6190.7	774.7	4419.6	357.4	3875.9
	mg cumulated consumed O ₃ per mg NPOC ₀	0.32	2.81	9.11	9.99	2.31	7.47	1.69	9.65	1.82	13.94
	NPOC eliminated (mg)	-	-	-	145	-	568	-	204	-	196
	N-NH ₄ ⁺ eliminated (mg)	-	-	-	34	-	296	-	244	-	172
	Consumed O ₃ / (NPOC + N-NH ₄ ⁺) eliminated (mol/mol)	-	-	-	2.5	-	1.9	-	2.7	-	2.8
	[O ₃] _L average (mg L ⁻¹)	absence	-	8.75	12.45	absence	-	absence	-	absence	-
During each period	Consumed O ₃ dose (mg)	56.8	425.3	1100.9	148.1	1917.9	4272.8	774.7	3644.9	357.4	3518.5
	Eliminated organic C from PhACs (mg)	0.07	0.04	-	-	0.61	-	0.55 (0-30 min)	-	0.13	-
	NPOC eliminated (mg)	2.64	23.0	90.5	28.7	200	368	32	172	8	188
	DIC eliminated (mg)	2.74	1.00	0.56		162	320	22	178	6	130
	Consumed O ₃ /organic C from PhACs (mol/mol)	218	2672	-	-	786	-	198 (0-30 min)	-	687	-
	Consumed O ₃ / NPOC eliminated (mol/mol)	5.4	4.6	3.0	1.3	2.4	2.9	6.1	5.3	11.2	4.7
	N-NH ₄ ⁺ eliminated (mg)	10	24	-	-	164	132	18	226	10	162
	N-NO ₃ ⁻ produced (mg)	0	100	-	-	75	196	16.6	224	7.8	156
	Consumed O ₃ / N-NH ₄ ⁺ eliminated (mol/mol)	1.7	5.2	-	-	3.4	9.4	12.6	4.7	10.4	6.3
	Consumed O ₃ / (NPOC + N-NH ₄ ⁺) eliminated (mol/mol)	1.3	2.4	3.0	1.3	1.4	2.2	4.1	2.5	5.4	2.7
	Reaction regimes	instantaneous	fast	moderate	slow	instantaneous	fast	instantaneous	fast	instantaneous	fast

V.6 Conclusions of this chapter

In this work, an integrated process that consisted of struvite precipitation, low-pressure reverse osmosis, together with ozonation system was performed for urine reclamation, aiming to recover valuable nutrients and to separate or to remove micropollutants from the hydrolysed urine. Several conclusions can be obtained from this study:

- Struvite crystallization with MgCl_2 as Mg^{2+} source was a successful solution to recover >90% P nutrients from the real urine. A major part of micropollutants and dissolved organic matters still remained in the urine solutions after struvite precipitation, indicating that a micropollutant-free solid fertilizer was produced.
- PhACs remaining in the urine solutions were not well rejected by the RO membrane, with observed retention between 43% for CAF and 79% for PRO (HUM-2 and HUM-3);
- At a consumed ozone dose of 0.3 - 1.3 mg per mg NPOC_0 , ozone-reactive PhACs were removed completely from the real urine solutions. However, much more ozone was consumed to degrade effectively ozone-refractory PhACs;
- The impacts of organic matters in the real urine on the ozonation efficiencies of micropollutants seemed to be complicated. The presence of organic matters inhibited significantly the overall elimination of micropollutants by ozonation. However, it appeared that a higher load of organic matters was more favourable to the oxidation of ozone-refractory PhACs;
- Organic matters and ammonia were two main contributors to ozone consumption. The ozone kinetic regimes were highly depending on their concentration in the urine matrix.

These results could be quite useful for the valorisation and the reuse of the real urine. If the purpose is to recover P nutrients from the hydrolysed urine, struvite precipitation is a feasible option. If the focus of the study is to reduce micropollutants from the hydrolysed urine, RO + ozonation / ozonation could be considered. It should be highlighted that, nonetheless, the application of RO needs to consider the reactivity of ozone towards micropollutants (ozone-reactive or ozone-recalcitrant micropollutants). That is to say: (1) If the compositions of ozone-recalcitrant PhACs is dominant in the real urine, RO process combined to ozonation of the RO concentrate was recommended; whereas (2) in the case of the hydrolysed urine mainly containing ozone-reactive micropollutants, direct ozonation was adequate to reduce such micropollutants to an acceptable level at a low consumed ozone dose.

In order to improve the removal efficiencies of PhACs by ozonation from the real urine, this work requires to be extended:

- Prior to ozonation, ammonia present in real urine could be removed by stripping, aiming to reduce the competitive effects of ammonia for the oxidant.
- two integrated processes for urine reclamation, i.e., precipitation + ozonation, and precipitation + RO process + ozonation, should be further evaluated in terms of performance and of cost-effectiveness.

Conclusions and Future research

In a context of growing water scarcity, wastewater reclamation or reuse has been increasingly recognized as an alternative source of water supply. However, trace micropollutants are not removed effectively by conventional treatment technologies in the wastewater treatment plants (WWTPs). To ensure safe reuse of municipal wastewater, it is necessary and important to establish advanced technologies, such as reverse osmosis (RO) process and ozonation, to reduce these non-desirable compounds to an acceptable level. In addition, a large fraction of trace micropollutants in the municipal wastewater, which are mainly referred to pharmaceutically active compounds (PhACs), mainly originate from urine wastewater. Separation and treatment of urine at the source not only provides an opportunity for urine valorisation by recovering N/P nutrients but also reduces the micropollutant load in the municipal wastewater.

In this context, the present thesis investigated the potential of the RO process, ozonation, and their combination for wastewater reuse including municipal MBR permeate and source-separated urine. The main objectives were:

- to study RO performance in an MBR-RO system, where RO concentrate was recirculated continuously to MBR;
- to examine the removal efficiency of trace micropollutants by RO process combining ozonation for municipal wastewater reuse.
- to investigate a combination consisted of struvite precipitation, RO process and ozonation for urine treatment by nutrients recovery and PhACs removal.

For these purposes, the performance of the RO process for MBR permeate was first examined in terms of RO membrane fouling and retention capacities for the target PhACs and for common water quality parameters. RO permeate flux decline, osmotic pressure model, saturation index of common scalants were used to study the RO membrane fouling potential in the MBR-RO system with RO concentrate recycling. Then RO process combining ozonation was applied to remove PhACs from municipal MBR permeate. At last, a combination of struvite precipitation, RO and ozonation was investigated for urine treatment with respect to P recovery and PhACs removal. At the same time, the impacts of matrix including ions, ammonia and organic matters on the degradation levels of the PhACs was also studied, aiming to better understand the ozonation behaviour of real urine with a complicated nature.

Based on the wastewater used in this thesis (MBR permeate and urine), the main conclusions are divided into two sections to present.

Treatment of MBR permeate by RO process and ozonation (Chapter III)

In the MBR- RO system, the continuous recirculation of RO concentrate to MBR did not affect significantly RO performance in terms of the retention capacities of the RO membrane for global water quality parameters. The retention efficiencies of the RO membrane for organic matters (NPOC) and conductivity were higher than 94% before and during RO concentrate recycling. However, RO

concentrate recycling increased significantly the concentration of inorganic ions and organic matters in both MBR permeate and RO concentrate. For instances, after two weeks of RO concentrate recycling, the conductivity and NPOC content in RO concentrate increased by a factor of 1.3 and 1.7, respectively. As a result, the RO membrane fouling propensity was enhanced with respect to RO permeate flux decline, which was mainly due to a gradual increase in the osmotic pressure of retained ions on the RO membrane surface. On the other hand, a colloidal cake layer or adsorption of organic matters to the RO membrane could happen, which represented around 15% of the RO permeate flux decline. Indeed, after RO concentrate recirculation, the 10- 100 kDa protein-like substances increased significantly in the bulk RO concentrate.

With respect to micropollutant removal from MBR permeate, RO process and ozonation can complement each other very well to remove trace organic micropollutants from MBR permeate. >91% of the target PhACs were retained in RO concentrate by the RO membrane. The followed ozonation was proven to be successful in eliminating these target PhACs retained in RO concentrate at a low ozone dose corresponding to 0.79 mg consumed O₃ per mg NPOC₀.

Treatment of urine by RO process and ozonation

In Chapter IV, the influence of water matrices (ions, NH₃ and organic matters) on the micropollutant elimination efficiency, ozone consumption and ozonation kinetic regimes were investigated and estimated. Ozone-reactive carbamazepine (CBZ) and ozone-refractory ketoprofen (KET) were selected as the model micropollutants. The results obtained in this work were useful for the oxidation of micropollutants by ozonation in the solutions with highly concentrated ions and organic matters such as real urine. Whatever the matrices were, less ozone was consumed to achieve a satisfactory abatement for ozone-reactive CBZ than ozone-refractory KET, which was attributed to their different reactivity towards molecular ozone. For example, ozone consumption of 1166 mg removed 66% of KET from synthetic urine with ions and ammonia, whereas an excellent elimination for CBZ (>95%) only consumed around 24 mg ozone dose. The presence of ions and NH₃ had a slight influence on the removal efficiency of ozone-reactive CBZ. However, once organic matters were involved (as in hydrolysed urine), the degradation of CBZ was inhibited strongly due to the competition for molecular ozone. With respect to ozone-refractory KET, ionic salts and ammonia inhibited significantly its degradation efficiency. The oxidation degree of micropollutants, the ozone consumption and the ozone kinetic regimes were strongly matrix-dependent.

In Chapter V, struvite crystallization with MgCl₂ as Mg²⁺ source was a feasible solution to recover all the P nutrients from the real urine. A major part of micropollutants and dissolved organic matters still remained in the urine solutions after struvite precipitation, indicating that a micropollutant-free solid fertilizer was produced. RO process with low-pressure operation was not effective in retaining PhACs remained in the hydrolysed urine (HUM), with the observed retention between 43% for caffeine (CAF) and 79% for propranolol (PRO) (HUM-2 and HUM-3). An ozone dose of 0.3 - 1.3 mg per mg NPOC₀

could remove completely ozone-reactive PhACs from the real urine solutions. However, a higher ozone dose was required to reduce ozone-refractory PhACs from real urine to an acceptable level, which was related to the presence of highly concentrated ammonia and organic matters with molecular ozone. Overall, during ozonation process of real urine, a relatively high dose of ozone consumption was required for a satisfactory removal of micropollutants, which was due to the competitive reactions of both organic matters and ammonia towards molecular ozone.

Future work

In this section, several recommendations with regard to the application of RO process combining ozonation for the wastewater reclamation are presented.

- In this thesis, RO performance in the integrated MBR-RO system with the recirculation of the treated RO concentrate by ozonation was not investigated, so the relevant studies should be conducted to gain more information on the management of RO concentrate.
- In the MBR-RO system, during the RO concentrate recycling, membrane fouling in MBR, due to ions accumulation in this system, was a main limitation. Therefore, in order to mitigate the RO membrane fouling during a long-term operation, the ion contents in this system should be controlled by technologies, such as capacitive deionization process.
- In order to improve the overall oxidation degree of micropollutants from real urine, it is essential to find effective solutions to reduce the amount of ozone-consuming constituents such as organic matters and NH_3 before ozonation. Biological treatment could be proposed to degrade organic matters from urine. With respect to NH_3 removal, stripping and biological nitrification could be considered.

REFERENCES

- Abdelmelek, S.B., Greaves, J., Ishida, K.P., Cooper, W.J., Song, W., 2011. Removal of pharmaceutical and personal care products from reverse osmosis retentate using advanced oxidation processes. *Environ. Sci. Technol.* 45, 3665–3671. <https://doi.org/10.1021/es104287n>
- Abdel-Shafy, H., Mohamed-Mansour, M.S., 2013. Issue of Pharmaceutical Compounds in Water and Wastewater: Sources, Impact and Elimination. *Egypt. J. Chem.* 56(5), 449–471.
- Aboussaoud, W., 2014. Étude du rôle d'adsorbants alumino-silicatés dans un procédé d'ozonation d'eaux usées pétrochimiques (Thèse de doctorat). Institut national polytechnique, Toulouse, France.
- Acero, J.L., Benitez, F.J., Real, F.J., Teva, F., 2016. Micropollutants removal from retentates generated in ultrafiltration and nanofiltration treatments of municipal secondary effluents by means of coagulation, oxidation, and adsorption processes. *Chem. Eng. J.* 289, 48–58. <https://doi.org/10.1016/j.cej.2015.12.082>
- Acero, J.L., Gunten, U. von, 2000. Influence of Carbonate on the Ozone/Hydrogen Peroxide Based Advanced Oxidation Process for Drinking Water Treatment. *Ozone Sci. Eng.* 22, 305–328. <https://doi.org/10.1080/01919510008547213>
- Akbari, A., Remigy, J.C., Aptel, P., 2002. Treatment of textile dye effluent using a polyamide-based nanofiltration membrane. *Chem. Eng. Process. Process Intensif.* 41, 601–609. [https://doi.org/10.1016/S0255-2701\(01\)00181-7](https://doi.org/10.1016/S0255-2701(01)00181-7)
- Alturki, A.A., Tadkaew, N., McDonald, J.A., Khan, S.J., Price, W.E., Nghiem, L.D., 2010. Combining MBR and NF/RO membrane filtration for the removal of trace organics in indirect potable water reuse applications. *J. Membr. Sci.* 365, 206–215. <https://doi.org/10.1016/j.memsci.2010.09.008>
- Asano, T., Metcalf & Eddy, Inc (Eds.), 2007. *Water reuse: issues, technology, and applications*, 1 ed. McGraw-Hill, New York, NY.
- Ashfaq, M., Li, Y., Wang, Y., Chen, W., Wang, H., Chen, X., Wu, W., Huang, Z., Yu, C.-P., Sun, Q., 2017. Occurrence, fate, and mass balance of different classes of pharmaceuticals and personal care products in an anaerobic-anoxic-oxic wastewater treatment plant in Xiamen, China. *Water Res.* 123, 655–667. <https://doi.org/10.1016/j.watres.2017.07.014>
- Azaïs, A., Mendret, J., Cazals, G., Petit, E., Brosillon, S., 2017. Ozonation as a pretreatment process for nanofiltration brines: Monitoring of transformation products and toxicity evaluation. *J. Hazard. Mater.* 338, 381–393. <https://doi.org/10.1016/j.jhazmat.2017.05.045>
- Azaïs, A., Mendret, J., Petit, E., Brosillon, S., 2016. Influence of volumetric reduction factor during ozonation of nanofiltration concentrates for wastewater reuse. *Chemosphere* 165, 497–506. <https://doi.org/10.1016/j.chemosphere.2016.09.071>

- Bagastyo, A.Y., Batstone, D.J., Rabaey, K., Radjenovic, J., 2013. Electrochemical oxidation of electrodialed reverse osmosis concentrate on Ti/Pt–IrO₂, Ti/SnO₂–Sb and boron-doped diamond electrodes. *Water Res.* 47, 242–250. <https://doi.org/10.1016/j.watres.2012.10.001>
- Bagastyo, A.Y., Keller, J., Poussade, Y., Batstone, D.J., 2011a. Characterisation and removal of recalcitrants in reverse osmosis concentrates from water reclamation plants. *Water Res.* 45, 2415–2427. <https://doi.org/10.1016/j.watres.2011.01.024>
- Bagastyo, A.Y., Radjenovic, J., Mu, Y., Rozendal, R.A., Batstone, D.J., Rabaey, K., 2011b. Electrochemical oxidation of reverse osmosis concentrate on mixed metal oxide (MMO) titanium coated electrodes. *Water Res.* 45, 4951–4959. <https://doi.org/10.1016/j.watres.2011.06.039>
- Bahr, C., Schumacher, J., Ernst, M., Luck, F., Heinzmann, B., Jekel, M., 2007. SUVA as control parameter for the effective ozonation of organic pollutants in secondary effluent. *Water Sci. Technol. J. Int. Assoc. Water Pollut. Res.* 55, 267–274.
- Ball, J.W., Nordstrom, D.K., 1991. User's manual for WATEQ4F, with revised thermodynamic data base and text cases for calculating speciation of major, trace, and redox elements in natural waters.
- Barbosa, S.G., Peixoto, L., Meulman, B., Alves, M.M., Pereira, M.A., 2016. A design of experiments to assess phosphorous removal and crystal properties in struvite precipitation of source separated urine using different Mg sources. *Chem. Eng. J.* 298, 146–153. <https://doi.org/10.1016/j.cej.2016.03.148>
- Bellona, C., Drewes, J.E., Xu, P., Amy, G., 2004. Factors affecting the rejection of organic solutes during NF/RO treatment—a literature review. *Water Res.* 38, 2795–2809. <https://doi.org/10.1016/j.watres.2004.03.034>
- Beltrán, F.J., 2004. Ozone reaction kinetics for water and wastewater systems. Lewis Publishers, Boca Raton, Fla.
- Beltran, F.J., 2003. Ozone Reaction Kinetics for Water and Wastewater Systems. CRC Press.
- Beltrán, F.J., Aguinaco, A., García-Araya, J.F., 2012. Application of Ozone Involving Advanced Oxidation Processes to Remove Some Pharmaceutical Compounds from Urban Wastewaters. *Ozone Sci. Eng.* 34, 3–15. <https://doi.org/10.1080/01919512.2012.640154>
- Beltrán, F.J., Pocostales, P., Alvarez, P., Oropesa, A., 2009. Diclofenac removal from water with ozone and activated carbon. *J. Hazard. Mater.* 163, 768–776. <https://doi.org/10.1016/j.jhazmat.2008.07.033>
- Bendz, D., Paxéus, N.A., Ginn, T.R., Loge, F.J., 2005. Occurrence and fate of pharmaceutically active compounds in the environment, a case study: Höje River in Sweden. *J. Hazard. Mater.* 122, 195–204. <https://doi.org/10.1016/j.jhazmat.2005.03.012>

- Benítez, F.J., Beltrán-Heredia, J., Acero, J.L., Pinilla, M.L., 1997. Ozonation Kinetics of Phenolic Acids Present in Wastewaters from Olive Oil Mills. *Ind. Eng. Chem. Res.* 36, 638–644. <https://doi.org/10.1021/ie9600250>
- Benner, J., 2009. Ozone reactivity in wastewater treatment plant effluent and reverse osmosis concentrate. Ozonation of beta blockers: kinetic studies, identification of oxidation products and pathways. Universität Koblenz-Landau, Mainz, Germany.
- Benner, J., Salhi, E., Ternes, T., von Gunten, U., 2008. Ozonation of reverse osmosis concentrate: Kinetics and efficiency of beta blocker oxidation. *Water Res.* 42, 3003–3012. <https://doi.org/10.1016/j.watres.2008.04.002>
- Blair, B., Nikolaus, A., Hedman, C., Klaper, R., Grundl, T., 2015. Evaluating the degradation, sorption, and negative mass balances of pharmaceuticals and personal care products during wastewater treatment. *Chemosphere* 134, 395–401. <https://doi.org/10.1016/j.chemosphere.2015.04.078>
- Cai, M.-J., Lin, Y.-P., 2016. Effects of effluent organic matter (EfOM) on the removal of emerging contaminants by ozonation. *Chemosphere* 151, 332–338. <https://doi.org/10.1016/j.chemosphere.2016.02.094>
- Cartagena, P., El Kaddouri, M., Cases, V., Trapote, A., Prats, D., 2013. Reduction of emerging micropollutants, organic matter, nutrients and salinity from real wastewater by combined MBR–NF/RO treatment. *Sep. Purif. Technol.* 110, 132–143. <https://doi.org/10.1016/j.seppur.2013.03.024>
- Cavaillé, L., Bounouba, M., Riboul, D., Morere, M., 2017. Quantification of micropollutants by QuEChERS method: optimization for different and complex environmental matrices. Presented at the 16th CONGRESS OF THE FRENCH CHEMICAL ENGINEERING SOCIETY, Nancy, France.
- Chen, Y., Liu, F., Wang, Y., Lin, H., Han, L., 2017. A tight nanofiltration membrane with multi-charged nanofilms for high rejection to concentrated salts. *J. Membr. Sci.* 537, 407–415. <https://doi.org/10.1016/j.memsci.2017.05.036>
- Chi, S.C., Jun, H.W., 1991. Release Rates of Ketoprofen from Poloxamer Gels in a Membraneless Diffusion Cell. *J. Pharm. Sci.* 80, 280–283. <https://doi.org/10.1002/jps.2600800318>
- Choi, H., Zhang, K., Dionysiou, D.D., Oerther, D.B., Sorial, G.A., 2005. Influence of cross-flow velocity on membrane performance during filtration of biological suspension. *J. Membr. Sci.* 248, 189–199. <https://doi.org/10.1016/j.memsci.2004.08.027>
- Coelho, A.D., Sans, C., Agüera, A., Gómez, M.J., Esplugas, S., Dezotti, M., 2009. Effects of ozone pre-treatment on diclofenac: Intermediates, biodegradability and toxicity assessment. *Sci. Total Environ.* 407, 3572–3578. <https://doi.org/10.1016/j.scitotenv.2009.01.013>
- Comerton, A.M., Andrews, R.C., Bagley, D.M., Hao, C., 2008. The rejection of endocrine disrupting and pharmaceutically active compounds by NF and RO membranes as a function of compound

- and water matrix properties. *J. Membr. Sci.* 313, 323–335. <https://doi.org/10.1016/j.memsci.2008.01.021>
- Comstock, S.E.H., Boyer, T.H., Graf, K.C., 2011. Treatment of nanofiltration and reverse osmosis concentrates: Comparison of precipitative softening, coagulation, and anion exchange. *Water Res.* 45, 4855–4865. <https://doi.org/10.1016/j.watres.2011.06.035>
- Crousier, C., Pic, J.-S., Albet, J., Baig, S., Roustan, M., 2016. Urban Wastewater Treatment by Catalytic Ozonation. *Ozone Sci. Eng.* 38, 3–13. <https://doi.org/10.1080/01919512.2015.1113119>
- Dai, G., Wang, B., Huang, J., Dong, R., Deng, S., Yu, G., 2015. Occurrence and source apportionment of pharmaceuticals and personal care products in the Beiyun River of Beijing, China. *Chemosphere* 119, 1033–1039. <https://doi.org/10.1016/j.chemosphere.2014.08.056>
- Dalhammar, G., 1997. Handling och koncentrerings av humanurin (personal communication). Royal Institute of Technology, Stockholm, Department of Biochemistry and Biochemical technology.
- de Vera, G.A., Keller, J., Gernjak, W., Weinberg, H., Farré, M.J., 2016. Biodegradability of DBP precursors after drinking water ozonation. *Water Res.* 106, 550–561. <https://doi.org/10.1016/j.watres.2016.10.022>
- De Vera, G.A., Stalter, D., Gernjak, W., Weinberg, H.S., Keller, J., Farré, M.J., 2015. Towards reducing DBP formation potential of drinking water by favouring direct ozone over hydroxyl radical reactions during ozonation. *Water Res.* 87, 49–58. <https://doi.org/10.1016/j.watres.2015.09.007>
- Derco, J., Dudáš, J., Valičková, M., Šimovičová, K., Kecskés, J., 2015. Removal of micropollutants by ozone based processes. *Chem. Eng. Process. Process Intensif., Novel engineering ideas for improved chemical processes* 94, 78–84. <https://doi.org/10.1016/j.cep.2015.03.014>
- Dialynas, E., Diamadopoulos, E., 2009. Integration of a membrane bioreactor coupled with reverse osmosis for advanced treatment of municipal wastewater. *Desalination* 238, 302–311. <https://doi.org/10.1016/j.desal.2008.01.046>
- Dodd, M.C., Buffle, M.-O., von Gunten, U., 2006. Oxidation of Antibacterial Molecules by Aqueous Ozone: Moiety-Specific Reaction Kinetics and Application to Ozone-Based Wastewater Treatment. *Environ. Sci. Technol.* 40, 1969–1977. <https://doi.org/10.1021/es051369x>
- Dodd, M.C., Zuleeg, S., von Gunten, U., Pronk, W., 2008. Ozonation of source-separated urine for resource recovery and waste minimization: process modeling, reaction chemistry, and operational considerations. *Environ. Sci. Technol.* 42, 9329–9337.
- Dolar, D., Gros, M., Rodriguez-Mozaz, S., Moreno, J., Comas, J., Rodriguez-Roda, I., Barceló, D., 2012. Removal of emerging contaminants from municipal wastewater with an integrated membrane system, MBR–RO. *J. Hazard. Mater.* 239–240, 64–69. <https://doi.org/10.1016/j.jhazmat.2012.03.029>
- Domenjoud, B., Ospina, A.G., Vulliet, E., Baig, S., 2015. Pharmaceuticals removal in wastewater by biological treatment and tertiary ozonation. Presented at the IOA world congress, Barcelona, Spain.

- Domenjoud, B., Tatari, C., Esplugas, S., Baig, S., 2011. Ozone-Based Processes Applied to Municipal Secondary Effluents. *Ozone Sci. Eng.* 33, 243–249. <https://doi.org/10.1080/01919512.2011.571166>
- Doyle, J.D., Parsons, S.A., 2002. Struvite formation, control and recovery. *Water Res.* 36, 3925–3940. [https://doi.org/10.1016/S0043-1354\(02\)00126-4](https://doi.org/10.1016/S0043-1354(02)00126-4)
- Dreywood, R., 1946. Qualitative Test for Carbohydrate Material. *Ind. Eng. Chem. Anal. Ed.* 18, 499–499. <https://doi.org/10.1021/i560156a015>
- Eichelsdörfer, D., Jandik, J., 1985. Long Contact Time Ozonation For Swimming Pool Water Treatment. *Ozone Sci. Eng.* 7, 93–106. <https://doi.org/10.1080/01919518508552328>
- El-taliawy, H., Ekblad, M., Nilsson, F., Hagman, M., Paxeus, N., Jönsson, K., Cimbritz, M., la Cour Jansen, J., Bester, K., 2017. Ozonation efficiency in removing organic micro pollutants from wastewater with respect to hydraulic loading rates and different wastewaters. *Chem. Eng. J.* 325, 310–321. <https://doi.org/10.1016/j.cej.2017.05.019>
- Escher, B.I., Pronk, W., Suter, M.J.F., Maurer, M., 2006. Monitoring the removal efficiency of pharmaceuticals and hormones in different treatment processes of source-separated urine with bioassays. *Environ. Sci. Technol.* 40, 5095–5101.
- EUROPEAN COMMISSION, 2019. European Union Strategic Approach to Pharmaceuticals in the Environment.
- EUROPEAN COMMISSION, 2018. Proposal for a REGULATION OF THE EUROPEAN PARLIAMENT AND OF THE COUNCIL on minimum requirements for water reuse.
- F, A.W.W.R., Langlais, B., Reckhow, D.A., Brink, D.R., 1991. *Ozone in Water Treatment: Application and Engineering*. CRC Press.
- Farias, E.L., Howe, K.J., Thomson, B.M., 2014. Effect of membrane bioreactor solids retention time on reverse osmosis membrane fouling for wastewater reuse. *Water Res.* 49, 53–61. <https://doi.org/10.1016/j.watres.2013.11.006>
- Field, R., Bekassy-Molnar, E., Lipnizki, F., Vatai, G. (Eds.), 2017. *Engineering aspects of membrane separation and application in food processing*, Contemporary food engineering series. CRC Press, Taylor & Francis Group, Boca Raton, Fla. London New York.
- Gajurel, D.R., Kucharek, K., Skwiot, R., Hammer, M., 2007. Ozonierung von Urin zur Entfernung von Pharmaka (Ozonation of urine for removal of pharmaceuticals). *Abwasserbehandlung* 148, 262–268.
- Ganiyu, S.O., van Hullebusch, E.D., Cretin, M., Esposito, G., Oturan, M.A., 2015. Coupling of membrane filtration and advanced oxidation processes for removal of pharmaceutical residues: A critical review. *Sep. Purif. Technol., Environmental Nanotechnology and Sustainability in Water Treatment in honor of Professor Chin-Pao Huang*, Ph.D, Harvard University, Donald C. Philips, Professor Civil and Environmental Engineering, University of Delaware, USA 156, Part 3, 891–914. <https://doi.org/10.1016/j.seppur.2015.09.059>

- Ganrot, Z., Dave, G., Nilsson, E., 2007. Recovery of N and P from human urine by freezing, struvite precipitation and adsorption to zeolite and active carbon. *Bioresour. Technol.* 98, 3112–3121. <https://doi.org/10.1016/j.biortech.2006.10.038>
- Giannakis, S., Jovic, M., Gasilova, N., Pastor Gelabert, M., Schindelholz, S., Furbringer, J.-M., Girault, H., Pulgarin, C., 2017. Iohexol degradation in wastewater and urine by UV-based Advanced Oxidation Processes (AOPs): Process modeling and by-products identification. *J. Environ. Manage., Advanced Oxidation Processes for Environmental Remediation* 195, 174–185. <https://doi.org/10.1016/j.jenvman.2016.07.004>
- Greenlee, L.F., Lawler, D.F., Freeman, B.D., Marrot, B., Moulin, P., 2009. Reverse osmosis desalination: Water sources, technology, and today's challenges. *Water Res.* 43, 2317–2348. <https://doi.org/10.1016/j.watres.2009.03.010>
- Guillossou, R., Le Roux, J., Mailler, R., Vulliet, E., Morlay, C., Nauleau, F., Gasperi, J., Rocher, V., 2019. Organic micropollutants in a large wastewater treatment plant: What are the benefits of an advanced treatment by activated carbon adsorption in comparison to conventional treatment? *Chemosphere* 218, 1050–1060. <https://doi.org/10.1016/j.chemosphere.2018.11.182>
- Guo, W., Ngo, H.-H., Li, J., 2012. A mini-review on membrane fouling. *Bioresour. Technol., Membrane Bioreactors (MBRs): State-of-Art and Future* 122, 27–34. <https://doi.org/10.1016/j.biortech.2012.04.089>
- Haag, W.R., Hoigné, J., 1983. Ozonation of water containing chlorine or chloramines. Reaction products and kinetics. *Water Res.* 17, 1397–1402. [https://doi.org/10.1016/0043-1354\(83\)90270-1](https://doi.org/10.1016/0043-1354(83)90270-1)
- Hille, B., 1992. *Ionic channels of excitable membranes*, 2. ed. ed. Sinauer, Sunderland, Mass.
- Hoek, E.M.V., Allred, J., Knoell, T., Jeong, B.-H., 2008. Modeling the effects of fouling on full-scale reverse osmosis processes. *J. Membr. Sci.* 314, 33–49. <https://doi.org/10.1016/j.memsci.2008.01.025>
- Hoigné, J., Bader, H., 1983. Rate constants of reactions of ozone with organic and inorganic compounds in water—I. *Water Res.* 17, 173–183. [https://doi.org/10.1016/0043-1354\(83\)90098-2](https://doi.org/10.1016/0043-1354(83)90098-2)
- Hoigne, J., Bader, H., 1978. Ozonation of water: kinetics of oxidation of ammonia by ozone and hydroxyl radicals. *Environ. Sci. Technol.* 12, 79–84. <https://doi.org/10.1021/es60137a005>
- Hoigné, J., Bader, H., 1976. The role of hydroxyl radical reactions in ozonation processes in aqueous solutions. *Water Res.* 10, 377–386. [https://doi.org/10.1016/0043-1354\(76\)90055-5](https://doi.org/10.1016/0043-1354(76)90055-5)
- Hoigné, J., Bader, H., Haag, W.R., Staehelin, J., 1985. Rate constants of reactions of ozone with organic and inorganic compounds in water—III. Inorganic compounds and radicals. *Water Res.* 19, 993–1004. [https://doi.org/10.1016/0043-1354\(85\)90368-9](https://doi.org/10.1016/0043-1354(85)90368-9)
- Huang, H., Xiao, X., Yang, L., Yan, B., 2010. Removal of ammonia nitrogen from washing wastewater resulting from the process of rare-earth elements precipitation by the formation of struvite. *Desalination Water Treat.* 24, 85–92. <https://doi.org/10.5004/dwt.2010.1223>

- Huber, M.M., Canonica, S., Park, G.-Y., von Gunten, U., 2003. Oxidation of Pharmaceuticals during Ozonation and Advanced Oxidation Processes. *Environ. Sci. Technol.* 37, 1016–1024. <https://doi.org/10.1021/es025896h>
- Huber, M.M., Göbel, A., Joss, A., Hermann, N., Löffler, D., McArdell, C.S., Ried, A., Siegrist, H., Ternes, T.A., von Gunten, U., 2005. Oxidation of Pharmaceuticals during Ozonation of Municipal Wastewater Effluents: A Pilot Study. *Environ. Sci. Technol.* 39, 4290–4299. <https://doi.org/10.1021/es048396s>
- Hübner, U., Keller, S., Jekel, M., 2013. Evaluation of the prediction of trace organic compound removal during ozonation of secondary effluents using tracer substances and second order rate kinetics. *Water Res.* 47, 6467–6474. <https://doi.org/10.1016/j.watres.2013.08.025>
- Hurwitz, G., Hoek, E.M.V., Liu, K., Fan, L., Roddick, F.A., 2014. Photo-assisted electrochemical treatment of municipal wastewater reverse osmosis concentrate. *Chem. Eng. J.* 249, 180–188. <https://doi.org/10.1016/j.cej.2014.03.084>
- Huyskens, C., Brauns, E., Vanhoof, E., Dewever, H., 2008. A new method for the evaluation of the reversible and irreversible fouling propensity of MBR mixed liquor. *J. Membr. Sci.* 323, 185–192. <https://doi.org/10.1016/j.memsci.2008.06.021>
- Ikehata, K., Naghashkar, N.J., El-Din, M.G., 2006. Degradation of Aqueous Pharmaceuticals by Ozonation and Advanced Oxidation Processes: A Review. *Ozone Sci. Eng.* 28, 353–414. <https://doi.org/10.1080/01919510600985937>
- Illés, E., Szabó, E., Takács, E., Wojnárovits, L., Dombi, A., Gajda-Schranz, K., 2014. Ketoprofen removal by O₃ and O₃/UV processes: Kinetics, transformation products and ecotoxicity. *Sci. Total Environ.* 472, 178–184. <https://doi.org/10.1016/j.scitotenv.2013.10.119>
- Jacob, M., 2011. Réutilisation des eaux usées épurées par association de procédés biologiques et membranaires. Université de Toulouse - INSA, Toulouse, France.
- Jacob, M., Guigui, C., Cabassud, C., Darras, H., Lavison, G., Moulin, L., 2010. Performances of RO and NF processes for wastewater reuse: Tertiary treatment after a conventional activated sludge or a membrane bioreactor. *Desalination* 250, 833–839. <https://doi.org/10.1016/j.desal.2008.11.052>
- Jacob, M., Li, C., Guigui, C., Cabassud, C., Lavison, G., Moulin, L., 2012. Performance of NF/RO process for indirect potable reuse: interactions between micropollutants, micro-organisms and real MBR permeate. *Desalination Water Treat.* 46, 75–86. <https://doi.org/10.1080/19443994.2012.677507>
- Jamil, S., Jeong, S., Vigneswaran, S., 2016. Application of pressure assisted forward osmosis for water purification and reuse of reverse osmosis concentrate from a water reclamation plant. *Sep. Purif. Technol.* 171, 182–190. <https://doi.org/10.1016/j.seppur.2016.07.036>
- Javier Benitez, F., Acero, J.L., Real, F.J., Roldán, G., Rodríguez, E., 2015. Ozonation of benzotriazole and methyldole: Kinetic modeling, identification of intermediates and reaction mechanisms.

- J. Hazard. Mater., *Advances in Analysis, Treatment Technologies, and Environmental Fate of Emerging Contaminants* 282, 224–232. <https://doi.org/10.1016/j.jhazmat.2014.05.085>
- Javier Rivas, F., Sagasti, J., Encinas, A., Gimeno, O., 2011. Contaminants abatement by ozone in secondary effluents. Evaluation of second-order rate constants. *J. Chem. Technol. Biotechnol.* 86, 1058–1066. <https://doi.org/10.1002/jctb.2609>
- Jiang, S., Li, Y., Ladewig, B.P., 2017. A review of reverse osmosis membrane fouling and control strategies. *Sci. Total Environ.* 595, 567–583. <https://doi.org/10.1016/j.scitotenv.2017.03.235>
- Jiménez Cisneros, B.E., Asano, T. (Eds.), 2008. *Water reuse: an international survey of current practice, issues and needs*, Scientific and technical report. IWA Publishing, London.
- Johir, M.A.H., Vigneswaran, S., Kandasamy, J., BenAim, R., Grasmick, A., 2013. Effect of salt concentration on membrane bioreactor (MBR) performances: Detailed organic characterization. *Desalination* 322, 13–20. <https://doi.org/10.1016/j.desal.2013.04.025>
- Joo, S.H., Tansel, B., 2015. Novel technologies for reverse osmosis concentrate treatment: A review. *J. Environ. Manage.* 150, 322–335. <https://doi.org/10.1016/j.jenvman.2014.10.027>
- Joss, A., Baenninger, C., Foa, P., Koepke, S., Krauss, M., McArdell, C.S., Rottermann, K., Wei, Y., Zapata, A., Siegrist, H., 2011. Water reuse: >90% water yield in MBR/RO through concentrate recycling and CO₂ addition as scaling control. *Water Res.* 45, 6141–6151. <https://doi.org/10.1016/j.watres.2011.09.011>
- Justo, A., González, O., Aceña, J., Pérez, S., Barceló, D., Sans, C., Esplugas, S., 2013. Pharmaceuticals and organic pollution mitigation in reclamation osmosis brines by UV/H₂O₂ and ozone. *J. Hazard. Mater.* 263, 268–274. <https://doi.org/10.1016/j.jhazmat.2013.05.030>
- Justo, A., González, O., Sans, C., Esplugas, S., 2015. BAC filtration to mitigate micropollutants and EfOM content in reclamation reverse osmosis brines. *Chem. Eng. J.* 279, 589–596. <https://doi.org/10.1016/j.cej.2015.05.018>
- Kappel, C., Kemperman, A.J.B., Temmink, H., Zwijnenburg, A., Rijnaarts, H.H.M., Nijmeijer, K., 2014. Impacts of NF concentrate recirculation on membrane performance in an integrated MBR and NF membrane process for wastewater treatment. *J. Membr. Sci.* 453, 359–368. <https://doi.org/10.1016/j.memsci.2013.11.023>
- Karak, T., Bhattacharyya, P., 2011. Human urine as a source of alternative natural fertilizer in agriculture: A flight of fancy or an achievable reality. *Resour. Conserv. Recycl.* 55, 400–408. <https://doi.org/10.1016/j.resconrec.2010.12.008>
- Kasprzyk-Hordern, B., Dinsdale, R.M., Guwy, A.J., 2008. The occurrence of pharmaceuticals, personal care products, endocrine disruptors and illicit drugs in surface water in South Wales, UK. *Water Res.* 42, 3498–3518. <https://doi.org/10.1016/j.watres.2008.04.026>
- Kemacheevakul, P., Chuangchote, S., Otani, S., Matsuda, T., Shimizu, Y., 2015. Effect of magnesium dose on amount of pharmaceuticals in struvite recovered from urine. *Water Sci. Technol.* 72, 1102–1110. <https://doi.org/10.2166/wst.2015.313>

- Kim, S.D., Cho, J., Kim, I.S., Vanderford, B.J., Snyder, S.A., 2007. Occurrence and removal of pharmaceuticals and endocrine disruptors in South Korean surface, drinking, and waste waters. *Water Res.* 41, 1013–1021. <https://doi.org/10.1016/j.watres.2006.06.034>
- Kimura, K., Hane, Y., Watanabe, Y., Amy, G., Ohkuma, N., 2004. Irreversible membrane fouling during ultrafiltration of surface water. *Water Res.* 38, 3431–3441. <https://doi.org/10.1016/j.watres.2004.05.007>
- Kimura, K., Hara, H., Watanabe, Y., 2005. Removal of pharmaceutical compounds by submerged membrane bioreactors (MBRs). *Desalination* 178, 135–140. <https://doi.org/10.1016/j.desal.2004.11.033>
- Kimura, K., Okazaki, S., Ohashi, T., Watanabe, Y., 2016. Importance of the co-presence of silica and organic matter in membrane fouling for RO filtering MBR effluent. *J. Membr. Sci.* 501, 60–67. <https://doi.org/10.1016/j.memsci.2015.12.016>
- Kirchmann, H., Pettersson, S., 1994. Human urine - Chemical composition and fertilizer use efficiency. *Fertil. Res.* 40, 149–154. <https://doi.org/10.1007/BF00750100>
- Knopp, G., Prasse, C., Ternes, T.A., Cornel, P., 2016. Elimination of micropollutants and transformation products from a wastewater treatment plant effluent through pilot scale ozonation followed by various activated carbon and biological filters. *Water Res.* 100, 580–592. <https://doi.org/10.1016/j.watres.2016.04.069>
- Kołodziejaska, M., Maszkowska, J., Białk-Bielińska, A., Steudte, S., Kumirska, J., Stepnowski, P., Stolte, S., 2013. Aquatic toxicity of four veterinary drugs commonly applied in fish farming and animal husbandry. *Chemosphere* 92, 1253–1259. <https://doi.org/10.1016/j.chemosphere.2013.04.057>
- Koros, W.J., Ma, Y.H., Shimidzu, T., 1996. Terminology for membranes and membrane processes (IUPAC Recommendations 1996). *Pure Appl. Chem.* 68, 1479–1489. <https://doi.org/10.1351/pac199668071479>
- Kumar, R., Pal, P., 2013. Turning hazardous waste into value-added products: production and characterization of struvite from ammoniacal waste with new approaches. *J. Clean. Prod.* 43, 59–70. <https://doi.org/10.1016/j.jclepro.2013.01.001>
- Kwon, G., Kang, J., Nam, J.-H., Kim, Y.-O., Jahng, D., 2018. Recovery of ammonia through struvite production using anaerobic digestate of piggery wastewater and leachate of sewage sludge ash. *Environ. Technol.* 39, 831–842. <https://doi.org/10.1080/09593330.2017.1312550>
- Landry, K.A., Boyer, T.H., 2016. Life cycle assessment and costing of urine source separation: Focus on nonsteroidal anti-inflammatory drug removal. *Water Res.* 105, 487–495. <https://doi.org/10.1016/j.watres.2016.09.024>
- Larsen, T.A., Gujer, W., 1996. Separate management of anthropogenic nutrient solutions (human urine). *Water Sci. Technol.* 34. [https://doi.org/10.1016/0273-1223\(96\)00560-4](https://doi.org/10.1016/0273-1223(96)00560-4)

- Larsen, T.A., Lienert, J., Joss, A., Siegrist, H., 2004. How to avoid pharmaceuticals in the aquatic environment. *J. Biotechnol., Highlights from the ECB11: Building Bridges between Biosciences and Bioengineering* 113, 295–304. <https://doi.org/10.1016/j.jbiotec.2004.03.033>
- Le Corre, K.S., Valsami-Jones, E., Hobbs, P., Parsons, S.A., 2005. Impact of calcium on struvite crystal size, shape and purity. *J. Cryst. Growth* 283, 514–522. <https://doi.org/10.1016/j.jcrysgro.2005.06.012>
- Lee, C.O., Howe, K.J., Thomson, B.M., 2012. Ozone and biofiltration as an alternative to reverse osmosis for removing PPCPs and micropollutants from treated wastewater. *Water Res.* 46, 1005–1014. <https://doi.org/10.1016/j.watres.2011.11.069>
- Lee, L.Y., Ng, H.Y., Ong, S.L., Hu, J.Y., Tao, G., Kekre, K., Viswanath, B., Lay, W., Seah, H., 2009. Ozone-biological activated carbon as a pretreatment process for reverse osmosis brine treatment and recovery. *Water Res., AOPs for Effluent Treatment* 43, 3948–3955. <https://doi.org/10.1016/j.watres.2009.06.016>
- Lee, S., Ang, W.S., Elimelech, M., 2006. Fouling of reverse osmosis membranes by hydrophilic organic matter: implications for water reuse. *Desalination, Integrated Concepts in Water Recycling* 187, 313–321. <https://doi.org/10.1016/j.desal.2005.04.090>
- Lee, Y., Gerrity, D., Lee, M., Bogeat, A.E., Salhi, E., Gamage, S., Trenholm, R.A., Wert, E.C., Snyder, S.A., von Gunten, U., 2013. Prediction of Micropollutant Elimination during Ozonation of Municipal Wastewater Effluents: Use of Kinetic and Water Specific Information. *Environ. Sci. Technol.* 47, 5872–5881. <https://doi.org/10.1021/es400781r>
- Lee, Y., Gunten, U. von, 2016. Advances in predicting organic contaminant abatement during ozonation of municipal wastewater effluent: reaction kinetics, transformation products, and changes of biological effects. *Environ. Sci. Water Res. Technol.* 2, 421–442. <https://doi.org/10.1039/C6EW00025H>
- Lee, Y., Kovalova, L., McArdell, C.S., von Gunten, U., 2014. Prediction of micropollutant elimination during ozonation of a hospital wastewater effluent. *Water Res.* 64, 134–148. <https://doi.org/10.1016/j.watres.2014.06.027>
- Levenspiel, O., 1999. *Chemical reaction engineering*, 3rd ed. Wiley, Hoboken, NJ.
- Li, C., 2014. Study of the effects of pharmaceutical micropollutants on the fouling of MBR used for municipal wastewater treatment : case of carbamazepine.
- Li, H., Xia, H., Mei, Y., 2016. Modeling organic fouling of reverse osmosis membrane: From adsorption to fouling layer formation. *Desalination* 386, 25–31. <https://doi.org/10.1016/j.desal.2016.02.037>
- Li, K., Cheng, Y., Wang, J., Zhang, J., Liu, J., Yu, D., Li, M., Wei, Y., 2016. Effects of returning NF concentrate on the MBR-NF process treating antibiotic production wastewater. *Environ. Sci. Pollut. Res.* 23, 13114–13127. <https://doi.org/10.1007/s11356-016-6467-x>

- Lide, D.R., 2005. CRC Handbook of Chemistry and Physics, Internet Version 2005. CRC Press, Boca Raton, FL.
- Lienert, J., Bürki, T., Escher, B.I., 2007. Reducing micropollutants with source control: substance flow analysis of 212 pharmaceuticals in faeces and urine. *Water Sci. Technol. J. Int. Assoc. Water Pollut. Res.* 56, 87–96. <https://doi.org/10.2166/wst.2007.560>
- Liu, K., Roddick, F.A., Fan, L., 2012. Impact of salinity and pH on the UVC/H₂O₂ treatment of reverse osmosis concentrate produced from municipal wastewater reclamation. *Water Res.* 46, 3229–3239. <https://doi.org/10.1016/j.watres.2012.03.024>
- Liu, P., Zhang, H., Feng, Y., Yang, F., Zhang, J., 2014. Removal of trace antibiotics from wastewater: A systematic study of nanofiltration combined with ozone-based advanced oxidation processes. *Chem. Eng. J.* 240, 211–220. <https://doi.org/10.1016/j.cej.2013.11.057>
- López-López, A., Pic, J.-S., Benbelkacem, H., Debellefontaine, H., 2007. Influence of t-butanol and of pH on hydrodynamic and mass transfer parameters in an ozonation process. *Chem. Eng. Process. Process Intensif.* 46, 649–655. <https://doi.org/10.1016/j.cep.2006.08.010>
- Lu, J., Fan, L., Roddick, F.A., 2013. Potential of BAC combined with UVC/H₂O₂ for reducing organic matter from highly saline reverse osmosis concentrate produced from municipal wastewater reclamation. *Chemosphere* 93, 683–688. <https://doi.org/10.1016/j.chemosphere.2013.06.008>
- Lu, Y., Li, M., 2016. Simultaneous Rapid Determination of the Solubility and Diffusion Coefficients of a Poorly Water-Soluble Drug Based on a Novel UV Imaging System. *J. Pharm. Sci.* 105, 131–138. <https://doi.org/10.1016/j.xphs.2015.11.021>
- Luo, H., Li, H., Lu, Y., Liu, G., Zhang, R., 2017. Treatment of reverse osmosis concentrate using microbial electrolysis desalination and chemical production cell. *Desalination* 408, 52–59. <https://doi.org/10.1016/j.desal.2017.01.003>
- Luo, W., Phan, H.V., Xie, M., Hai, F.I., Price, W.E., Elimelech, M., Nghiem, L.D., 2017. Osmotic versus conventional membrane bioreactors integrated with reverse osmosis for water reuse: Biological stability, membrane fouling, and contaminant removal. *Water Res.* 109, 122–134. <https://doi.org/10.1016/j.watres.2016.11.036>
- Luo, Y., Guo, W., Ngo, H.H., Nghiem, L.D., Hai, F.I., Zhang, J., Liang, S., Wang, X.C., 2014. A review on the occurrence of micropollutants in the aquatic environment and their fate and removal during wastewater treatment. *Sci. Total Environ.* 473–474, 619–641. <https://doi.org/10.1016/j.scitotenv.2013.12.065>
- Malaeb, L., Ayoub, G.M., 2011. Reverse osmosis technology for water treatment: State of the art review. *Desalination* 267, 1–8. <https://doi.org/10.1016/j.desal.2010.09.001>
- Mamo, J., García-Galán, M.J., Stefani, M., Rodríguez-Mozaz, S., Barceló, D., Monclús, H., Rodríguez-Roda, I., Comas, J., 2018. Fate of pharmaceuticals and their transformation products in integrated membrane systems for wastewater reclamation. *Chem. Eng. J.* 331, 450–461. <https://doi.org/10.1016/j.cej.2017.08.050>

- Marce, M., Domenjoud, B., Esplugas, S., Baig, S., 2016. Ozonation treatment of urban primary and biotreated wastewaters: Impacts and modeling. *Chem. Eng. J.* 283, 768–777. <https://doi.org/10.1016/j.cej.2015.07.073>
- Márquez, G., Rodríguez, E.M., Beltrán, F.J., Álvarez, P.M., 2013. Determination of Rate Constants for Ozonation of Ofloxacin in Aqueous Solution. *Ozone Sci. Eng.* 35, 186–195. <https://doi.org/10.1080/01919512.2013.771530>
- Maurer, M., Pronk, W., Larsen, T.A., 2006. Treatment processes for source-separated urine. *Water Res.* 40, 3151–3166. <https://doi.org/10.1016/j.watres.2006.07.012>
- McDowell, D.C., Huber, M.M., Wagner, M., von Gunten, U., Ternes, T.A., 2005. Ozonation of Carbamazepine in Drinking Water: Identification and Kinetic Study of Major Oxidation Products. *Environ. Sci. Technol.* 39, 8014–8022. <https://doi.org/10.1021/es050043l>
- Merle, T., 2009. Couplage des procédés d'adsorption et d'ozonation pour l'élimination de molécules bio-récalcitrantes. Université de Toulouse-INSA, Toulouse.
- Miralles-Cuevas, S., Oller, I., Agüera, A., Llorca, M., Sánchez Pérez, J.A., Malato, S., 2017. Combination of nanofiltration and ozonation for the remediation of real municipal wastewater effluents: Acute and chronic toxicity assessment. *J. Hazard. Mater.* 323, 442–451. <https://doi.org/10.1016/j.jhazmat.2016.03.013>
- Moffat, A.C., Osselton, M.D., Widdop, B., Watts, J. (Eds.), 2011. Clarke's analysis of drugs and poisons: in pharmaceuticals, body fluids and postmortem material, Fourth edition. ed. Pharmaceutical Press, London ; Chicago.
- Moreno, J., Monclús, H., Stefani, M., Cortada, E., Aumatell, J., Adroer, N., De Lamo-Castellví, S., Comas, J., 2013. Characterisation of RO fouling in an integrated MBR/RO system for wastewater reuse. *Water Sci. Technol.* 67, 780–788. <https://doi.org/10.2166/wst.2012.619>
- Nebout, P., Chedeville, O., Delpoux, S., Di Giusto, A., 2015. Removal of pharmaceuticals from water by the ozone/activated carbon coupling. Presented at the IOA world congress, Barcelona, Spain.
- Nikolaou, A., Méric, S., Fatta, D., 2007. Occurrence patterns of pharmaceuticals in water and wastewater environments. *Anal. Bioanal. Chem.* 387, 1225–1234. <https://doi.org/10.1007/s00216-006-1035-8>
- Nikolova, J.D., Islam, M.A., 1998. Contribution of adsorbed layer resistance to the flux-decline in an ultrafiltration process. *J. Membr. Sci.* 146, 105–111. [https://doi.org/10.1016/S0376-7388\(98\)00086-6](https://doi.org/10.1016/S0376-7388(98)00086-6)
- Nilsson, M., Trägårdh, G., Östergren, K., 2008. The influence of pH, salt and temperature on nanofiltration performance. *J. Membr. Sci.* 312, 97–106. <https://doi.org/10.1016/j.memsci.2007.12.059>
- Nöthe, T., Fahlenkamp, H., Sonntag, C. von, 2009. Ozonation of Wastewater: Rate of Ozone Consumption and Hydroxyl Radical Yield. *Environ. Sci. Technol.* 43, 5990–5995. <https://doi.org/10.1021/es900825f>

- Olson, B.J.S.C., Markwell, J., 2007. Assays for Determination of Protein Concentration, in: Coligan, J.E., Dunn, B.M., Speicher, D.W., Wingfield, P.T. (Eds.), *Current Protocols in Protein Science*. John Wiley & Sons, Inc., Hoboken, NJ, USA, pp. 3.4.1-3.4.29. <https://doi.org/10.1002/0471140864.ps0304s48>
- O'Neal, J.A., Boyer, T.H., 2013. Phosphate recovery using hybrid anion exchange: Applications to source-separated urine and combined wastewater streams. *Water Res.* 47, 5003–5017. <https://doi.org/10.1016/j.watres.2013.05.037>
- Pabby, A.K. (Ed.), 2015. *Handbook of membrane separations: chemical, pharmaceutical, food and biotechnology applications*, 2. ed. ed. CRC Press, Boca Raton, Fla.
- Papageorgiou, A., Stylianou, S.K., Kaffes, P., Zouboulis, A.I., Voutsas, D., 2017. Effects of ozonation pretreatment on natural organic matter and wastewater derived organic matter – Possible implications on the formation of ozonation by-products. *Chemosphere Complete*, 33–40. <https://doi.org/10.1016/j.chemosphere.2016.12.005>
- Parkhurst, D.L., Appelo, C.A.J., 1999. User's guide to PHREEQC (Version 2) : a computer program for speciation, batch-reaction, one-dimensional transport, and inverse geochemical calculations (USGS Numbered Series No. 99–4259), *Water-Resources Investigations Report*. U.S. Geological Survey : Earth Science Information Center, Open-File Reports Section [distributor],.
- Peldszus, S., Hallé, C., Peiris, R.H., Hamouda, M., Jin, X., Legge, R.L., Budman, H., Moresoli, C., Huck, P.M., 2011. Reversible and irreversible low-pressure membrane foulants in drinking water treatment: Identification by principal component analysis of fluorescence EEM and mitigation by biofiltration pretreatment. *Water Res.* 45, 5161–5170. <https://doi.org/10.1016/j.watres.2011.07.022>
- Pérez, G., Fernández-Alba, A.R., Urriaga, A.M., Ortiz, I., 2010. Electro-oxidation of reverse osmosis concentrates generated in tertiary water treatment. *Water Res.* 44, 2763–2772. <https://doi.org/10.1016/j.watres.2010.02.017>
- Pérez-González, A., Urriaga, A.M., Ibáñez, R., Ortiz, I., 2012. State of the art and review on the treatment technologies of water reverse osmosis concentrates. *Water Res.* 46, 267–283. <https://doi.org/10.1016/j.watres.2011.10.046>
- Pinto, O.A., Tabaković, A., Goff, T.M., Liu, Y., Adair, J.H., 2011. Calcium Phosphate and Calcium Phosphosilicate Mediated Drug Delivery and Imaging, in: Prokop, A. (Ed.), *Intracellular Delivery*. Springer Netherlands, Dordrecht, pp. 713–744. https://doi.org/10.1007/978-94-007-1248-5_23
- Pocostales, J.P., Sein, M.M., Knolle, W., von Sonntag, C., Schmidt, T.C., 2010. Degradation of Ozone-Refractory Organic Phosphates in Wastewater by Ozone and Ozone/Hydrogen Peroxide (Peroxone): The Role of Ozone Consumption by Dissolved Organic Matter. *Environ. Sci. Technol.* 44, 8248–8253. <https://doi.org/10.1021/es1018288>

- Pradhan, S., Fan, L., Roddick, F.A., 2015. Removing organic and nitrogen content from a highly saline municipal wastewater reverse osmosis concentrate by UV/H₂O₂–BAC treatment. *Chemosphere* 136, 198–203. <https://doi.org/10.1016/j.chemosphere.2015.05.028>
- Pradhan, S., Fan, L., Roddick, F.A., Shahsavari, E., Ball, A.S., 2016. Impact of salinity on organic matter and nitrogen removal from a municipal wastewater RO concentrate using biologically activated carbon coupled with UV/H₂O₂. *Water Res.* 94, 103–110. <https://doi.org/10.1016/j.watres.2016.02.046>
- Prasse, C., Wagner, M., Schulz, R., Ternes, T.A., 2012. Oxidation of the Antiviral Drug Acyclovir and Its Biodegradation Product Carboxy-acyclovir with Ozone: Kinetics and Identification of Oxidation Products. *Environ. Sci. Technol.* 46, 2169–2178. <https://doi.org/10.1021/es203712z>
- Pronk, W., Koné, D., 2009. Options for urine treatment in developing countries. *Desalination* 248, 360–368. <https://doi.org/10.1016/j.desal.2008.05.076>
- Pronk, W., Palmquist, H., Biebow, M., Boller, M., 2006. Nanofiltration for the separation of pharmaceuticals from nutrients in source-separated urine. *Water Res.* 40, 1405–1412. <https://doi.org/10.1016/j.watres.2006.01.038>
- Pronk, W., Zuleeg, S., Lienert, J., Escher, B., Koller, M., Berner, A., Koch, G., Boller, M., 2007. Pilot experiments with electrodialysis and ozonation for the production of a fertiliser from urine. *Water Sci. Technol. J. Int. Assoc. Water Pollut. Res.* 56, 219–227. <https://doi.org/10.2166/wst.2007.575>
- Prywer, J., Torzewska, A., Płociński, T., 2012. Unique surface and internal structure of struvite crystals formed by *Proteus mirabilis*. *Urol. Res.* 40, 699–707. <https://doi.org/10.1007/s00240-012-0501-3>
- Quay, A.N., Tong, T., Hashmi, S.M., Zhou, Y., Zhao, S., Elimelech, M., 2018. Combined Organic Fouling and Inorganic Scaling in Reverse Osmosis: Role of Protein–Silica Interactions. *Environ. Sci. Technol.* 52, 9145–9153. <https://doi.org/10.1021/acs.est.8b02194>
- Radjenovic, J., Bagastyo, A., Rozendal, R.A., Mu, Y., Keller, J., Rabaey, K., 2011. Electrochemical oxidation of trace organic contaminants in reverse osmosis concentrate using RuO₂/IrO₂-coated titanium anodes. *Water Res.* 45, 1579–1586. <https://doi.org/10.1016/j.watres.2010.11.035>
- Radjenović, J., Petrović, M., Ventura, F., Barceló, D., 2008. Rejection of pharmaceuticals in nanofiltration and reverse osmosis membrane drinking water treatment. *Water Res.* 42, 3601–3610. <https://doi.org/10.1016/j.watres.2008.05.020>
- Rautenbach, R., Mellis, R., 1994. Waste water treatment by a combination of bioreactor and nanofiltration. *Desalination* 95, 171–188. [https://doi.org/10.1016/0011-9164\(94\)00012-3](https://doi.org/10.1016/0011-9164(94)00012-3)
- Real, F.J., Benitez, F.J., Acero, J.L., Sagasti, J.J.P., Casas, F., 2009a. Kinetics of the Chemical Oxidation of the Pharmaceuticals Primidone, Ketoprofen, and Diatrizoate in Ultrapure and Natural Waters. *Ind. Eng. Chem. Res.* 48, 3380–3388. <https://doi.org/10.1021/ie801762p>

- Real, F.J., Benitez, F.J., Acero, J.L., Sagasti, J.J.P., Casas, F., 2009b. Kinetics of the Chemical Oxidation of the Pharmaceuticals Primidone, Ketoprofen, and Diatrizoate in Ultrapure and Natural Waters. *Ind. Eng. Chem. Res.* 48, 3380–3388. <https://doi.org/10.1021/ie801762p>
- Reid, E., Liu, X., Judd, S.J., 2006. Effect of high salinity on activated sludge characteristics and membrane permeability in an immersed membrane bioreactor. *J. Membr. Sci.* 283, 164–171. <https://doi.org/10.1016/j.memsci.2006.06.021>
- Rischbieter, E., Stein, H., Schumpe, A., 2000. Ozone Solubilities in Water and Aqueous Salt Solutions. *J. Chem. Eng. Data* 45, 338–340. <https://doi.org/10.1021/je990263c>
- Ronteltap, M., Biebow, M., Maurer, M., Gujer, W., 2003. Thermodynamics of struvite precipitation in source separated urine. Presented at the Second interational symposium on ecological sanitation, IWA, Baltic Sea, Germany, pp. 463–470.
- Ronteltap, M., Maurer, M., Gujer, W., 2007. The behaviour of pharmaceuticals and heavy metals during struvite precipitation in urine. *Water Res.* 41, 1859–1868. <https://doi.org/10.1016/j.watres.2007.01.026>
- Ronteltap, M., Maurer, M., Hausherr, R., Gujer, W., 2010. Struvite precipitation from urine – Influencing factors on particle size. *Water Res.* 44, 2038–2046. <https://doi.org/10.1016/j.watres.2009.12.015>
- Rosal, R., Rodríguez, A., Perdigón-Melón, J.A., Petre, A., García-Calvo, E., Gómez, M.J., Agüera, A., Fernández-Alba, A.R., 2009. Degradation of caffeine and identification of the transformation products generated by ozonation. *Chemosphere* 74, 825–831. <https://doi.org/10.1016/j.chemosphere.2008.10.010>
- Sablani, S., Goosen, M., Al-Belushi, R., Wilf, M., 2001. Concentration polarization in ultrafiltration and reverse osmosis: a critical review. *Desalination* 141, 269–289. [https://doi.org/10.1016/S0011-9164\(01\)85005-0](https://doi.org/10.1016/S0011-9164(01)85005-0)
- Sadrnourmohamadi, M., Gorczyca, B., 2015. Effects of ozone as a stand-alone and coagulation-aid treatment on the reduction of trihalomethanes precursors from high DOC and hardness water. *Water Res.* 73, 171–180. <https://doi.org/10.1016/j.watres.2015.01.023>
- Sahar, E., David, I., Gelman, Y., Chikurel, H., Aharoni, A., Messalem, R., Brenner, A., 2011. The use of RO to remove emerging micropollutants following CAS/UF or MBR treatment of municipal wastewater. *Desalination*, Special issue to mark the 45th Anniversary of launching *Desalination* journal and to honour Professor David Hasson for his enormous support and contribution to *Desalination* 273, 142–147. <https://doi.org/10.1016/j.desal.2010.11.004>
- Schäfer, A.I. (Ed.), 2006. *Nanofiltration - principles and applications*, Reprint. ed. Elsevier, Oxford.
- Shanmuganathan, S., Loganathan, P., Kazner, C., Johir, M.A.H., Vigneswaran, S., 2017. Submerged membrane filtration adsorption hybrid system for the removal of organic micropollutants from a water reclamation plant reverse osmosis concentrate. *Desalination*, 50th anniversary of *Desalination* 401, 134–141. <https://doi.org/10.1016/j.desal.2016.07.048>

- She, Q., Wang, R., Fane, A.G., Tang, C.Y., 2016. Membrane fouling in osmotically driven membrane processes: A review. *J. Membr. Sci.* 499, 201–233. <https://doi.org/10.1016/j.memsci.2015.10.040>
- Silva, B.F. da, Jelic, A., López-Serna, R., Mozeto, A.A., Petrovic, M., Barceló, D., 2011. Occurrence and distribution of pharmaceuticals in surface water, suspended solids and sediments of the Ebro river basin, Spain. *Chemosphere* 85, 1331–1339. <https://doi.org/10.1016/j.chemosphere.2011.07.051>
- Singh, S., Seth, R., Tabe, S., Yang, P., 2015. Oxidation of Emerging Contaminants during Pilot-Scale Ozonation of Secondary Treated Municipal Effluent. *Ozone Sci. Eng.* 37, 323–329. <https://doi.org/10.1080/01919512.2014.998755>
- Solley, D., Gronow, C., Tait, S., Bates, J., Buchanan, A., 2010. Managing the reverse osmosis concentrate from the Western Corridor Recycled Water Scheme. *Water Pract. Technol.* 5, wpt2010018. <https://doi.org/10.2166/wpt.2010.018>
- Sonntag, C. von, Gunten, U. von, 2012. *Chemistry of Ozone in Water and Wastewater Treatment*. IWA Publishing.
- Suarez, S., Dodd, M.C., Omil, F., von Gunten, U., 2007. Kinetics of triclosan oxidation by aqueous ozone and consequent loss of antibacterial activity: Relevance to municipal wastewater ozonation. *Water Res.* 41, 2481–2490. <https://doi.org/10.1016/j.watres.2007.02.049>
- Sui, Q., Gebhardt, W., Schröder, H.F., Zhao, W., Lu, S., Yu, G., 2017. Identification of New Oxidation Products of Bezafibrate for Better Understanding of Its Toxicity Evolution and Oxidation Mechanisms during Ozonation. *Environ. Sci. Technol.* 51, 2262–2270. <https://doi.org/10.1021/acs.est.6b03548>
- Sun, C., Leiknes, T., Weitzenböck, J., Thorstensen, B., 2010. Salinity effect on a biofilm-MBR process for shipboard wastewater treatment. *Sep. Purif. Technol.* 72, 380–387. <https://doi.org/10.1016/j.seppur.2010.03.010>
- Taheran, M., Brar, S.K., Verma, M., Surampalli, R.Y., Zhang, T.C., Valero, J.R., 2016. Membrane processes for removal of pharmaceutically active compounds (PhACs) from water and wastewaters. *Sci. Total Environ.* 547, 60–77. <https://doi.org/10.1016/j.scitotenv.2015.12.139>
- Tang, F., Hu, H.-Y., Sun, L.-J., Wu, Q.-Y., Jiang, Y.-M., Guan, Y.-T., Huang, J.-J., 2014. Fouling of reverse osmosis membrane for municipal wastewater reclamation: Autopsy results from a full-scale plant. *Desalination* 349, 73–79. <https://doi.org/10.1016/j.desal.2014.06.018>
- Tang, F., Hu, H.-Y., Wu, Q.-Y., Tang, X., Sun, Y.-X., Shi, X.-L., Huang, J.-J., 2013. Effects of chemical agent injections on genotoxicity of wastewater in a microfiltration-reverse osmosis membrane process for wastewater reuse. *J. Hazard. Mater.* 260, 231–237. <https://doi.org/10.1016/j.jhazmat.2013.05.035>

- Tansel, B., 2012. Significance of thermodynamic and physical characteristics on permeation of ions during membrane separation: Hydrated radius, hydration free energy and viscous effects. *Sep. Purif. Technol.* 86, 119–126. <https://doi.org/10.1016/j.seppur.2011.10.033>
- Tay, K.S., Madehi, N., 2015. Ozonation of ofloxacin in water: by-products, degradation pathway and ecotoxicity assessment. *Sci. Total Environ.* 520, 23–31. <https://doi.org/10.1016/j.scitotenv.2015.03.033>
- Tettenborn, F., Behrendt, J., Otterpohl, R., 2007. Resource recovery and removal of pharmaceutical residues Treatment of separate collected urine. Hamburg University of Technology.
- Tiraferri, A., 2014. Membrane-based water treatment to increase water supply.
- Tizaoui, C., Grima, N., 2011. Kinetics of the ozone oxidation of Reactive Orange 16 azo-dye in aqueous solution. *Chem. Eng. J.* 173, 463–473. <https://doi.org/10.1016/j.cej.2011.08.014>
- Treguer, R., Tatin, R., Couvert, A., Wolbert, D., Tazi-Pain, A., 2010. Ozonation effect on natural organic matter adsorption and biodegradation – Application to a membrane bioreactor containing activated carbon for drinking water production. *Water Res.* 44, 781–788. <https://doi.org/10.1016/j.watres.2009.10.023>
- Triger, A., 2012. Procédé hybride cristallisation et séparation membranaire pour le traitement d'un fluide complexe (urine). Toulouse, INSA.
- Triger, A., Pic, J.-S., Cabassud, C., 2012. Determination of struvite crystallization mechanisms in urine using turbidity measurement. *Water Res.* 46, 6084–6094. <https://doi.org/10.1016/j.watres.2012.08.030>
- Udert, K.M., Wächter, M., 2012. Complete nutrient recovery from source-separated urine by nitrification and distillation. *Water Res.* 46, 453–464. <https://doi.org/10.1016/j.watres.2011.11.020>
- Umar, M., Roddick, F., Fan, L., 2016a. Comparison of coagulation efficiency of aluminium and ferric-based coagulants as pre-treatment for UVC/H₂O₂ treatment of wastewater RO concentrate. *Chem. Eng. J.* 284, 841–849. <https://doi.org/10.1016/j.cej.2015.08.109>
- Umar, M., Roddick, F., Fan, L., 2016b. Impact of coagulation as a pre-treatment for UVC/H₂O₂-biological activated carbon treatment of a municipal wastewater reverse osmosis concentrate. *Water Res.* 88, 12–19. <https://doi.org/10.1016/j.watres.2015.09.047>
- Umar, M., Roddick, F., Fan, L., 2014. Effect of coagulation on treatment of municipal wastewater reverse osmosis concentrate by UVC/H₂O₂. *J. Hazard. Mater.* 266, 10–18. <https://doi.org/10.1016/j.jhazmat.2013.12.005>
- Umar, M., Roddick, F.A., Fan, L., Autin, O., Jefferson, B., 2015. Treatment of municipal wastewater reverse osmosis concentrate using UVC-LED/H₂O₂ with and without coagulation pre-treatment. *Chem. Eng. J.* 260, 649–656. <https://doi.org/10.1016/j.cej.2014.09.028>

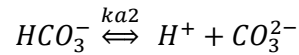
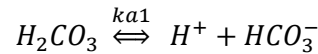
- Urfer, D., Von Cuntzen, U., Revelly, P., Courbat, R., Ramseier, S., Jordan, R., Kaiser, H.-P., Walther, J.-L., Gaille, P., Stettler, R., 2001. Utilisation de l'ozone pour le traitement des eaux potables en Suisse. 3e partie. : Étude de cas spécifiques. *GWA* 81, 29–41.
- Urriaga, A.M., Pérez, G., Ibáñez, R., Ortiz, I., 2013. Removal of pharmaceuticals from a WWTP secondary effluent by ultrafiltration/reverse osmosis followed by electrochemical oxidation of the RO concentrate. *Desalination* 331, 26–34. <https://doi.org/10.1016/j.desal.2013.10.010>
- Van der Bruggen, B., Lejon, L., Vandecasteele, C., 2003. Reuse, Treatment, and Discharge of the Concentrate of Pressure-Driven Membrane Processes. *Environ. Sci. Technol.* 37, 3733–3738. <https://doi.org/10.1021/es0201754>
- von Gunten, U., 2003. Ozonation of drinking water: Part I. Oxidation kinetics and product formation. *Water Res.* 37, 1443–1467. [https://doi.org/10.1016/S0043-1354\(02\)00457-8](https://doi.org/10.1016/S0043-1354(02)00457-8)
- Vu, T.T.N., 2017. Impacts of reverse osmosis concentrate recirculation on MBR performances in the field of wastewater reuse.
- Vu, T.T.N., Montaner, M., Guigui, C., 2017. Recycling of Reverse Osmosis Concentrates to the Membrane Bioreactor in the MBR-RO Process for Water Reuse: effect on mbr performances. *J. Water Sci.* 30, 1. <https://doi.org/10.7202/1040057ar>
- Wang, J., Li, K., Wei, Y., Cheng, Y., Wei, D., Li, M., 2015. Performance and fate of organics in a pilot MBR–NF for treating antibiotic production wastewater with recycling NF concentrate. *Chemosphere* 121, 92–100. <https://doi.org/10.1016/j.chemosphere.2014.11.034>
- Wang, J., Wei, Y., Li, K., Cheng, Y., Li, M., Xu, J., 2014. Fate of organic pollutants in a pilot-scale membrane bioreactor-nanofiltration membrane system at high water yield in antibiotic wastewater treatment. *Water Sci. Technol.* 69, 876–881. <https://doi.org/10.2166/wst.2013.789>
- Weng, M., Pei, J., 2016. Electrochemical oxidation of reverse osmosis concentrate using a novel electrode: Parameter optimization and kinetics study. *Desalination* 399, 21–28. <https://doi.org/10.1016/j.desal.2016.08.002>
- Wilsenach, J.A., Schuurbijs, C.A.H., van Loosdrecht, M.C.M., 2007. Phosphate and potassium recovery from source separated urine through struvite precipitation. *Water Res.* 41, 458–466. <https://doi.org/10.1016/j.watres.2006.10.014>
- Wintgens, T., Melin, T., Schäfer, A., Khan, S., Muston, M., Bixio, D., Thoeue, C., 2005. The role of membrane processes in municipal wastewater reclamation and reuse. *Desalination* 178, 1–11. <https://doi.org/10.1016/j.desal.2004.12.014>
- Wu, B., Kitade, T., Chong, T.H., Uemura, T., Fane, A.G., 2013. Impact of membrane bioreactor operating conditions on fouling behavior of reverse osmosis membranes in MBR–RO processes. *Desalination* 311, 37–45. <https://doi.org/10.1016/j.desal.2012.11.020>
- Xu, P., Drewes, J.E., Bellona, C., Amy, G., Kim, T.-U., Adam, M., Heberer, T., 2005. Rejection of Emerging Organic Micropollutants in Nanofiltration–Reverse Osmosis Membrane Applications. *Water Environ. Res.* 77, 40–48. <https://doi.org/10.2175/106143005X41609>

- Yang, Y., Pignatello, J.J., Ma, J., Mitch, W.A., 2016. Effect of matrix components on UV/H₂O₂ and UV/S₂O₈²⁻ advanced oxidation processes for trace organic degradation in reverse osmosis brines from municipal wastewater reuse facilities. *Water Res.* 89, 192–200. <https://doi.org/10.1016/j.watres.2015.11.049>
- Yu, T., Sun, H., Chen, Z., Wang, Y.-H., Huo, Z.-Y., Ikuno, N., Ishii, K., Jin, Y., Hu, H.-Y., Wu, Y.-H., Lu, Y., 2018. Different bacterial species and their extracellular polymeric substances (EPSs) significantly affected reverse osmosis (RO) membrane fouling potentials in wastewater reclamation. *Sci. Total Environ.* 644, 486–493. <https://doi.org/10.1016/j.scitotenv.2018.06.286>
- Yu, Y., Wu, L., Chang, A.C., 2013. Seasonal variation of endocrine disrupting compounds, pharmaceuticals and personal care products in wastewater treatment plants. *Sci. Total Environ.* 442, 310–316. <https://doi.org/10.1016/j.scitotenv.2012.10.001>
- Zeng, Y., Lin, X., Li, F., Chen, P., Kong, Q., Liu, G., Lv, W., 2018. Ozonation of ketoprofen with nitrate in aquatic environments: kinetics, pathways, and toxicity. *RSC Adv.* 8, 10541–10548. <https://doi.org/10.1039/C7RA12894K>
- Zhang, R., Sun, P., Boyer, T.H., Zhao, L., Huang, C.-H., 2015. Degradation of Pharmaceuticals and Metabolite in Synthetic Human Urine by UV, UV/H₂O₂, and UV/PDS. *Environ. Sci. Technol.* 49, 3056–3066. <https://doi.org/10.1021/es504799n>
- Zhang, T., Ding, L., Ren, H., 2009. Pretreatment of ammonium removal from landfill leachate by chemical precipitation. *J. Hazard. Mater.* 166, 911–915. <https://doi.org/10.1016/j.jhazmat.2008.11.101>
- Zhou, T., Lim, T.-T., Chin, S.-S., Fane, A.G., 2011. Treatment of organics in reverse osmosis concentrate from a municipal wastewater reclamation plant: Feasibility test of advanced oxidation processes with/without pretreatment. *Chem. Eng. J.* 166, 932–939. <https://doi.org/10.1016/j.cej.2010.11.078>

Appendix

Appendix 1 Dissociation of bicarbonate, ammonium and phosphate

1.1 Dissociation of carbonate-containing solution



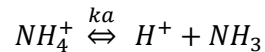
$$k_{a1} = \frac{[H^+][HCO_3^-]}{[H_2CO_3]} = 10^{-6.3}$$

$$k_{a2} = \frac{[H^+][CO_3^{2-}]}{[HCO_3^-]} = 10^{-10.3}$$

$$[DIC] = [H_2CO_3] + [HCO_3^-] + [CO_3^{2-}]$$

- when $\text{pH} < \text{pka1}(6.3)$, H_2CO_3 is the predominant species;
- when $\text{pka1}(6.3) < \text{pH} < \text{pka2}(10.3)$, HCO_3^- is the predominant species;
- when $\text{pH} > \text{pka2}(10.3)$, CO_3^{2-} is the predominant species.

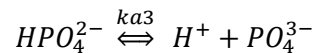
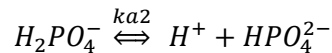
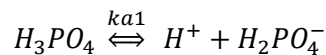
1.2 Dissociation of ammonium-containing solution



$$k_a = \frac{[H^+][NH_3]}{[NH_4^+]} = 10^{-9.24}$$

- when $\text{pH} < \text{pka}(9.24)$, NH_4^+ is the predominant species;
- when $\text{pH} > \text{pka}(9.24)$, NH_3 is the predominant species.

1.3 Dissociation of phosphate-containing solution



$$k_{a1} = \frac{[H^+][H_2PO_4^-]}{[H_3PO_4]} = 10^{-2.2}$$

$$k_{a2} = \frac{[H^+][HPO_4^{2-}]}{[H_2PO_4^-]} = 10^{-7.2}$$

$$k_{a3} = \frac{[H^+][PO_4^{3-}]}{[HPO_4^{2-}]} = 10^{-12.7}$$

- when $\text{pka1}(2.2) < \text{pH} < \text{pka2}(7.2)$, $H_2PO_4^-$ is the predominant species;
- when $\text{pka2}(7.2) < \text{pH} < \text{pka3}(12.7)$, HPO_4^{2-} is the predominant species.

Appendix 2 Determination of uncertainty of RO permeate flux

2.1 Dead-end cell

RO permeate flux (J) is defined as:

$$J = \frac{m_t - m_{t-1}}{t S}$$

where t is operating time (h). m_t is the measured mass during the period of t (kg). S is the membrane surface (m^2), as expressed in the following equation.

$$S = \pi \frac{D^2}{4}$$

where D is the diameter of RO membrane (0.073m)

To determine the uncertainty of permeate flux, the following uncertainty values are taken into account:

$$\Delta t = 1 \text{ s} = 0.0003 \text{ h}$$

$$\Delta m = 0.01 \text{ g} = 0.00001 \text{ kg}$$

$$\Delta D = 1 \text{ mm} = 0.001 \text{ m}$$

$$\Delta s = (\pi/2) \times D \times \Delta D = 0.0002 \text{ m}^2$$

$$\text{Thus, } S = 0.0042 \pm 0.0001 \text{ m}^2$$

And

$$\frac{\Delta J}{J} = 2 \frac{\Delta m}{m_1 - m_0} + \frac{\Delta t}{t} + \frac{\Delta S}{S}$$

Taking the extreme case of recording a point every minute and a mass of one gram maximum in this period of time, the relative uncertainty on J is at most 6.1%.

2.2 Cross-flow RO pilot

RO permeate flux (J) is defined as:

$$J = \frac{Q_t - Q_{t-1}}{S}$$

where Q_t is the measured flowrate of RO permeate during the period of t ($L \text{ h}^{-1}$). S is the membrane surface, as expressed in the following equation.

$$S = L \times W$$

where L is the length of RO membrane (0.607 m). W is the width of RO membrane (0.092 m).

To determine the uncertainty of permeate flux, the following uncertainty values are taken into account:

$$\Delta Q = 0.015 \text{ L h}^{-1}$$

$$\Delta L = 1 \text{ mm} = 0.001 \text{ m}$$

$$\Delta W = 1 \text{ mm} = 0.001 \text{ m}$$

$$\text{Thus, } S = 0.0558 \pm 0.0007 \text{ m}^2$$

And

$$\frac{\Delta J}{J} = 2 \frac{\Delta Q}{Q_1 - Q_0} + \frac{\Delta S}{S}$$

If RO pilot is run at a CF 3, $Q_t - Q_{t-1}$ is around 0.38. thus, the relative uncertainty on J is at most 5.2%.

For J/J_i ,

$$\frac{J}{J_i} = \frac{\frac{Q_1 - Q_0}{S}}{\frac{Q_t - Q_{t-1}}{S}} = \frac{Q_1 - Q_0}{Q_t - Q_{t-1}}$$

And

$$\frac{\Delta J/J_i}{J/J_i} = \frac{\Delta Q}{Q_1 - Q_0} + \frac{\Delta Q}{Q_t - Q_{t-1}}$$

Thus, the relative uncertainty on J/J_i is at most 7.8%.

Appendix 3 Solubility of ozone in the ionic solution (Chapter IV)

The effect of salts presence on the solubility of ozone in a concentrated aqueous solution is usually described by the Sechenov equation (Beltrán, 2004; Rischbieter et al., 2000).

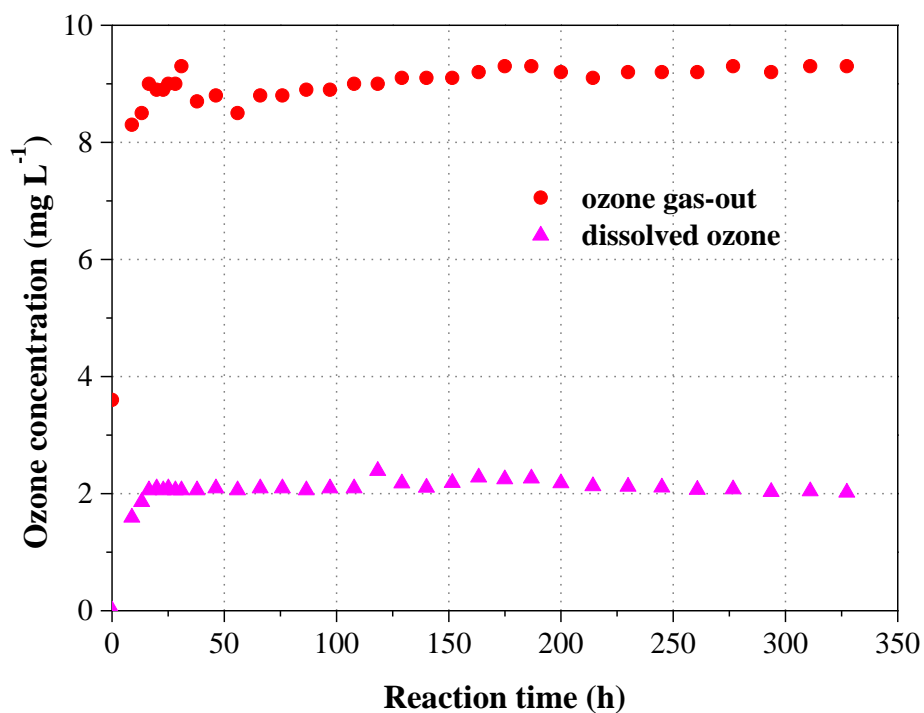
$$\log\left(\frac{m_0}{m}\right) = \sum (h_i + h_G) C_i$$

$$h_G = h_{G,0} + h_T(T - 298.15)$$

Where m_0 and m are the solubility parameter of ozone in pure water and in the salt solution, respectively. C_i is the molar concentration of ion i . h_i is an ionic-specific parameter. h_G , $h_{G,0}$ and h_T are the gas-specific parameters. The relevant values and the solubility of ozone in the salt solution are summarized in Table A.3.1.

Table A.3.1 The solubility of ozone in the SAM and SUM

SAM	C_i (mol L ⁻¹)	h_i (mol L ⁻¹)	$h_{G,0}$ (mol L ⁻¹)	h_T (mol L ⁻¹ K ⁻¹)	T (K)	h_G (mol L ⁻¹)	m
Cl ⁻	0.105	0.0318	0.00396	1.79E-06	293.15	0.00395	0.25
HCO ₃ ⁻	0.318	0.0967					
SO ₄ ²⁻	0.016	0.1117					
PO ₄ ³⁻	0.006	0.2119					
Na ⁺	0.377	0.1143					
K ⁺	0.038	0.0922					
SUM	C_i (mol L ⁻¹)	h_i (mol L ⁻¹)	$h_{G,0}$ (mol L ⁻¹)	h_T (mol L ⁻¹ K ⁻¹)	T (K)	h_G (mol L ⁻¹)	m
Cl ⁻	0.117	0.0318	0.00396	1.79E-06	293.15	0.00395	0.25
HCO ₃ ⁻	0.227	0.0967					
SO ₄ ²⁻	0.016	0.1117					
PO ₄ ³⁻	0.014	0.2119					
Na ⁺	0.072	0.1143					
K ⁺	0.059	0.0922					
NH ₄ ⁺	0.638	0.0556					
CO ₃ ²⁻	0.020	0.1423					

Appendix 4 Ozonation of saline solution (SA) without micropollutant spike (Chapter IV)

A 4.1 Concentration of ozone gas-out and of dissolved ozone as a function of cumulated consumed ozone dose during the ozonation of SA. ozone gas-in concentration: $\sim 10 \text{ mg L}^{-1}$ gaseous ozone flow rate: 30 L h^{-1} . liquid volume: 2 L , temperature: $20 \pm 1 \text{ }^\circ\text{C}$.